Rhodium-catalyzed cascade C–H bond functionalization for the synthesis of nitrogen-containing heterocycles

Marie Peng

DOCTORAT MATIERE BRETAGNE MOLECULES LOIRE ET MATERIAUX

UNIVERSITÉ DE RENNES 1

THESE DE DOCTORAT DE

L'UNIVERSITE DE RENNES 1

ECOLE DOCTORALE N° 596
Matière, Molécules, Matériaux
Spécialité : Chimie Moléculaire et Macromoléculaire

Par

Marie PENG

Rhodium-Catalyzed Cascade C–H Bond Functionalization for the Synthesis of Nitrogen-Containing Heterocycles

Thèse présentée et soutenue à Rennes, le 24 Novembre 2022

Unité de recherche : UMR 6226, CNRS, Université de Rennes 1, Institut des Sciences Chimiques de Rennes 1

Rapporteurs avant soutenance :

Tatiana BESSET	Directrice de Recherche, CNRS, INSA de Rouen
Patrick TOULLEC	Professeur, Université de Bordeaux

Composition du Jury :

Tatiana BESSET	Directrice de Recherche, CNRS, INSA de Rouen
Patrick TOULLEC	Professeur, Université de Bordeaux
Jean-François SOULÉ	Professeur, Chimie-Paris Tech (PSL), Université de Rennes 1
Henri DOUCET	Directeur de Recherche, Université de Rennes 1

Acknowledgments

Ce n'est pas sans émotion que je m'apprête à conclure un petit chapitre de vie, après sept ans de vie estudiantine et professionnelle rennaise.

J'adresse tout d'abord mes remerciements à Prof. Patrick Toullec et à Dr. Tatiana Besset de me faire l'honneur de constituer mon jury de thèse et d'investir de votre temps pour examiner ces travaux de recherches.

Je tiens à exprimer ma profonde gratitude envers mon directeur de thèse, Prof. Jean-François Soulé et mon co-directeur de thèse, Dr. Henri Doucet. Depuis le stage de master 2 jusqu'au doctorat, j'ai eu la chance d'évoluer auprès de ces chercheurs passionnés et passionnants qui ont su m'épauler et m'apporter tous les outils pour mener à bien ces travaux de recherches. Malgré un contexte sanitaire un peu capricieux, je suis chanceuse d'avoir été soutenue à chaque moment de la thèse. Merci pour votre patience, votre disponibilité, les précieux conseils ainsi que les critiques constructives, toujours teintées de bienveillance, dont vous m'avez fait bénéficier. Merci de m'avoir encouragée et guidée quand le moral n'y était pas toujours, mais également de m'avoir apportée la confiance nécessaire pour affronter chaque défi. Je suis sincèrement reconnaissante d'avoir eu l'opportunité d'explorer sous votre tutelle et votre expertise, un domaine de recherche passionnant et excitant. J'ai grandement apprécié les nombreux échanges que nous avons eu et souhaite à tout doctorant de bénéficier de la même qualité d'encadrement dont j'ai pu profiter.

Ces travaux de thèse n'auraient certainement pas vu le jour sans l'investissement de toutes les personnes qui y sont également impliquées. Je tiens tout d'abord à remercier Dr. Chang-Sheng Wang, ancien doctorant sous la tutelle de Prof. Jean-François Soulé et Prof. Pierre H. Dixneuf, d'avoir initié les travaux sur les nitroarènes, et d'avoir ouvert la voie à un domaine d'exploration challengeant et intéressant. Je souhaite également remercier Dr. Thierry Roisnel d'avoir effectué les analyses de Diffraction des Rayons X, pour votre efficacité et votre disponibilité. Mes remerciements sont également dirigés aux membres du CRMPO, notamment Clément Orione, en charge du service des analyses RMN, pour ta patience infinie et les agréables échanges que nous avons pu avoir. Merci également à l'équipe d'analyses de Spectroscopie de Masse, Jérôme Ollivier, Phillippe Jéhan, Fabian Lambert, Dr. Nicolas Le Yondre pour votre implication (voire acharnement !), et surtout pour la qualité de nos échanges.

Je souhaite adresser ma gratitude à la grande équipe de Catalyse - OMC avec qui j'ai eu le plaisir d'échanger au cours de ces trois années. Bien entendu, je ne peux débuter sans remercier sincèrement mon ancien professeur d'Organométalliques et de Catalyse, et ce depuis la 2ème année de licence, Prof. Christophe Darcel. Merci de m'avoir transmis le goût de la catalyse, de m'avoir encouragé à réaliser mon stage au Canada dans ce domaine et de m'avoir présentée à Prof. Jean-François Soulé et Dr. Henri Doucet. Je vous remercie pour votre bienveillance, vos conseils, mais surtout les verres que vous avez pu me payer. Plus sérieusement, je vous suis redevable dans bien des domaines et je suis chanceuse d'avoir pu vous côtoyer pendant toutes ces années. Je tiens également à remercier Prof. Pierre H. Dixneuf, pour les intéressantes discussions et votre aide pour élargir mon réseau grâce votre fameuse phrase d'accroche « *Have you met this young researcher ?* ». Mes sincères remerciements sont également adressés à Dr. Cédric Fischmeister, Dr. Rafael Gramage-Doria, Dr. Christian Bruneau, Dr. Sylvie Dérien, Dr. Mathieu Achard pour votre aide et vos conseils avisés au niveau de la recherche ou de l'enseignement au cours de ces trois années. J'adresse mes remerciements à Jérôme Ollivier, oreille toujours attentive, pour les discussions, les repas partagés et ton soutien tout au long de cette thèse. Je tiens également à remercier Cécile Valter, Catherine Jolivet, et Dominique Paris pour votre gentillesse, efficacité et disponibilité.

Merci également aux nombreux doctorants, post-doctorants, stagiaires et amis que j'ai pu rencontrer au labo. Je souhaite d'abord remercier les copains de la « *JF's dream team* », Jian, Loris, Bin pour les bons moments, votre aide et votre soutien. Merci également à Javid, mon binôme de labo pendant deux ans, vecteur de bonne humeur au quotidien. Merci aux anciens doctorants, Amal, Cindy, Zhuan, Hai-Yun, Haoran, Arpan, Mohammed et Rabab pour tous les bons souvenirs, et les bons gâteaux d'anniversaire. Je remercie également Linhao, Jonathan, Raphaël, Gabriel, Naba, Liwei, Zilong, Yumeng, Camille, Tony, Meriem, Lucie, Armelle et Jiajun d'avoir rendu l'ambiance agréable au labo et pour les bons moments que nous avons passés ensemble cette année. Un merci tout spécial à Jiajun, aka, *my brother from another mother*, avec qui j'ai débuté la thèse, cherché des produits, bu de nombreux cafés pendant la rédaction, et surtout, toujours le plus motivé pour aller boire une petite mousse après une dure journée de labeur. Je tiens également à remercier les anciennes stagiaires de l'équipe devenues de précieuses amies, Natacha et Kharla, pour votre bonne humeur et soutien permanent. Je souhaite aussi remercier Denis, certainement le stagiaire le plus enthousiaste et motivé de l'Institut, pour toute l'aide qu'il m'a apportée au cours de son stage de master 1.

Un grand merci également aux membres de l'équipe OMC du sous-sol, Dr. Olivier Galangau, Dr. Marc Devillard pour les agréables échanges et les encouragements, ainsi que les

doctorants Marie et William avec qui j'ai toujours le plaisir de discuter. J'aimerais remercier les membres de l'équipe MaCSE que j'ai eu le plaisir de côtoyer au cours de ces années. Merci Dr. Corinne Lagrost et Dr. Yann Leroux pour votre bienveillance. Merci également aux copains de l'équipe, Timothé, Max, Fabien, Kiseok, Cong, et Clément pour les (trop) nombreux apéros.

Je tiens également à remercier l'ensemble des chercheurs-enseignants avec qui j'ai eu le plaisir de discuter pendant les missions d'enseignements notamment Dr. Viatcheslav Jouikov et Dr. William Erb pour les nombreuses anecdotes et conseils partagés.

La vie de doctorante a notamment été plus douce grâce à l'association ACiD. Ce fut un plaisir d'en faire partie et d'avoir contribué à petite échelle à la vie de l'ISCR en compagnie des meilleurs. Merci à Claire, Déborah, Louis, Jeanne, avec qui j'ai partagé les bons comme les mauvais moments au cours de ces trois années. Merci également à Guillaume, Cécile, Alexandre, Julie, Myriam, Romain, Clément, Etienne, Charlène, … et tous les autres doctorants investis et rencontrés grâce à l'ACiD.

Un immense merci à mes amis rencontrés au cours de ces années rennaises pour tous les merveilleux souvenirs. Merci aux copains de licence, Thibault, Rebecca, Léry, Justyna et Ménélik, pour votre soutien et les soirées qui continuent de perpétuer malgré la distance. Je tiens également à remercier sincèrement mes acolytes devenus ma famille au cours de ces quelques années, Marine, Nicolas, Barthélémy, Nocibée, Corentin, Roland, Giulia, Robin et Nicolas. Entre soirées mémorables, débats houleux et vacances farnientes, merci d'être toujours si prévenants, bienveillants et présents au quotidien.

Toute ma gratitude est portée vers ma famille, mes parents, mon grand-frère, Thomas, et ma petite sœur, Alice, pour leur soutien indéfectible, de m'encourager et de me pousser à donner le meilleur au quotidien. Papa, maman, bien que je ne tiendrais pas rigueur des nombreuses questions posées sur le déroulement de « mon stage » au cours de ces années, merci d'être toujours là pour moi. J'aimerais chaleureusement remercier ma deuxième famille, Arnaud, Marina, et Fanny de me soutenir et de faire partie de ma vie.

Enfin, ces travaux de thèse n'auraient certainement pas abouti si je n'avais pas bénéficié du meilleur partenaire au quotidien. Merci Quentin d'être là, depuis les fonds de la classe de la 4ème E, jusqu'aux bancs de l'Université de Rennes 1 et de nos thèses respectives au sein de l'ISCR. Merci d'être une source d'inspiration dans la vie personnelle comme professionnelle, et de toujours me tirer vers le haut. Je ne pourrais jamais assez te remercier pour ton soutien inébranlable au cours de toutes ces années.

Table of Contents

General Introduction

Over the past two decades, transition metal-catalyzed C−H bond functionalization has emerged as a robust methodology to create carbon-carbon and carbon-heteroatom bonds. This approach involving the formal "activation" of inert carbon-hydrogen bonds enables a straightforward diversification of readily available materials in contrast to classical cross-coupling reactions that require organometallic and organohalide reagents.[1] Hence, the direct functionalization of C−H bonds brings a sustainable alternative in a viewpoint of atom- and step-economy by reducing the number of synthetic steps and limiting the generation of toxic waste and undesired by-products. Due to the ubiquity of C−H bonds in organic compounds, achieving selective C−H bond activation remains one of the key challenges. The most effective approach is introducing a directing group with a chelating heteroatom such as N or O atom (but not limited to) that can coordinate or act as a ligand with the transition-metal catalyst to direct the C–H bond cleavage at its *ortho*-position.[2] This concept was initiated by Murai and co-workers in 1993, where they succeeded in the selective C−H bond alkylation of aromatic ketone, in which the carbonyl group acts as the *ortho*-directing group.[3] This transformation was further extended to other functional groups such as esters, imines, or nitriles.[4] This concept has been a huge source of inspiration, and many research groups worldwide have also studied this reaction in varying catalysts (*e.g.*, Ru, Pd, Rh, Ir, Co, and others), steering groups, and transformations. However, in many cases, it turned out that the directing group was only there to guide the selectivity of the *ortho* C–H bond functionalization, thus limiting the potential of this approach or requiring additional steps to transform the directing group into a functional group.

An alternative approach consisted in developing new directing-assisted C−H bond transformations by employing a traceless directing group.[5] In this case, the functional group is pre-installed and directly removed in a one-pot process after C−H bond functionalization. The first example of directed C−H bond activation with a traceless directing group was reported by Miura and co-workers in 2008.[6] In this work, carboxylic acid was employed to selectively undergo C2-vinylation of indoles followed by decarboxylation to release the directing group in a single step.

A second alternative approach revolved around the elaboration of directing groups that can be directly converted into useful functional groups. Indeed, the presence of such directing groups associated with various coupling partners can make them prone to other intramolecular reactions leading to the simultaneous formation of multiple bonds such as C−C and C−X bonds (X = O, N). In this context, C−H bond "activation" is a compelling strategy to trigger further transformations in a single one-pot process. Such reactions can be defined as

cascade reactions.[7] For example, the formation of several bonds can be achieved in one reaction process without additional reagents or additional catalysts. Besides improving the atom- and step-economy, this methodology brings an efficient, eco-friendly route to enhance the complexity of desired scaffolds. Over the years, several examples of cascade C−H bond activation reactions have been reported, such as sequential C−H activation/annulation or a combination of C−H activation/annulation and further interactions with a functional group allowing access to complex polyheterocyclic compounds.[8]

Nitrogen-containing heterocycles are important organic scaffolds as they are widely represented in natural compounds, pharmaceutics, agrochemicals, and organic materials.[9, 10] Therefore, their transformations and diversifications face increasing demand. While the synthesis of nitrogen-containing heterocycles motifs often involves multi-step synthesis, this research aims to develop eco-friendly routes by using low-functionalized commercially available substrates to form multiple bonds such as carbon-carbon bonds, carbon-nitrogen bonds, or carbon-oxygen bonds. This Ph.D. thesis will focus on developing new rhodium-catalyzed C−H bond functionalization to access various nitrogen-containing heterocycles in a few steps by exploring these two strategies of traceless directing groups. Despite the generally elevated cost of rhodium complexes, their unique reactivities and selectivity make it always a metal of choice for C–H bond activation/functionalization. Moreover, rates, selectivity, and catalyst lifetime are generally more important variables than the cost of the metal itself.

The manuscript is divided into four chapters.

Chapter 1 presents a literature survey on recent Rh-catalyzed C−H annulation transformations to access nitrogen-containing heterocycles. Mechanistic studies on rhodium catalysis are also discussed.

Chapter 2 reports the cascade reaction of C–H alkylation – amidation of phosphanamines using Rh(I) catalyst and trivalent phosphorus as a traceless directing group. This strategy provides straightforward access to dihydroquinolinone scaffolds. The optimization of the reaction of conditions and the exploration of the scope of the reaction are provided. A deep mechanistic investigation with kinetic studies is also presented in this chapter to underpin the catalytic pathway of this novel transformation.

Chapter 3 discloses a novel route to provide 3,3-disubstituted oxindoles from nitroarenes, alkynes, and anhydrides. This work represents one of the rare examples of the nitro group as a directing group for Rh-catalyzed C–H bond functionalization. Optimization and design of cyclopentadienyl-pro ligands are developed in the first part and are followed by exploring the

scope of this multicomponent reaction. Post-modifications allow the synthesis of disubstituted indolines. Mechanistic studies with the isolation of three rhodacycles intermediates are provided to rationalize this new unpredictable cascade reaction.

Finally, in chapter 4, we describe a new approach to build bi(hetero)aryl compounds using twofold C–H bond activation catalyzed by Rh(III)/Ag(I) at room temperature. Using one of the η^5-cyclopentadienyl rhodium complexes developed in the chapter 3, we showed better reactivity than with the commercially available $[Rh(Cp^*)Cl_2]_2$. The scope of the reaction is investigated, and post-transformations are ongoing to extend the strategy to the synthesis of 3,4-fused isoquinolin-1-*2H*-one scaffolds.

References

1. Recent reviews on C–H bond functionalization: (a) Yang, Z.; Yu, J.-T.; Pan, C. *Org. Biomol. Chem.* **2021**, *19*, 8442–8465; (b) Rej, S.; Das, A.; Chatani, N. *Coord. Chem. Rev.* **2021**, *431,* 213683; (c) Yu, X.; Zhang, Z.-Z.; Niu, J.-L.; Shi, B.-F. *Org. Chem. Front.* **2022**, *9*, 1458-1484; (d) Wang, K.; Zhang, J.; Hu, R.; Liu, C.; Bartholome, T. A.; Ge, H.; Li, B. *ACS Catal.* **2022**, *12*, 2796–2820.
2. Rej, S.; Ano, Y.; Chatani, N. *Chem. Rev.* **2020**, *120*, 1788–1887.
3. Murai, S.; Kakiuchi, F.; Sekine, S.; Tanaka, Y.; Kamatani, A.; Sonoda, M.; Chatani, N. *Nature*. **1993**, *366*, 529–531.
4. Kakiuchi, F.; Murai, S. *Acc. Chem. Res.* **2002**, *35*, 826–834.
5. Rani, G.; Luxami, V.; Paul, K. *Chem. Commun.* **2020**, *56*, 12479–12521.
6. Maehara, A.; Tsurugi, H.; Satoh, T.; Miura, M. *Org. Lett.* **2008**, 1159–1162.
7. Nicolaou, K. C.; Edmonds, D. J.; Bulger, P. G. *Angew. Chem. Int. Ed.* **2006**, *45*, 7134–7186.
8. Selected reviews on cascade C–H bond functionalization: (a) Peneau, A.; Guillou, C.; Chabaud, L. *Eur. J. Org. Chem.* **2018**, *2018*, 5777–5794 ; (b) Baccalini, A.; Faita, G.; Zanoni, G.; Maiti, D. *Chem. – Eur. J.* **2020**, *26*, 9749–9783; (c) Song, L.; Van der Eycken, E. V. *Chem. – Eur. J.* **2021**, *27*, 121–144; (d) Kumar, S.; Nunewar, S.; Oluguttula, S.; Nanduri, S.; Kanchupalli, V. *Org. Biomol. Chem.* **2021**, *19*, 1438–1458.
9. Heravi, M. M.; Zadsirjan, V. *RSC Adv.* **2020**, *10*, 44247–44311.
10. Chen, D.; Su, S.-J.; Cao, Y. *J. Mater. Chem. C.* **2014**, *2*, 9565–9578.

Chapter 1. Literature Survey on Rh-Catalyzed C–H Bond Annulation for the Formation of *N*-Heterocycles Building Blocks

1.1. Introduction

N-heterocycles are key structural units embedded in many active pharmaceutical ingredients (APIs), biologically exciting molecules, natural products, and functional materials.[1] Therefore, developing novel synthetic routes of *N*-heterocycles, respecting some of the 12 principles of green chemistry, has gained increased attention in academia and industry. The development of novel catalytic transformations can unlock the preparation of unprecedented *N*-heterocycles with further potential applications in medicinal or material sciences. Over the past decades, many metal-catalyzed C–N bond formation methodologies, such as Buchwald-Hartwig cross-coupling and Ullmann reaction, have been widely applied to prepare *N*-heterocycles with high efficiencies.[2] However, these approaches required pre-functionalized starting materials, limiting the exploration of *N*-heterocycle structures to target-oriented rather than diversity-oriented synthesis. To avoid the generation of wastes, intramolecular C–H bond amination has been applied to the synthesis of *N*-heterocycles,[3] but once again, specific substrates must be designed.

Thanks to the deep investigation of C–H bond functionalizations,[4] more and more complex transformations have flourished, notably, the C–H bond functionalization with the concomitant C–N bond formation, so-called C–H bond annulation, which furnishes diverse nitrogen-containing heterocycles in a single step. This rapid construction of diverse and functional nitrogen-containing heterocycles from simple building blocks entirely fits with the idea of suitable synthesis in terms of atom economy. In most cases, the *N*-atom present on the starting materials (*e.g.*, anilines, amides, triazenes, imidamides, *N*-arylhydrazine, and others) helps to direct the C–H bond functionalization at the *ortho*-position and then, reacts intramolecularly to create the C–N bond under oxidative conditions. Among the diverse metal catalysts, rhodium has been predominant in achieving these *ortho*-directed C–H bond annulations. However, the use of an external oxidant to regenerate the catalyst, mainly $Cu(OAc)_2$, could misrepresent the sustainability of the C–H bond annulation reaction. Alternatively, oxidizing directing groups can replace the external conditions, resulting in milder reaction conditions.[5] Oxidizing directing groups are generally composed of N–O or N–N bonds, which can reoxidize the metal catalyst at the end of the catalytic cycles through an oxidative addition step of the N–X bond. During these last 15 years, these two strategies for Rh(III)-catalyzed C–H bond annulation have been applied to the construction of diverse heterocycles depending on the choice of the starting materials.

In this chapter, we would like to summarize the different *N*-heterocycles than can be prepared by this method, asides (iso)quinolines, because their preparations have been widely covered by precedent reviews[6] and are not related to this Ph.D. thesis. The contents were categorized by the type of *N*-heterocycles: indoles, pyrroles, indolines, (iso)quinolinones, dihydroquinolines, and pyrrolidones. We focus on 1) reaction design, including catalyst choice and substrate design, and 2) mechanistic insights of cascade C–H bond functionalizations. Finally, the challenges and future developments in this research field are also discussed.

1.2. Formation of Five-Membered Ring *N*-Heterocycles

1.2.1. Preparation of Indole Scaffolds

1.2.1.1 C–H Bond Functionalization Under Oxidative Conditions

In 2008, Fagnou and co-workers reported the first synthesis of indoles starting from readily available *N*-acetyl anilines and alkynes as starting materials through Rh(III)-catalyzed C–H bond annulation reaction (Scheme 1.1-A).[7] Initially, the conditions employed $[Cp^*RhCl_2]_2$ in conjunction with a stochiometric amount of $Cu(OAc)_2$ as oxidant at 120 °C. Both electron-rich and electron-deficient acetanilides were efficiently coupled with internal alkynes. The reaction is fully regioselective with aryl-alkyl di-substituted alkynes, while mixtures of regioisomers were obtained using unsymmetrical alkynes with two different alkyl groups. This regioselectivity arises from the alkyne insertion event owing to the electronic factors. In 2010, Fagnou and co-workers upgraded the reaction conditions by using a catalytic amount of $Cu(OAc)_2$ in the presence of atmospheric oxygen as the terminal oxidant at a lower temperature of 60 °C (Scheme 1.1-B).[8] The substrate scope was enlarged to 35 examples demonstrating a high functional group tolerance, including sensitive ones such as benzyl, silyl, (protected) alcohols, cyclopropyl, and ester groups. This Rh(III)-catalyzed formation of indole scaffold was also applied to the preparation of Paullone, a complex natural product (Scheme 1.1-C).[8] The authors conducted a deep mechanistic study using kinetics and deuterium-labeling experiments, enabling them to propose the catalytic cycle depicted in Scheme 1.1-D. Cationic Rh complex **I** is formed (by halogen abstraction using silver salts) in the presence of 1 equivalent of acetate. A deactivation pathway was revealed in the presence of alkyne to form nonproductive coordination complexes. After the coordination of acetanilides through the Lewis basic amide oxygen, C–H bond cleavage occurs from rhodacyle **II** in an irreversible and rate-determining step. Alkyne may then coordinate **II**, followed by carbo-rhodation to yield **III**. C–N bond reductive elimination extrudes the desired indole product along with Cp*Rh(I). The reduced catalyst is then oxidized back to the active species *via* catalytic copper(II) acetate

which is then reoxidized by the combination of molecular oxygen and acetic acid (generated in the reaction) in the case of conditions 2.

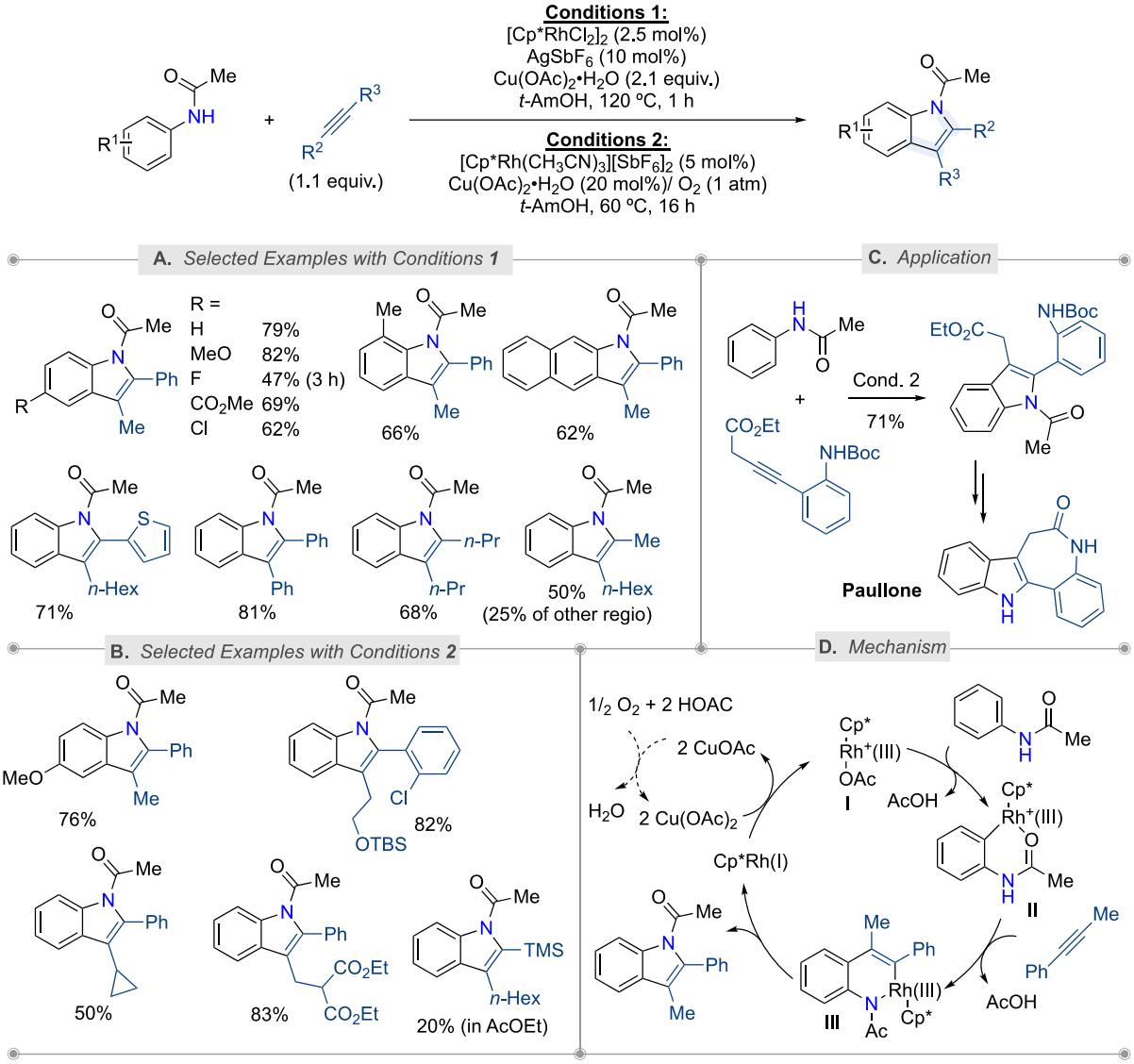

Scheme 1.1. Indole Synthesis *via* Rhodium(III)-Catalyzed Oxidative Coupling of Acetanilides and Internal Alkynes.

In 2010, Li and co-workers reported a similar formation of indoles, but they used pyridine as directing group instead of amide (Scheme 1.2, top).[9] From *N*-aryl-2-aminopyridines and symmetrical alkynes, the corresponding *N*-pyridinyl-substituted indoles were obtained in good yields using $[Cp^*RhCl_2]_2$ in the presence of a stochiometric amount of $Cu(OAc)_2$ as oxidant at 120 °C in DMF. The reaction proceeded through a similar catalytic cycle to the one proposed by Fagnou (Scheme 1.1-D).[7] The reaction exhibited poor functional group tolerance as only substrates bearing Me, MeO, F, and Cl substituents were employed. Later on, the same

group showed that this indole synthesis is also applicable to *trans*-crotylamide, albeit using a cationic Cp*Rh catalyst (Scheme 1.2, bottom).[10]

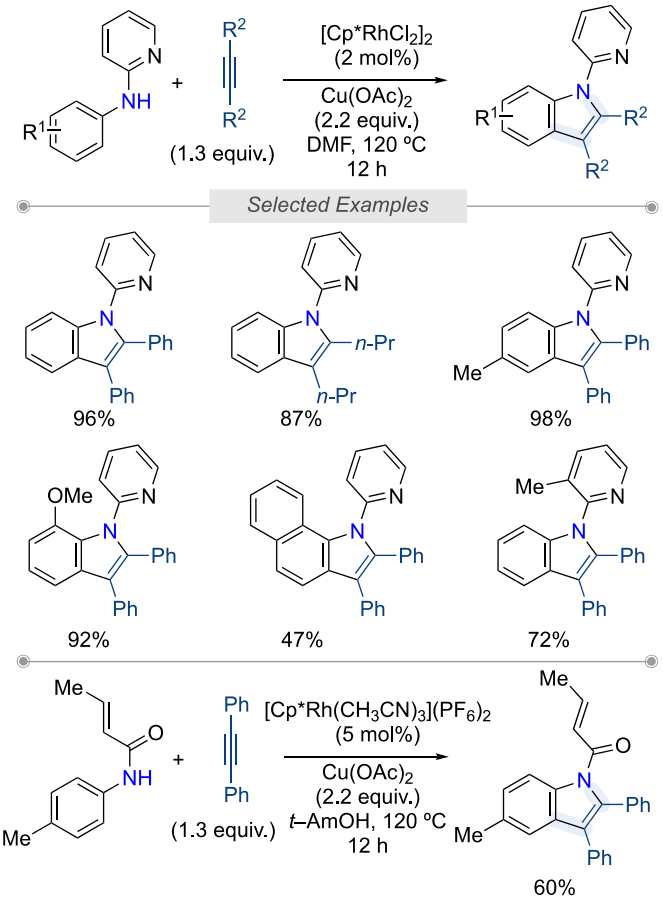

Scheme 1.2. Rh(III)-Catalyzed Oxidative C–H Bond Annulation of *N*-Aryl-2-aminopyridine with Alkynes.

In 2011, after the unfortunate death of Keith Fagnou, his group reported the preparation of unsymmetrical 2,3-substituted indoles through rhodium(III)-catalyzed oxidative C–H bond annulation of N-arylurea with enynes (Scheme 1.3).[11] Similarly to aryl-alkyl di-substituted alkynes,[7-8] the alkyne insertion reaction was highly regioselective, leading to the production of C2-vinyl-substituted indoles. Nevertheless, acetamide (–NHAc as directing group) was not a suitable partner for this transformation, and *N*-arylurea (–NHCONMe$_2$ as directing group) had to be employed. Several functional groups were compatible with the optimized conditions on the aniline unit, such as trifluoromethyl, methoxy, chloro, and methyl. α,β-Unsaturated esters could also be employed, including those containing functional groups such as *tert*-butylcarbamate-protected amines and triphenylmethyl ethers. Notably, olefin isomerization was observed with (*Z*)-alkenes, and 2,2-disubstituted alkenes were also tolerated. An allylic alcohol, protected as the *tert*-butyldimethylsilyl ether, was also installed alongside another indolyl ring. The authors demonstrated that these C2-vinyl-substituted indoles could serve as

building blocks for the preparation of unsymmetrical 2,3-aliphatic-substituted indoles through hydrogenation using Pd/C as catalyst. Notably, such compounds are not directly accessible by rhodium-catalyzed synthesis with alkyl-alkyl di-substituted alkynes due to regioselectivity issues.

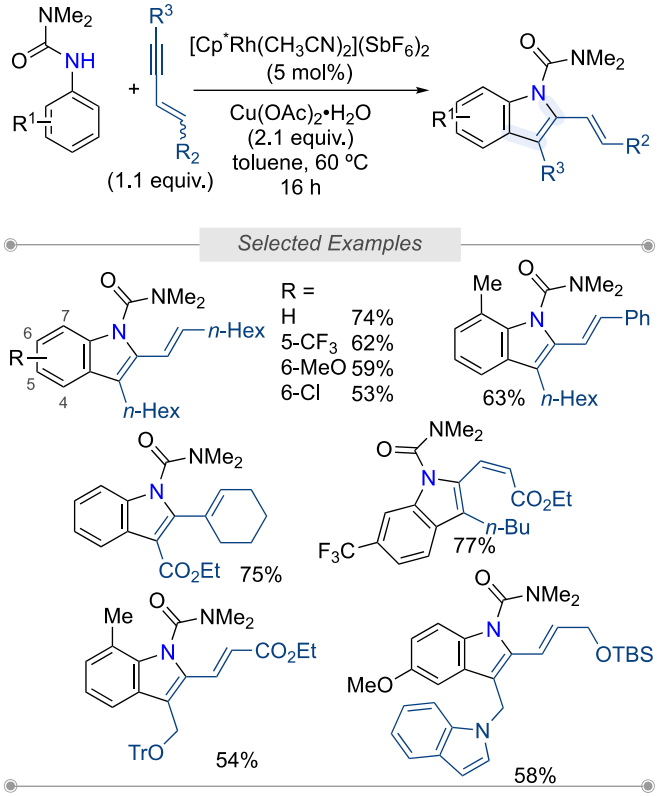

Scheme 1.3. Indole Synthesis *via* Rhodium(III)-Catalyzed Oxidative Coupling of *N*-Arylurea and Enynes.

With the emergence of Cp*Rh-catalyzed C–H bond functionalizations, several sterically or electronically tuned cyclopentadienyl ligands have been investigated in rhodium catalysis to improve selectivity and/or reactivity.[12] In 2014, Tanaka and co-workers employed an electron-deficient $Cp^{R}Rh$ catalyst, namely $[Cp^{E}RhCl_2]_2$,[13] to succeed in Fagnou's indole synthesis at room temperature (Scheme 1.4).[14] Indeed, the electron-deficient dicationic Rh(III) complex derived from $[Cp^{E}RhCl_2]_2$ exhibited a higher reactivity than Cp^*Rh^{2+} owing to the easiest electrophilic C–H bond activation of the acetanilide. For instance, the reaction of acetanilide with diphenylacetylene proceeded at room temperature under air to give the corresponding indoles in quantitative yield, while using Cp^*Rh^{2+}, a lower yield of 28% was obtained. The reaction is quite general, as diversely substituted indoles have been prepared by this method, including those containing sensitive groups such as alkyl halides. The reaction was not limited to acetamide as a directing group, as carbamate (NHBoc) and benzamide (COPh) have also been successfully employed. The authors mentioned that this electron-deficient rhodium

catalyst displays a preference for annulation across electron-rich substrates over electron-deficient substrates.

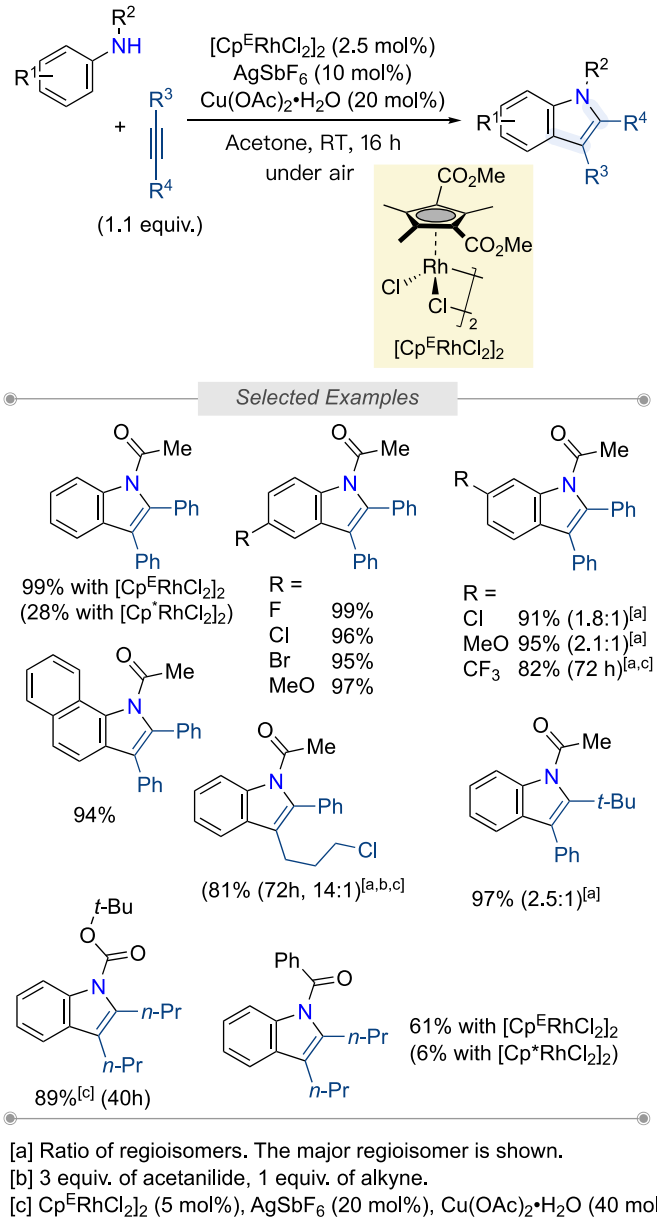

[a] Ratio of regioisomers. The major regioisomer is shown.
[b] 3 equiv. of acetanilide, 1 equiv. of alkyne.
[c] $Cp^{E}RhCl_2]_2$ (5 mol%), $AgSbF_6$ (20 mol%), $Cu(OAc)_2$•H_2O (40 mol%)

Scheme 1.4. Room-Temperature Oxidative Annulation of Anilides with Internal Alkynes Using $[Cp^{E}RhCl_2]_2$ Catalyst.

In 2014, Huang and co-workers also reinvestigated the Fagnou reaction starting from anilines in the presence of acetic anhydride (Scheme 1.5).[15] The reaction goes through the *in-situ* anilides formation from anilines and acetic anhydride, then, after C–H bond annulation, the addition of NaOH allows the "one-pot sequential" diacylation to afford the NH-indole derivatives. The reactivity was affected by the nature of the cationic counterion, and the best result was obtained with $Cp^*Rh(H_2O)_3(OTf)_2$ as the catalyst precursor. It should also be

mentioned that these conditions did not require additional copper, as O_2 acts as the sole oxidant enabling to regenerate Cp*Rh(III) from Cp*Rh(I) at the end of the catalytic cycle.

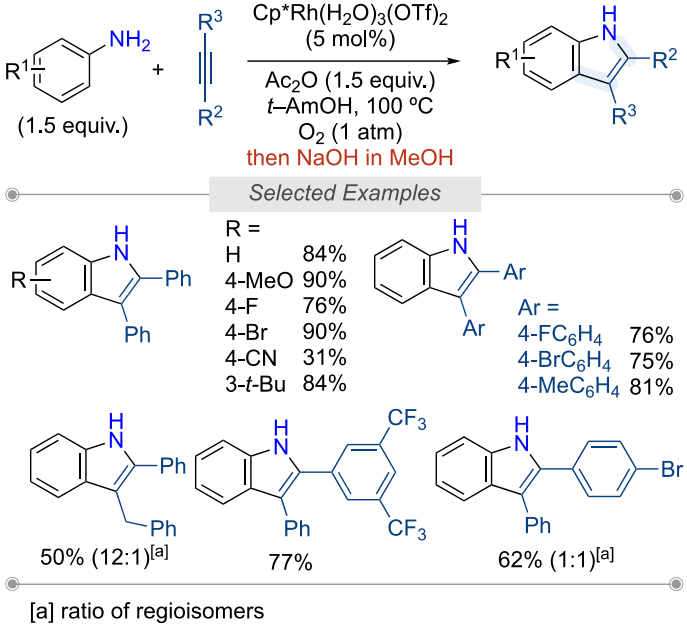

Scheme 1.5. Rh(III)-Catalyzed Oxidative C–H Bond Annulation of Anilines with Alkynes.

In 2013, Huang reported a novel synthetic approach for unprotected indoles through a triazene-directed C–H annulation using alkynes (Scheme 1.6).[16] The optimized reaction conditions were found using 5 mol% $[Cp^*RhCl_2]_2$ associated with $AgSbF_6$ (20 mol%) in the presence of 2 equivalents of $Cu(OAc)_2{\cdot}H_2O$ as an external oxidant in methanol at 90 °C. Diversely substituted triazenyl arenes (F, Cl, Br, I, NO_2, MeO, Me) were efficiently coupled with alkynes (diaryl or dialkyl). Moreover, excellent regioselectivity was achieved when non-symmetrical alkynes were employed. The authors demonstrated the potential of this reaction by preparing specific indoles for materials applications or drug molecules. The author proposed a catalytic cycle involving 1,2-rhodium shift ring contraction (path a) or an N=N insertion mechanism (path b) as key steps (Scheme 1.6-B). After the classical C–H bond metalation directed by the middle nitrogen atom of the triazene moiety (complex **I**) and insertion of the alkyne, the resulting 7-membered metallacycle **II** is obtained**.** In path a, **II** rearranges into a more stable six-membered Rh complex **III**, then reductive elimination releases the indole product and Rh(I), which is reoxidized by $Cu(OAc)_2$. In path b, N=N insertion to Rh–C, followed by subsequent reduction and hydrolysis, would also generate the desired heterocycle.

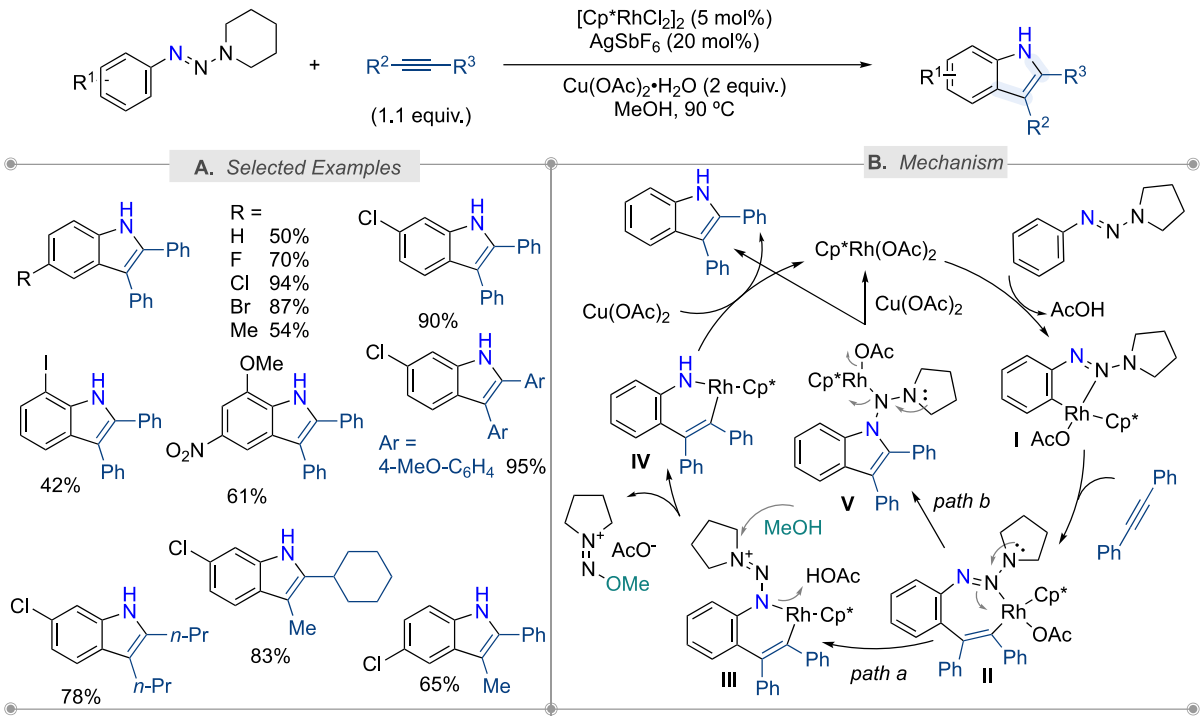

Scheme 1.6. Synthesis of Indoles through Triazene-Directed C–H Bond Annulation.

In 2014, Nicholls and co-workers extended Fagnou's indole synthesis to *N*-arylurea, in which the $NHCONR_2$ group acts as the directing group (Scheme 1.7).[17] The conditions were similar to the first conditions reported by Fagnou [stochiometric amount of $Cu(OAc)_2$], albeit 1,2-dichloroethane was used as the solvent. Various *ortho*-, *para*-, and *meta*-substituted *N*-arylureas with either electron-donating (*e.g.*, alkyl, MeO) or electron-withdrawing functional groups (*e.g.,* I, Br, Cl, F, or CO_2Me) were efficiently coupled with diphenylacetylene. Dialkyl-substituted acetylenes displayed better reactivity than diaryl-substituted acetylenes, while aryl-alkyl-substituted acetylenes regioselectivity reacted.

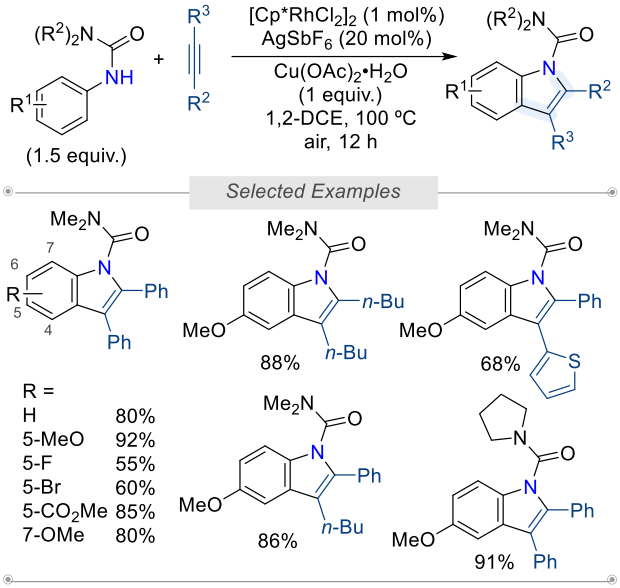

Scheme 1.7. Rh(III)-Catalyzed Oxidative C–H Bond Annulation of *N*-Arylurea with Alkynes.

The same year, Liu and co-workers succeeded in the C–H bond annulation of *N*-arylacetohydrazide to form indolyl scaffolds (Scheme 1.8-A).[18] The reaction was catalyzed by $[Cp^*RhCl_2]_2$ using unprecedented 1,3-dinitrobenzene as a terminal oxidant. Various substituted (*e.g.*, alkyl, methoxy, halo, cyano) *N*-arylacetohydrazide were efficiently coupled with internal alkynes. In most cases, substrates holding an electron-withdrawing group gave lower yields. Other substituents at the R^2 position on the hydrazine, such as benzyl or long chain alkyl chlorides, were also tolerated. Based on control experiments to clarify the role of 1,3-dinitrobenzene as a terminal oxidant, the authors have proposed the catalytic cycle depicted in Scheme 1.8-B. Firstly, $[Cp^*RhCl_2]_2$ reacts with NaOAc to generate the active catalyst $[Cp^*Rh(OAc)_2]$, which undergoes CMD process with *N*-arylacetohydrazide to form the rhodacycle **II**. Then, alkyne coordination followed by insertion affords the seven-membered rhodacycle **III**, which rearranges to a more stable six-membered rhodium complex **IV**. Then, reductive elimination releases the annulated product and [Cp*Rh(I)]. Finally, external oxidant 1,3-dinitrobenzene reoxidizes [Cp*Rh(I)] in the presence of acetic acid to regenerate the active catalyst $[Cp^*Rh(OAc)_2]$.

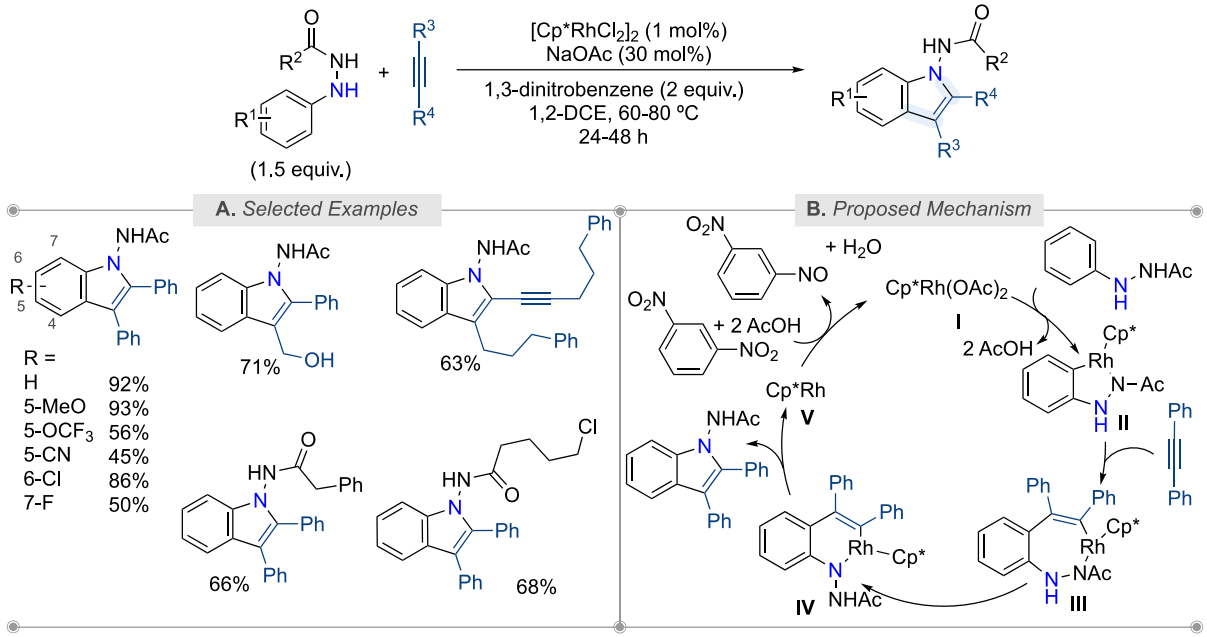

Scheme 1.8. Rh(III)-Catalyzed Oxidative C–H bond Annulation of *N*-Arylacetohydrazide with Alkynes Using a Nitrobenzene Oxidant.

As reported by Saá and co-workers, indolyl scaffold could also be generated through Cp*Rh(III)-catalyzed oxidative coupling of anilides with allyl carbonates using a slight excess of $AgSbF_6$ salt and $Cu(OAc)_2$ as oxidant (Scheme 1.9-A).[19] This approach is equivalent to C–H bond annulation of anilides with terminal alkynes, as it gives rise to indoles with substituents at the C2 position but not at the C3 position. 18 examples were reported by introducing methyl, methoxy, fluoro, chloro substituent at *para*-, *meta*-, or *ortho*-positions of the anilides. The reaction is limited to the use of AcNH- as directing group. Moreover, the yields are inferior when allyl partners are substituted, such as 1-methyl-2-propenylmethyl carbonate or *E*-2-butenyl acetate. The authors proposed a catalytic cycle based on deuterium labelling and KIE experiments (Scheme 1.9-B). After the initial formation of the previously proposed rhodacycle **II** through *ortho*-C–H bond cleavage of anilides *via* a CMD process, migratory insertion of the allyl double bond into the Rh–C bond gives a seven-membered rhodacycle **IIIa**. β-Oxygen elimination delivers the new olefin-coordinated Rh(III) species **IV** through an oxidative Mizoroki Heck/β-elimination pathway. Alternatively, the same species **III** could be formed by coordination of the allyl-bearing the carbonate oxygen to Rh(III) species **IIIb** which facilitates an intramolecular S_N2 process. *Syn*-amidorhodation occurs in **IV**, followed by β-hydrogen elimination and isomerization, then releases the observed product. Finally, the reduced Cp*Rh(I) catalyst is oxidized by copper(II) acetate.

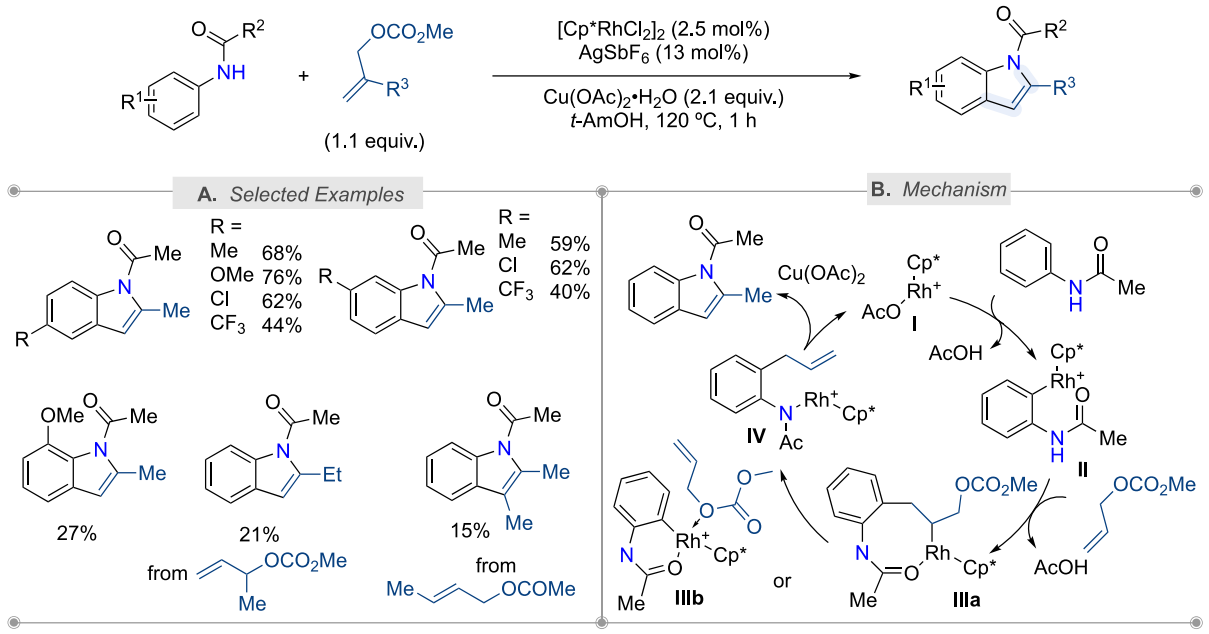

Scheme 1.9. Indole Synthesis *via* Rhodium(III)-Catalyzed Tandem C–H allylation – Oxidative Cyclization of Anilides.

A more atom-economy protocol for the synthesis of C2-substituted indoles was reported by Kim and co-workers using allyl acetate instead of carbonates (Scheme 1.10).[20] However, the reaction is limited to access 2-methylindoles, as only allyl acetate has been employed. The reaction conditions are similar to those previously reported, namely 2.5 mol% $[Cp^*RhCl_2]_2$ associated with 10 mol% $AgSbF_6$ in the presence of a stochiometric amount of $Cu(OAc)_2$ as oxidant.

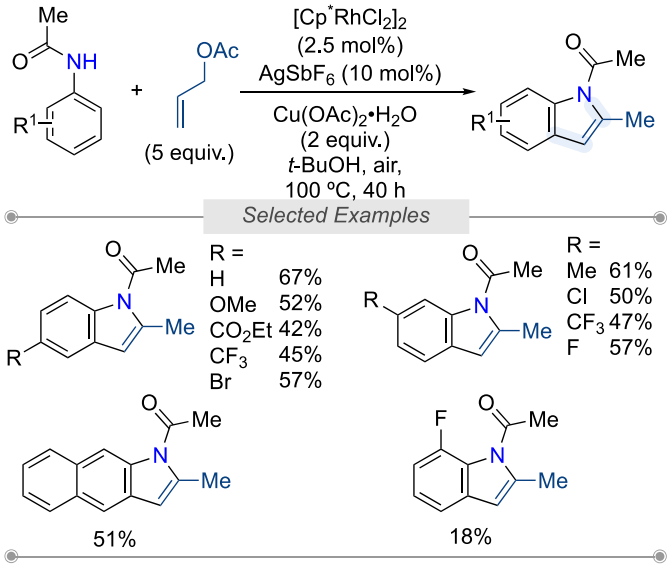

Scheme 1.10. Synthesis of 2-Methylindoles from Anilides and Allyl Acetate Using Rhodium Catalysis.

In 2016, Li and co-workers discovered the synthesis of *N*-unprotected indoles through Rh(III)-catalyzed C–H bond annulation of imidamides with α-diazo β-ketoesters (Scheme 1.11-A).[21] The reaction occurs in the presence of $[Cp^*RhCl_2]_2$ catalysts associated with CsOAc in the presence of AcOH in DCE at 80 °C. An amide is co-generated from C–N cleavage of the imidamide and C–C (acyl) cleavage of the diazo compounds. Diversely substituted *N*-unprotected indoles were isolated in good to high yields by varying the substituent on imidamides. However, the reaction is limited to the use of α-diazo β-ketoesters entailing that *N*-unprotected indoles hold an ester substituent (or acetyl) at the C3 position. The authors proposed the mechanism depicted in Scheme 1.11-B. After the formation of active catalyst $[RhCp^*(OAc)_2]$, C–H bond cleavage of imidamides occurs through an *ortho*-coordination assisted CMD mechanism (*this rhodacyclic intermediate* ***I*** *has been isolated with Cl ligand instead of AcO*). Then, coordination of the diazo substrate and nitrogen elimination gives rhodium carbene species **II**. The Rh–Ar bond undergoes migratory insertion into the carbene unit to give intermediate **III**. The Rh–C(alkyl) bond then undergoes migratory insertion into the C–N bond to afford amide species **IV**. Acidic hydrolysis releases **V** and the active Rh(III) catalyst. Finally, unprotected indole is formed from **V** by the elimination of amide.

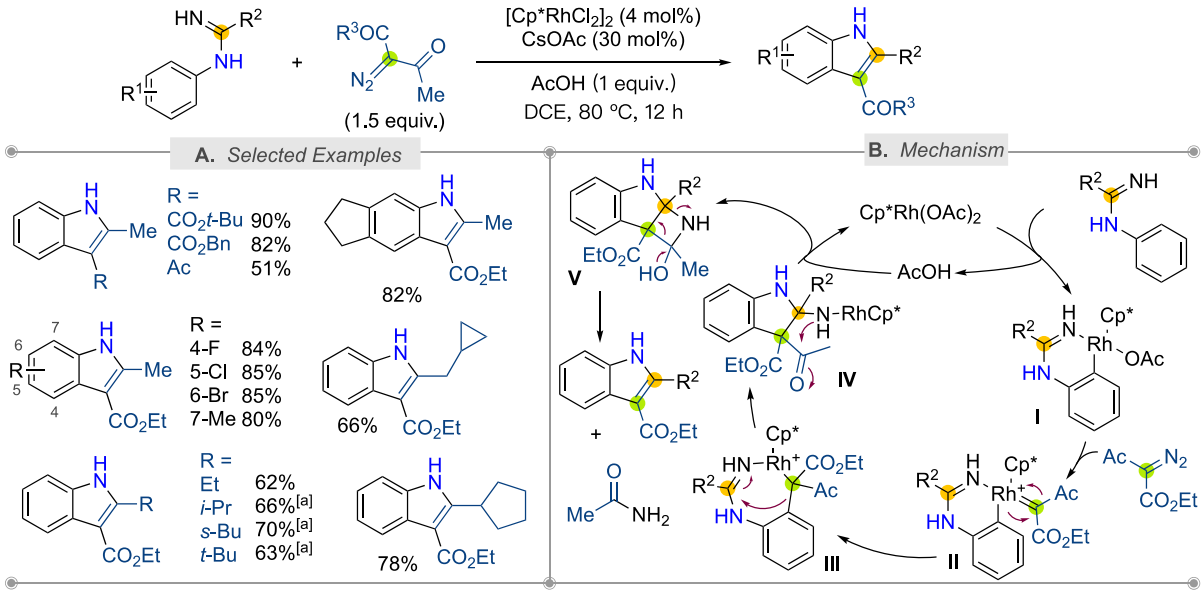

[a] Using 1.3 equivalents of imidamide

Scheme 1.11. Rhodium(III)-Catalyzed C–H, C–C, and C–N Bond Cleavages for the Synthesis of *N*-Unprotected Indoles from Imidamides and Diazo Ketoesters.

Zhou, Liu, and co-workers later reported a similar protocol using α-chloroketones instead of α-diazo β-ketoesters (Scheme 1.12-A).[22] The optimum catalytic system was found using $[Cp^*RhCl_2]_2$ (5 mol %), AgOAc (50 mol %), and $NaHCO_3$ (200 mol %) in MeOH at 90 °C for 24 h.

N-Phenylamidines bearing various electron-donating, electron-withdrawing, or halogen substituents reacted with diversely mono- and di-substituted *α*-chloroketones to give the corresponding 2-substituted-3-acylindoles in good to high yields. The reactivity trend shows better yields with electron-donating groups on the benzamidine ring. Moreover, C-alkyl imidamides were also successfully employed. The authors proposed the following catalytic cycle (Scheme 1.12-B). The reaction of *N*-phenylamidine with $Cp^*Rh(OAc)_2$ through a CMD mechanism affords the cyclometalated intermediate **I**. After coordination of *α*-chloroketone by the oxygen atom to the Rh center, nucleophilic substitution affords the seven-membered rhodacyclic intermediate **II,** followed by Rh−C(alkyl) migratory insertion into the C=N bond to afford **III.** Finally, the desired indole is produced by aromatization with the release of NH_3.

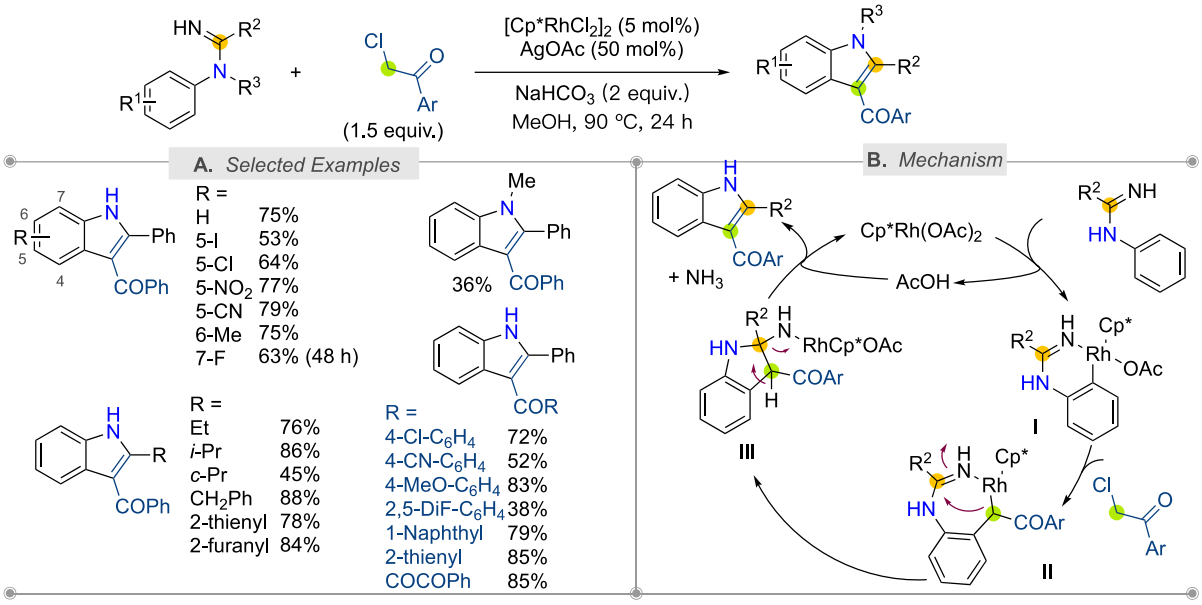

Scheme 1.12. Synthesis of 3-Acylindoles through Rhodium(III)-Catalyzed Annulation of *N*-Phenylamidines with *α*-Chloro Ketones.

In 2017, Xi and co-workers accomplished the C–H bond annulation of azobenzenes with vinyl ketones to deliver 2-acyl-NH-indole compounds using Rh(III) catalysis (Scheme 1.13-A).[23] The optimized conditions, namely 5 mol% $[Cp^*RhCl_2]_2$ in the presence of 2 equivalents of $Cu(OAc)_2$, tolerated synthetically useful functional groups, such as Me, OMe, F, CF_3, Cl, and Br, on azobenzene to give the expected indole products in moderate to good yields. Various vinyl aryl ketones and *N*,*N*-dimethyl acrylamides were also efficiently coupled. Interestingly, the reaction is regioselective with unsymmetrically substituted azobenzenes, the reaction occurred on the electron-poorer aryl ring. The authors proposed the mechanism shown in Scheme 1.13-B. First, the C–H bond cleavage of azobenzene by Rh(III) specie gives five-membered cyclo-rhodium species **I**, followed by alkene coordination and insertion to afford

the seven-membered rhodacycle **II**. In the presence of $Cu(OAc)_2$, a rearrangement involving nucleophilic addition toward the N–N bond delivers **IV**, which further undergoes N–N bond cleavage and aromatization to give free indole products.

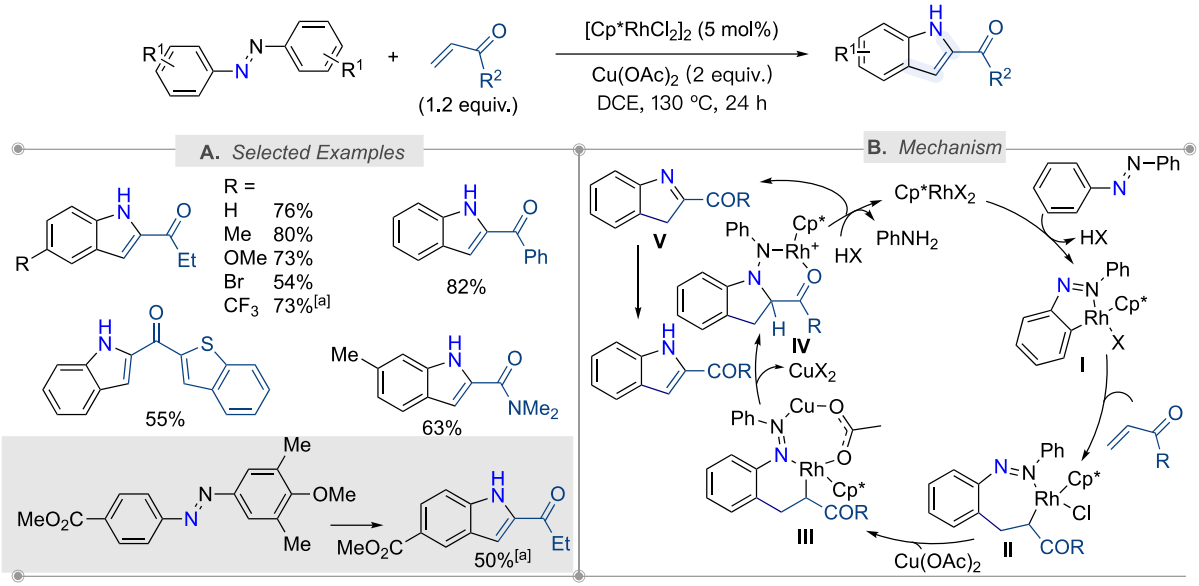

[a] $AgSbF_6$ (20 mol%) was added.

Scheme 1.13. 2-Acyl-NH-Indole Synthesis from Azobenzenes and Vinyl Ketones using Rhodium Catalysis.

1.2.1.2 C–H Bond Functionalization Using Internal N–O Bond as Oxidant

Despite the outstanding advances in Rh(III)-catalyzed C–H bond annulation to prepare indolyl scaffolds, the use of a stochiometric amount of oxidants, often $Cu(OAc)_2$, remains a significant weakness of these synthetic methodologies in terms of green chemistry. Recent developments in redox-neutral strategy employing an oxidizing directing group have made these protocols more eco-friendly.[5] In 2015, Wang, Wan, and co-workers reported the first example of redox-neutral Rh(III)-catalyzed C–H bond annulation of nitrones with alkyne to prepare indoles (Scheme 1.14-A).[24] The nitrone acts as a directing group and oxidizing agent, allowing the regeneration of Rh(III)-catalysts through the N–O bond. One of the two aryl substituents on the indole ring arises from the aryl ring of the nitrone and the other one from the alkyne moiety through C–C bond cleavage, thus, providing the indole products with exclusive regioselectivity. Optimized conditions still required a stoichiometric amount of copper salts. The scope of the reaction is quite general, tolerating ether, alkyl, aryl, ester, nitro, fluoro, chloro, or trifluoromethyl substituents at diverse positions. After a mechanistic study, the authors proposed the complex mechanism depicted in Scheme 1.14-B. In a first step, nitrone-assisted C–H bond affords the five-membered rhodacycle intermediate **I,** followed by alkyne insertion to generate the seven-membered rhodacycle intermediate **IIa** (path a), which

undergoes reductive elimination to provide cationic heterocyclic intermediate **IIIa** together with Rh(I) complex. Then, oxygen-atom transfer followed by oxidative addition occurs to generate intermediate **IV**. This intermediate might be alternatively generated from **I** through alkyne insertion at the *N*-oxide side of the Rh center (intermediate **IIb**). Intramolecular electrophilic attack of the imino moiety of **IV** furnishes intermediate **V**. Then transmetalation with Cu coupled with a β-H elimination gives **VI**, which generates the desired indole by eliminating one molecule of PhCHO. It should be noted that Cu does not serve as an oxidant in this reaction, as the N–O bond plays this role.

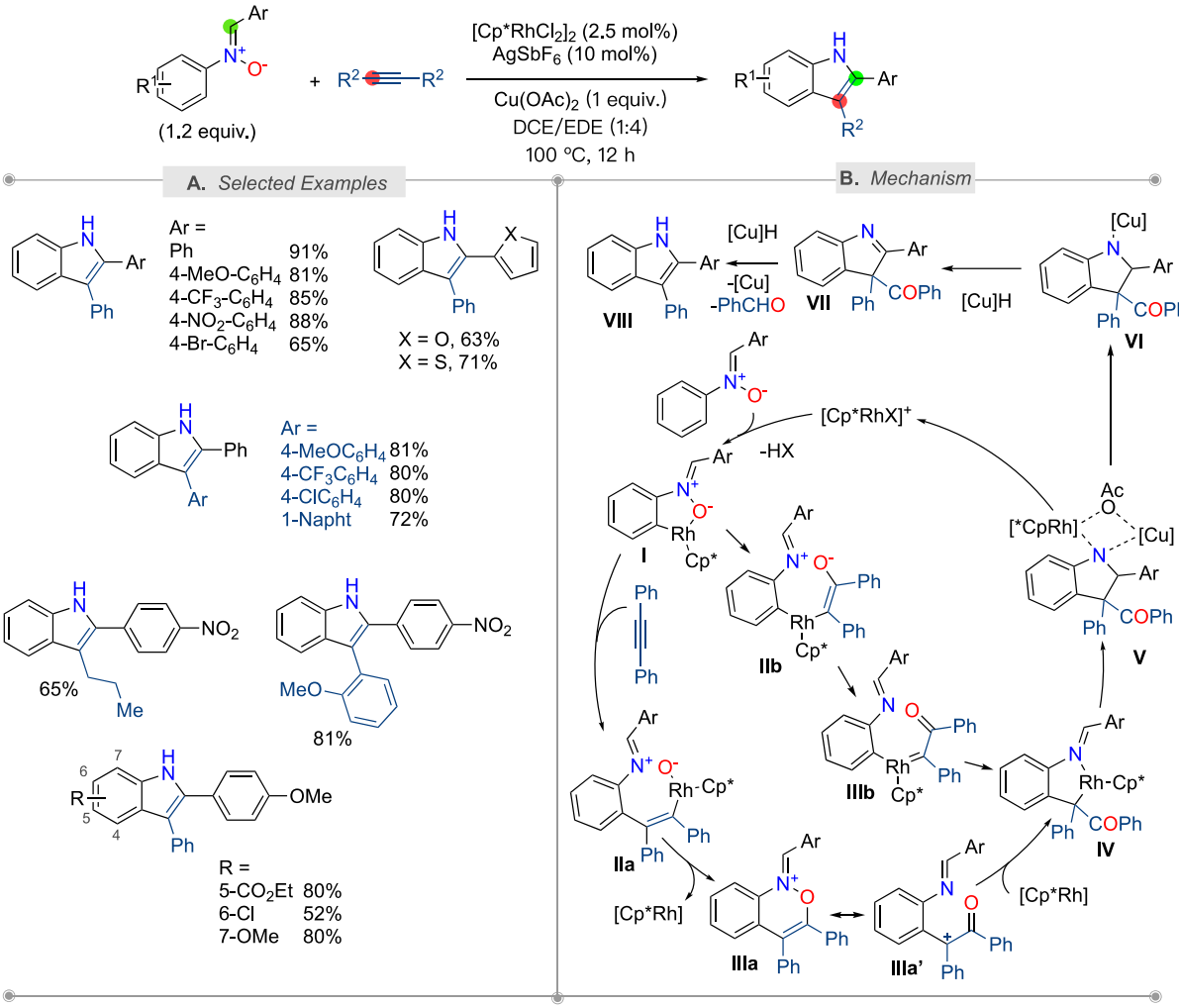

Scheme 1.14. Rh(III)-Catalyzed C–H Bond Annulation of Nitrones with Alkynes.

Interestingly, when sterically hindered nitrones were employed, the reaction also afforded 2,3-di-substituted indoles without C–C bond cleavage but through a different pathway, as shown by Liu, Lu, and co-workers (Scheme 1.15-B).[25] The conditions are slightly different, employing PivOH instead of $Cu(OAc)_2$ and a well-defined cationic Rh(III) complex. This change may induce a different pathway, especially for the final step, which is now the hydrolysis of **IV** to deliver the enolate intermediate **V**, which is in equilibrium with the keto intermediate **VI**.

Then, the second hydrolysis occurred with the liberation of mesitylaldehyde, followed by cyclization to afford the desired indole products. The scope of the reaction was similar to previously reported conditions. A mixture of regioisomers was obtained with unsymmetrical alkynes unless aryl-alkyl di-substituted alkynes were employed.

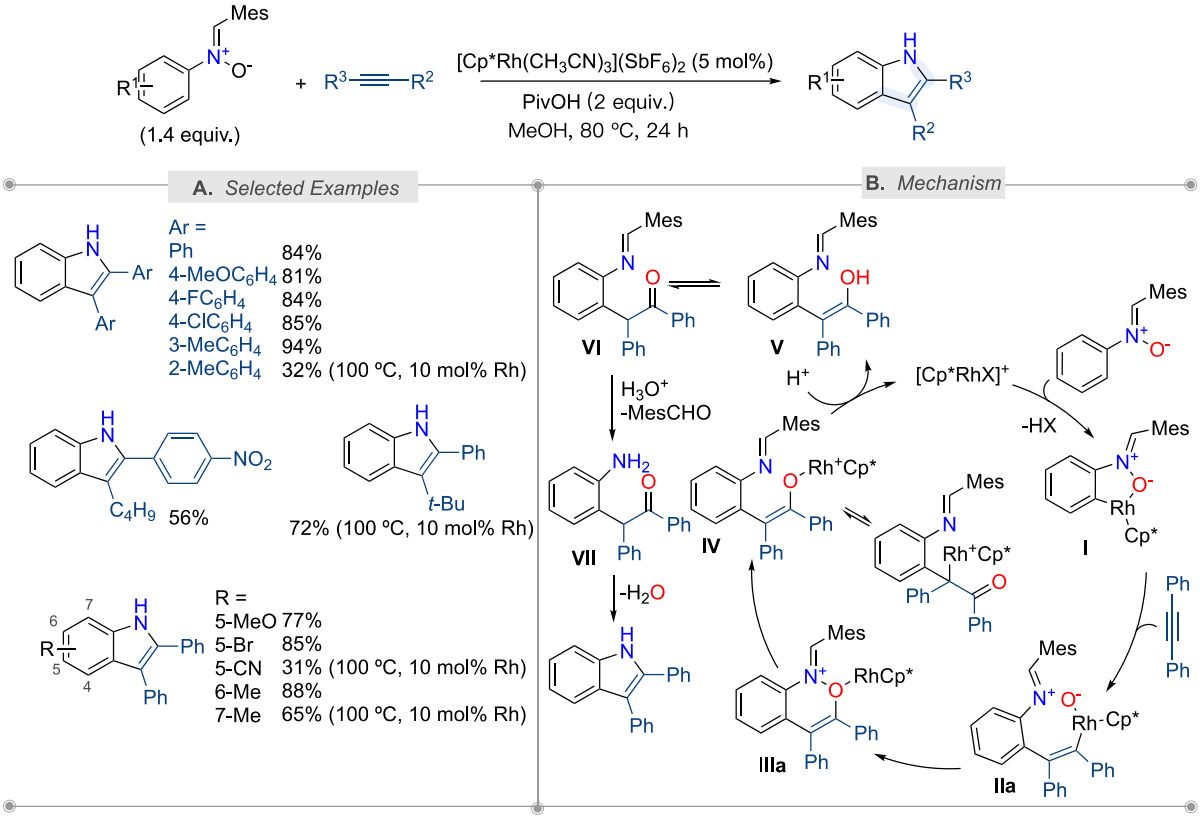

Scheme 1.15. Rh(III)-Catalyzed Redox-Neutral C–H Annulation of Arylnitrones with Alkynes for the Synthesis of Indole Derivatives.

Nitrones can also be annulated with diazo compounds to prepare indolyl scaffolds. Two conditions were published at almost the same time.[26] Although the same conditions were employed, namely, $[Cp^*RhCl_2]_2$ (5 mol%) associated with $AgSbF_6$ (16-20 mol%) in the presence of $Cu(OAc)_2$, two different products were obtained. In the first case, the reaction run in 1,4-dioxane at 100 °C gave *N*-hydroxyindole (Scheme 1.16, Conditions A),[26a] while in 1,2-dichloroethane (DCE) at 120 °C, the reduced indoles were obtained (Scheme 1.16, Conditions B).[26b] The scope of both reactions is relatively identical, tolerating electron-donating or electron-withdrawing groups. Both mechanisms start with the cyclometalation of nitrone to generate rhodacycle **I** through C−H bond activation. Then, *α*-acyldiazoacetate reacts with **I** to form a rhodium(III) carbene intermediate **II**. Migratory insertion of the Rh−C bond into the activated carbene generates the six-membered rhodacyclic intermediate **III**, in which an electrophilic attack of the imino moiety occurs to form the five-membered ring heterocycle

IV. Then transmetalation of the Rh catalyst with the copper salt and subsequent β-hydride elimination releases intermediate **VIIa** or **VIIb**. At last, with the elimination of one acetic acid unit, the desired products are obtained. The mechanism of final deoxygenation remains unclear, and the role of DCE as solvent and hydride provider[27] might be further explored in detail.

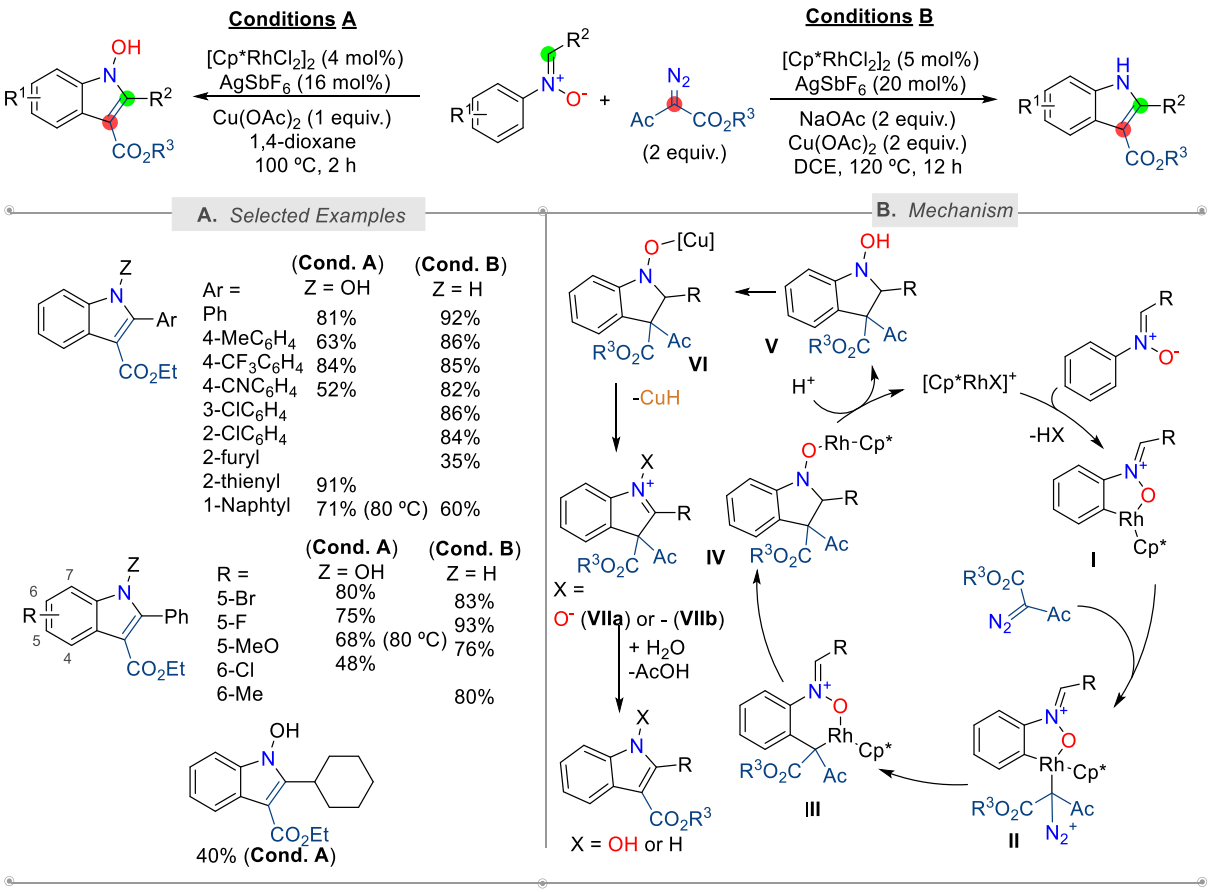

Scheme 1.16. Rh(III)-Catalyzed Redox-Neutral C–H Annulation of Arylnitrones with Diazo Compounds for the Synthesis of Indole Derivatives.

In 2016, Wang and co-workers reported an Rh(III)-catalyzed redox-free C–H bond annulation of aniline *N*-oxides with internal alkynes (Scheme 1.17).[28] The reaction conditions are regular for C–H bond activation catalyzed by Cp*Rh(III) catalyst, albeit no additional oxidant is required. Indeed, the N–O bond plays the role of directing group for the C–H bond cleavage and also of oxidant through an *O*-atom transfer. Excellent functional group tolerance was observed. After the classical formation of five-membered cyclometalated species **I** *via ortho*-C–H bond activation of aniline *N*-oxides, alkyne insertion into the Rh–C bond generates a seven-membered rhodacycle intermediate (**II**) (Path A). Then, reductive elimination of the C–O bond of **II** gives intermediates **III** or **IV** (tautomerization from **III** through OAT) with the release of Rh(I) catalyst. Then, oxidative addition affords enolate intermediates **V** or **VI**, and such

intermediates could react with aniline *N*-oxides to release **VII** and close the catalytic cycle. Finally, in the presence of silver(I), the C–N bond cleavage followed by intramolecular nucleophilic cyclization gives the final indole product. However, a catalytic cycle based on Rh(III)/Rh(V) was also proposed, in which the alkyne insertion into the Rh–O bond leads to intermediates **VIII**, **IX**, and **V** (Path B). At the same time, You and co-workers reported the same Rh(III)-catalyzed redox-free C–H bond annulation of aniline *N*-oxides with internal alkynes, albeit they employed a catalytic amount of Ag(I) salts.[29]

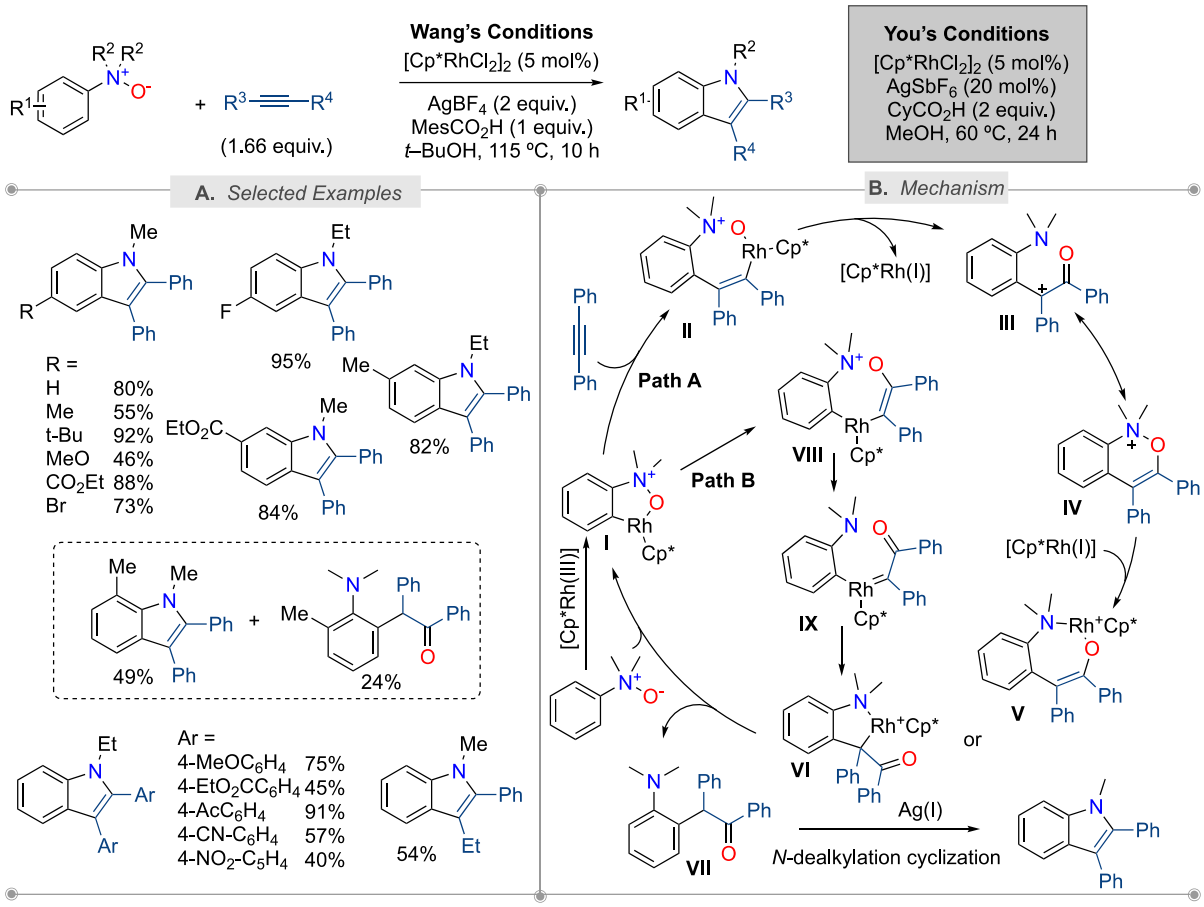

Scheme 1.17. Rh(III)-Catalyzed Redox-Neutral C–H Annulation of Aniline *N*-Oxides with Internal Alkynes.

In 2021, Anbarasan and co-workers developed Rh(III)-catalyzed redox-neutral annulation of *N*-acetoxyacetanilides with alkynes to synthesize substituted indole derivatives (Scheme 1.18).[30] The reaction conditions are straightforward as no additive is required, and only cationic Rh(III) complex in DCE was used. Substituted 2,3-diarylindoles holding a wide range of functional groups (alkyl, ether, ester, halo, formyl, acetamide, and amino) were prepared from various substituted *N*-acetoxyacetanilides and symmetrical/unsymmetrical alkynes in good to excellent yields. Even the intermolecular version has been investigated. Moreover,

they described a one-pot procedure from nitroarenes through a reduction carried out by Zn powder in the presence of Ac_2O. Based on deuterium/hydrogen exchange, competitive reactions, and stoichiometric experiments, the authors proposed the catalytic cycle depicted in Scheme 1.18-B. The reaction starts with the C–H bond cleavage and the formation of six-membered rhodacycle complex **I** *via* acyl oxygen-directed metalation of the *ortho* C–H bond. This complex was isolated. Then, insertion of the alkyne into the Rh–C bond delivers **II**, followed by a rearrangement of the eight-membered ring in intermediate **II** to produce intermediate **III**. Then, two pathways are possible. In Path A, a C–N bond formation through reductive elimination from **III** to ammonium ion **IV**, along with the formation of Cp*Rh(I), occurs. The Rh(I) undergoes oxidative addition and hydrolysis to give the indole and regenerate the active rhodium species. In Path B, oxidative addition of the N–O bond in **III** would result in Rh(V) specie **V**, which after reductive elimination would afford the product and regenerate the active catalyst.

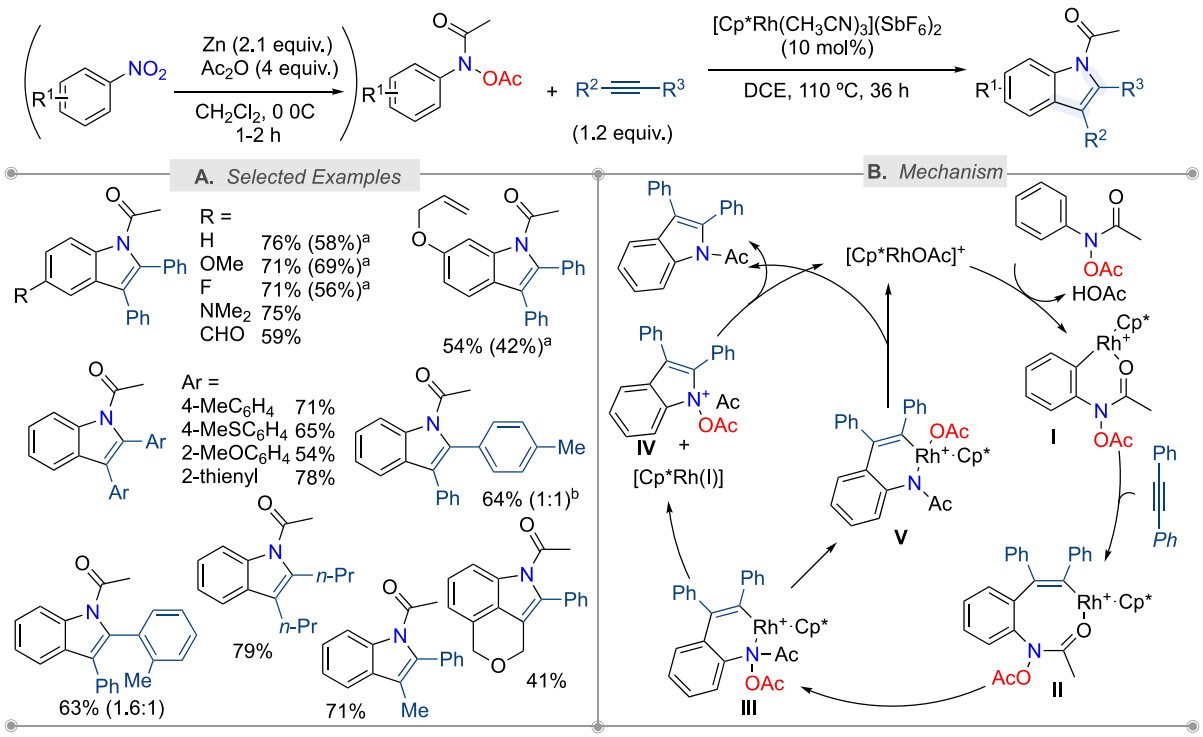

[a] From $ArNO_2$; [b] Regioselectivity and only major regioisomers are shown.

Scheme 1.18. Rh(III)-Catalyzed Annulation of *N*-Acetoxyacetanilide with Substituted Alkynes.

1.2.1.3 C–H Bond Functionalization Using Internal N–N Bond as Oxidant

In 2013, Glorius and co-workers offered a new method for synthesizing unprotected indoles from 2-acetyl-1-arylhydrazines and alkynes through rhodium(III)-catalyzed redox-neutral C–H bond annulation (Scheme 1.19).[31] This work represents an early example of the use of the N–

N bond as an internal oxidant for the regeneration of catalysts in C–H bond functionalization. The optimized conditions, 2.5 mol% of $[Cp^*RhCl_2]_2$ associated with 25 mol% of CsOAc in the presence of 1.2 equivalents of AcOH, allowed the formation of diversely substituted indoles in high yields from well-decorated acetyl-1-arylhydrazine partners (*e.g.*, F, Cl, Br, I, CN, OCF_3, or CO_2Me) and symmetrical diaryl, or dialkyl internal alkynes. Moreover, reactions with alkyl phenyl acetylenes proceeded with complete regioselectivity. From mechanistic investigation, notably using [^{15}N]-2-acetyl-1-phenylhydrazine, the authors proposed the catalytic cycle depicted in Scheme 1.19-B. Like other reactions, the reaction starts with an *ortho*-directed C–H bond metalation followed by alkyne insertion to afford the seven-membered rhodacycle **I**. This metallacycle rearranges to a more stable six-membered rhodium complex **II,** which might undergo a reductive elimination, protonation, and oxidative addition to break the N–N bond with the aid of acetic acid to form intermediate **III**, which is finally protonated by acetic acid to yield the desired indole and regenerate the catalyst (path a). Alternatively, the authors proposed that **II** could lead to a cyclic Rh(V)-nitrene intermediate **V** by acylamino migration, and **V** could easily undergo reductive elimination to form the desired heterocycle and regenerate the Rh(III) catalyst (path b). DFT calculation performed by Lin and co-workers also evoked an Rh(V)/Rh(III) scenario for this transformation.[32]

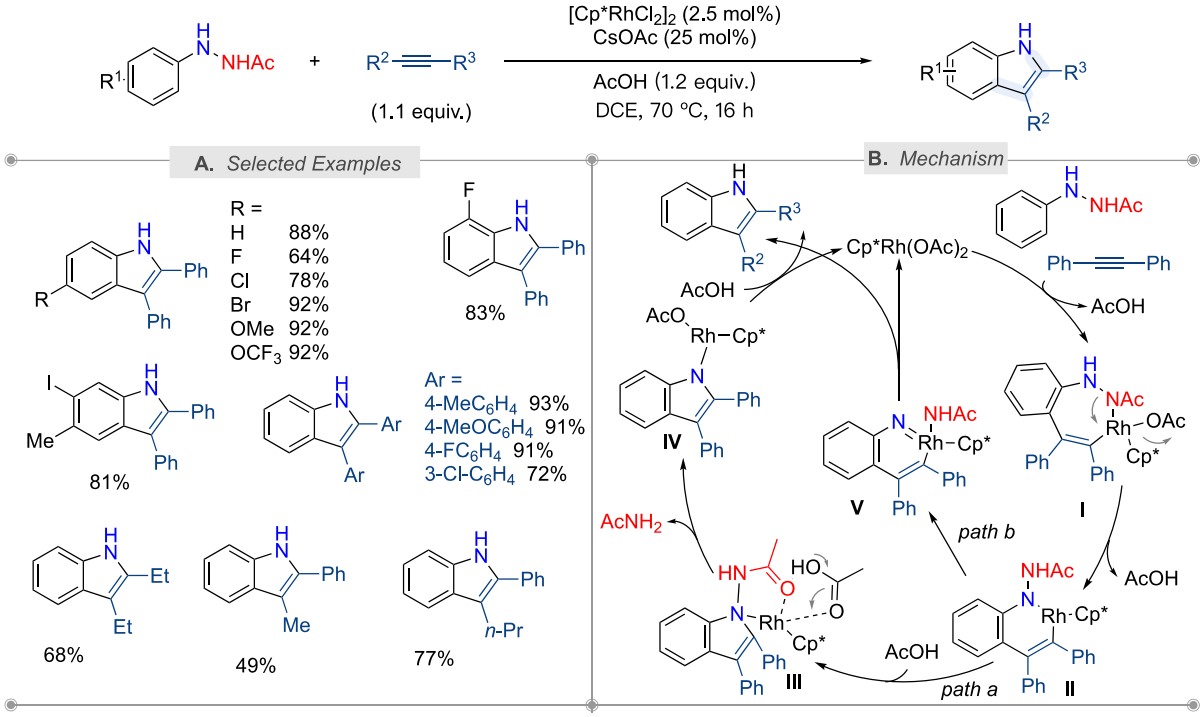

Scheme 1.19. Rhodium(III)-Catalyzed Hydrazine-Directed C–H Activation: Redox-Neutral and Traceless by N–N Bond Cleavage.

C–H Bond annulation of 2-acetyl-1-arylhydrazines was not limited to the use of internal alkynes as annulative reagents, as Wang and co-workers reported the use of diazo compounds for preparing 1-aminoindoles (Scheme 1.20).[33] However, in this case, no oxidant was required, therefore, the N–N bond is not cleaved. The reaction was run in water using 2.5 mol% of $[Cp^*RhCl_2]_2$ associated with 25 mol% of CsOAc in the presence of 0.5 equivalents of AcOH. Like the previous methodologies, a broad tolerance to functional groups was observed, including halogen atoms, cyano, and ester groups. $[Cp^*Rh(OAc)_2]$ is proposed to be the active catalyst undergoing C–H bond cleavage followed by generation of Rh(III)-carbene **II**. Subsequently, migratory insertion of the carbene into the Rh–C bond might deliver rhodacyclic intermediate **III**, which is protonated by acetic acid to release **IV** and Rh(III). Then, intramolecular condensation with the elimination of water affords the indolyl scaffold.

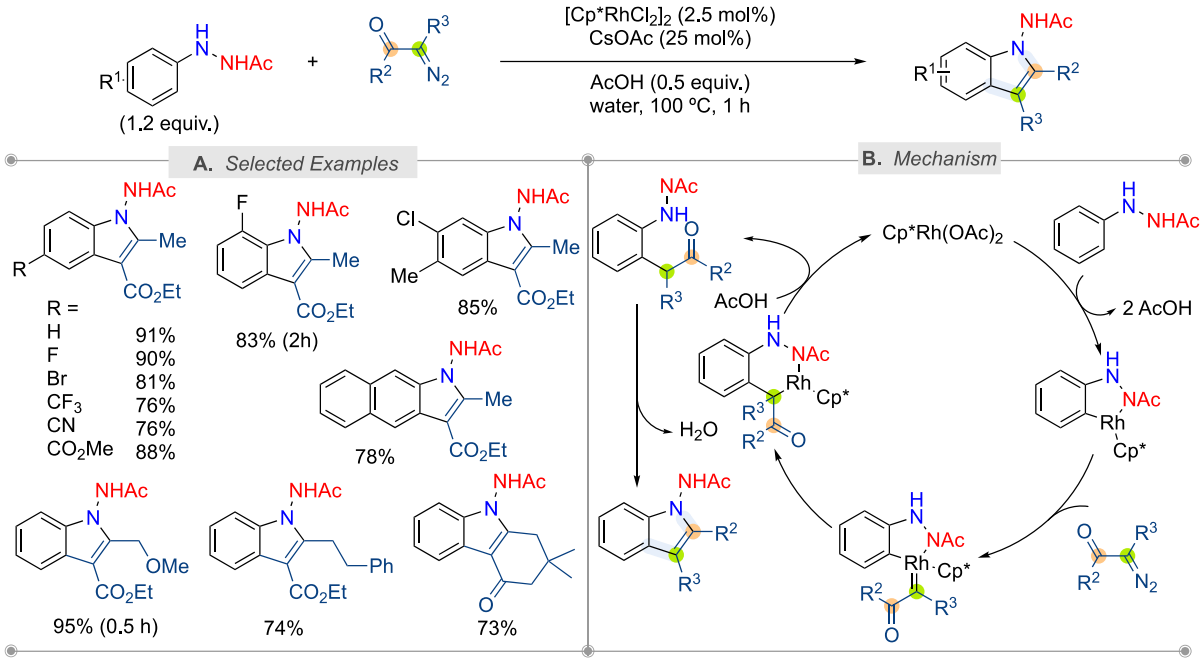

Scheme 1.20. Rhodium(III)-Catalyzed Synthesis of 1-Aminoindoles from 2-Acetyl-1-arylhydrazines and Diazo Compounds.

In 2013, Zhu and co-workers also reported the synthesis of indoles through C–H bond annulation using the N–N bond as an internal oxidant, albeit from *N*-nitrosoanilines (Scheme 1.21).[34] They developed two sets of conditions (acid and basic) to ensure a broad functional group tolerance. In contrast to acid conditions, the basic ones are compatible with *N*-nitrosoaniline holding an electron-withdrawing cyano group at the *para*-position, and the reaction is regioselective with *meta*-substituted (Me) electron-rich *N*-nitrosoaniline derivative. A few months later, an additive-free version was reported by Huang and co-workers using 8 mol% $Cp^*Rh(OAc)_2$ in MeOH at 90 °C.[35] Comprehensive mechanistic studies

by Zhu,[34] under acidic conditions, support $[RhCp^*]^{2+}$ as catalyst resting state (switchable to $[RhCp^*(OOCt\text{-}Bu)]^+$ under specific circumstances) and C–H activation as the turnover-limiting step. The key step is the regeneration of the catalyst from alkenylrhodium intermediate **VI**, which occurred by internal oxidation through H^+-promoted concerted N–N bond cleavage – C–N bond formation with the concomitant abstraction of NO^-, later decomposed into detectable NO_2 and H_2O.

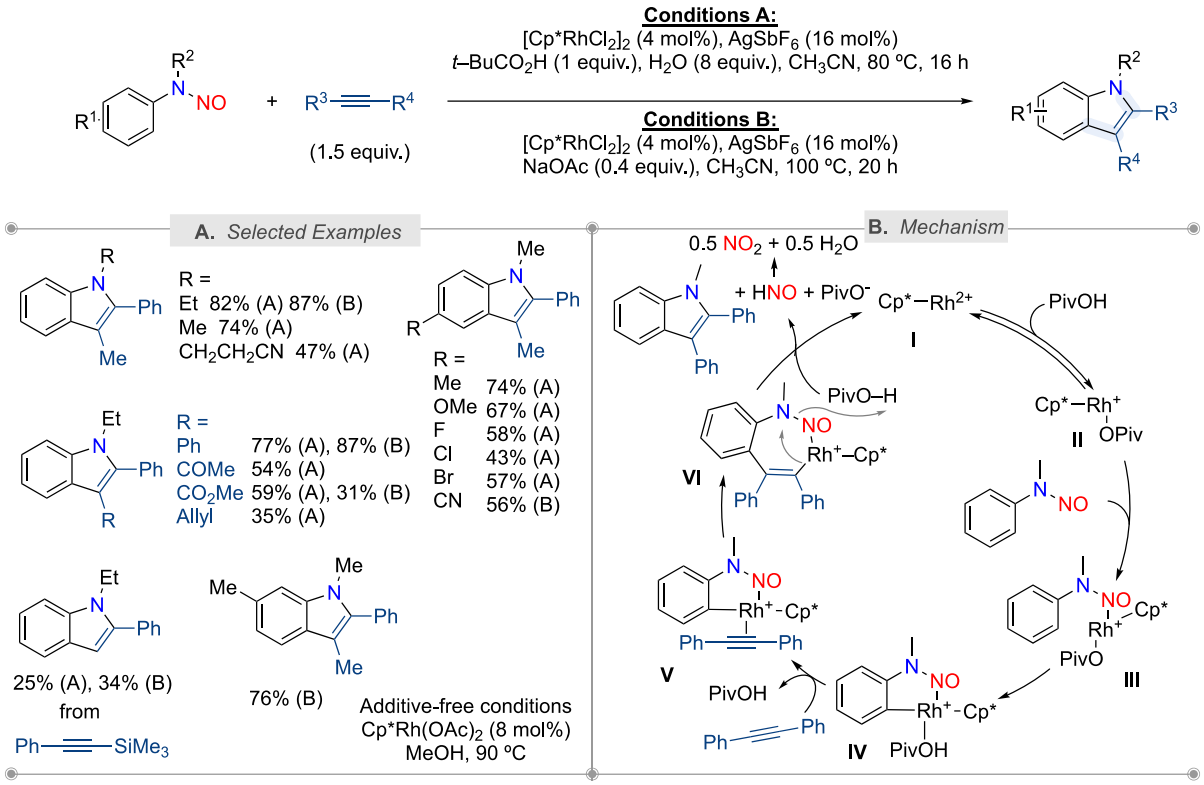

Scheme 1.21. Rhodium(III)-Catalyzed Indole Synthesis from *N*-Nitrosoanilines using N–N Bond as an Internal Oxidant.

This C–H bond annulation reaction was later extended to synthesize 2-alkenylindoles and 2-alkenylindole-3-carboxylates using propargyl alcohols instead of internal alkynes as annulative reagents (Scheme 1.22).[36] After C–H bond annulation, dehydration of the tertiary alcohol occurred, leading to the formation of the vinyl substituents. However, this transformation required the use of AgOAc or $Cu(OAc)_2$, therefore, the authors could not completely rule out an external oxidation process. Post-functionalizations of such building blocks have allowed the preparation of various polycycles such as 2-acylindole, benzocarbazole, indoloquinoline, pyridoindolone, cyclopentaindolone, and indenoindolone.

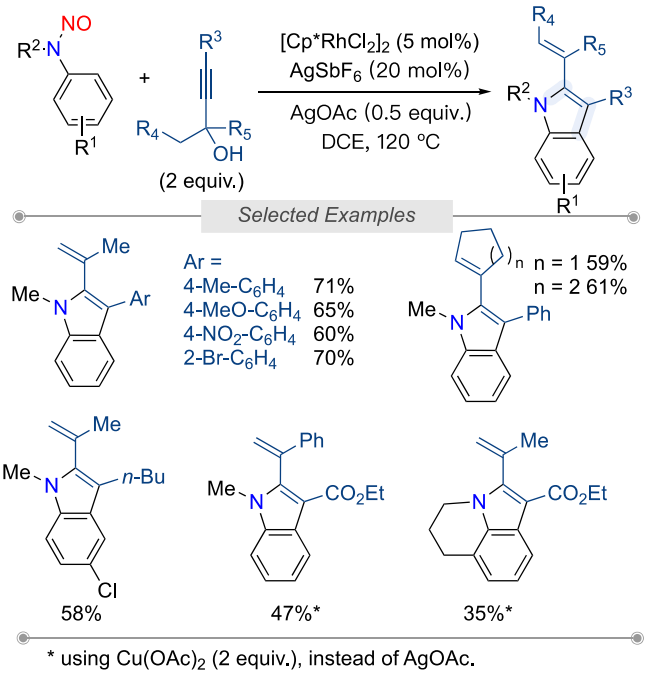

Scheme 1.22. Rhodium(III)-Catalyzed Synthesis of 2-Alkenylindoles and 2-Alkenylindole-3-carboxylates from *N*-Nitrosoanilines and Propargyl Alcohols using N−N Bond as an Internal Oxidant.

In 2020, Messaoudi and co-workers employed this *N*-nitrosoanilines C–H bond annulation approach with alkynes for preparing 2,3-substituted *β*-*N*-glycosyl indoles (Scheme 1.23).[37] They prepared various *β*-*N*-nitrosophenyl glucopyranoside derivatives before subjecting them to C–H bond annulation in the presence of 5 mol% $[Cp^*RhCl_2]_2$ in conjunction with $AgSbF_6$ (20 mol%) in DCE at 90 °C. Various 2,3-disubstituted *N*-glycosyl indoles were prepared in moderate to good yields depending on the substitution of both partners. Interestingly, the reaction was also applied to prepare bioactive compounds.

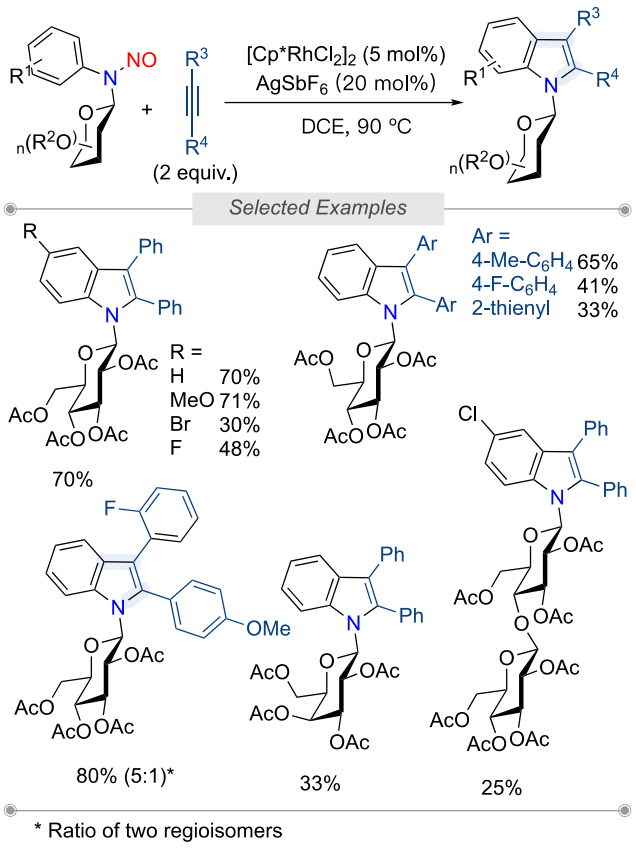

Scheme 1.23. Rhodium(III)-Catalyzed Synthesis of 2,3-Substituted *β*-*N*-Glycosyl Indoles from *N*-Nitrosoanilines using N–N Bond as an Internal Oxidant

In 2014, Matsuda and co-workers succeeded the C–H bond annulation of alkylidenehydrazine, in which the N–N bond also acts as an internal oxidant by releasing isobutyronitrile (Scheme 1.24-A).[38] Surprisingly, these conditions still employed $Cu(OAc)_2$ as an oxidant, but the authors did not indicate the results in the absence of copper salts. In the meantime, Huan and co-workers reported the same transformation but with the *in-situ* formation of alkylidene from *N*-arylhydrazines and isobutyraldehyde (Scheme 1.24-B).[39] The authors called this strategy auto-formed and auto-cleavable directing group. This time, no external oxidant was required, and the reaction scope was quite general. They proposed the mechanism depicted in Scheme 1.24-C. First, hydrazone was rapidly formed *in-situ* from hydrazine and *i*-PrCHO, with the release of 1 equivalent of HOAc. Then, cyclometalation followed by alkyne insertion affords a seven-membered rhodacycle **II**, which rearranges to a more stable six-membered rhodacycle **III**. Reductive elimination of **III** gives **IV**, and H^+-promoted N–N cleavage generates **V**. Protonation of **V** delivers the indole product and regenerates the Rh(III) catalyst. They also proposed an alternative mechanism in which the N–N cleavage occurs in **III** to afford Rh(V) nitrene intermediate **V**, which could undergo reductive elimination to form the indole product.

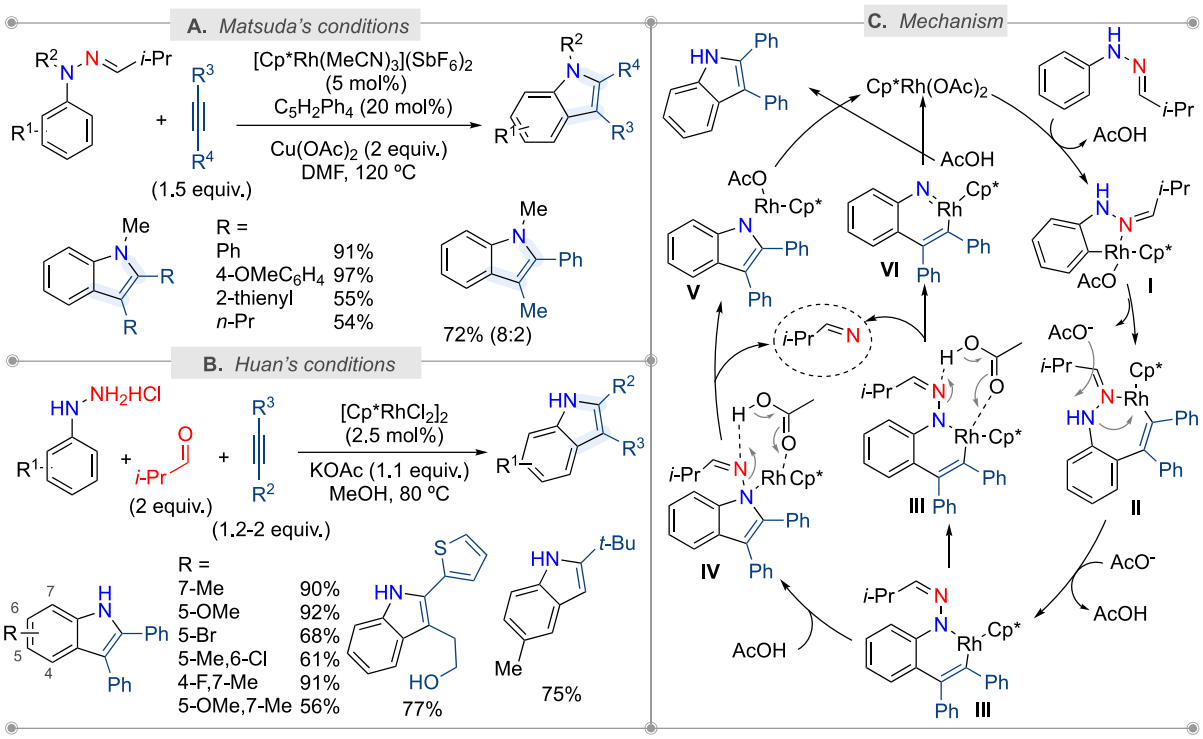

Scheme 1.24. Rhodium(III)-Catalyzed Synthesis of Indoles from 1-Alkylidene-2-arylhydrazines and Alkynes *via* C–H and N–N Bond Cleavages.

1.2.1.4 C–H Bond Functionalization Under Reductive Conditions

In 2020, Patureau and co-workers prepared indoles from nitroarenes and alkynes *via* Rh(III)-catalyzed C–H bond annulation using zinc metal to reduce *in-situ* NO_2 into NH functions (Scheme 1.25).[40] This method from nitroarenes as abundant feedstocks by-passes the reduction steps required to prepare *N*-functionalized anilines, commonly used in Rh(III)-catalyzed C–H bond annulation. Using $[Cp^*RhCl_2]_2$ in the presence of elemental zinc in conjunction with TMSCl as a reductant system, they achieved the C–H bond annulation of diversely substituted nitroarenes with symmetrical alkynes. The authors did not report a reaction pathway, but they showed some control experiments with a different intermediate that can be obtained from the reduction of nitroarenes. They conclude that the C–H bond annulation event did not proceed from anilines, 1,2-diphenylhydrazine, and trace amounts with azobenzene, while slightly better yield was observed with nitrosobenzene (14%) or *N*-phenylhydroxylamine (5%) opening the way for multiple intermediates.

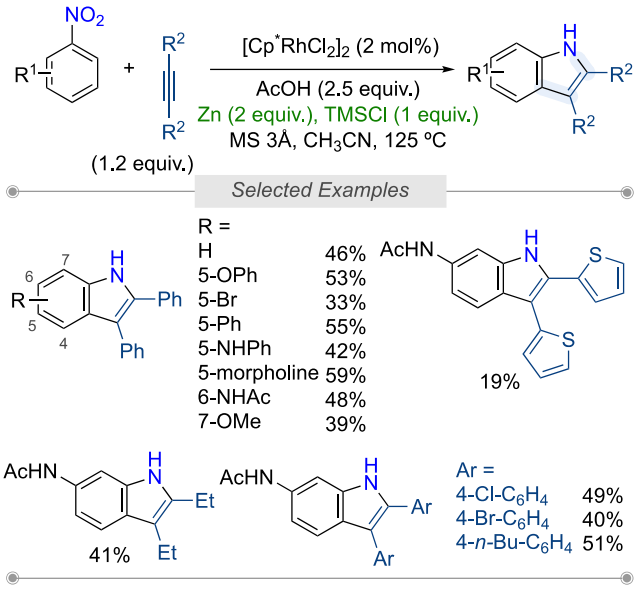

Scheme 1.25. Rh(III)-Catalyzed C–H Bond Annulation of Nitroarenes with Alkynes.

1.2.2. Preparation of Pyrrole Scaffolds

1.2.2.1 C–H Bond Functionalization Under Oxidative Conditions

In 2010, during their investigations on Rh(III)-catalyzed C–H bond annulation reaction of acetanilides for the preparation of indoles (Scheme 1.1-B),[8] Fagnou and co-workers also explored the extension of this method to vinylic C–H bond functionalization in the context of a pyrrole synthesis (Scheme 1.26).[8] The reaction is quite general, with different substituted enamines and internal alkynes. The reaction can also be performed at room temperature, provided it was run in acetone.

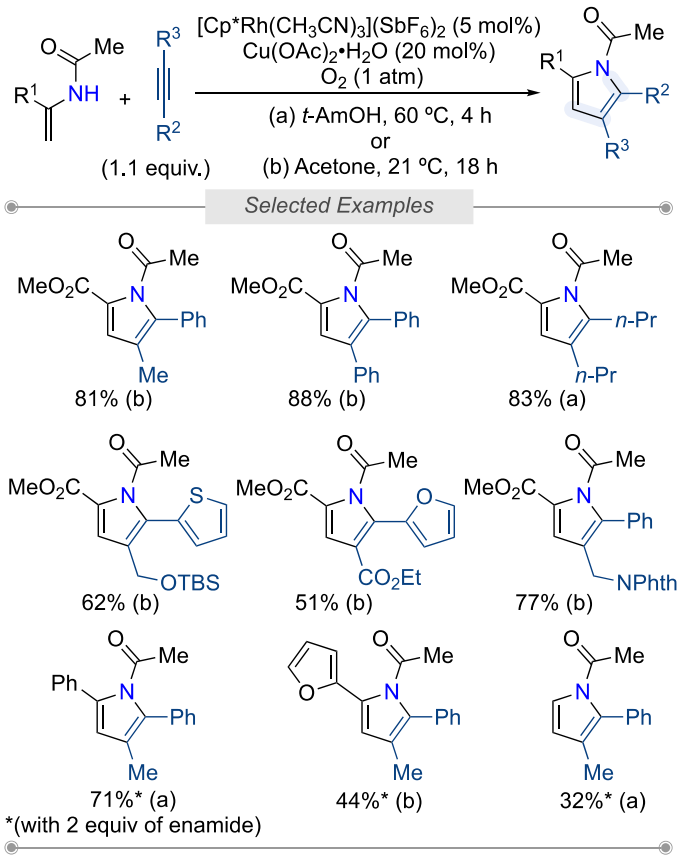

Scheme 1.26. Pyrrole Synthesis *via* Rhodium(III)-Catalyzed Oxidative Coupling of Enamides and Internal Alkynes.

During their investigations on indole synthesis from *N*-arylurea and enynes (Scheme 1.3),[11] Huestis and co-workers also extended this enyne chemistry to the synthesis of 2-alkenyl pyrroles using an enamide coupling partner (Scheme 1.27).[11] The reaction was accomplished at room temperature in cyclohexanone using NHAc as directing group. Consistent with the indole chemistry, triphenylmethyl and *tert*-butyldimethylsilylethers were well tolerated on the enyne coupling partners. TMS-functionalized enynes were also employed to deliver C3-TMS-substituted pyrrole building blocks. Pyrroles having a styryl or *N*-vinylacetamide substituent at the C2 position were also prepared.

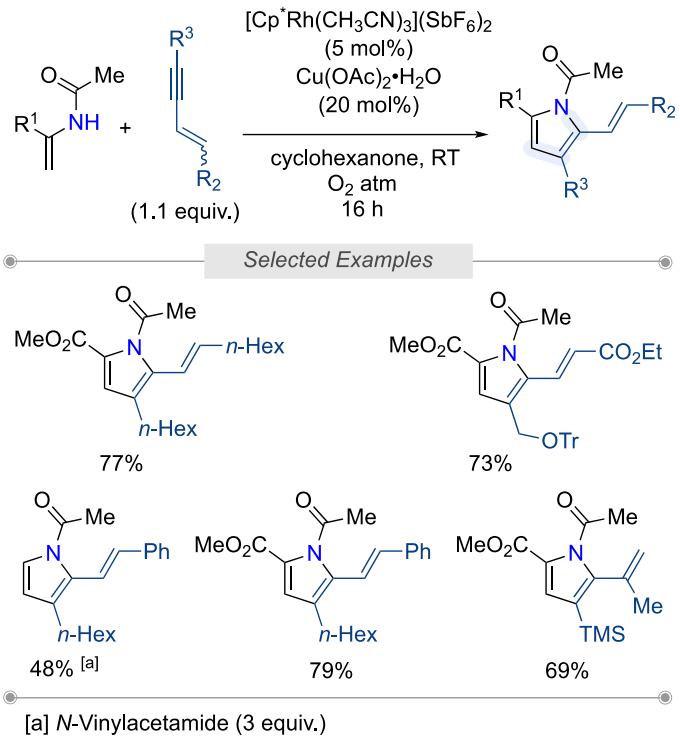

Scheme 1.27. Pyrrole Synthesis *via* Rhodium(III)-Catalyzed Oxidative Coupling of Enamides and Enynes.

Tanaka and co-workers have shown that electron-deficient $[Cp^{E}RhCl_2]_2$ outperformed commercially available $[Cp^{*}RhCl_2]_2$ in the synthesis of pyrrole through rhodium(III)-catalyzed oxidative coupling of enamides and internal alkynes at room temperature (Scheme 1.28).[14]

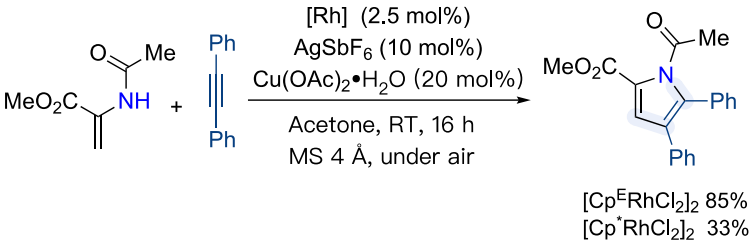

Scheme 1.28. Effect of the Catalysts in Rhodium(III)-Catalyzed Oxidative Coupling of Enamides and Internal Alkynes.

1.2.3. Preparation of Indoline Scaffolds

1.2.3.1 Oxidative Couplings Using External Oxidant

In 2018, Mascareñas, Gulías, and co-workers prepared indolinyl scaffolds by C–H bond annulation of 2-alkenyl anilides with alkynes using electron-deficient $[Cp^{E}RhCl_2]_2$ (3 mol%) associated with 0.25 equivalents of $Cu(OAc)_2$ in toluene (Scheme 1.29).[41] The presence of oxygen plays the role of terminal oxidant in this reaction. The use of an electron-deficient

catalyst is essential for the outcome of the reaction, as $[Cp^*RhCl_2]_2$ catalyzes this transformation in only 16% yield. Moreover, the choice of the group at the nitrogen atom (R) is also an essential factor as other tested groups than Ns give lower yields (R = Tf 40%, or Ts 25%) or no reaction (R = H, Ac). The optimized conditions tolerate various functional groups on the 2-alkenyl anilides partners. Moreover, symmetrical alkynes with electron-rich or electron-poor aromatic substituents have been employed as annulative reagents. In the case of non-symmetrical alkynes, the regioselectivity of the transformation was very high in favor of products with the aryl substituent at the terminal position of the alkene. The reaction is not limited to *ortho*-propenylanilides, as the authors reported one example with but-1-en-2-yl substituent, but the corresponding indoline product was obtained as a mixture of *Z* and *E* isomers in a 1.7:1 ratio. A catalytic cycle using rhodium acetate complexes as active catalysts has been proposed. The activation of an olefinic C–H bond gives rhodacycle **I**, followed by carbometalation to generate **II**, and a 1,5-hydrogen shift to generate the key π-allyl intermediate **III**, which evolves by reductive elimination to form the corresponding indoline product. The resulting Rh(I) complex is then reoxidized to Rh(III) by the Cu(II) salt and air. The authors also proposed an alternative pathway for forming **III** from **V** through 1,3-rhodium migration.

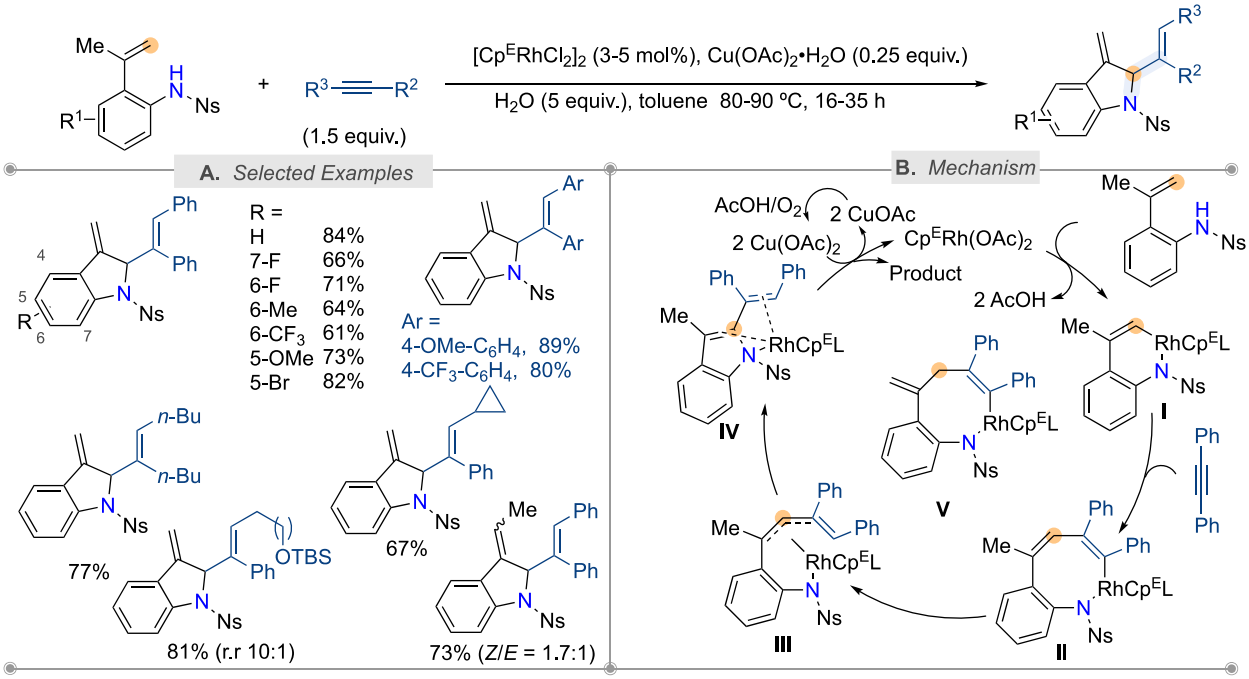

Scheme 1.29. Rhodium(III)-Catalyzed C–H Bond Annulation of 2-Alkenyl Anilides with Alkynes to Access 2-Substituted Indolines.

In 2021, Chatani and co-workers showed that aniline derivatives that contain a pyrimidine directing group reacted with vinylsilanes using $[Cp^*RhCl_2]_2$ to form C3-substituted indolines (Scheme 1.30).[42] The reaction proceeds *via* C–H bond alkylation – internal amination cascade reaction. Aniline derivatives holding electron-donating or electron-withdrawing groups at the *ortho*-position, including the highly bulky *tert*-butyl group, afforded the expected indoline products. The reaction showed high functional group compatibility, including substituents such as OMe, F, Cl, Br, CF_3, and NO_2 groups. Alkyl- and phenyl-substituted vinylsilanes can be used for this transformation, while reactions with siloxy-substituted vinylsilane gave a mixture of the indoline product with the linear alkenylated product. Based on a deep mechanistic investigation, the authors built the catalytic cycle depicted in Scheme 1.30-B. The catalyst **I** is generated from $[Cp^*RhCl_2]_2$ in the presence of $AgSbF_6$, Ag_2CO_3, and aniline through the directed *ortho*-rhodation. The coordination of an alkene to the rhodium complex **I,** followed by the migratory insertion of an alkene into an Rh–C bond, generates the eight-membered rhodium complex **II**. The insertion of an alkene into the Rh–C bond is governed by steric repulsion between the Cp*Rh moiety and SiR_3 group. A subsequent 1,3-Rh migration with the elimination of $HSbF_6$ forms the six-membered complex **III**, which undergoes reductive elimination to form the indoline with the regeneration of the active complex **I** in the presence of aniline, $AgSbF_6$, and Ag_2CO_3.

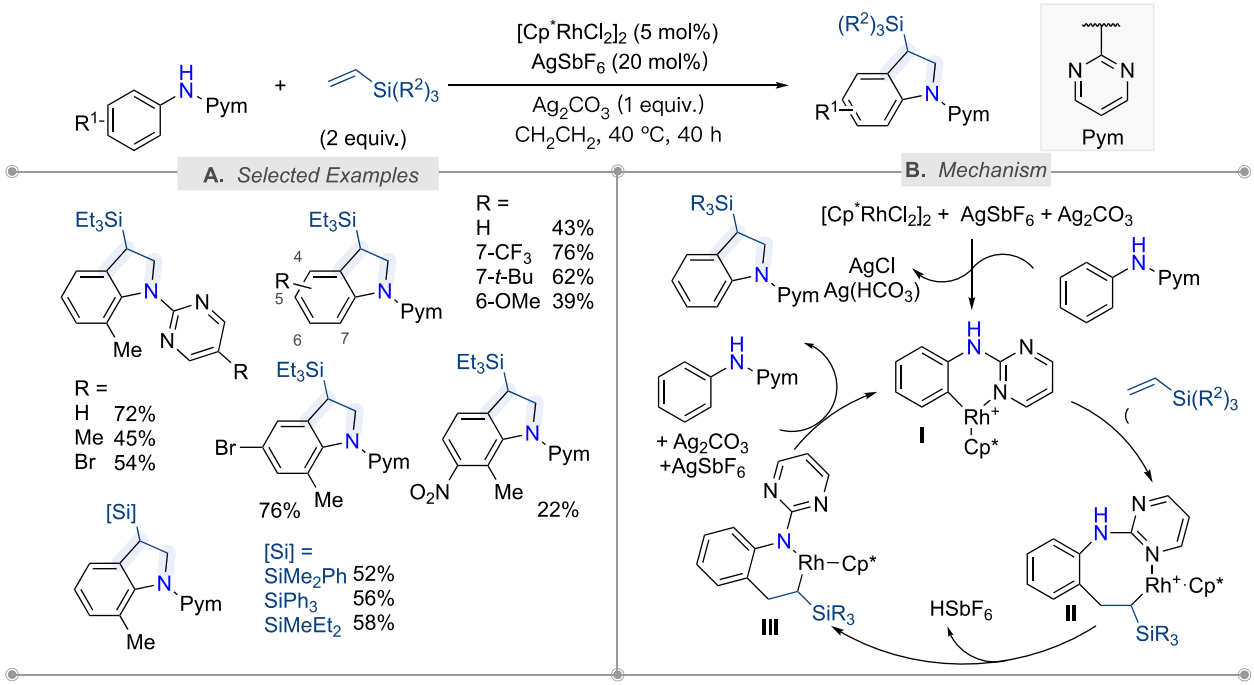

Scheme 1.30. Rhodium(III)-Catalyzed [3 + 2] Annulation of Aniline Derivatives with Vinylsilanes.

1.2.3.2 Redox-neutral Conditions

In 2015, Glorius and and-workers reported the synthesis of 1-aminoindolines from arylsubstituted diazenecarboxylates and alkenes through the concomitant C–H bond alkylation and *N*-alkylation reaction (Scheme 1.31).[43] The conditions are mild, as the reaction could be performed at room temperature in the presence of $[Cp^*RhCl_2]_2$ (2.5 mol%) and AgOAc (10 mol%) in a mixture of HOAc and DCE (1:3). A variety of important functional groups such as halogens (F, Cl, and Br), ester, and methoxy groups on the aryl-substituted diazenecarboxylates were well tolerated. Different alkenes such as acrylates, acrylamides, acrylonitriles, styrenes, and alkyl alkenes have been employed in this reaction delivering the 2-substituted 1-aminoindoline products in good to high yields. Based on a set of mechanistically insightful experiments, the authors proposed that $[Cp^*Rh(OAc)_2]$ is the active catalyst. After cyclometalation of arylsubstituted diazenecarboxylates followed by alkene insertion into the Rh–C bond, the seven-membered ring rhodacycle **I** rearranges to the more stable six-membered coordinately saturated Rh species **II.** Complex **II** undergoes a nucleophilic addition to the N=N bond to form intermediate **III**, which is finally protonated by HOAc to yield the desired 1-aminoindoline.

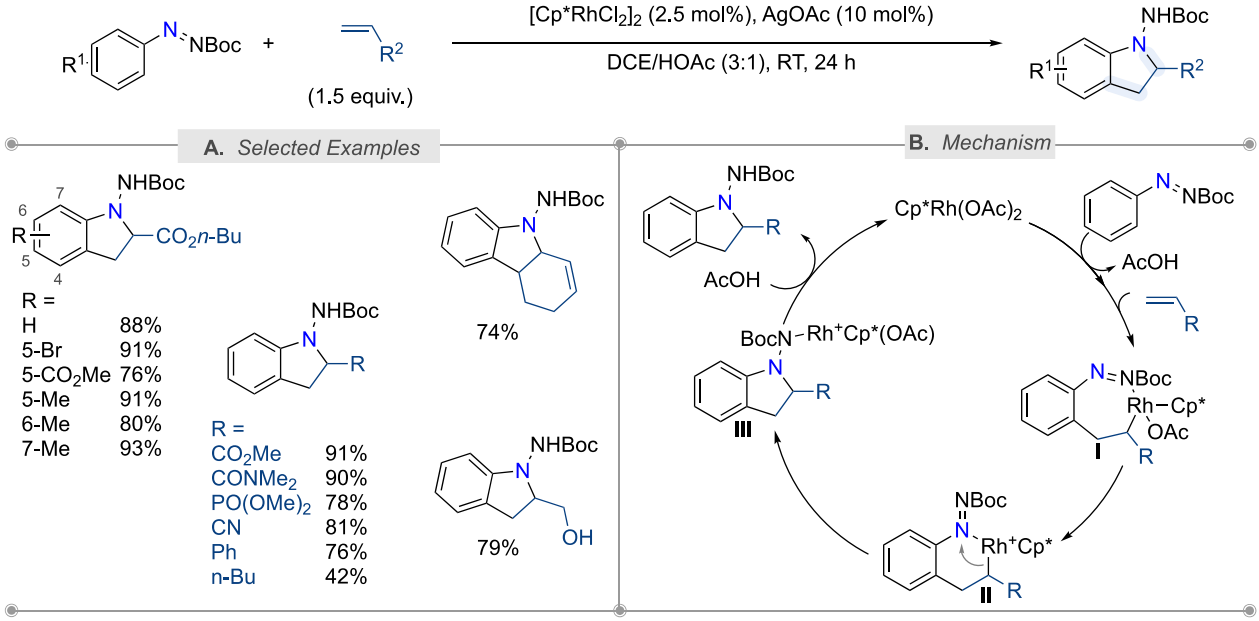

Scheme 1.31. Rhodium(III)-Catalyzed Cyclative Capture Approach to Diverse 1-Aminoindoline Derivatives at Room Temperature.

Indoline scaffolds can also be built from nitrone and diazomalonate via Rh(III)-catalyzed C–H bond annulation, as demonstrated by Zhou and co-workers (Scheme 1.32).[44] In the presence of an acid, the reaction proceeds through the first rhodium(III)-catalyzed chelation-assisted

(N–O) insertion of aromatic C(sp^2)–H bonds into diazo compounds, followed by direct intramolecular nucleophilic attack of the C(sp^3)–Rh intermediate on the C=N bond to afford the corresponding *N*-hydroxyindoline compounds (Scheme 1.32, left). Interestingly, over-oxidation occulted in the presence of a base (AgOAc), delivering the 3-indole-*N*-oxide derivatives (Scheme 1.32, right).

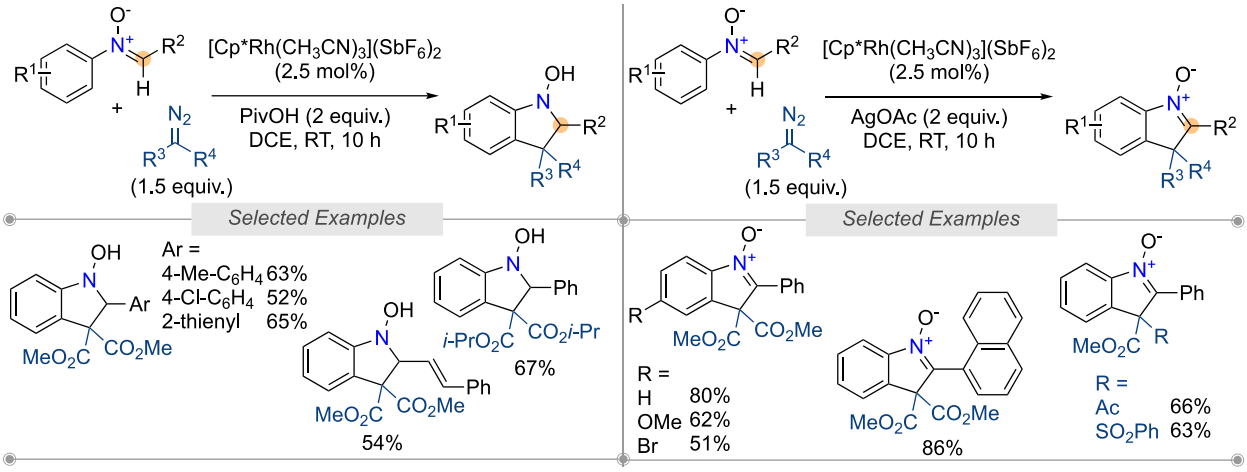

Scheme 1.32. Rhodium(III)-Catalyzed C–H Bond Annulation of Nitrones with Diazomalonates.

1.2.3.3 By Merging O-Atom Transfer

In 2015, Chang and co-workers reported the first example of Rh(III)-catalyzed coupling reaction of arylnitrones with internal alkynes under external oxidant-free conditions (Scheme 1.33).[45] They proposed a dual role of the rhodium catalyst: *i)* C–H bond activation/functionalization and *ii) O*-atom transfer process. The cyclization proceeds smoothly under mild conditions giving rise to indoline products in good yields together with moderate to high diastereoselectivity with an excellent functional group tolerance (*e.g.,* Me, OCF_3, F, Cl, Br). Li and co-workers later reported the same reaction and almost the same conditions (EtOAc instead of 1,4-dioxane).[46] Most indoline products were obtained as a mixture of diastereoisomers, and the major isomer has two phenyl groups at the C2 and C3 positions of a newly generated five-membered ring in an *anti*-relationship. The authors proposed the mechanism depicted in Scheme 1.-B. After the classical formation of rhodacycle **I** *via* a CMD process and alkyne insertion into the Rh–C bond, the alkenyl intermediate **II** is formed. Then, a subsequent *O*-atom transfer (OAT) might occur in two pathways: (i) cleavage of the N−O bond to form an Rh(V) oxo species that undergo the reductive elimination to afford an Rh(III)-enolate (IV) or (ii) reductive elimination of **II** to form a benzoxazine and Rh(I) followed by oxidation of Rh(I) to Rh(III) *via* N−O cleavage leading to **IV**. A rearrangement of rhodium enolate (IV) and then cyclization proceeds *via* **III**.

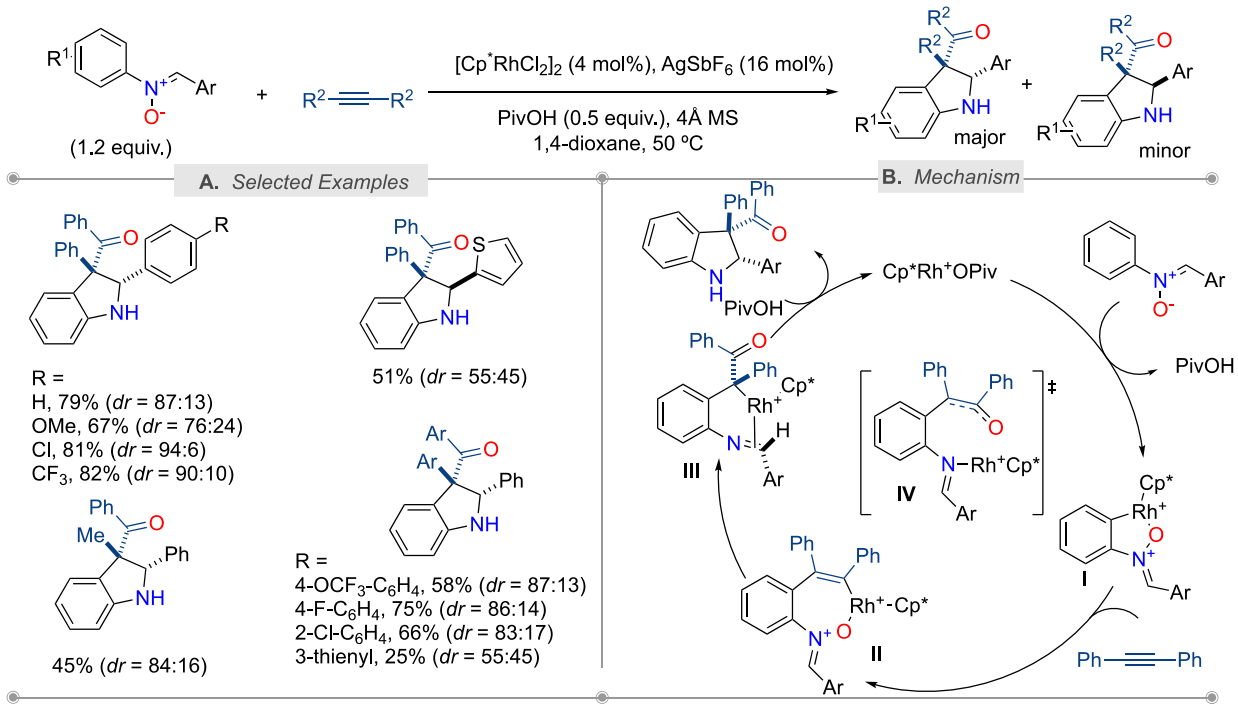

Scheme 1.33. Rhodium(III)-Catalyzed C–H Bond Annulation of Arylnitrones to Indolines under External Oxidant-Free Conditions.

In the same year, Zhou, Yang, Zhu, and co-workers described the C–H bond annulation of arylamine *N*-oxides with diazo compounds, in which an *O*-atom transfer acts as an internal oxidant (Scheme 1.34).[47] Various 1H-benzo[*g*]indolines were prepared in good yields whatever the substituent on the *N*,*N*-dimethyl-1-naphthylamine *N*-oxides (*e.g.,* Me, MeO, F, Br, CO_2Me). Primary C(sp^3)–H bonds and secondary C(sp^3)–H bonds have been annulated to provide the tetracyclic products. The N–O bond acts as a directing group to allow the formation of complex **I** from [Cp*Rh($OAc)_2$] and *N*,*N*-dimethyl-1-naphthylamine *N*-oxides. Then, coordination of the diazo substrate, followed by denitrogenation and Rh–aryl migratory insertion, affords **II.** Then, with the assistance of acetate, **II** undergoes a methyl C(sp^3)–H activation to give a more stable complex **III** with a new C–Rh bond formed. Subsequent C–C reductive elimination of **III** delivers the rhodium(I) complex **IV**. Finally, rhodium(I) oxidation with *N*-oxide irreversibly gives the indoline product. The authors also proposed an alternative pathway *via* an Rh-iminium intermediate.

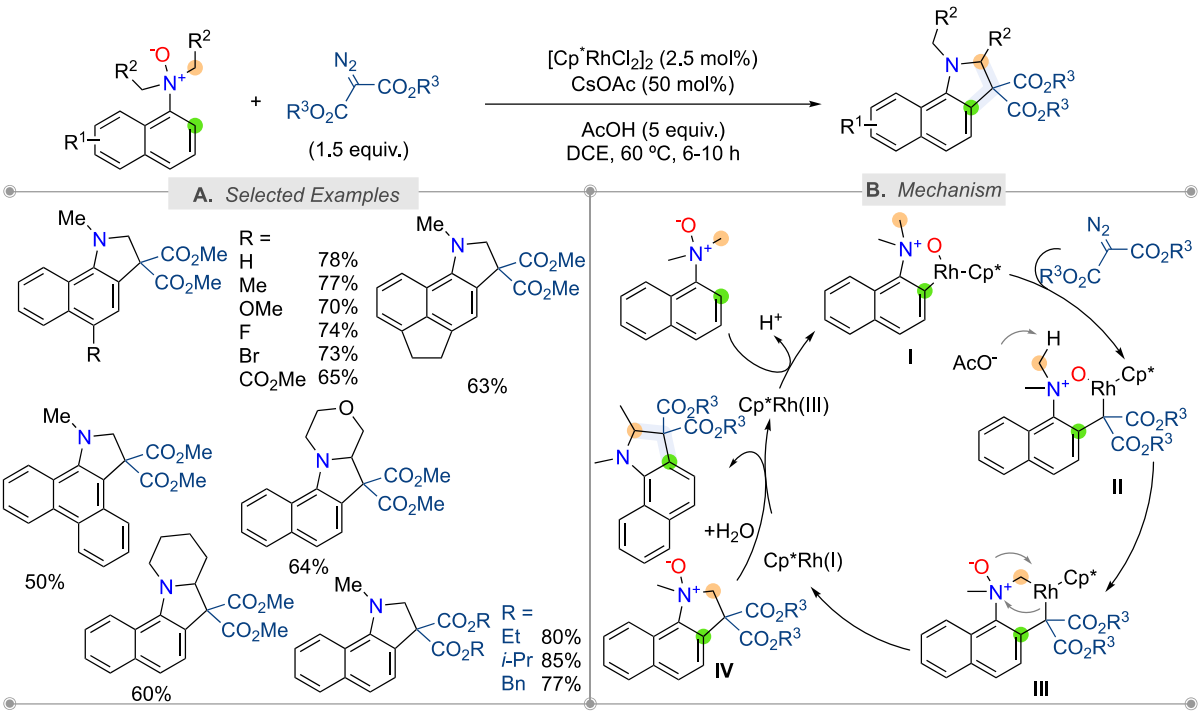

Scheme 1.34. Rhodium(III)-Catalyzed C–H Bond Annulation of Arylamine *N*-Oxides with Diazo Compounds.

1.3. Formation of Six-Membered Ring *N*-Heterocycles

1.3.1. Preparation of Quinolinone and Isoquinolone Scaffolds

1.3.1.1 C–H Bond Functionalization Under Oxidative Conditions

In 2010, Li and co-workers reported the oxidative C–H bond annulation of *N*-aryl-2-aminopyridine with benzylacrylate to generate isoquinolone scaffolds (Scheme 1.35).[9] The optimized conditions were found using 1 mol% $[Cp^*RhCl_2]_2$ in the presence of 2.2 equivalents of $Cu(OAc)_2$ as the oxidant in DMF at 100 °C over 12 h. Other alkyl acrylates have been successfully employed to deliver the same products. It should be mentioned that replacing benzylacrylate with styrene delivered the mono and bis-alkenylated products.

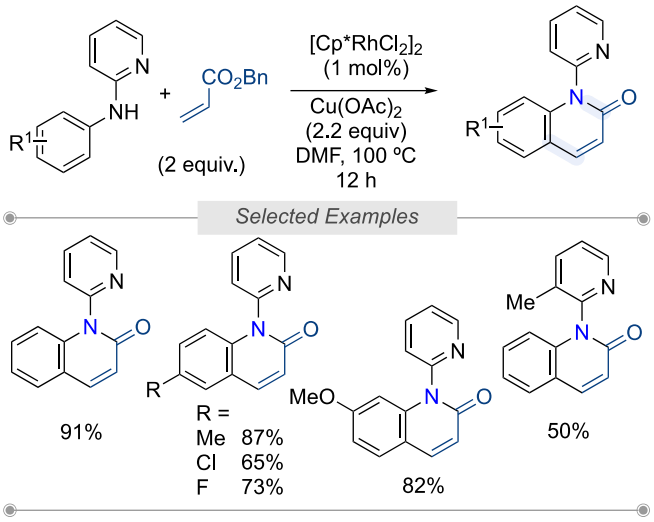

Scheme 1.35. Rh(III)-Catalyzed Oxidative C–H Bond Annulation of *N*-Aryl-2-aminopyridine with Acrylates.

In 2010, isoquinolone heterocycles were prepared from amide and alkynes using Rh(III)-catalyzed C–H bond annulation, a catalytic transformation developed by Rovis and co-workers (Scheme 1.36).[48] The reactions conditions are similar to those described by Fagnou for indoles synthesis,[7] asides $AgSbF_6$ [2.5 mol% of $[Cp^*RhCl_2]_2$ as a catalyst with $Cu(OAc)_2$ (2.1 equivalents) as a stoichiometric oxidant in *t*–AmOH]. Electron-rich and electron-poor *N*-methyl benzamides reacted in good yields. *Meta*-substituted benzamides gave isoquinolone products as single regioisomers (less hindered position), while *ortho*-substituted ones afforded the isoquinolone products in slightly lower yields. Moreover, heteroaryl carboxamides have also been employed. The reaction displayed a broad substrate tolerance among internal alkynes, including unsymmetrical dialkyl alkynes, for which good regioselectivity was observed. After conducting mechanistic studies (deuterium-labelling experiments and competitive reactions), the authors proposed the following mechanism (Scheme 1.36-B). In the presence of $Cu(OAc)_2$, the active catalyst $Cp^*Rh(OAc)_n$ is formed. After the classical C–H bond activation *ortho*-directed by the amide group (**I**) and alkyne insertion, seven-membered rhodacycle **II** with an open coordination site is generated. Then, reductive elimination formed the desired isoquinolone and generated a rhodium(I) species that can undergo oxidation to regenerate the catalytically active rhodium(III) complex with $Cu(OAc)_2$.

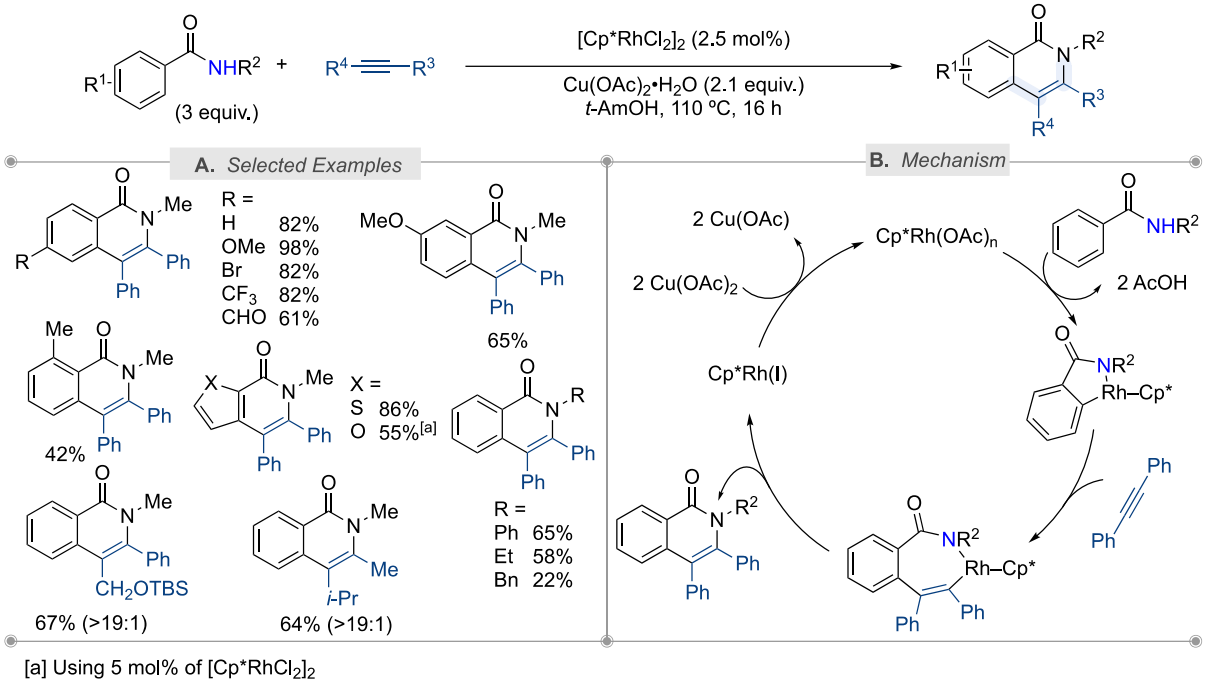

[a] Using 5 mol% of $[Cp^*RhCl_2]_2$

Scheme 1.36. Rhodium(III)-Catalyzed Oxidative Cycloaddition of Benzamides and Alkynes *via* C–H/N–H Activation.

Satoh, Miura, and co-workers reported a similar transformation in the same year, albeit using alkynes and primary amides in a 1 to 1 ratio to achieve the double C–H bond annulation reaction to prepare tetracyclic compounds (Scheme 1.37).[49]

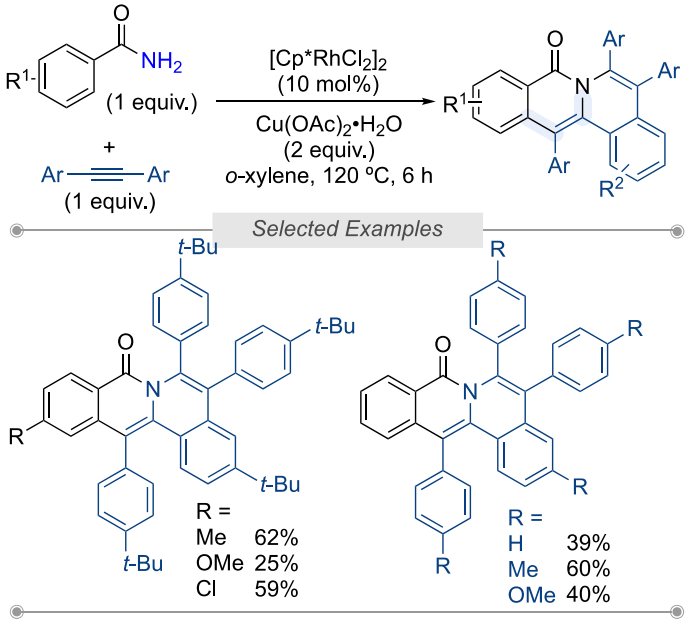

Scheme 1.37. Rhodium(III)-catalyzed Oxidative Coupling/Cyclization of Benzamides with Alkynes *via* C–H Bond Cleavage.

In 2014, during their investigation of indole synthesis through Rh(III)-catalyzed C–H bond annulation of *N*-protected anilines (Scheme 1.4),[14] Tanaka and co-workers also described one example of the formation of isoquinolone scaffold when they conducted the reaction from *N*-phenylbenzamide and 1,2-diphenylacetylene in the presence of $[Cp^*RhCl_2]_2$ associated with 2 equivalents of $Cu(OAc)_2$ in *tert*-amyl alcohol (Scheme 1.38). Interestingly, in contrast with five-membered ring formation, $[Cp^*RhCl_2]_2$ displays a better activity than electron-deficient $[Cp^ERhCl_2]_2$ catalysts for the formation of isoquinolone scaffold.

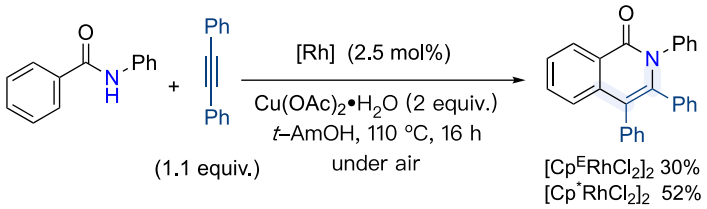

Scheme 1.38. Preparation of Isoquinolone Scaffold *via* Rhodium(III)-Catalyzed Oxidative Coupling of *N*-Phenylbenzamide and an Internal Alkyne.

In 2017, Huang and co-workers reported the C–H bond annulation of *N*-arylpyridin-2-amines with *α*,*β*-unsaturated aldehydes for synthesizing dihydroquinolines using rhodium catalysis (Scheme 1.39).[50] The optimized conditions, namely $[Cp^*RhCl_2]_2$ (2.5 mol%) and $AgSbF_6$ (10 mol%) in the presence of PivOH (2 equivalents) in MeOH at 50 °C, tolerate various electron-withdrawing or electron-donating functional groups on the benzene rings of *N*-arylpyridin-2-amines. Most reactions were performed with acrylaldehyde, but 3-methyl and 3-ethyl propenal have also been employed. After the *ortho*-C–H bond alkylation of *N*-arylpyridin-2-amines catalyzed by Rh(III) in a regular catalytic cycle, the amino group of intermediate **I** intramolecularly adds to the carbonyl group, forming *α*-hydroxyl tetrahydroquinoline intermediate **II**. The ligand exchange of the Cp*Rh(III) complex with intermediate **II** leads to rhodium intermediate **III**. Then, *β*-hydride elimination of intermediate **III** results in tetrahydroquinoline and Cp*Rh(III)–H. After the addition of anion Y^- onto Cp*Rh(III)–H, losing HY by reductive-elimination leads to Cp*Rh(I), which is oxidized into Cp*Rh(III) for catalytic recycling by oxygen in the air.

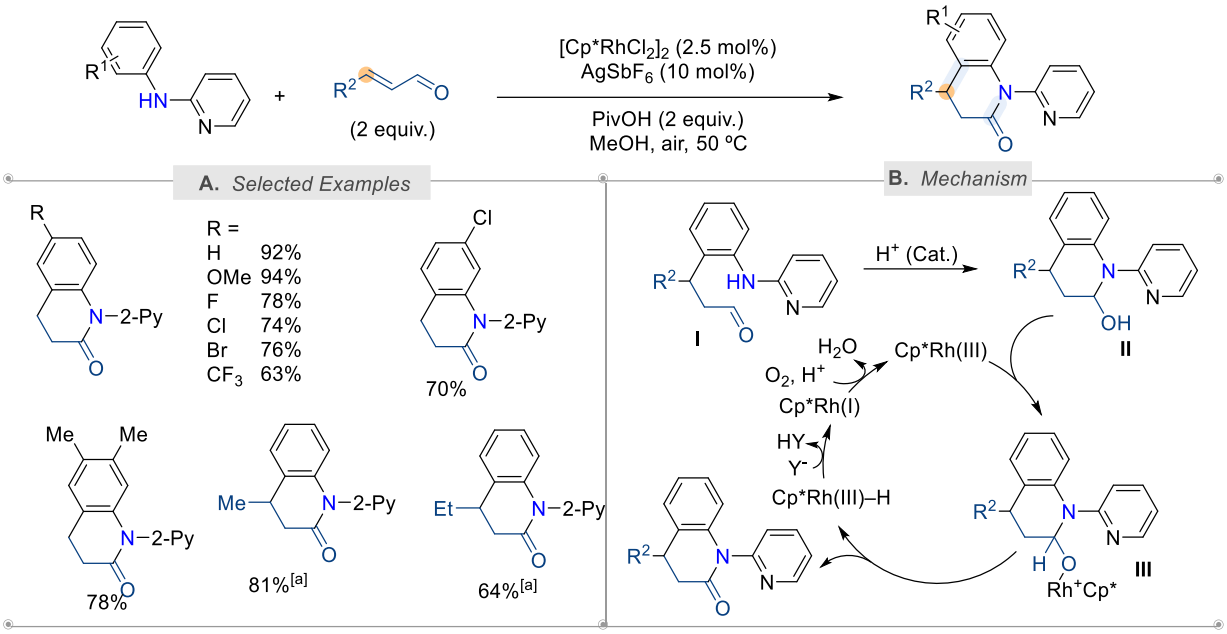

[a] Reaction performed using $[Cp^*RhCl_2]_2$ (4 mol%), $AgSbF_6$ (20 mol%) at 90 °C.

Scheme 1.39. Rhodium(III)-Catalyzed C–H Bond Annulation of *N*-arylpyridin-2amines with α,β-Unsaturated Aldehydes.

1.3.1.2 C–H Bond Functionalization Using Redox-Neutral Conditions

In 2011, during their investigation on Rh(III)-catalyzed directed C–H bond olefination using an oxidizing directing group, Glorious and co-workers succeeded in preparing tetrahydroisoquinolinones (Scheme 1.40).[51] In the presence of 2.5 mol% of $[Cp^*RhCl_2]_2$, 30 mol% of CsOPiv, and 20 mol% of PivOH in MeOH, *N*-(pivaloyloxy)benzamides were annulated using mere alkenes. This reaction works with acrylates and styrenes. Moreover, under standard reaction conditions, gaseous ethylene (5 bar) has also been employed as an alkene coupling partner.

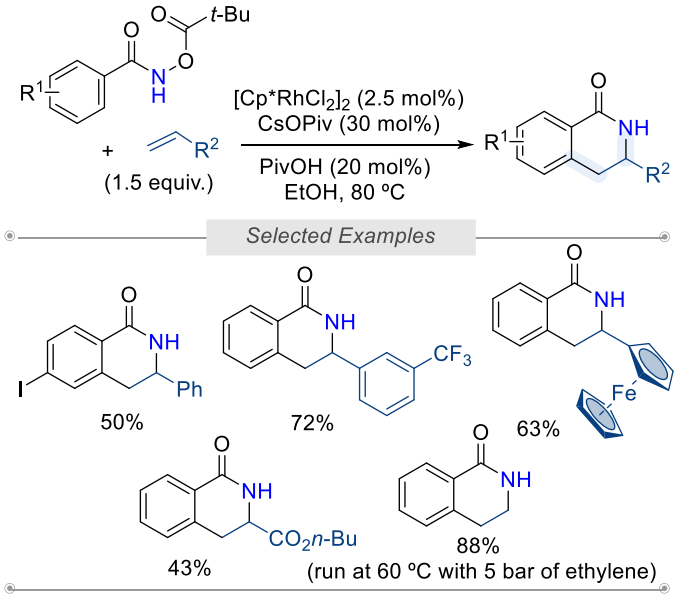

Scheme 1.40. Rhodium(III)-catalyzed C–H Bond Annulation of *N*-(Pivaloyloxy)benzamides with Alkenes for Tetrahydroisoquinolinone Synthesis.

Later, by employing *α*-(pseudo)halo ketones as annulative reagents, the same group succeeded in preparing isoquinolones (Scheme 1.41).[52] Various *α*-(pseudo)halo ketones were evaluated, and the best results were obtained with OMs or OTs groups. Diversely substituted *N*-OMe substituted amides were employed. However, the OMe group was critical as no reaction occurred with other *N*-substituted amides (with H, Me, Ph, OPiv). Besides the aryl ketones, they found that a dialkyl ketone derivative, 2-oxopropyl tosylate, also worked efficiently. A classical mechanism based on a CMD process catalyzed by Rh(III) is proposed for the generation of **I**. However, the cyclization reaction occurred in a non-catalyzed process. Depending on the substitution patterns of the amide, the enols **II** could be more favored and could slower down the cyclization process. Then, an intramolecular attack of the *N*-atom to ketone affords **III**, which provides the desired product after dehydration.

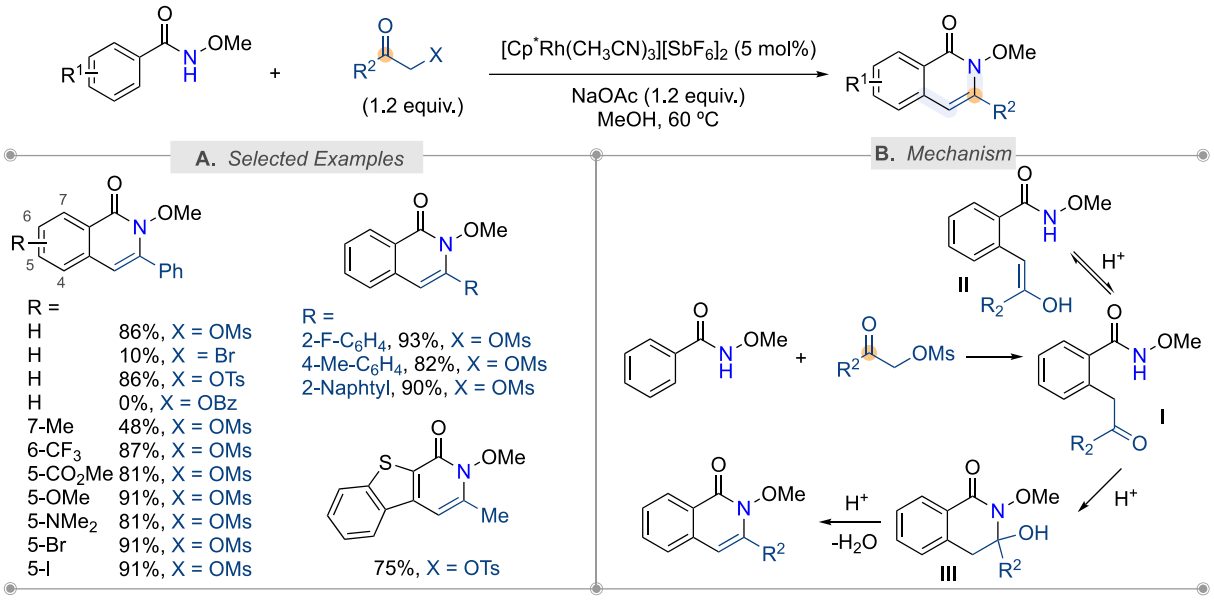

Scheme 1.41. Rhodium(III)-Catalyzed C–H Bond Annulation of Amide with *α*-(Pseudo)halo Ketones as Annulating Agents.

1.3.2. Preparation of Dihydroquinoline Scaffolds

In 2022, Volla and co-workers reported the synthesis of dihydroquinolines from alkenyl anilides and allenyl acetates (Scheme 1.42).[53] This format [5 + 1]-annulation of 2-alkenylanilides is catalyzed by 2.5 mol% of $[Cp^*RhCl_2]_2$, and 30 mol% of NaOAc in DCE at room temperature. Diversely substituted 2-alkenylanilides have been coupled with phenyl allene to afford the desired 1,2-dihydroquinoline derivatives in good to excellent yields (R = Me, OMe, F, Cl, Br, CO_2Et). Regarding the alkenyl substituent fragment, methyl, ethyl, *i*-propyl, *n*-butyl and phenyl derivatives were successfully used, while mere vinyl substituted aniline (R = H) and trisubstituted alkenylanilides did not show any reactivity for the annulation. Moreover, electron-donating and -withdrawing substituents at the *ortho*-, *meta*- and *para*-positions of the aryl ring of allenyl acetate were well tolerated, demonstrating the generality of this method. Based on deuterium-labelling, competitive, and control experiments, the authors proposed the catalytic cycle depicted in Scheme 1.42-B. First, vinyl C–H activation to form six-membered rhodacycle **I** occurs, followed by regioselective 2,3-migratory insertion of allene to give the eight-membered Rh(III) intermediate **II**. Subsequent *β*-oxygen elimination from species **II** gives the diene intermediate **III**, which undergoes intramolecular nucleophilic addition of the nitrogen–rhodium bond resulting in [5 + 1]-annulation. Finally, protonation of **IV** provides the desired 1,2-dihydroquinolines and regenerates the active Rh(III) catalyst.

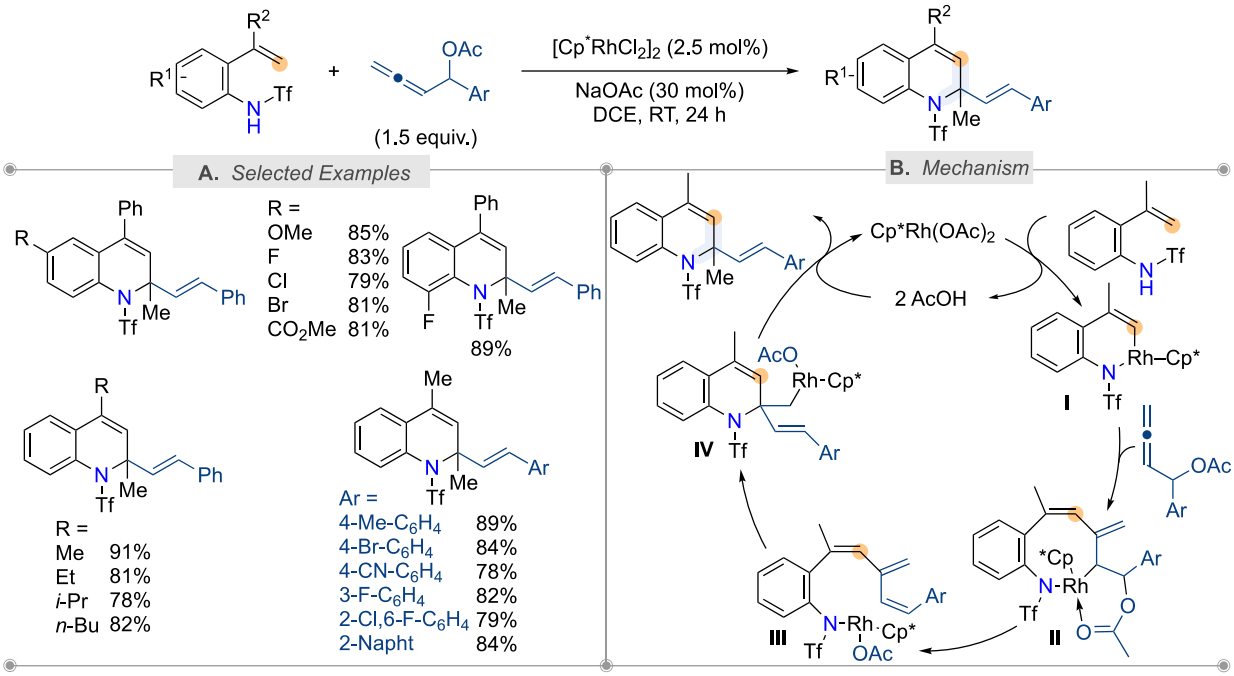

Scheme 1.42. Rhodium(III)-Catalyzed C–H Bond Annulation of 2-Alkenylanilides and 2-Alkenylphenols with Allenyl Acetates.

1.3.3. Preparation of Pyridone Scaffolds

In 2010, Li and co-workers reported an elegant method to prepare 2-pyridones from acrylamides and alkynes through Rh(III)-catalyzed C–H bond annulation (Scheme 1.43, top).[10] Interestingly the C–H bond activation occurred exclusively on the vinylic C–H bond using 0.5 mol% $[Cp^*RhCl_2]_2$ catalyst while using cationic Rh(III) complex afforded the functionalization of the aryl C–H bond (Scheme 1.43, bottom).[10] Again $Cu(OAc)_2$ was employed as the terminal oxidant to promote the C–N bond formation. In addition to the coupling of alkynes with secondary acrylamides, the coupling of primary methacrylamides with an excess of 1,2-diphenylacetylene gave a tricyclic product as a result of a second oxidative insertion of the second equivalent of 1,2-diphenylacetylene (Scheme 1.43, bottom).

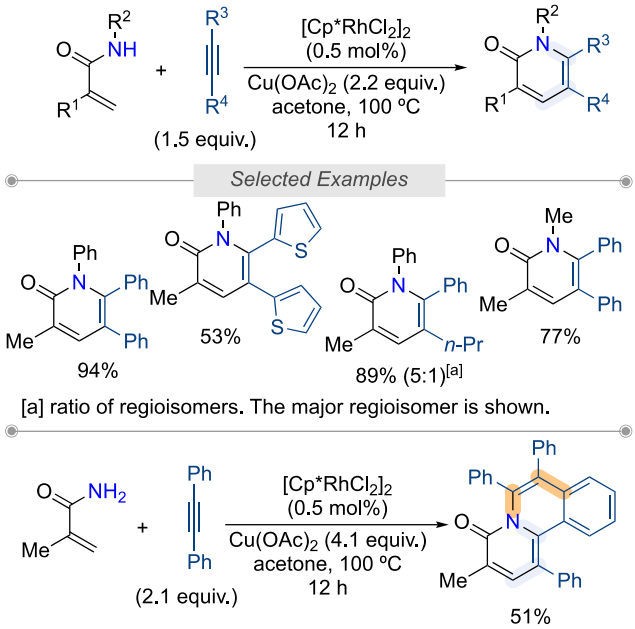

Scheme 1.43. Synthesis of 2-Pyridones *via* Rh(III)-Catalyzed Oxidative C–H Bond Annulation of Acrylamides with Alkynes.

1.4. Conclusion

This review has highlighted the recent advances in developing Rh(III)-catalyzed C–H bond annulation to access *N*-heterocycles from readily available materials. The excellent contributions demonstrate that the development of novel and green approaches for the heterocyclic scaffold synthesis by concomitant C–N/C–C bond formation triggered by C–H bond activation offers a straightforward way to the structural diversity molecules. Rh(III)-catalysis has predominated this chemistry, exhibiting broad functional group tolerances, including X–halo bonds, even C–I ones allowing further post modifications to access better molecular diversity. It is noted that amide units were the most popular directing groups to control the regioselectivity, and depending on the annulative partners, different *N*–heterocycles have been prepared. Furthermore, some oxidizing directing groups have been specifically designed to avoid the use of external oxidants leading to better molecular diversity *via* cascade reactions, including an additional *O*–atom transfer step.

Although significant advances in this research field have been made, some challenges persist. First, large amounts of catalysts and generally high temperatures are necessary for the reported C–H bond annulation. To overcome these limitations, novel $Cp^{R}Rh(III)$ catalysts such as electron-deficient $Cp^{E}Rh(III)$ have been developed. In our opinion, the design of more reactive $Cp^{R}Rh(III)$ will be a hot topic to unlock novel C–H bond annulation processes in the coming years. Secondly, compared with external oxidants, reactions involving oxidizing

directing groups have limited successful examples, and most of them are based on non-natural oxidizing directing groups. Therefore, the development of new strategies based on directing groups containing a native N–O bond would provide new opportunities to access *N*-heterocycles of interest. Finally, discovering new strategies based on C–H bond annulation would provide opportunities to access *N*-heterocycles of interest in a minimum of steps. This field will soon find more opportunities to synthesize functional materials and drugs on academic and even industrial levels.

1.5. References

1. (a) Kim, J.; Movassaghi, M., *Chem. Soc. Rev.* **2009**, *38*, 3035-3050; (b) Chen, D.; Su, S.-J.; Cao, Y., *J. Mat. Chem. C.* **2014**, *2*, 9565-9578; (c) Heravi, M. M.; Zadsirjan, V., *RSC Adv.* **2020**, *10*, 44247-44311; (d) Bhutani, P.; Joshi, G.; Raja, N.; Bachhav, N.; Rajanna, P. K.; Bhutani, H.; Paul, A. T.; Kumar, R., *J. Med. Chem.* **2021**, *64*, 2339-2381.
2. (a) Lu, H.; Li, C., *Org. Lett.* **2006**, *8*, 5365-5367; (b) Newman, S. G.; Lautens, M., *J. Am. Chem. Soc.* **2010**, *132*, 11416-11417; (c) Carvalho, L. C. R.; Fernandes, E.; Marques, M. M. B., *Chem. Eur. J.* **2011**, *17*, 12544-12555; (d) Cho, S. H.; Kim, J. Y.; Kwak, J.; Chang, S., *Chem. Soc. Rev.* **2011**, *40*, 5068-5083; (e) Shimbayashi, T.; Matsushita, G.; Nanya, A.; Eguchi, A.; Okamoto, K.; Ohe, K., *ACS Catal.* **2018**, *8*, 7773-7780.
3. Liu, Z.-K.; Zhao, Q.-Q.; Gao, Y.; Hou, Y.-X.; Hu, X.-Q., *Adv. Synth. Catal.* **2021**, *363*, 411-424.
4. (a) Ackermann, L.; Vicente, R.; Kapdi, A. R., *Angew. Chem. Int. Ed.* **2009**, *48*, 9792-9826; (b) McGlacken, G. P.; Bateman, L. M., *Chem. Soc. Rev.* **2009**, *38*, 2447-2464; (c) Lyons, T. W.; Sanford, M. S., *Chem. Rev.* **2010**, *110*, 1147-1169; (d) Rossi, R.; Bellina, F.; Lessi, M.; Manzini, C., *Adv. Synth. Catal.* **2014**, *356*, 17-117; (e) He, J.; Wasa, M.; Chan, K. S. L.; Shao, O.; Yu, J.-Q., *Chem. Rev.* **2017**, *117*, 8754-8786; (f) Cheng, H.-G.; Chen, S.; Chen, R.; Zhou, Q., *Angew. Chem. Int. Ed.* **2019**, *58*, 5832-5844; (g) Hagui, W.; Doucet, H.; Soulé, J.-F., *Chem* **2019**, *5*, 2006-2078; (h) Rej, S.; Ano, Y.; Chatani, N., *Chem. Rev.* **2020**, *120*, 1788-1887; (i) Yorimitsu, H.; Yoshimura, A.; Misaki, Y., *Synthesis* **2020**, *52*, 3326-3336.
5. Patureau, F. W.; Glorius, F., *Angew. Chem. Int. Ed.* **2011**, *50*, 1977-1979.
6. (a) Prajapati, S. M.; Patel, K. D.; Vekariya, R. H.; Panchal, S. N.; Patel, H. D., *RSC Adv.* **2014**, *4*, 24463-24476; (b) Li, L.-H.; Niu, Z.-J.; Liang, Y.-M., *Chem. Asian J.* **2020**, *15*, 231-241; (c) Zhang, B.; Studer, A., *Chem. Soc. Rev.* **2015**, *44*, 3505-3521.
7. Stuart, D. R.; Bertrand-Laperle, M.; Burgess, K. M. N.; Fagnou, K., *J. Am. Chem. Soc.* **2008**, *130*, 16474-16475.
8. Stuart, D. R.; Alsabeh, P.; Kuhn, M.; Fagnou, K., *J. Am. Chem. Soc.* **2010**, *132*, 18326-18339.

9. Chen, J.; Song, G.; Pan, C.-L.; Li, X., *Org. Lett.* **2010**, *12*, 5426-5429.
10. Su, Y.; Zhao, M.; Han, K.; Song, G.; Li, X., *Org. Lett.* **2010**, *12*, 5462-5465.
11. Huestis, M. P.; Chan, L.; Stuart, D. R.; Fagnou, K., *Angew. Chem. Int. Ed.* **2011**, *50*, 1338-1341.
12. (a) Greed, S., *Nat. Rev. Chem.* **2022**, *6*, 301-301; (b) Piou, T.; Rovis, T., *Acc. Chem. Res.* **2018**, *51*, 170-180.
13. Shibata, Y.; Tanaka, K., *Angew. Chem. Int. Ed.* **2011,** *123*, 10917-10921.
14. Hoshino, Y.; Shibata, Y.; Tanaka, K., *Adv. Synth. Catal.* **2014**, *356*, 1577-1585.
15. Zhang, G.; Yu, H.; Qin, G.; Huang, H., *Chem. Commun.* **2014**, *50*, 4331-4334.
16. Wang, C.; Sun, H.; Fang, Y.; Huang, Y., *Angew. Chem. Int. Ed.* **2013**, *52*, 5795-5798.
17. Kathiravan, S.; Nicholls, I. A., *Chem. Commun.* **2014**, *50*, 14964-14967.
18. Li, D. Y.; Chen, H. J.; Liu, P. N., *Org. Lett.* **2014**, *16*, 6176-6179.
19. Cajaraville, A.; López, S.; Varela, J. A.; Saá, C., *Org. Lett.* **2013**, *15*, 4576-4579.
20. Kim, M.; Park, J.; Sharma, S.; Han, S.; Han, S. H.; Kwak, J. H.; Jung, Y. H.; Kim, I. S., *Org. Biomol. Chem.* **2013**, *11*, 7427-7434.
21. Qi, Z.; Yu, S.; Li, X., *Org. Lett.* **2016**, *18*, 700-703.
22. Zhou, J.; Li, J.; Li, Y.; Wu, C.; He, G.; Yang, Q.; Zhou, Y.; Liu, H., *Org. Lett.* **2018**, *20*, 7645-7649.
23. Cai, S.; Lin, S.; Yi, X.; Xi, C., *J. Org. Chem.* **2017**, *82*, 512-520.
24. Yan, H.; Wang, H.; Li, X.; Xin, X.; Wang, C.; Wan, B., *Angew. Chem. Int. Ed.* **2015**, *54*, 10613-10617.
25. Zhou, Z.; Liu, G.; Chen, Y.; Lu, X., *Adv. Synth. Catal.* **2015**, *357*, 2944-2950.
26. (a) Li, Y.; Li, J.; Wu, X.; Zhou, Y.; Liu, H., *J. Org. Chem.* **2017**, *82*, 8984-8994; (b) Guo, X.; Han, J.; Liu, Y.; Qin, M.; Zhang, X.; Chen, B., *J. Org. Chem.* **2017**, *82*, 11505-11511.
27. Lee, B. H.; Biswas, A.; Miller, M. J., *J. Org. Chem.* **1986**, *51*, 106-109.
28. Li, B.; Xu, H.; Wang, H.; Wang, B., *ACS Catal.* **2016**, *6*, 3856-3862.
29. Huang, X.; Liang, W.; Shi, Y.; You, J., *Chem. Commun.* **2016**, *52*, 6253-6256.
30. Ghorai, J.; Ramachandran, K.; Anbarasan, P., *J. Org. Chem.* **2021**, *86*, 14812-14825.
31. Zhao, D.; Shi, Z.; Glorius, F., *Angew. Chem. Int. Ed.* **2013**, *52*, 12426-12429.
32. Chen, W.-J.; Lin, Z., *Organometallics* **2015**, *34*, 309-318.
33. Liang, Y.; Yu, K.; Li, B.; Xu, S.; Song, H.; Wang, B., *Chem. Commun.* **2014**, *50*, 6130-6133.
34. Liu, B.; Song, C.; Sun, C.; Zhou, S.; Zhu, J., *J. Am. Chem. Soc.* **2013**, *135*, 16625-16631.
35. Wang, C.; Huang, Y., *Org. Lett.* **2013**, *15*, 5294-5297.
36. Song, X.; Gao, C.; Li, B.; Zhang, X.; Fan, X., *J. Org. Chem.* **2018**, *83*, 8509-8521.
37. Zhao, G.; Zhu, M.; Provot, O.; Alami, M.; Messaoudi, S., *Org. Lett.* **2020**, *22*, 57-61.

38. Matsuda, T.; Tomaru, Y., *Tetrahedron Lett.* **2014**, *55*, 3302-3304.
39. Zheng, L.; Hua, R., *Chem. Eur. J.* **2014**, *20*, 2352-2356.
40. Özkaya, B.; Bub, C. L.; Patureau, F. W., *Chem. Commun.* **2020**, *56*, 13185-13188.
41. Font, M.; Cendón, B.; Seoane, A.; Mascareñas, J. L.; Gulías, M., *Angew. Chem. Int. Ed.* **2018**, *57*, 8255-8259.
42. Khake, S. M.; Chatani, N., *ACS Catal.* **2021**, *11*, 12375-12383.
43. Zhao, D.; Vásquez-Céspedes, S.; Glorius, F., *Angew. Chem. Int. Ed.* **2015**, *54*, 1657-1661.
44. Yang, Y.; Wang, X.; Li, Y.; Zhou, B., *Angew. Chem. Int. Ed.* **2015**, *54*, 15400-15404.
45. Dateer, R. B.; Chang, S., *J. Am. Chem. Soc.* **2015**, *137*, 4908-4911.
46. Kong, L.; Xie, F.; Yu, S.; Qi, Z.; Li, X., *Chin. J. Catal.* **2015**, *36*, 925-932.
47. Zhou, B.; Chen, Z.; Yang, Y.; Ai, W.; Tang, H.; Wu, Y.; Zhu, W.; Li, Y., *Angew. Chem. Int. Ed.* **2015**, *54*, 12121-12126.
48. Hyster, T. K.; Rovis, T., *J. Am. Chem. Soc.* **2010**, *132*, 10565-10569.
49. Mochida, S.; Umeda, N.; Hirano, K.; Satoh, T.; Miura, M., *Chem. Lett.* **2010**, *39*, 744-746.
50. Wu, Z.-J.; Huang, K. L.; Huang, Z.-Z., *Org. Biomol. Chem.* **2017**, *15*, 4978-4983.
51. Rakshit, S.; Grohmann, C.; Besset, T.; Glorius, F., *J. Am. Chem. Soc.* **2011**, *133*, 2350-2353.
52. Yu, D. G.; de Azambuja, F.; Glorius, F., *Angew. Chem. Int. Ed.* **2014,** *53*, 2754-2758.
53. Singh, A.; Shukla, R. K.; Volla, C. M. R., *Chem. Sci.* **2022**, *13*, 2043-2049.

Chapter 2. Rhodium(I)-Catalyzed Cascade C–H Bond Alkylation – Amidation of Phosphanamines: Phosphorus as Traceless Directing Group

2.1. Introduction

Benzo-fused *N*-heterocycles are valuable building blocks in molecular sciences, including medicinal and materials chemistry. Remarkably, several drug leads feature dihydroquinolinone scaffolds (Figure 2.1).[1] For instance, Carteolol is a non-selective beta blocker used to treat glaucoma, Cilostazol is a medication used to help the symptoms of intermittent claudication in peripheral vascular disease, and Vesnarinone is a cardiotonic agent.

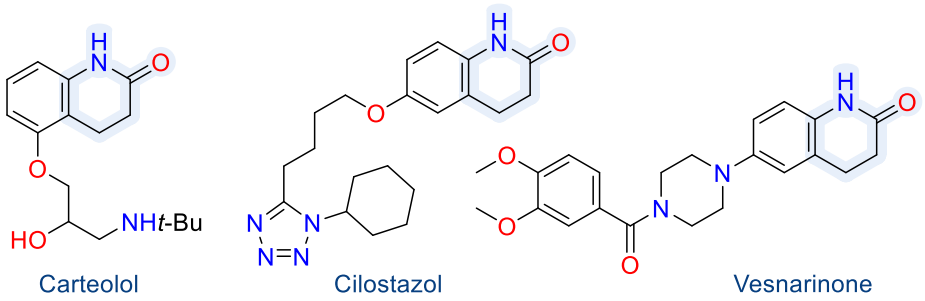

Figure 2.1. Selected Examples of Dihydroquinolinones-Containing Drug Leads.

Dihydroquinolinones were formerly prepared from aniline derivatives *via* amidation reaction followed by intramolecular Friedel-Crafts reaction in the presence of an excess amount of Lewis acid, typically $AlCl_3$ (Figure 2.2-a, left).[2] Due to their importance, several strategies considering better process sustainability have been developed, ranging from transition metal-catalyzed cyclization reactions[3] and radical cyclizations.[4] Since these approaches require multi-step synthesis of the precursors and specific starting materials, they are often limited to preparing a few particular examples. On the other hand, a more direct approach for synthesizing dihydroquinolinones through the concomitant formation of C–C and C–N bonds, so-called C(sp^2)–H bond annulation remains unexplored (Figure 2.2-a, right). This approach is highly desirable as mere anilines and acrylates are the starting materials. However, this C(sp^2)–H bond annulation for the formation of dihydroquinolinones has proven to be incredibly challenging given the inherent nucleophilic characters of anilines which are prone to react in 1,4-addition reaction affording trisubstituted anilines (Figure 2.2-b, 1).[5] To swap the selectivity toward C(sp^2)–H bond functionalization at the *ortho*-position of the *N*-atom, a directing group (DG) needs to be installed. The second issue to face is the selectivity between alkenylation versus alkylation. For instance, in 2015, Lui and co-workers demonstrated that the installation of a transient acetamido as a directing group on aniline partners allows the synthesis of 2-quinolinones through a cascade reaction of Pd-catalyzed C(sp^2)−H alkenylation – cyclization

reaction (Figure 2.2-b, 2).[6] Therefore, a subsequent hydrogenation step of the double bound is required to deliver dihydroquinolinones.[7] The alkenylation versus alkylation selectivity generally depends on the choice of the directing group. Indeed, Chang and co-workers demonstrated that the acetamido group affords alkenylation, while pyridine, pyrazole, and pyrimidine lead to alkylation products using $[Cp^*IrCl_2]_2$ catalyst (Figure 2.2-b, 3).[8]

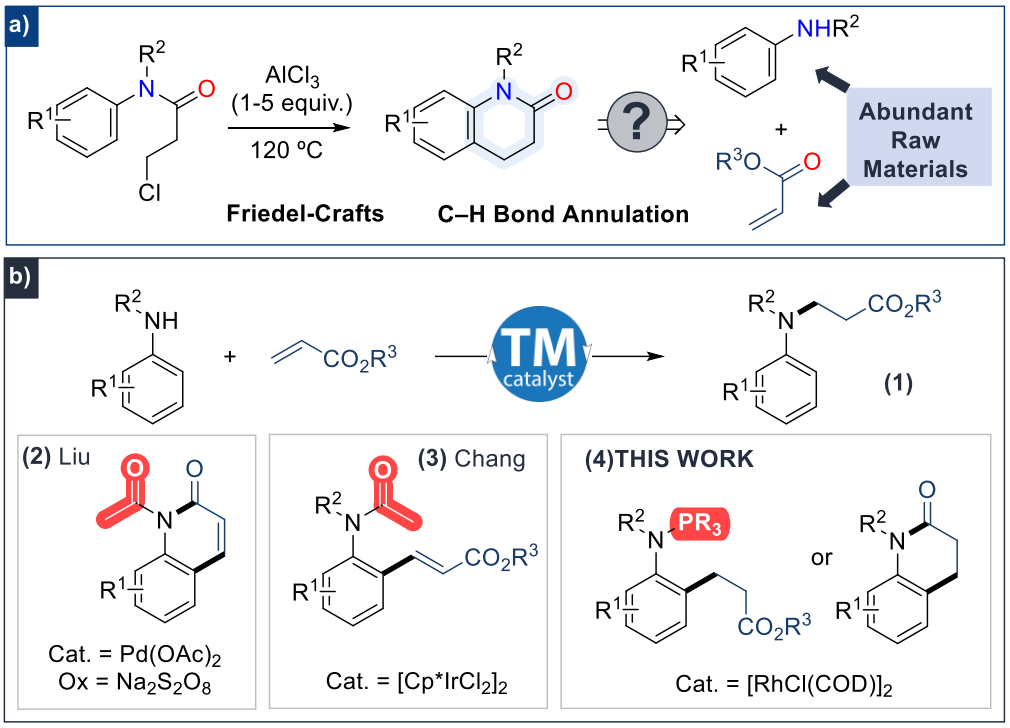

Figure 2.2. a) Traditional Synthesis of Dihydroquinolinones *vs.* C(sp^2)–H Bond Annulation. b) Key Role of the Directing Group for Anilines Acrylates Couplings: Amination, Alkenylation *vs.* Alkylation.

Following the discovery that trivalent phosphorus P(III) acts as directing group for the C(sp^2)–H bond functionalization of phosphines[9] or indoles,[10] and given the fact that P(III) favors alkylation products with acrylates using Rh(I) catalysts,[11] we hypothesized that if *N*-arylphosphanamines could be alkylated at *ortho*-position with acrylates, such intermediate would rapidly undergo intramolecular amidation reaction driven by N–P bond hydrolysis provided that suitable conditions are found (Figure 2.2-b, 4). Herein, we describe the reaction development with mechanistic aspects showcasing that trivalent phosphorus acts as a traceless directing group in rhodium(I)-catalyzed cascade reaction of C(sp^2)–H bond activation/alkylation – amidation of anilines with acrylate derivatives for the one-pot synthesis of dihydroquinolinones.

2.2. Results and Discussion

2.2.1. Optimization of the Reaction Conditions

To demonstrate the feasibility of the one-pot cascade of the C(sp^2)–H bond alkylation – amidation reaction, we carried out optimization with phosphanamine **1a** and *tert*-butylacrylate (**2a**) as the annulative agent. Using our previously published method for the C(sp^2)–H bond alkylation of phosphines as the starting point,[11a] we quickly recognized that the most important aspect of reaction optimization was the determination of the optimal solvent (and additive) to promote C(sp^2)–H bond alkylation followed by the one-pot removal of P(*i*-Pr)$_2$ directing group to trigger amidation reaction and deliver the dihydroquinolin-2-one scaffold. Indeed, in toluene or 1,4-dioxane, desired product **3a** was obtained among intermediate **4a,** which could be converted into **3a** by acidic hydrolysis (Table 2.1, entries 1 and 2). In contrast, the one-pot process occurred in 1,2-dichloroethane or *N*,*N*-dimethylformamide (DMF), affording dihydroquinolin-2-one **3a** in 24% and 40% yield, respectively, without additional treatment (Table 2.1, entries 3 and 4). The addition of base to favor C(sp^2)–H bond cleavage,[12] or Lewis acid to promote the amination reaction have both a negative effect on the reaction outcomes (Table 2.1, entries 5 and 6). Next, we examined the effect of ligands with the aim of increasing the reactivity. Protected amino-acid such as Ac-Ala (**L1**) slightly improved the reaction to afford **3a** in 54% yield, while diphosphine **L2** failed to affect the title reaction (Table 2.1, entries 7 and 8). Diols, such as BINOL (**L3**), previously employed by Shi in Rh(I)-catalyzed phosphine-directed C(sp^2)−H functionalization,[10b] did not gave better results (Table 2.1, entry 9). A set of bidentate acac-type ligands **L4**-**L6** was tested and 2,2,6,6-tetramethylheptane-3,5-dione (**L6**) was the most efficient, providing **3a** in 58% yield (Table 2.1, entries 10-12). However, the formation of **3a** was not reproducible, and in most cases, the reaction terminated after the formation of **4a**. This may be due to the amount of water necessary to hydrolyze the *N*-arylphosphanamine into aniline derivatives. In the presence of 4 Å molecular sieves, the reaction was much less effective, while in the presence of a small amount of water, reproductible results were obtained, and 10 equivalents of water was the best stoichiometry affording **3a** in 81% isolated yield (Table 2.1, entries 13-17). Control experiment without **L6** and with 10 equivalents of water gave a lower yield of 35% in **1a**, revealing the importance of **L6** in the catalytic conditions (Table 2.1, entry 18).

Table 2.1. Optimization of the Reaction Conditions.

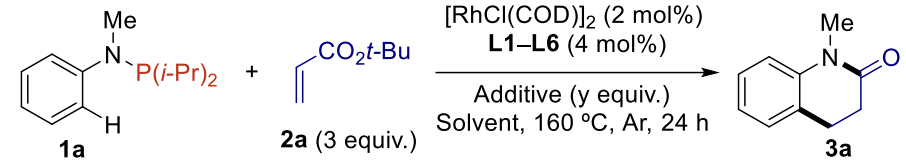

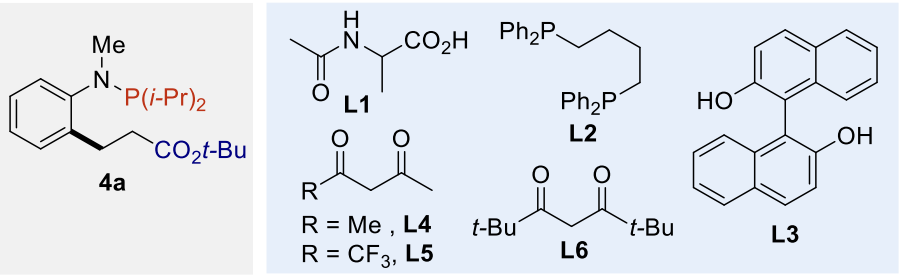

Entry	Ligand	Additive	Solvent	**3a** (%)[a]
1	–	–	toluene	42[b]
2	–	–	1,4-dioxane	12[b]
3	–	–	DCE	24
4	–	–	DMF	40
5	–	NaOAc (0.3)	DMF	30
6	–	$AlMe_3$ (0.2)	DMF	20
7	**L1**	–	DMF	54
8	**L2**	–	DMF	36
9	**L3**	–	DMF	46
10	**L4**	–	DMF	45
11	**L5**	–	DMF	22
12	**L6**	–	DMF	58
13	**L6**	MS 4Å (50 mg)	DMF	21
14	**L6**	H_2O (2 equiv.)	DMF	62
15	**L6**	H_2O (6 equiv.)	DMF	75
16	**L6**	H_2O (10 equiv.)	DMF	90 (81)
17	**L6**	H_2O (20 equiv.)	DMF	54
18	–	H_2O (10 equiv.)	DMF	35

[a]Determined by GC-analysis using *n*-dodecane as internal standard, isolated yield is shown in parentheses. [b]Yield obtained after hydrolysis: HCl 1 N at 80 °C, 2 h.

2.2.2. Scope of the Reaction

With the aforementioned optimal reaction conditions established, the substrate scopes of this reaction were then investigated (Scheme 2.1). First, different substituents on the aromatic ring of the aniline moiety were examined. Electron-donating (MeO, Me) and electron-withdrawing (OCF_3, F, Cl) groups at *the para*-position of the *N*-atom were tolerated providing dihydroquinolinones **3b-f** in good to high yields. However, the conditions were incompatible with Br substituent on the *N*-arylphosphanamine partner. When *meta*-substituted phosphanamines were employed, the C(sp^2)–H bond alkylation regioselectivity occurred at the less hindered position, whatever the substituent, as exemplified by products **3h-k** containing F, Cl, Me, or MeO groups. From *N*-(3,5-difluorophenyl)-1,1-diisopropyl-*N*-methylphosphanamine and *tert*-butylacrylate, the dihydroquinolinone **3l** was isolated in 72% yield. The reaction is slightly sensitive to steric factors, as from *ortho*-substituted *N*-arylphosphanamine (**1m**, R = F), **3m** was isolated in a moderate yield of 42%. Other alkyl groups on the *N*-atom such as Et or *n*-Bu were also tolerated affording **3n-p** in 75-83% yields.[13] Beyond *N*–alkyl phosphanamines, 1,2,3,4-tetrahydroquinoline was also subjected to this C(sp^2)–H bond annulation to afford tricyclic amide **3q** in 70% yield. α-Substituted acrylates such as dimethyl 2-methylenesuccinate (**2b**) and methyl methacrylate (**2c**) were also successfully coupled with phosphanamine **1a** to produce 3-substituted *N*-methyl-dihydroquinolinones **3r** and **3s** in 57% and 60% yield, respectively.

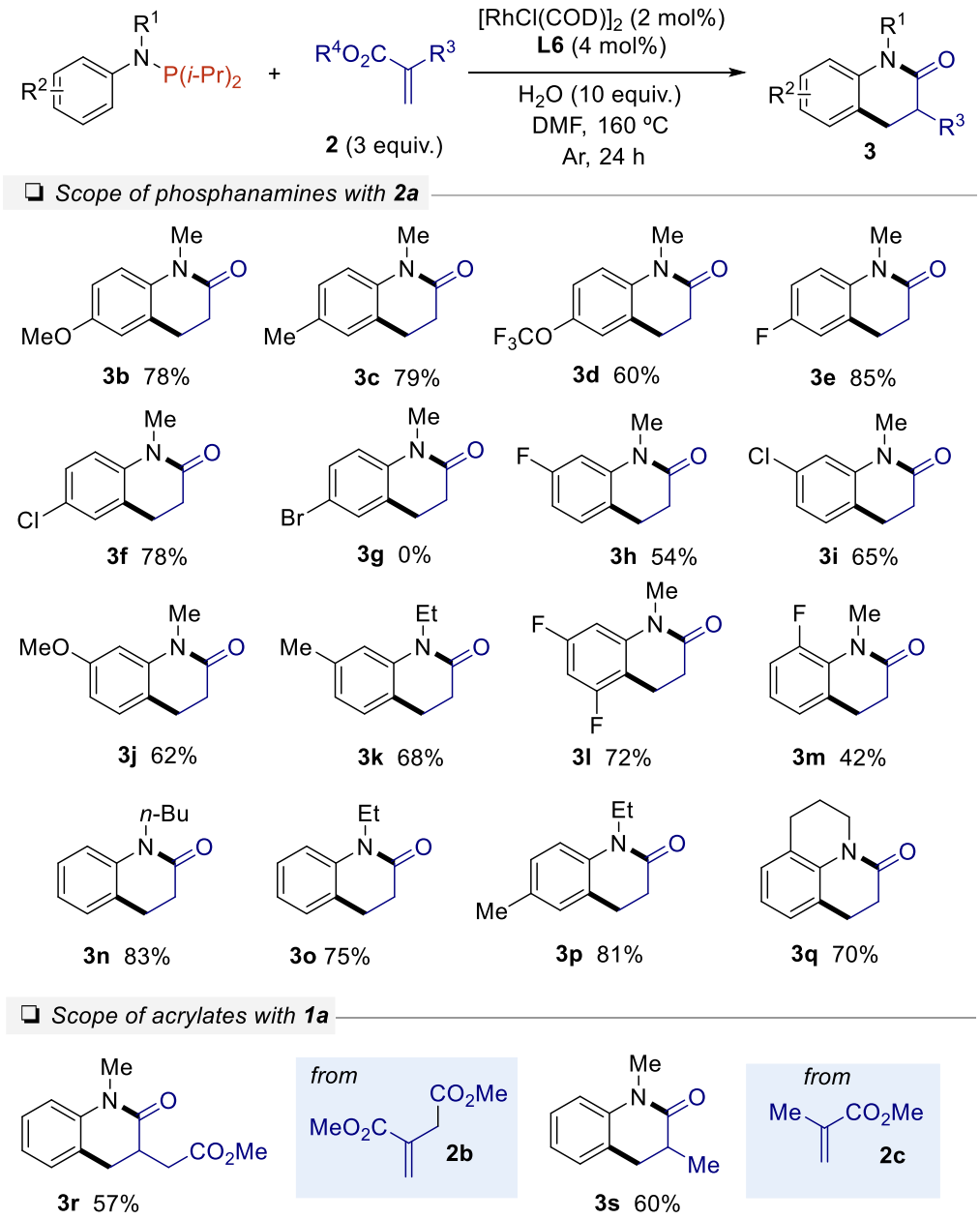

Reaction conditions: *N*-arylphosphanamine **1** (0.3 mmol, 1 equiv.), acrylate **2** (0.9 mmol, 3 equiv.), $[RhCl(COD)]_2$ (0.006 mmol, 2 mol%), **L6** (0.012 mmol, 4 mol%), water (3 mmol, 10 equiv.) in DMF (1.5 mL) at 160 °C.

Scheme 2.1. Scope of Cascade of C(sp^2)–H Bond Alkylation – Amidation from *N*-Arylphosphanamines and Acrylates.

We then moved to extend this trivalent phosphorus traceless directing group strategy to *ortho*-C(sp^2)–H bond functionalization of anilines with styrene derivatives (Scheme 2.2). Accordingly, *ortho*-alkylated *N*-methyl aniline **5a** was obtained in 60% yield from **1a** and styrene (**2d**) using the same catalytic system, namely 2 mol% of $[RhCl(COD)]_2$ associated with

4 mol% of **L6** in the presence of 10 equivalents of water in DMF. Noteworthy, the C–P bond was not fully hydrolyzed when the reaction was performed without water. Electron-rich 1-(*tert*-butyl)-4-vinylbenzene displayed a higher reactivity, as exemplified by forming **5b** and **5c** in 65-73% yield. This reactivity trend was also confirmed with 1-methoxy-4-vinylbenzene and 2,4-dimethyl-1-vinylbenzene, with which **1a** was coupled to give the *ortho*-alkylated *N*-methyl anilines **5d** and **5e** in 75% and 69% yield, respectively. Conversely, the reaction was more sluggish with styrenes holding an electron-withdrawing group such as F and Cl, as the resulting products **5f** and **5g** were isolated in only 32% and 42% yields.

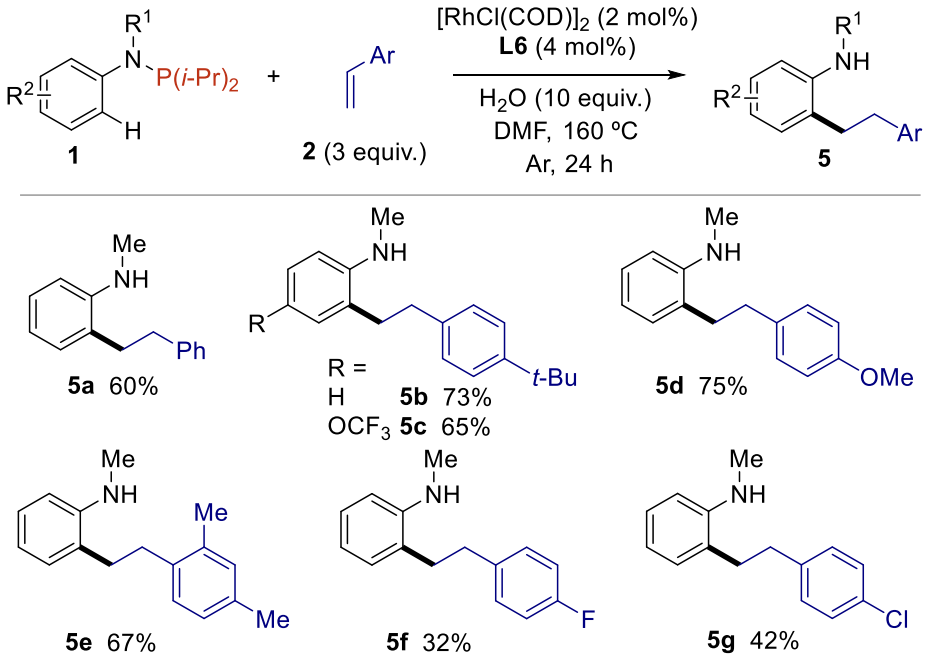

Reaction conditions: *N*-arylphosphanamine **1** (0.3 mmol, 1 equiv.), styrene **2** (0.9 mmol, 3 equiv.), $[RhCl(COD)]_2$ (0.006 mmol, 2 mol%), **L6** (0.012 mmol, 4 mol%), water (3 mmol, 10 equiv.) in DMF (1.5 mL) at 160 °C.

Scheme 2.2. Scope of C(sp^2)–H Bond Alkylation of *N*-Arylphosphanamines with Styrenes.

2.2.3. Application to the Synthesis of Aripiprazole *N*-Methylated Analog

Having established a method to construct dihydroquinolinones with good functional group compatibility, we investigated the feasibility of applying it to prepare Aripiprazole *N*-methylated analog **8**. Aripiprazole treats schizophrenia, bipolar disorder, major depressive disorder, tic disorders.[14] In 2020, the Aripiprazole market was dominated by two brand companies (Otsuka & Bristol-Myers Squibb) and is expected to grow at a CAGR of 4.60% in the forecast period of 2022-2029. The majority of previous routes toward Aripiprazole (or its *N*-

alkyl congeners) involved multi-step synthesis for the construction of the dihydroquinolinone scaffold[15] (*e.g.*, intramolecular Friedel-Craft reaction followed by Pd-catalyzed hydrogenation of double bond,[16] or through a Beckmann rearrangement from indanone derivative). Owing to the increasing demand for Aripiprazole and its *N*-alkyl analogs, and the lack of synthetic routes for the construction of dihydroquinolinones from simple starting materials prompted us to develop an efficient route to Aripiprazole *N*-methylated analog **8**, employing our rhodium(I)-catalyzed cascade reaction of C(sp^2)–H bond alkylation – amidation of anilines (Scheme 2.3). A gram-scale reaction (5 mmol) performed from 1,1-diisopropyl-*N*-(3-methoxyphenyl)-*N*-methylphosphanamine with *tert*-butylacrylate (**2a**) gave 0.54 g of **3j** (57% yield). Then, classical deprotection of phenol group by BBr_3, followed by Williamson reaction using 2 equivalents of 1,4-dibromobutane in the presence of K_2CO_3 afforded **7** in good yield. Final coupling with 1-(2,3-dichlorophenyl)piperazine in the presence of KI as a relay-nucleofuge and triethylamine as base led to the formation of desired Aripiprazole *N*-methylated analog **8** in 70% yield.

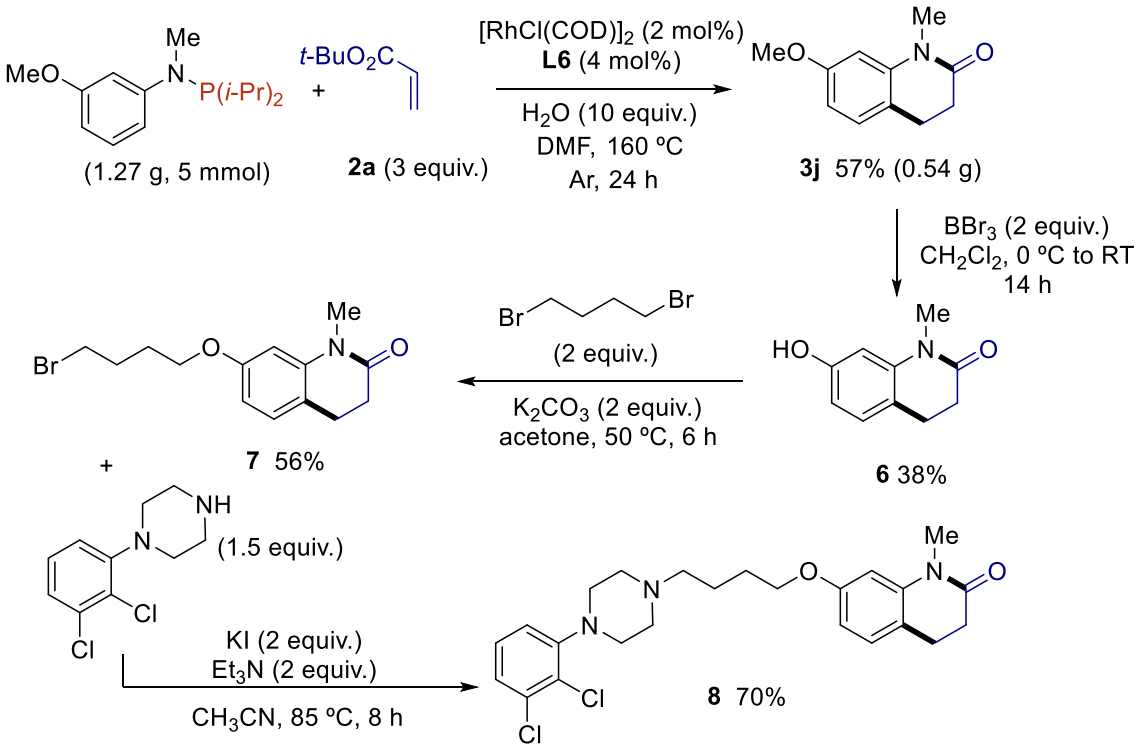

Scheme 2.3. Gram-Scale and Synthesis of Aripiprazole *N*-Methylated Analog.

2.3. Mechanistic Study

2.3.1. Control and Deuterium-Labelling Experiments

Intrigued by the exact role and the becoming of the phosphorus group along this reaction, we started a mechanistic investigation by carrying out some control experiments. No reaction occurred from *P*,*P*-diisopropyl-*N*-methyl-*N*-phenylphosphinic amide, indicating that trivalent phosphorus is not oxidized at least before the C(sp^2)–H bond cleavage. The use of classical acetamide as a directing group or reaction from *N*-methylaniline also failed to deliver cyclized amide **3a** (Scheme 2.4-a). These results indicate that trivalent phosphorus is the active directing group. A standard reaction between phosphanamine **1a** and **2a** in the presence of 1 equivalent of 3-fluoro-*N*-methylaniline revealed that there is no phosphorus-directing group scrambling (Scheme 2.4-b). A careful analysis of the reaction outcomes by GC-MS and ^{31}P NMR has allowed us to identify the formation hydroxydiisopropylphosphane (**9a**) as the side product, which may explain that -P(*i*-Pr)$_2$ acts as a traceless directing group rather than a transient directing group (Scheme 2.4-c).[17] A standard reaction performed using 10 equivalents of deuterated water gave 57% deuterium incorporation at *ortho*-position of the NMeP(*i*-Pr)$_2$ group (Scheme 2.4-d). This deuterium labelling experiment suggests that the C(sp^2)–H bond cleavage is reversible. Moreover, H-D exchange also occurred at the α-position of the ester group, suggesting reductive elimination (or Rh–C protonolysis). At the same time, the incorporation of the D atom at the β-position might arise from the deprotonation of the acidic benzylic C(sp^2)–H bond after forming product **3a**. The deuterium incorporation in the NMe group may result from the formation of amide rhodacycle through C(sp^3)–H bond activation. To determine the role of **L6**, we decided to prepare the well-defined Rh(COD)(**L6**) complex, but it was completely inactive for this cascade reaction (Scheme 2.4-e).

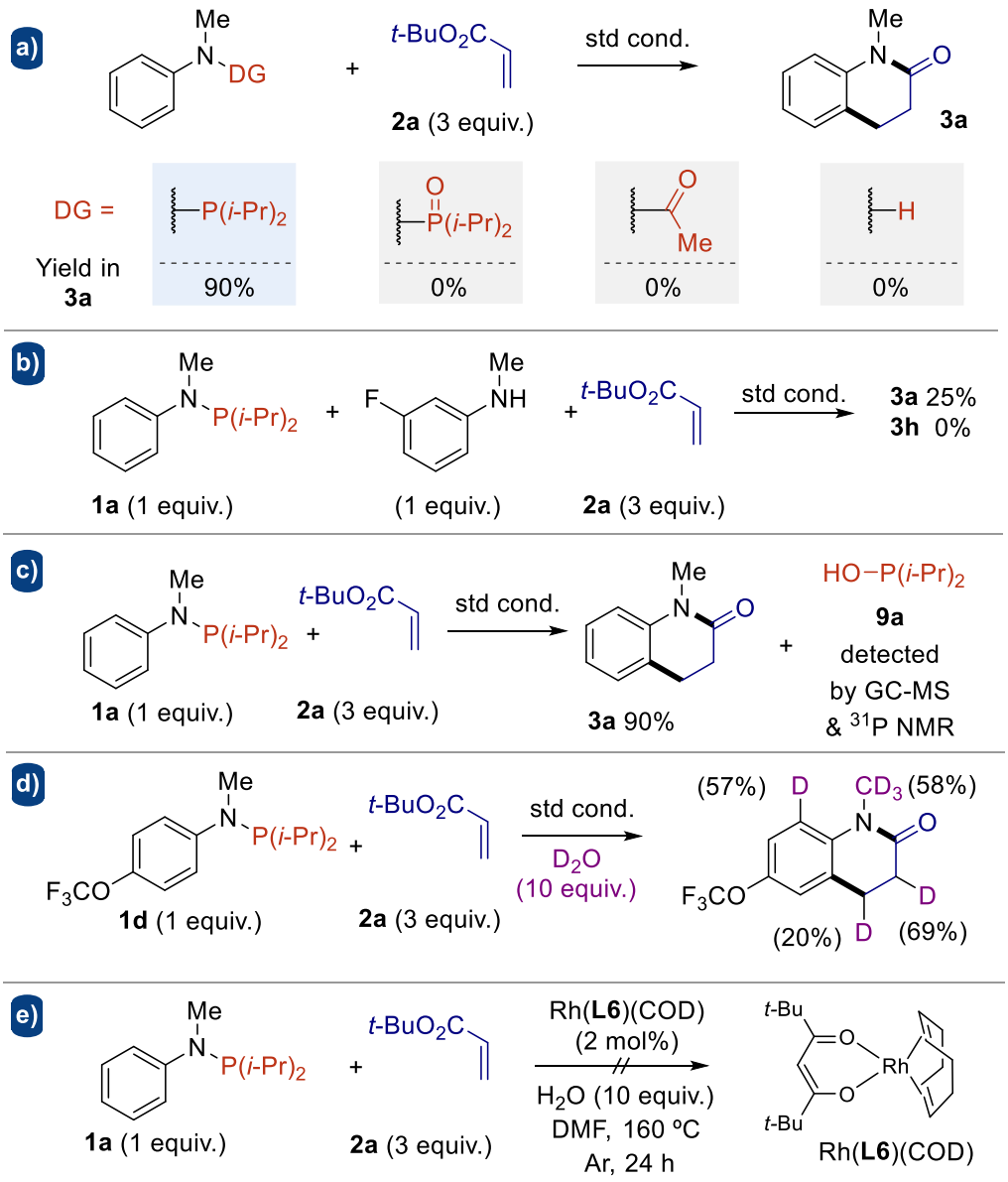

Scheme 2.4. Control and D-Labelling Experiments.

2.3.2. Kinetic Study

We conducted a kinetic study to obtain a better picture of the reaction pathway. First, we plotted the kinetic profile of the reaction by following the consumption of **1a**, the production and consumption of **4a** by ^{31}P NMR, while the production of **3a** was followed by ^{1}H NMR (Figure 2.3). The gaussian-shape kinetic profile of **4a** indicates that $k_1 > k_2$ meaning that **4a** is a latent intermediate of the reaction. However, we could never observe hydrolyzed aniline **10a** during the reaction, possibly due to a spontaneous cyclization affording **3a**. Some *de facto* approximations were formulated. If [**10a**] ≈ 0 during the reaction, then $k_3 \gg k_2$; steps 2 and 3 can be considered as a single operation, and the rate determining step (RDS) is the hydrolysis of N–P(*i*-Pr)$_2$ bond.

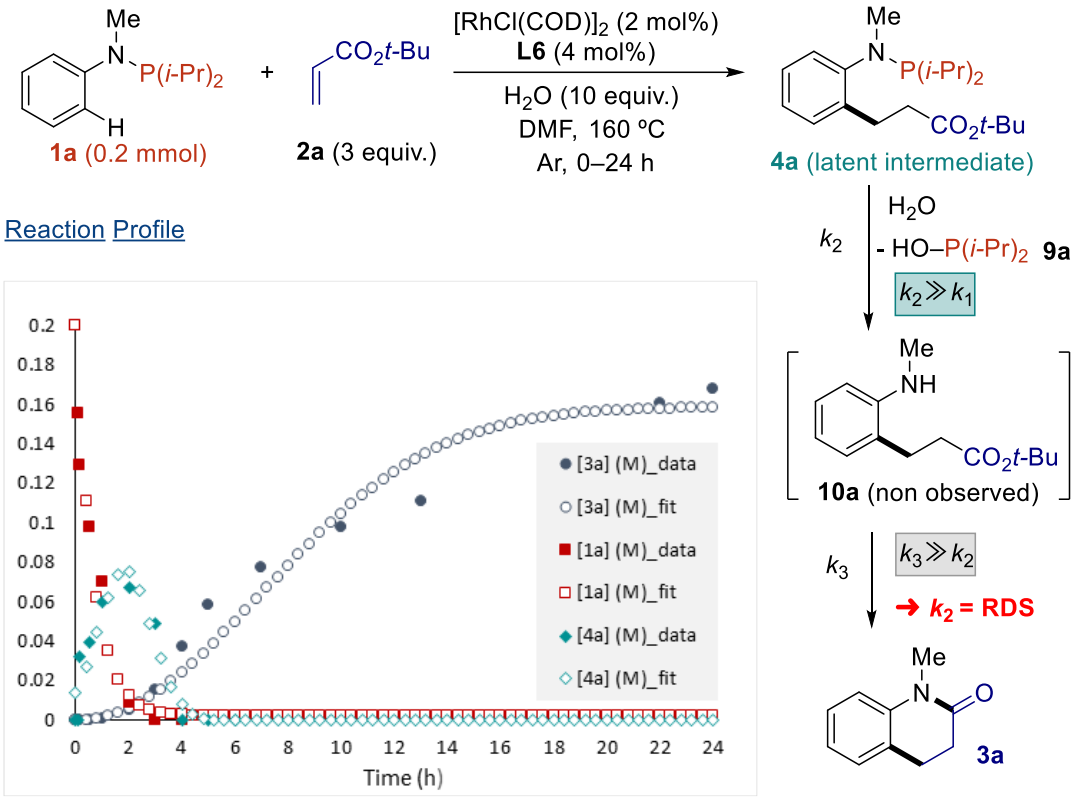

Figure 2.3. Kinetic Reaction Profile.

Our attention next turned toward determining the factors influencing the kinetic efficiency of Rh(I)-catalyzed cascade C(sp^2)–H bond alkylation – amidation of anilines. Reaction progress kinetic analysis revealed that catalyst deactivation was not caused by substrates or product formation, including **9a**. Then, we measured the initial reaction rate for the model reaction as a function of the concentration of water, catalyst, *tert*-butylacrylate (**2a**) and phosphanamine **1a** in DMF at 160 °C. Interestingly, we observed a zero-order dependence on water for the consumption of **1a**, and a first-order dependence for the production of **3a** (Figure 2.4-a). These observations indicate that the water is required for the second step, namely the hydrolysis of N–P(*i*-Pr)$_2$ bond, and its presence (up to 10 equivalents) has a negligible influence on the Rh(I) catalytic activity. In contrast, first-order dependence on Rh/**L6** catalytic system was observed for the consumption of **1a** (Figure 2.4-b). The first-order dependence of the reaction rate on acrylate concentration was obtained from the linear plot of initial rate (Δ[**1a**]/Δt) *vs*. initial acrylate concentration ([**2a**]) (Figure 2.4-c). Saturation kinetics were observed with respect to phosphanamine concentration ([**1a**]) when experiments were carried out by measuring the initial rate over a range of **1a** concentrations (Figure 2.4-d). These data advocate that the phosphanamine reversibly binds to rhodium *via* its phosphorus

atom. Therefore, we suggest that the catalyst might be saturated with phosphanamine as a coordination complex prior to reversible C(sp^2)–H bond cleavage.

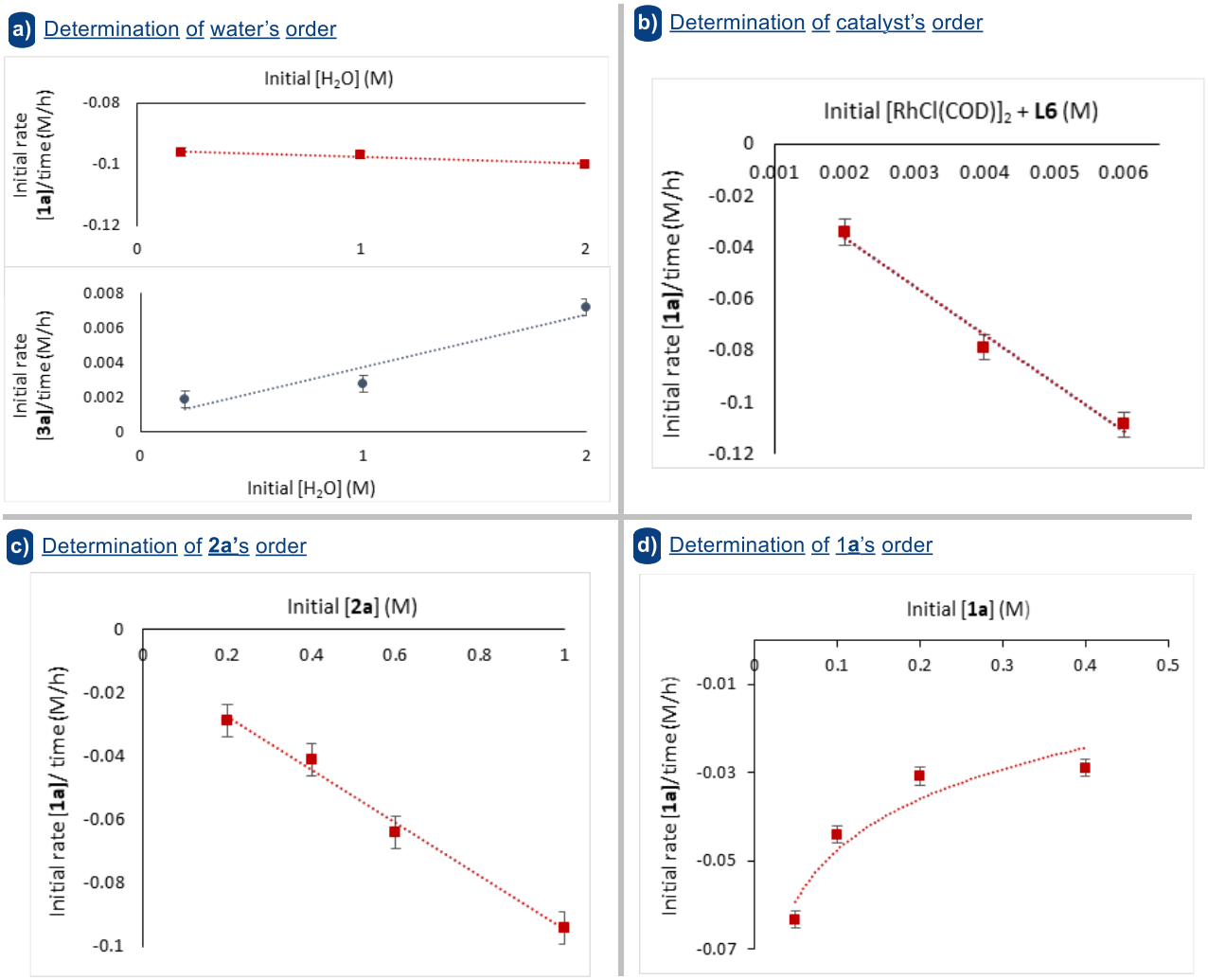

Figure 2.4. Kinetic Order of Reagents.

2.4. Proposed Mechanism

The catalytic cycle depicted in Figure 2.5 could be proposed based on control experiments and the kinetic data. $[RhCl(COD)]_2$ complex reacts with 1 equivalent of phosphanamine **1a** to form the active catalytic specie **I**. However, **I** may react with 2 additional equivalents of **1a** in an inhibitory manner to form resting state rhodium catalyst **II**. Therefore, decoordination of at least 1 molecule of **1a** promoted by **L6** is mandatory to undergo C(sp^2)–H bond activation producing Rh–H complex **III**. Acrylate **2a** may then coordinate **III**, followed by carbo-rhodation to yield **V**. Then, reductive elimination affords **4a** and regenerates the active catalyst after P–Rh exchange with **1a**. In the presence of water, P–N bond of **4a** is hydrolyzed*, in-situ* promoting

the intramolecular amidation to afford the desired dihydroquinolinone **3a** together with phosphinous acid **9a**.

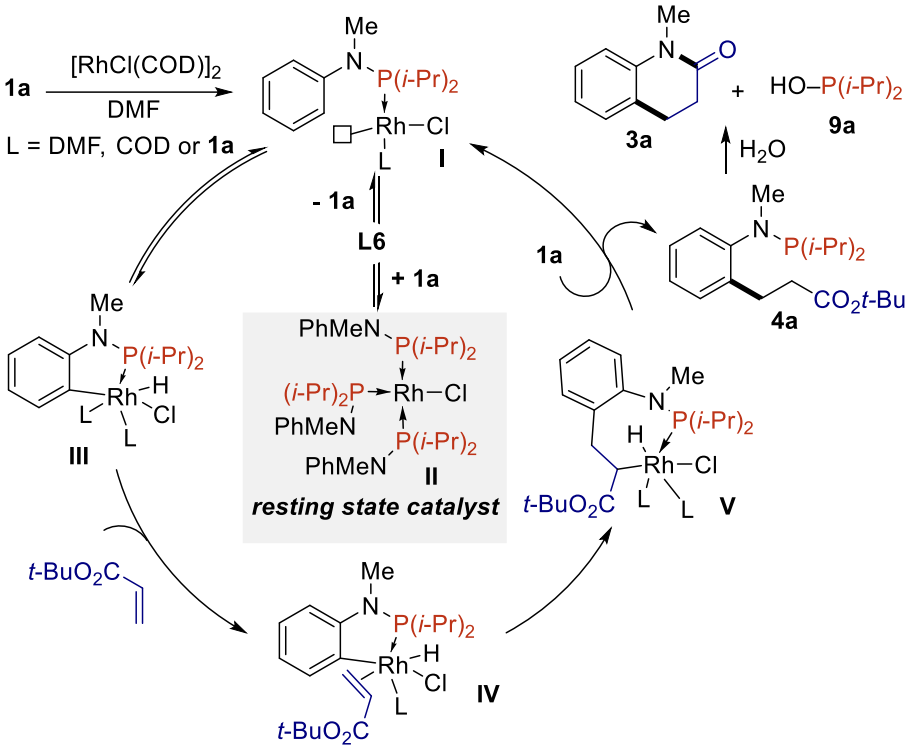

Figure 2.5. Proposed Mechanism.

2.5. Conclusion

We have developed a novel and mild method for the construction of a highly functionalized dihydroquinolinone scaffold based on a cascade reaction of rhodium(I)-catalyzed C(sp^2)–H bond functionalization of phosphamamines with acrylates followed by N–P hydrolysis and intramolecular amidation. The reaction features good substrate scope with respect to both coupling partners. A mechanistic investigation established a viable catalytic cycle that was consistent with the kinetic data obtained. The formal C(sp^2)–H bond alkylation of anilines was also extended to styrene derivatives to afford the corresponding *ortho*-alkylated anilines. Finally, the utility of this protocol was demonstrated by the synthesis of Aripiprazole *N*-methylated analog from easily accessible and cheap *N*-methylaniline. These findings provide a general framework for improving and expanding the scope of rhodium(I)-catalyzed C(sp^2)–H bond activation in synthetic organic chemistry of *N*-heterocycles, and the collected mechanistic insights should benefit in the future development of rhodium(I)-catalyzed P(III)-directed C–H bond activation.

2.6. Experimental Data

2.6.1. General Information

All reactions were carried out under argon atmosphere with standard Schlenk techniques or set up in a glovebox (Mbraun, MB10-Compact). All reagents were obtained from commercial sources and used as supplied unless stated otherwise. *N,N*-Dimethylformamide was distilled with $MgSO_4$ under argon and stored in a glovebox before use. ^{1}H NMR spectra were recorded on Bruker AV III 400 MHz spectrometer fitted with a BBFO probe. Chemical shifts (δ) were reported in parts per million relatives to residual chloroform (7.26 ppm for 1H; 77.16 ppm for 13C). Coupling constants were reported in Hertz. ^{1}H NMR assignment abbreviations were the following: singlet (s), doublet (d), triplet (t), quartet (q), doublet of doublets (dd), doublet of triplets (dt), doublet of doublet of doublets (ddd), multiplet (m). ^{13}C NMR spectra were recorded at 101 MHz on the same spectrometer and reported in ppm. ^{19}F NMR spectra were recorded at 376 MHz on the same spectrometer and reported in ppm. ^{31}P NMR spectra were recorded at 162 MHz on the same spectrometer and reported in ppm.

GC analyses were performed with a gas chromatograph (GC-2014 Shimadzu) instrument equipped with a capillary column (UptibondTM UB5P- 5% phenyl-95% dimethyl polysiloxane), which was coupled to a flame ionization detector (FID). The following GC conditions were used: flow rate (77.7 kPa, N_2), Inject (250 °C), Detect. (280 °C), Int. T. (50 °C), Int. T. (2 min), Rate (20°C /min), Fin. T. (280 °C), Fin. T. (20 min).

Mass spectroscopy were recorded on a Waters Q-Tof 2 mass spectrometer or a Bruker Ultraflex III mass spectrometer at the corresponding facilities of the CRMPO, Centre Régional de Mesures Physiques de l'Ouest, Université de Rennes 1.

Column chromatography was carried out on a Teledyne ISCO CombiFlash NextGen 300 using FlashPure silica flash columns (4, 12, 25 g; 35–45 µm). Substrates were purified using heptane and ethyl acetate on a gradient of 100:0 to 0:100 with flow rates of 13 – 400 mL/min depending on the size of column and ΔRf.

Complex (2,2,6,6-tetramethyl-3,5-heptanedionato)-(1,5- cyclooctadiene) Rh(COD)(**L6**) was already reported and prepared according to the literature.[18]

2.6.2. General Procedure for the Synthesis of Starting Materials 1a-1g and Compounds Characterization

Procedure: To a solution of aniline (1.5 mmol, 1 equiv.) in anhydrous THF (4.5 mL) was added *n*-BuLi (1.1 M in hexanes, 1.6 mL, 1.8 mmol, 1.2 equiv.) dropwise at -78 °C. The reaction was warmed up to room temperature and stirred over 1 h. Then, Cl-P(*i*-Pr)$_2$ (310 µL, 1.95 mmol, 1.6 equiv.) was added dropwise at -78 °C, the mixture was allowed to warm up to room temperature and stirred overnight. The crude product was concentrated and the residue was dissolved in pentane. The precipitate was filtered over celite and pentane was removed under vacuum. Then the product was heated at 60 °C under vacuum over 3 h to remove the excess of Cl-P(*i*-Pr)$_2$ and stored in a glovebox.

1,1-Diisopropyl-*N*-methyl-*N*-phenylphosphanamine (1a)

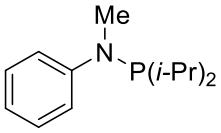

Following the general procedure using *N*-methylaniline (180 µL, 1.5 mmol, 1 equiv.), the product was obtained in 95% yield (318 mg, 1.4 mmol).

^{1}H NMR (400 MHz, $CDCl_3$) δ (ppm) 7.28 – 7.16 (m, 4H), 6.78 (tt, *J* = 6.5, 1.8 Hz, 1H), 2.97 (d, *J* = 1.4 Hz, 3H), 2.08 (heptd, *J* = 7.0, 3.6 Hz, 2H), 1.13 (dd, *J* = 16.7, 6.9 Hz, 6H), 1.03 (dd, *J* = 16.7, 6.9 Hz, 6H).

^{31}P{^{1}H} NMR (162 MHz, $CDCl_3$) δ (ppm) 72.2.

^{13}C NMR (101 MHz, $CDCl_3$) δ (ppm) 153.1 (d, *J* = 20.4 Hz), 128.7 (d, *J* = 1.8 Hz), 118.4 (d, *J* = 1.8 Hz), 116.5 (d, *J* = 16.5 Hz), 34.4 (d, *J* = 7.5 Hz), 26.8 (d, *J* = 15.1 Hz), 19.7 (d, *J* = 10.3 Hz), 19.5 (d, *J* = 25.9 Hz).

1,1-Diisopropyl-*N*-(4-methoxyphenyl)-*N*-methylphosphanamine (1b)

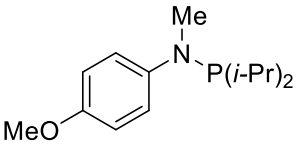

Following the general procedure using 4-methoxy-*N*-methylaniline (206 mg, 1.5 mmol, 1 equiv.), the product was obtained in 70 % yield (266 mg, 1.05 mmol).

^{1}H NMR (400 MHz, $CDCl_3$) δ (ppm) 7.16 – 7.13 (m, 2H), 6.82 – 6.79 (m, 2H), 3.76 (s, 3H), 2.96 (d, *J* = 0.8 Hz, 3H), 2.06 (hetptd, J = 7.2, 3.0 Hz, 2H), 1.15 – 1.03 (m, 12H).

^{31}P{^{1}H} NMR (162 MHz, $CDCl_3$) δ (ppm) 73.9.

^{13}C NMR (101 MHz, $CDCl_3$) δ (ppm) 152.6 (d, *J* = 2.0 Hz), 147.0 (d, *J* = 20.8 Hz), 118.0 (d, *J* = 14.8 Hz), 114.1, 55.7, 34.9 (d, *J* = 7.2 Hz), 26.7 (d, *J* = 15.2 Hz), 19.7 (d, *J* = 10.1 Hz), 19.5 (d, *J* = 25.4 Hz).

1,1-Diisopropyl-*N*-methyl-*N*-(*p*-tolyl)phosphanamine (1c)

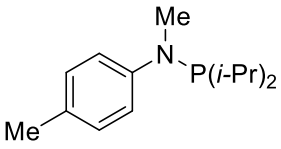

Following the general procedure using *N*-methyl-*para*-toluidine (190 µL, 1.5 mmol, 1 equiv.), the product was obtained in 78% yield (277 mg, 1.17 mmol).

^{1}H NMR (400 MHz, $CDCl_3$) δ (ppm) 7.19 – 7.10 (m, 2H), 7.08 – 6.99 (m, 2H), 2.96 (d, *J* = 1.6 Hz, 3H), 2.27 (s, 3H), 2.08 (heptd, *J* = 7.0, 3.6 Hz, 2H), 1.13 (dd, *J* = 16.6, 7.0 Hz, 6H), 1.04 (dd, *J* = 12.0, 7.0 Hz, 6H).

^{31}P{^{1}H} NMR (162 MHz, $CDCl_3$) δ (ppm) 72.2.

^{13}C NMR (101 MHz, $CDCl_3$) δ (ppm) 150.7 (d, *J* = 20.4 Hz), 129.2 (d, *J* = 1.3 Hz), 127.6 (d, *J* = 1.7 Hz), 116.5 (d, *J* = 15.8 Hz), 34.5 (d, *J* = 7.4 Hz), 26.8 (d, *J* = 15.2 Hz), 20.4, 19.7 (d, *J* = 10.1 Hz), 19.5 (d, *J* = 25.8 Hz).

1,1-Diisopropyl-*N* -(4-(trifluoromethoxy)phenyl)-*N*-methyl-phosphanamine (1d)

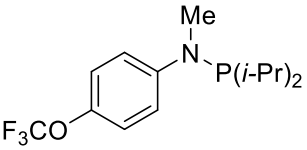

Following the general procedure using *N*-methyl-4-(trifluoromethoxy)aniline (231 µL, 1.5 mmol, 1 equiv.), the product was obtained in 77% yield (355 mg, 1.16 mmol).

^{1}H NMR (400 MHz, $CDCl_3$) δ (ppm) 7.23 – 7.20 (m, 2H), 7.06 – 7.04 (m, 2H), 2.96 (d, *J* = 1.3 Hz, 3H), 2.07 (heptd, J = 7.0, 3.5 Hz, 2H), 1.13 (dd, *J* = 16.8, 7.0 Hz, 4H), 1.03 (dd, *J* = 12.1, 7.0 Hz, 3H).

^{31}P{^{1}H} NMR (162 MHz, $CDCl_3$) δ (ppm) 73.6.

^{19}F{^{1}H} RMN (376 MHz, $CDCl_3$) δ (ppm) -58.3.

^{13}C NMR (101 MHz, $CDCl_3$) δ (ppm) 151.8 (d, *J* = 21.1 Hz), 141.2 (t, *J* = 2.2 Hz), 120.8 (q, *J* = 255.3 Hz), 121.5, 116.7 (d, *J* = 17.1 Hz), 34.4 (d, *J* = 7.8 Hz), 26.8 (d, *J* = 15.3 Hz), 19.7 (d, *J* = 10.0 Hz), 19.4 (d, *J* = 25.7 Hz).

1,1-Diisopropyl-*N*-(4-fluorophenyl) -*N*-methylphosphanamine (1e)

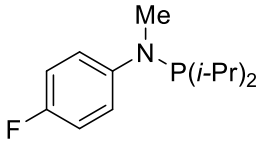

Following the general procedure using 4-fluoro-*N*-methylaniline (180 µL, 1.5 mmol, 1 equiv.), the product was obtained in 85% yield (308 mg, 1.28 mmol).

^{1}H NMR (400 MHz, $CDCl_3$) δ (ppm) 7.22 – 7.15 (m, 2H), 6.96 – 6.88 (m, 2H), 2.96 (d, *J* = 1.5 Hz, 3H), 2.09 (heptd, *J* = 7.0, 3.5 Hz, 2H), 1.15 (dd, *J* = 16.6, 7.0 Hz, 6H), 1.06 (dd, *J* = 12.0, 7.0 Hz, 6H).

^{31}P{^{1}H} NMR (162 MHz, $CDCl_3$) δ(ppm) 74.1.

^{19}F{^{1}H} NMR (376 MHz, $CDCl_3$) δ (ppm) -127.0.

^{13}C NMR (101 MHz, $CDCl_3$) δ (ppm) 156.2 (dd, *J* = 237.0, 2.4 Hz), 149.3 (dd, *J* = 21.0, 2.1 Hz), 117.4 (dd, *J* = 16.0, 7.3 Hz), 114.8 (d, *J* = 21.8 Hz), 34.5 (d, *J* = 7.6 Hz), 26.7 (d, *J* = 15.2 Hz), 19.6 (d, *J* = 10.1 Hz), 19.3 (d, *J* = 25.7 Hz).

_N_-(4-Chlorophenyl)-1,1-diisopropyl-_N_-methylphosphanamine (1f)

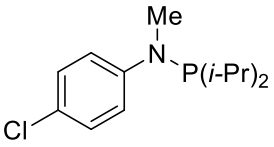

Following the general procedure using 4-chloro-*N*-methylaniline (181 µL, 1.5 mmol, 1 equiv.), the product was obtained in 85% yield (329 mg, 1.28 mmol).

^{1}H NMR (400 MHz, $CDCl_3$) δ (ppm) 7.34 – 7.05 (m, 4H), 2.94 (d, *J* = 1.3 Hz, 3H), 2.08 (heptd, *J* = 7.0, 3.5 Hz, 2H), 1.15 (dd, *J* = 16.8, 7.0 Hz, 6H), 1.04 (dd, *J* = 12.1, 7.0 Hz, 6H).

^{31}P{^{1}H} NMR (162 MHz, $CDCl_3$) δ (ppm) 73.0.

^{13}C NMR (101 MHz, $CDCl_3$) δ (ppm) 151.6 (d, *J* = 20.9 Hz), 128.3 (d, *J* = 1.5 Hz), 123.0 (d, *J* = 2.8 Hz), 117.2 (d, *J* = 17.1 Hz), 34.2 (d, *J* = 7.7 Hz), 26.6 (d, *J* = 15.4 Hz), 19.5 (d, *J* = 10.1 Hz), 19.3 (d, *J* = 25.9 Hz).

_N_-(4-Bromophenyl)-1,1-diisopropyl-_N_-methylphosphanamine (1g)

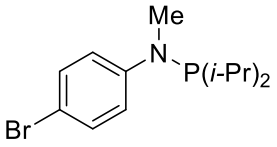

Following the general procedure using 4-bromo-*N*-methylaniline (170 µL, 1.5 mmol, 1 equiv.), the product was obtained in 80% yield (361 mg, 1.2 mmol).

^{1}H NMR (400 MHz, $CDCl_3$) δ (ppm) 7.32 – 7.26 (m, 2H), 7.17 – 7.12 (m, 2H), 2.95 (d, *J* = 1.2 Hz, 3H), 2.09 (heptd, *J* = 7.0, 3.6 Hz, 2H), 1.14 (dd, *J* = 16.8, 6.9 Hz, 6H), 1.03 (dd, *J* = 12.1, 7.0 Hz, 6H).

^{31}P{^{1}H} NMR (162 MHz, $CDCl_3$) δ (ppm) 72.9.

^{13}C NMR (101 MHz, $CDCl_3$) δ (ppm) 148.4, 131.9, 114.0, 108.8, 30.8, 25.5, 24.8, 16.3, 15.1 (d, *J* = 3.2 Hz).

1,1-Diisopropyl- _N_-(3-fluorophenyl)-_N_-methylphosphanamine (1h)

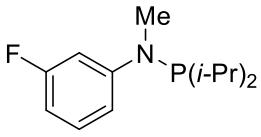

Following the general procedure using 3-fluoro-*N*-methylaniline (170 µL, 1.5 mmol, 1 equiv.), the product was obtained in 63% yield (228 mg, 0.95 mmol).

^{1}H NMR (400 MHz, $CDCl_3$) δ (ppm) 7.13 (td, *J* = 8.2, 7.0 Hz, 1H), 7.07 – 6.91 (m, 2H), 6.46 (tdd, *J* = 8.2, 2.4, 0.9 Hz, 1H), 2.94 (d, *J* = 1.2 Hz, 3H), 2.08 (heptd, *J* = 7.0, 3.6 Hz, 2H), 1.13 (dd, *J* = 16.8, 6.9 Hz, 6H), 1.02 (dd, *J* = 16.8, 6.9 Hz, 6H).

$^{31}P\{^{1}H\}$ NMR (162 MHz, $CDCl_3$) δ (ppm) 72.7.

$^{19}F\{^{1}H\}$ RMN (376 MHz, $CDCl_3$) δ (ppm) -113.0 (dd, *J* = 13.6, 7.0 Hz).

^{13}C NMR (101 MHz, $CDCl_3$) δ (ppm) 163.6 (dd, *J* = 241.9, 1.6 Hz), 155.0 (dd, *J* = 21.5, 10.4 Hz), 130.0 (dd, *J* = 10.1, 1.6 Hz), 111.7 (dd, *J* = 18.0, 2.4 Hz), 104.7 (dd, *J* = 21.6, 1.5 Hz), 103.1 (dd, *J* = 25.8, 17.3 Hz), 34.3 (d, *J* = 7.7 Hz), 26.7 (d, *J* = 15.5 Hz), 19.5 (d, *J* = 10.1 Hz), 19.3 (d, *J* = 26.1 Hz).

***N*-(3-Chlorophenyl)-1,1-diisopropyl-*N*-methylphosphanamine (1i)**

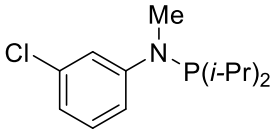

Following the general procedure using 3-chloro-*N*-methylaniline (181 µL, 1.5 mmol, 1 equiv.), the product was obtained in 72% yield (278 mg, 1.08 mmol).

^{1}H NMR (400 MHz, $CDCl_3$) δ (ppm) 7.24 – 7.06 (m, 3H), 6.74 (dd, *J* = 7.6, 1.9, 1.1 Hz, 1H), 2.93 (d, *J* = 1.2 Hz, 3H), 2.07 (heptd, *J* = 7.0, 3.6 Hz, 2H), 1.12 (dd, *J* = 16.8, 7.0 Hz, 6H), 1.01 (dd, *J* = 16.8, 7.0 Hz, 6H).

$^{31}P\{^{1}H\}$ NMR (162 MHz, $CDCl_3$) δ (ppm) 72.8.

^{13}C NMR (101 MHz, $CDCl_3$) δ (ppm) 154.4 (d, *J* = 21.0 Hz), 134.6, 129.5 (d, *J* = 1.7 Hz), 118.2 (d, *J* = 1.6 Hz), 116.0 (d, *J* = 16.6 Hz), 115.0 (d, *J* = 18.6 Hz), 34.3 (d, *J* = 7.8 Hz), 26.8 (d, *J* = 15.4 Hz), 19.7 (d, *J* = 10.1 Hz), 19.4 (d, *J* = 26.0 Hz).

1,1-Diisopropyl-*N*-(3-methoxyphenyl)-*N*-methylphosphanamine (1j)

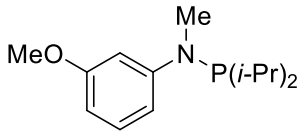

Following the general procedure using 3-methoxy-*N*-methylaniline (206 mg, 1.5 mmol, 1 equiv.), the product was obtained in 80% yield (304 mg, 1.2 mmol).

^{1}H NMR (400 MHz, $CDCl_3$) δ 7.11 (t, *J* = 8.2 Hz, 1H), 6.89 (dt, *J* = 8.3, 2.4 Hz, 2H), 6.80 (q, *J* = 2.5 Hz, 1H), 6.35 (dd, *J* = 8.0, 2.3 Hz, 1H), 3.79 (s, 3H), 2.95 (d, *J* = 1.2 Hz, 3H), 2.07 (heptd, *J* = 7.0, 3.5 Hz, 2H), 1.12 (dd, *J* = 16.7, 6.9 Hz, 7H), 1.02 (dd, *J* = 12.0, 7.0 Hz, 7H).

$^{31}P\{^{1}H\}$ NMR (162 MHz, $CDCl_3$) δ (ppm) 72.0.

^{13}C NMR (101 MHz, $CDCl_3$) δ (ppm) 160.3, 154.5 (d, *J* = 20.7 Hz), 129.2, 109.4 (d, *J* = 17.8 Hz), 103.3, 102.7 (d, *J* = 16.7 Hz), 55.3, 34.5 (d, *J* = 7.5 Hz), 26.8 (d, *J* = 15.5 Hz), 19.7 (d, *J* = 10.1 Hz), 19.5 (d, *J* = 26.1 Hz).

1,1-Diisopropyl-*N*-ethyl-*N*-(*m*-tolyl)phosphanamine (1k)

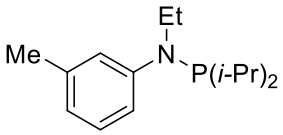

Following the general procedure using *N*-ethyl-*meta*-toluidine (190 µL, 1.5 mmol, 1 equiv.), the product was obtained in 90% yield (339 mg, 1.35 mmol).

^{1}H NMR (400 MHz, $CDCl_3$) δ 7.09 (t, *J* = 7.8 Hz, 1H), 7.03 – 6.92 (m, 2H), 6.63 (d, *J* = 7.4 Hz, 1H), 3.52 (qd, *J* = 7.0, 2.6 Hz, 2H), 2.30 (s, 3H), 2.09 (heptd, *J* = 7.0, 3.1 Hz, 2H), 1.15 – 1.05 (m, 15H).

^{31}P{^{1}H} NMR (162 MHz, $CDCl_3$) δ (ppm) 80.9.

^{13}C NMR (101 MHz, $CDCl_3$) δ (ppm) 150.1 (d, *J* = 17.1 Hz), 137.9, 128.2, 120.3, 120.1, 116.3 (d, *J* = 12.3 Hz), 42.1, 26.7 (d, *J* = 16.6 Hz), 21.7, 19.7 (d, *J* = 11.3 Hz), 19.4 (d, *J* = 24.9 Hz), 14.0.

***N*-(3,5-Difluorophenyl)-1,1-diisopropyl-*N*-methylphosphanamine (1l)**

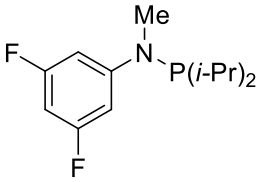

Following the general procedure using 3,5-difluoro-*N*-methylaniline (176 µL, 1.5 mmol, 1 equiv.), the product was obtained in 75% yield (291 mg, 1.13 mmol).

^{1}H NMR (400 MHz, $CDCl_3$) δ (ppm) 6.79 – 6.75 (m, 2H), 6.20 (tt, *J* = 8.9, 2.2 Hz, 1H), 2.90 (d, *J* = 1.0 Hz, 2H), 2.06 (heptd, *J* = 10.5, 7.0, 3.5 Hz, 1H), 1.12 (dd, *J* = 17.0, 6.9 Hz, 4H), 1.00 (dd, *J* = 12.2, 7.0 Hz, 4H).

^{31}P{^{1}H} NMR (162 MHz, $CDCl_3$) δ (ppm) 73.2.

^{19}F{^{1}H} RMN (376 MHz, $CDCl_3$) δ (ppm) -110.7.

^{13}C NMR (101 MHz, $CDCl_3$) δ (ppm) 163.6 (ddd, *J* = 242.7, 16.1, 1.8 Hz), 155.6 (dt, *J* = 22.9, 12.9 Hz), 98.7 (dd, *J* = 29.3, 18.7 Hz), 93.3 (t, *J* = 26.2 Hz), 34.3 (d, *J* = 8.0 Hz), 26.7 (d, *J* = 15.5 Hz), 19.6 (d, *J* = 10.2 Hz), 19.3 (d, *J* = 26.1 Hz).

1,1-Diisopropyl-*N*-(2-fluorophenyl)-*N*-methylphosphanamine (**1m**)

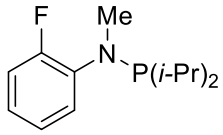

Following the general procedure using 2-fluoro-*N*-methylaniline (180 µL, 1.5 mmol, 1 equiv.), the product was obtained in 90% yield (325 mg, 1.35 mmol).

^{1}H NMR (400 MHz, $CDCl_3$) δ (ppm) 7.20 (tt, *J* = 8.2, 1.9 Hz, 1H), 7.04 – 6.81 (m, 3H), 3.01 (dd, *J* = 2.6, 1.6 Hz, 3H), 2.07 (heptd, *J* = 7.0, 3.3 Hz, 2H), 1.32 – 0.98 (m, 12H).

^{31}P{^{1}H} NMR (162 MHz, $CDCl_3$) δ (ppm) 84.0 (d, *J* = 32.6 Hz).

^{19}F{^{1}H} NMR (376 MHz, $CDCl_3$) δ (ppm) -120.4 (d, *J* = 32.4 Hz).

^{13}C NMR (101 MHz, $CDCl_3$) δ (ppm) 156.9 (dd, *J* = 245.9, 3.5 Hz), 141.4 (dd, *J* = 20.9, 9.0 Hz), 126.1 (dd, *J* = 12.4, 3.3 Hz), 124.1 (d, *J* = 3.4 Hz), 122.8 (dd, *J* = 7.7, 1.7 Hz), 116.4 (d, *J* = 21.2 Hz), 36.6 (t, *J* = 5.7 Hz), 26.5 (d, *J* = 15.5 Hz), 19.7 (d, *J* = 10.0 Hz), 19.3 (d, *J* = 24.4 Hz).

1,1-Diisopropyl-*N*-ethyl-*N*-phenylphosphanamine (1n)

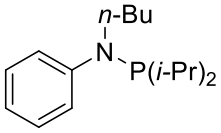

Following the general procedure using *N*-butylaniline (240 µL, 1.5 mmol, 1 equiv.), the product was obtained in 87% yield (346 mg, 1.31 mmol).

^{1}H NMR (400 MHz, $CDCl_3$) δ (ppm) 7.26 – 7.13 (m, 4H), 3.47 – 3.41 (m, 2H), 2.12 (heptd, *J* = 7.0, 3.5 Hz, 2H), 1.58 – 1.47 (m, 2H), 1.32 (dt, *J* = 14.4, 7.3 Hz, 2H), 1.20 – 1.03 (m, 12H), 0.94 (t, *J* = 7.3 Hz, 3H).

^{31}P{^{1}H} NMR (162 MHz, $CDCl_3$) δ (ppm) 82.0.

^{13}C NMR (101 MHz, $CDCl_3$) δ (ppm) 150.7 (d, *J* = 16.3 Hz), 128.6, 119.5 (d, *J* = 12.4 Hz), 112.7, 32.0, 26.9 (d, *J* = 16.5 Hz), 22.8, 20.6, 19.9 (d, *J* = 11.3 Hz), 19.5 (d, *J* = 24.7 Hz), 14.2.

1,1-Diisopropyl-*N*-ethyl-*N*-phenylphosphanamine (1o)

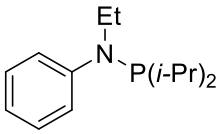

Following the general procedure using *N*-ethylaniline (189 µL, 1.5 mmol, 1 equiv.), the product was obtained in 90 % yield (320 mg, 1.35 mmol).

^{1}H NMR (400 MHz, $CDCl_3$) δ (ppm) 7.24 – 7.12 (m, 4H), 6.84 – 6.78 (m, 1H), 3.54 (qd, *J* = 7.0, 2.7 Hz, 2H), 2.10 (heptd, *J* = 7.0, 3.5 Hz, 2H), 1.17 – 1.04 (m, 15H).

^{31}P{^{1}H} NMR (162 MHz, $CDCl_3$) δ (ppm) 81.4.

^{13}C NMR (101 MHz, $CDCl_3$) δ (ppm) 150.3 (d, *J* = 17.0 Hz), 128.7, 119.5 (d, *J* = 12.8 Hz), 119.3 (d, *J* = 1.7 Hz), 42.5, 26.9 (d, *J* = 16.4 Hz), 19.9 (d, *J* = 11.1 Hz), 19.6 (d, *J* = 24.8 Hz), 14.1.

1,1-Diisopropyl-*N*-ethyl-*N*-(*p*-tolyl)phosphanamine (1p)

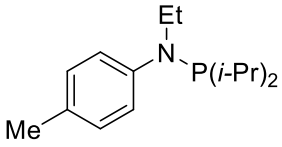

Following the general procedure using *N*-ethyl-*para*-toluidine (190 µL, 1.5 mmol, 1 equiv.), the product was obtained in 88% yield (332 mg, 1.32 mmol).

^{1}H NMR (400 MHz, $CDCl_3$) δ (ppm) 7.10 – 6.98 (m, 4H), 3.52 (qd, *J* = 7.0, 2.9 Hz, 2H), 2.26 (s, 3H), 2.08 (heptd, *J* = 7.0, 3.0 Hz, 2H), 1.17 – 1.04 (m, 15H).

^{31}P{^{1}H} NMR (162 MHz, $CDCl_3$) δ (ppm) 81.4.

^{13}C NMR (101 MHz, $CDCl_3$) δ (ppm) 147.8 (d, *J* = 16.5 Hz), 129.3, 128.7 (d, *J* = 1.7 Hz), 119.8 (d, *J* = 11.9 Hz), 42.8, 26.9 (d, *J* = 16.2 Hz), 20.6, 19.9 (d, *J* = 11.1 Hz), 19.6 (d, *J* = 24.7 Hz), 14.2.

1-(Diisopropylphosphaneyl)-1,2,3,4-tetrahydroquinoline (1q)

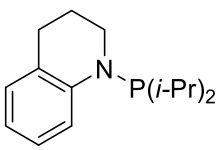

Following the general procedure using 1,2,3,4-tetrahydroquinolinone (189 µL, 1.5 mmol, 1 equiv.), the product was obtained in 64% yield (239 mg, 0.96 mmol).

^{1}H RMN (400 MHz, $CDCl_3$) δ (ppm) 7.72 (s, 1H), 7.07 – 6.98 (m, 2H), 6.70 – 6.60 (m, 1H), 3.37 (t, *J* = 5.5 Hz, 2H), 2.78 (t, *J* = 6.5 Hz, 2H), 2.14 (q, *J* = 9.7 Hz, 2H), 1.91 (p, *J* = 6.4 Hz, 2H), 1.19 – 1.03 (m, 12H).

^{31}P{^{1}H} RMN (162 MHz, $CDCl_3$) δ (ppm) 64.0.

^{13}C NMR (101 MHz, $CDCl_3$) δ (ppm) 129.6 (d, *J* = 1.3 Hz), 126.3 (d, *J* = 2.6 Hz), 124.1, 117.6, 117.3, 117.0, 28.2, 25.8 (d, *J* = 15.3 Hz), 23.1, 19.9 (d, *J* = 10.8 Hz), 19.6 (d, *J* = 25.5 Hz).

2.6.3. Optimization of the Reaction Conditions

Procedure: In a glovebox, an oven-dried Schlenk tube was charged with phosphanamine **1a** (44 mg, 0.2 mmol, 1 equiv.). Then the Schlenk tube was closed and removed from the glovebox. Under argon atmosphere, the catalyst (0.004 mmol, 2 mol%), additive (n. equiv.), *tert*-butyl acrylate **2a** (87 µL, 0.6 mmol, 3 equiv.) and solvent (1 mL) were added. The resulting mixture was stirred at 160 °C over 24h. The crude product was then cooled down, diluted with ethyl acetate and injected in a calibrated GC-FID using *n*-dodecane (10 µL) as an internal standard to give the corresponding yields: t_R (min) 8.2 (*n*-dodecane), 10.7 (product **3a**).

Table 2.2. Screening of Solvents.

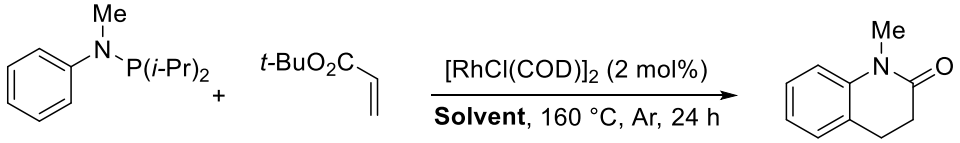

1a **2a** **3a**

Entry	Solvent	Yield **3a** (%)
1	Toluene	42[a]
2	Xylene	29[a]
3	1,2-Dichloroethane	24
4	Dimethyl carbonate	35
5	*N,N*-Dimethylformamide	40
6	*N,N*-Dimethylacetamide	27
7	1,4-Dioxane	12[a]

[a]Yield obtained after acid hydrolysis HCl 1 N at 80 °C.

Table 2.3. Screening of Additives and Catalysts.

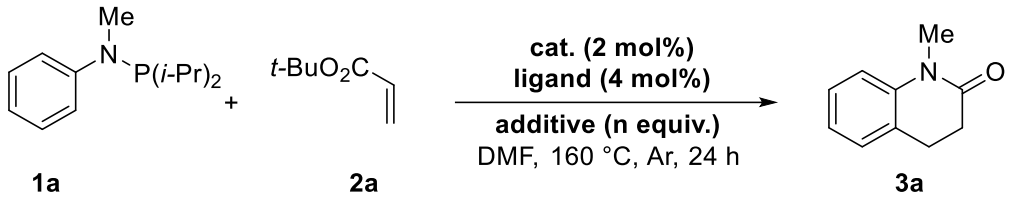

1a **2a** **3a**

Entry	Catalyst	Additive or Ligand	Yield **3a** (%)
1	$[RhCl(COD)]_2$	-	40
2	$[RhCl(COD)]_2$	NaOAc (30 mol%)	30
3	$[RhCl(COD)]_2$	$AlMe_3$ (20 mol%)	34
4	$[RhCl(COD)]_2$	*N*-acetyl-DL alanine (**L1**)	54
5	$[RhCl(COD)]_2$	*N*-acetyl-DL leucine	38
6	$[RhCl(COD)]_2$	PPh_3	30
7	$[RhCl(COD)]_2$	Dppb (**L2**)	36
8	$[RhCl(COD)]_2$	BINOL (**L3**)	46
9	$[RhCl(COD)]_2$	Bathophenanthroline	32
10	$[RhCl(COD)]_2$	Acetylacetone (**L4**)	45
11	$[RhCl(COD)]_2$	1,1,1-Trifluoropentane-2,4-dione (**L5**)	22
12	$[RhCl(COD)]_2$	2,2,6,6-Tetramethylheptane-3,5-dione (**L6**)	58
13	$[IrCl(COD)]_2$	2,2,6,6-Tetramethylheptane-3,5-dione (**L6**)	22
14	$[Rh(Cp^*)Cl_2]_2$	2,2,6,6-Tetramethylheptane-3,5-dione (**L6**)	n.d.[a]
15	$[Ru(p\text{-Cymene})Cl_2]_2$	2,2,6,6-Tetramethylheptane-3,5-dione (**L6**)	n.d.[a]
16	$[Rh(OAc)(COD)]_2$	2,2,6,6-Tetramethylheptane-3,5-dione (**L6**)	traces
17	$[RhCl(NBD)]_2$	2,2,6,6-Tetramethylheptane-3,5-dione (**L6**)	45
18	$[RhCl(COE)_2]_2$	2,2,6,6-Tetramethylheptane-3,5-dione (**L6**)	39
19	$[RhOH(COD)]_2$	2,2,6,6-Tetramethylheptane-3,5-dione (**L6**)	17
20	Rh(acac)(COD)	2,2,6,6-Tetramethylheptane-3,5-dione (**L6**)	17
21	$[Rh(OMe)(COD)]_2$	2,2,6,6-Tetramethylheptane-3,5-dione (**L6**)	32
22	$RhCl(PPh_3)_3$	2,2,6,6-Tetramethylheptane-3,5-dione (**L6**)	17

[a]Reaction set up in presence of $AgSbF_6$ (8 mol%) as additive.

Table 2.4. Control of Water Amount.

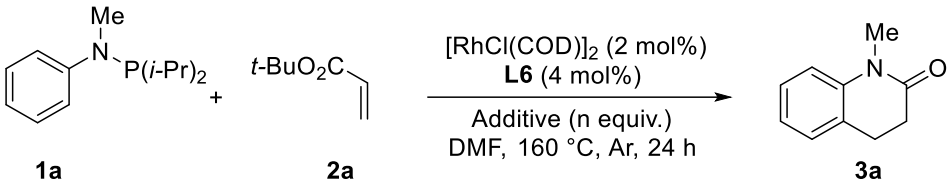

1a **2a** **3a**

Entry	Additive (n equiv.)	Yield **3a** (%)
1	MS 4 Å (50 mg)	58
2	H_2O (1)	60
3	H_2O (2)	62
4	H_2O (4)	67
5	H_2O (6)	75
6	H_2O (8)	77
7	H_2O (10)	90 (81)
8	H_2O (20)	54
9	H_2O (10)	35[a]

[a]Reaction was performed without **L6**. Isolated yield is shown in parentheses.

2.6.4. Representative Procedure for the Synthesis of 3a-3s and Compounds Characterization

Procedure: In a glovebox, an oven-dried Schlenk tube was charged with *N*-arylphosphanamines **1** (0.3 mmol, 1 equiv.) and distilled DMF (1.5 mL). Then, the Schlenk tube was closed and removed from the glovebox. Under argon atmosphere, $[RhCl(COD)]_2$ (3 mg, 0.006 mmol, 2 mol%), 2,2,6,6-tetramethylheptane-3,5-dione **L6** (3 µL, 0.012 mmol, 4 mol%), water (54 µL, 3 mmol, 10 equiv.) and acrylate derivative **2** (0.9 mmol, 3 equiv.) were added. The resulting mixture was stirred at 160 °C over 24 h. The crude product was purified on flash chromatography on silica gel using heptane and ethyl acetate as eluents to provide the pure products.

1-Methyl-3,4-dihydroquinolin-2(1H)-one (3a)

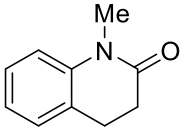

Following the general procedure using **1a** (67 mg, 0.3 mmol, 1 equiv.) and *tert*-butyl acrylate **2a** (131 µL, 0.9 mmol, 3 equiv.), the residue was purified

by flash chromatography on silica gel (Heptane/Ethyl Acetate = 80:20) to afford **3a** as a white solid in 81% yield (39 mg, 0.24 mmol).

^{1}H NMR (400 MHz, $CDCl_3$) δ (ppm) 7.27 – 7.21 (m, 1H), 7.16 – 7.13 (m, 1H), 7.03 – 6.94 (m, 2H), 3.34 (s, 3H), 2.93 – 2.83 (m, 2H), 2.68 – 2.55 (m, 2H).

^{13}C NMR (101 MHz, $CDCl_3$) δ (ppm) 170.6, 140.8, 127.8, 127.6, 126.4, 122.9, 114.8, 31.9, 29.7, 25.5.

HRMS m/z (ESI) calcd for $C_{10}H_{11}NONa$ $[M+Na]^+$ 184.0733, found 184.0733.

6-Methoxy-1-methyl-3,4-dihydroquinolin-2(1H)-one (3b)

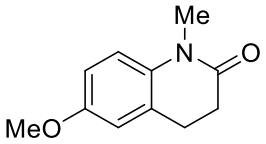

Following the general procedure using **1b** (76 mg, 0.3 mmol, 1 equiv.) and *tert*-butyl acrylate **2a** (131 µL, 0.9 mmol, 3 equiv.), the residue was purified by flash chromatography on silica gel (Heptane/Ethyl Acetate = 80:20) to afford **3b** as a yellow oil in 78% yield (45 mg, 0.23 mmol).

^{1}H RMN (400 MHz, $CDCl_3$) δ (ppm) 6.90 (d, *J* = 8.7 Hz, 1H), 6.78 (dd, *J* = 8.7, 2.9 Hz, 1H), 6.73 (d, *J* = 2.9 Hz, 1H), 3.79 (s, 3H), 3.33 (s, 3H), 2.91 – 2.84 (m, 2H), 2.66 – 2.59 (m, 2H).

^{13}C RMN (101 MHz, $CDCl_3$) δ (ppm) 170.2, 155.4, 134.4, 127.9, 115.7, 114.0, 112.0, 55.7, 31.9, 29.8, 25.8.

HRMS m/z (ESI) calcd for $C_{11}H_{13}NO_2Na$ $[M+Na]^+$ 214,0839 found 214.0839.

1,6-Dimethyl-3,4-dihydroquinolin-2(1H)-one (3c)

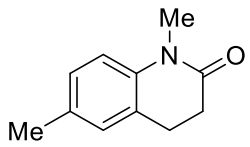

Following the general procedure using **1c** (71 mg, 0.3 mmol, 1 equiv.) and *tert*-butyl acrylate **2a** (131 µL, 0.9 mmol, 3 equiv.), the residue was purified by flash chromatography on silica gel (Heptane/Ethyl Acetate = 80:20) to afford **3c** as an orange oil in 79 % yield (41 mg, 0.24 mmol).

^{1}H RMN (400 MHz, $CDCl_3$) δ (ppm) 7.05 (d, *J* = 8.2 Hz, 1H), 6.98 (s, 1H), 6.86 (d, *J* = 8.2 Hz, 1H), 3.33 (s, 3H), 2.90 – 2.80 (m, 2H), 2.69 – 2.59 (m, 2H), 2.30 (s, 3H).

^{13}C RMN (101 MHz, $CDCl_3$) δ (ppm) 170.4, 138.3, 132.3, 128.5, 127.8, 126.1, 114.6, 31.8, 29.5, 25.4, 20.6.

HRMS m/z (ESI) calcd for $C_{11}H_{13}NONa$ $[M+Na]^+$ 198.0889, found 198.0889.

1-Methyl-6-(trifluoromethoxy)-3,4-dihydroquinolin-2(1H)-one (3d)

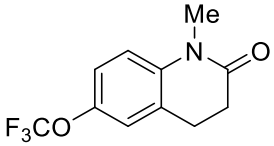

Following the general procedure using **1d** (92 mg, 0.3 mmol, 1 equiv.) and *tert*-butyl acrylate **2a** (131 µL, 0.9 mmol, 3 equiv.), the residue was

purified by flash chromatography on silica gel (Heptane/Ethyl Acetate = 80:20) to afford **3d** as a yellow oil in 60% yield (44 mg, 0.18 mmol).

^{1}H RMN (400 MHz, $CDCl_3$) δ (ppm) 7.13 – 7.07 (m, 1H), 7.03 (s, 1H), 6.95 (d, *J* = 8.8 Hz, 1H), 3.34 (s, 3H), 2.93 – 2.87 (m, 2H), 2.67 – 2.62 (m, 2H).

^{19}F{1H} RMN (376 MHz, $CDCl_3$) δ (ppm) -58.2.

^{13}C RMN (101 MHz, $CDCl_3$) δ (ppm) 170.1, 144.3 (d, *J* = 2.1 Hz), 139.5, 128.0, 120.7, 120.0, 119.9 (q, *J* = 256.2 Hz), 115.6, 31.4, 29.8, 25.4.

HRMS m/z (ESI) calcd for $C_{11}H_{10}NO_2F_3Na$ $[M+Na]^+$ 268.0556, found 268.0557.

6-Fluoro-1-methyl-3,4-dihydroquinolin-2(1H)-one (3e)

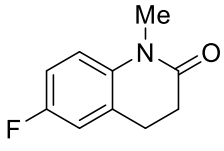

Following the general procedure using **1e** (72 mg, 0.3 mmol, 1 equiv.) and *tert*-butyl acrylate (131 µL, 0.9 mmol, 3 equiv.), the residue was purified by flash chromatography on silica gel (Heptane/Ethyl Acetate = 80:20) to afford **3e** as an orange solid in 85% yield (46 mg, 0.25 mmol).

^{1}H NMR (400 MHz, $CDCl_3$) δ (ppm) 6.96 – 6.85 (m, 3H), 3.34 (s, 3H), 2.84 (m, 2H), 2.68 – 2.56 (m, 2H).

^{19}F{^{1}H} NMR (376 MHz, $CDCl_3$) δ (ppm) -121.0.

^{13}C NMR (101 MHz, $CDCl_3$) δ (ppm) 170.1, 158.6 (d, *J* = 242.9 Hz), 128.4 (d, *J* = 7.6 Hz), 115.9 (d, *J* = 8.1 Hz), 114.9 (d, *J* = 22.9 Hz), 113.8, 113.6, 31.6, 29.9, 25.6.

HRMS m/z (ESI) calcd for $C_{10}H_{10}NOFNa$ $[M+Na]^+$ 202.0639, found 202.0640.

6-Chloro-1-methyl-3,4-dihydroquinolin-2(1H)-one (3f)

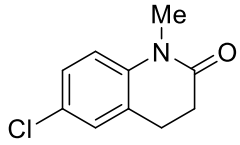

Following the general procedure using **1f** (77 mg, 0.3 mmol, 1 equiv.) and *tert*-butyl acrylate **2a** (131 µL, 0.9 mmol, 3 equiv.), the residue was purified by flash chromatography on silica gel (Heptane/Ethyl Acetate = 80:20) to afford **3f** as an orange solid in 78% yield (46 mg, 0.23 mmol).

^{1}H NMR (400 MHz, $CDCl_3$) δ (ppm) 7.21 (dd, *J* = 8.6, 2.4 Hz, 1H), 7.15 (s, 1H), 6.89 (d, *J* = 8.6 Hz, 1H), 3.33 (s, 3H), 2.91 – 2.83 (m, 2H), 2.70 – 2.58 (m, 2H).

^{13}C NMR (101 MHz, $CDCl_3$) δ (ppm) 170.2, 139.4, 128.1, 128.0, 127.8, 127.4, 115.9, 31.5, 29.8, 25.3.

HRMS m/z (ESI) calcd for $C_{10}H_{10}NOClNa$ $[M+Na]^+$ 218.0343, found 218.0343.

7-Fluoro-1-methyl-3,4-dihydroquinolin-2(1H)-one (3h)

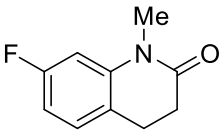

Following the general procedure using **1h** (72 mg, 0.3 mmol, 1 equiv.) and *tert*-butyl acrylate **2a** (131 µL, 0.9 mmol, 3 equiv.), the residue was purified by flash chromatography on silica gel (Heptane/Ethyl Acetate = 80:20) to afford **3h** as an orange oil in 54% yield (29 mg, 0.16 mmol).

^{1}H RMN (400 MHz, $CDCl_3$) δ (ppm) 7.12 – 7.06 (m, 1H), 6.72 (s, 1H), 6.71 – 6.68 (m, 1H), 3.32 (s, 3H), 2.89 – 2.85 (m, 2H), 2.68 – 2.60 (m, 2H).

^{19}F{1H} RMN (376 MHz, $CDCl_3$) δ (ppm) -114.1.

^{13}C RMN (101 MHz, $CDCl_3$) δ (ppm) 170.4, 162.4 (d, *J* = 243.3 Hz), 142.1 (d, *J* = 10.1 Hz), 128.7 (d, *J* = 9.3 Hz), 121.7 (d, *J* = 3.2 Hz), 109.0 (d, *J* = 21.2 Hz), 102.9 (d, *J* = 26.6 Hz), 31.9, 29.7, 24.9.

HRMS m/z (ESI) calcd for $C_{10}H_{10}NOFNa$ $[M+Na]^+$ 202.0638 found 202.0638.

7-Chloro-1-methyl-3,4-dihydroquinolin-2(1H)-one (3i)

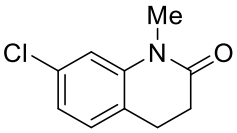

Following the general procedure using **1i** (77 mg, 0.3 mmol, 1 equiv.) and *tert*-butyl acrylate **2a** (131 µL, 0.9 mmol, 3 equiv.), the residue was purified by flash chromatography on silica gel (Heptane/Ethyl Acetate = 80:20) to afford **3i** as a yellow solid in 65% yield (38 mg, 0.19 mmol).

^{1}H RMN (400 MHz, $CDCl_3$) δ (ppm) 7.08 (d, *J* = 7.8 Hz, 1H), 7.01 – 6.93 (m, 2H), 3.33 (s, 3H), 2.93 – 2.83 (m, 2H), 2.69 – 2.61 (m, 2H).

^{13}C RMN (101 MHz, $CDCl_3$) δ (ppm) 170.3, 141.9, 133.2, 128.8, 124.6, 122.6, 115.2, 31.6, 29.7, 25.0.

HRMS m/z (ESI) calcd for $C_{10}H_{10}NOClNa$ $[M+Na]^+$ 218.0343 found 218.0343.

7-Methoxy-1-methyl-3,4-dihydroquinolin-2(1H)-one (3j)

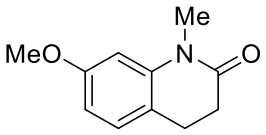

Following the general procedure using **1j** (76 mg, 0.3 mmol, 1 equiv.) and *tert*-butyl acrylate **2a** (131 µL, 0.9 mmol, 3 equiv.), the residue was purified by flash chromatography on silica gel (Heptane/Ethyl Acetate = 80:20) to afford **3j** as a yellow solid in 62% yield (36 mg, 0.19 mmol).

^{1}H RMN (400 MHz, $CDCl_3$) δ (ppm) 7.06 (d, *J* = 8.3 Hz, 1H), 6.64 – 6.41 (m, 2H), 3.81 (s, 3H), 3.33 (s, 3H), 2.89 – 2.79 (m, 2H), 2.71 – 2.56 (m, 2H).

^{13}C RMN (101 MHz, $CDCl_3$) δ (ppm) 170.8, 159.3, 141.8, 128.3, 118.6, 106.6, 102.6, 55.6, 32.2, 29.7, 24.7.

HRMS m/z (ESI) calcd for $C_{11}H_{13}NO_2Na$ $[M+Na]^+$ 214.0838, found 214.0838.

1-Ethyl-7-methyl-3,4-dihydroquinolin-2(1H)-one (3k)

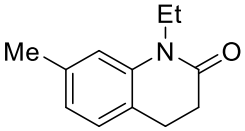

Following the general procedure using **1k** (75 mg, 0.3 mmol, 1 equiv.) and *tert*-butyl acrylate **2a** (131 µL, 0.9 mmol, 3 equiv.), the residue was purified by flash chromatography on silica gel (Heptane/Ethyl Acetate = 80:20) to afford **3k** as a yellow oil in 68% yield (39 mg, 0.20 mmol).

^{1}H RMN (400 MHz, $CDCl_3$) δ (ppm) 7.04 (d, *J* = 7.4 Hz, 1H), 6.85 – 6.77 (m, 2H), 3.97 (q, *J* = 7.1 Hz, 2H), 2.86 – 2.80 (m, 2H), 2.64 – 2.57 (m, 2H), 2.36 (s, 3H), 1.26 (t, *J* = 7.1 Hz, 3H).

^{13}C RMN (101 MHz, $CDCl_3$) δ (ppm) 170.2, 139.6, 137.3, 127.9, 123.6, 123.3, 115.5, 37.5, 32.2, 25.3, 21.7, 13.0

HRMS m/z (ESI) calcd for $C_{12}H_{15}NONa$ $[M+Na]^+$ 212.1046, found 212.1046.

5,7-Difluoro-1-methyl-3,4-dihydroquinolin-2(1H)-one (3l)

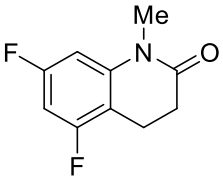

Following the general procedure using **1l** (78 mg, 0.3 mmol, 1 equiv.) and *tert*-butyl acrylate **2a** (131 µL, 0.9 mmol, 3 equiv.), the residue was purified by flash chromatography on silica gel (Heptane/Ethyl Acetate = 80:20) to afford **3l** as a yellow oil in 72% yield (43 mg, 0.22 mmol).

^{1}H RMN (400 MHz, $CDCl_3$) δ (ppm) 6.66 – 6.35 (m, 2H), 3.31 (s, 3H), 2.90 – 2.86 (m, 2H), 2.67 – 2.60 (m, 2H).

^{19}F{1H} RMN (376 MHz, $CDCl_3$) δ (ppm) -111.2 (d, *J* = 6.9 Hz), -114.8 (d, *J* = 6.8 Hz).

^{13}C RMN (101 MHz, $CDCl_3$) δ (ppm) 170.0, 162.1 (dd, *J* = 244.8, 14.7 Hz), 159.6 (dd, *J* = 244.8, 14.5 Hz), 143.2 (dd, *J* = 12.3, 9.1 Hz), 109.0 (dd, *J* = 22.2, 3.8 Hz), 98.9 (dd, *J* = 26.6, 3.5 Hz), 98.1 (dd, *J* = 26.7, 25.4 Hz), 30.8, 29.9, 17.3 (d, *J* = 3.5 Hz).

HRMS m/z (ESI) calcd for $C_{10}H_9NOF_2Na$ $[M+Na]^+$ 220.0544, found 220.0546.

8-Fluoro-1-methyl-3,4-dihydroquinolin-2(1H)-one (3m)

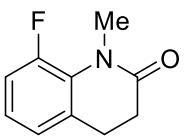

Following the general procedure using **1m** (72 mg, 0.3 mmol, 1 equiv.) and *tert*-butyl acrylate **2a** (131 µL, 0.9 mmol, 3 equiv.), the residue was purified by flash chromatography on silica gel (Heptane/Ethyl Acetate = 85:15) to afford **3m** as an orange solid in 42% yield (23 mg, 0.13 mmol).

^{1}H NMR (400 MHz, $CDCl_3$) δ (ppm) 7.09 – 6.87 (m, 3H), 3.44 (d, *J* = 6.4 Hz, 3H), 2.91 – 2.86 (m, 2H), 2.63 – 2.58 (m, 2H).

^{19}F{^{1}H} NMR (376 MHz, $CDCl_3$) δ (ppm) -122.5.

^{13}C NMR (101 MHz, $CDCl_3$) δ (ppm) 171.3, 152.2 (d, *J* = 247.1 Hz), 131.3 (d, *J* = 2.0 Hz), 127.7 (d, *J* = 27.5 Hz), 124.3 (d, *J* = 8.4 Hz), 123.1 (d, *J* = 3.1 Hz), 115.9 (d, *J* = 22.0 Hz), 33.5 (d, *J* = 11.3 Hz), 32.2, 26.1 (d, *J* = 2.5 Hz).

HRMS m/z (ESI) calcd for $C_{10}H_{10}NOFNa$ $[M+Na]^+$ 202.0638, found 202.0636.

1-Butyl-3,4-dihydroquinolin-2(1H)-one (3n)

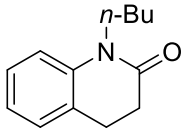

Following the general procedure using **1n** (71 mg, 0.3 mmol, 1 equiv.) and *tert*-butyl acrylate **2a** (131 µL, 0.9 mmol, 3 equiv.), the residue was purified by flash chromatography on silica gel (Heptane/Ethyl Acetate = 80:20) to afford **3n** as a yellow oil in 83% yield (51 mg, 0.25 mmol).

^{1}H NMR (400 MHz, $CDCl_3$) δ (ppm) 7.30 – 7.22 (m, 1H), 7.21 – 7.14 (m, 1H), 7.05 – 6.97 (m, 2H), 3.93 (t, *J* = 7.5 Hz, 2H), 2.94 – 2.85 (m, 2H), 2.69 – 2.62 (m, 2H), 1.79 – 1.52 (m, 2H), 1.48 – 1.20 (m, 2H), 0.98 (t, *J* = 7.3 Hz, 3H).

^{13}C NMR (101 MHz, $CDCl_3$) δ (ppm) 170.2, 139.7, 128.1, 127.5, 126.7, 122.7, 114.9, 42.0, 32.1, 29.4, 25.7, 20.3, 13.9.

HRMS m/z (ESI) calcd for $C_{13}H_{17}NONa$ $[M+Na]^+$ 226.1202, found 226.1201.

1-Ethyl-3,4-dihydroquinolin-2(1H)-one (3o)

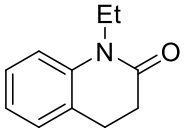

Following the general procedure using **1o** (71 mg, 0.3 mmol, 1 equiv.) and *tert*-butyl acrylate **2a** (131 µL, 0.9 mmol, 3 equiv.), the residue was purified by flash chromatography on silica gel (Heptane/Ethyl Acetate = 80:20) to afford **3o** as a yellow oil in 75% yield (39 mg, 0.22 mmol).

^{1}H NMR (400 MHz, $CDCl_3$) δ (ppm) 7.26 – 7.22 (m, 1H), 7.16 (dd, *J* = 7.3, 1.3 Hz, 1H), 7.04 – 6.95 (m, 2H), 3.99 (q, *J* = 7.1 Hz, 2H), 3.00 – 2.80 (m, 2H), 2.76 – 2.33 (m, 2H), 1.26 (t, *J* = 7.1 Hz, 3H).

^{13}C NMR (101 MHz, $CDCl_3$) δ (ppm) 170.0, 139.7, 128.1, 127.6, 126.7, 122.8, 114.7, 37.5, 32.1, 25.7, 12.9.

HRMS m/z (ESI) calcd for $C_{11}H_{13}NONa$ $[M+Na]^+$ 198.0889, found 198.0888.

1-Ethyl-6-methyl-3,4-dihydroquinolin-2(1H)-one (3p)

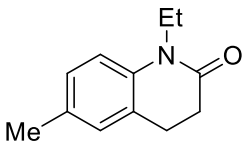

Following the general procedure using **1p** (75 mg, 0.3 mmol, 1 equiv.) and *tert*-butyl acrylate **2a** (131 µL, 0.9 mmol, 3 equiv.), the residue was purified by flash chromatography on silica gel (Heptane/Ethyl Acetate = 80:20) to afford **3p** as an orange oil in 81% yield (46 mg, 0.24 mmol).

^{1}H NMR (400 MHz, $CDCl_3$) δ (ppm) 7.04 (d, *J* = 8.2 Hz, 1H), 6.98 (s, 1H), 6.90 (d, *J* = 8.2 Hz, 1H), 3.97 (q, *J* = 7.1 Hz, 2H), 2.88 – 2.78 (m, 2H), 2.65 – 2.52 (m, 2H), 2.30 (s, 3H), 1.24 (t, *J* = 7.1 Hz, 3H).

^{13}C NMR (101 MHz, $CDCl_3$) δ (ppm) 169.9, 137.2, 132.3, 128.9, 127.9, 126.6, 114.6, 37.4, 32.1, 25.7, 20.6, 12.9.

HRMS m/z (ESI) calcd for $C_{12}H_{15}NONa$ $[M+Na]^+$ 212.1046, found 212.1048.

2,3,6,7-Tetrahydro-*1H*,*5H*-pyrido[3,2,1-ij]quinolin-5-one (3q)

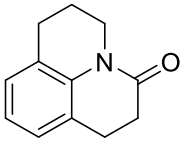

Following the general procedure using **1q** (72 mg, 0.3 mmol, 1 equiv.) and *tert*-butyl acrylate **2a** (131 µL, 0.9 mmol, 3 equiv.), the residue was purified by flash chromatography on silica gel (Heptane/Ethyl Acetate = 80:20) to afford **3q** as a yellow oil in 70% yield (39 mg, 0.21 mmol).

^{1}H NMR (400 MHz, $CDCl_3$) δ (ppm) 7.02 – 6.96 (m, 2H), 6.93 – 6.88 (m, 1H), 3.90 – 3.85 (m, 2H), 2.91 – 2.84 (m, 2H), 2.79 (t, *J* = 6.3 Hz, 2H), 2.68 – 2.61 (m, 2H), 1.97 – 1.90 (m, 2H).

^{13}C NMR (101 MHz, $CDCl_3$) δ (ppm) 169.7, 136.2, 127.9, 125.8, 125.5, 125.4, 122.5, 41.0, 31.6, 27.4, 25.4, 21.6.

HRMS m/z (ESI) calcd for $C_{12}H_{13}NONa$ $[M+Na]^+$ 210.0889, found 210.0891.

Methyl 2-(1-methyl-2-oxo-1,2,3,4-tetrahydroquinolin-3-yl)acetate (3r)

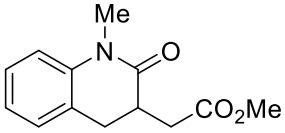

Following the general procedure using **1a** (67 mg, 0.3 mmol, 1 equiv.) and dimethyl itaconate **2b** (142 mg, 0.9 mmol, 3 equiv.), the residue was purified by flash chromatography on silica gel (Heptane/Ethyl Acetate = 70:30) to afford **3r** as an orange oil in 57% yield (40 mg, 0.17 mmol).

^{1}H NMR (400 MHz, $CDCl_3$) δ (ppm) 7.31 – 7.22 (m, 1H), 7.21 – 7.13 (m, 1H), 7.07 – 6.94 (m, 2H), 3.72 (s, 3H), 3.36 (s, 3H), 3.09 – 2.77 (m, 4H), 2.46 (dd, *J* = 16.1, 6.8 Hz, 1H).

^{13}C NMR (101 MHz, $CDCl_3$) δ (ppm) 172.8, 171.2, 140.4, 127.9, 127.8, 125.6, 123.1, 114.8, 52.0, 37.6, 34.9, 31.2, 30.1.

HRMS m/z (ESI) calcd for $C_{13}H_{15}NO_3Na$ $[M+Na]^+$ 256.0944, found 256.0945.

1,3-Dimethyl-3,4-dihydroquinolin-2(1H)-one (3s)

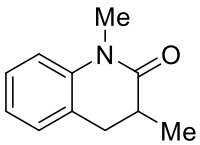

Following the general procedure using **1a** (67 mg, 0.3 mmol, 1 equiv.) and methyl methacrylate **2c** (96 µL, 0.9 mmol, 3 equiv.), the residue was purified by flash chromatography on silica gel (Heptane/Ethyl Acetate = 80:20) to afford **3s** as a yellow oil in 60% yield (32 mg, 0.18 mmol).

^{1}H NMR (400 MHz, $CDCl_3$) δ (ppm) 7.28 – 7.23 (m, 1H), 7.17 – 7.15 (m, 1H), 7.03 – 6.95 (m, 2H), 3.36 (s, 3H), 2.93 (dd, *J* = 14.5, 4.8 Hz, 1H), 2.73 – 2.62 (m, 2H), 1.26 (d, *J* = 6.6 Hz, 3H).

^{13}C NMR (101 MHz, $CDCl_3$) δ (ppm) 173.4, 140.6, 128.0, 127.5, 125.9, 122.8, 114.6, 35.7, 33.5, 29.9, 15.8.

HRMS m/z (ESI) calcd for $C_{11}H_{13}NONa$ $[M+Na]^+$ 198.0889, found 198.0891.

_N_-Methyl-2-phenethylaniline (5a)

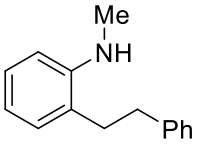

Following the general procedure using **1a** (66 mg, 0.3 mmol, 1 equiv.) and styrene **2d** (99 µL, 0.9 mmol, 3 equiv.), the residue was purified by flash chromatography on silica gel (Heptane/Ethyl Acetate = 95:5) to afford **5a** as a colorless oil in 60% yield (38 mg, 0.18 mmol).

^{1}H NMR (400 MHz, $CDCl_3$) δ (ppm) 7.35 – 7.29 (m, 2H), 7.26 – 7.17 (m, 4H), 7.09 (d, *J* = 7.3 Hz, 1H), 6.74 (t, *J* = 7.3 Hz, 1H), 6.67 (d, *J* = 8.0 Hz, 1H), 2.97 – 2.93 (m, 2H), 2.83 (s, 3H), 2.81 – 2.74 (m, 2H).

^{13}C NMR (101 MHz, $CDCl_3$) δ (ppm) 146.8, 142.1, 128.9, 128.6, 128.5, 127.5, 126.2, 125.8, 117.4, 110.1, 35.3, 33.3, 31.1.

HRMS m/z (ESI) calcd for $C_{15}H_{18}N$ $[M+H]^+$ 212.1433, found 212.1431.

2-(4-(Tert-butyl)phenethyl)-_N_-methylaniline (5b)

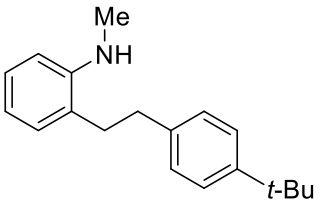

Following the general procedure using **1a** (66 mg, 0.3 mmol, 1 equiv.) and 4-*tert*-butyl-styrene **2e** (163 µL, 0.9 mmol, 3 equiv.), the residue was purified by flash chromatography on silica gel (Heptane/Ethyl Acetate = 95:5) to afford **5b** as a colorless oil in 73% yield (59 mg, 0.22 mmol).

^{1}H NMR (400 MHz, $CDCl_3$) δ (ppm) 7.43 – 7.37 (m, 2H), 7.25 – 7.19 (m, 3H), 7.17 (d, *J* = 7.4 Hz, 1H), 6.79 (t, *J* = 7.4 Hz, 1H), 6.69 (d, *J* = 8.0 Hz, 1H), 3.00 – 2.93 (m, 2H), 2.83 (s, 3H), 2.83 – 2.77 (m, 2H), 1.39 (s, 9H).

^{13}C NMR (101 MHz, $CDCl_3$) δ (ppm) 149.0, 147.0, 139.0, 128.8, 128.1, 127.5, 125.9, 125.5, 117.3, 109.9, 34.8, 34.5, 33.3, 31.6, 31.0.

HRMS m/z (ESI) calcd for $C_{19}H_{26}N$ $[M+H]^+$ 268.2060, found 268.2061.

2-(4-Tert-butyl)phenethyl)-*N*-methyl-4-(trifluoromethoxy)aniline (5c)

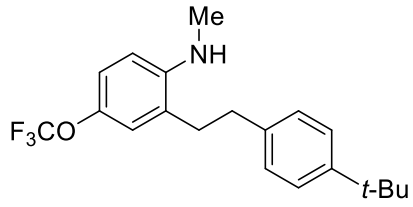

Following the general procedure using **1d** (92 mg, 0.3 mmol, 1 equiv.) and 4-*tert*-butyl-styrene **2e** (163 µL, 0.9 mmol, 3 equiv.), the residue was purified by flash chromatography on silica gel (Heptane/Ethyl Acetate = 90:10) to afford **5c** as a colorless oil in 65% yield (69 mg, 0.19 mmol).

^{1}H NMR (400 MHz, $CDCl_3$) δ (ppm) 7.36 (d, *J* = 8.3 Hz, 2H), 7.14 (d, *J* = 8.2 Hz, 2H), 7.07 – 7.02 (m, 1H), 6.98 – 6.94 (m, 1H), 6.56 (d, *J* = 8.8 Hz, 1H), 2.97 – 2.86 (m, 2H), 2.79 (s, 3H), 2.78 – 2.67 (m, 2H), 1.36 (s, 9H).

^{19}F NMR (376 MHz, $CDCl_3$) δ (ppm) -58.3.

^{13}C NMR (101 MHz, $CDCl_3$) δ (ppm) 149.3, 145.8, 140.4 (d, *J* = 2.0 Hz), 138.4, 128.2, 126.9, 125.6, 122.1, 120.9 (q, *J* = 255.0 Hz), 120.1, 109.9, 34.6, 34.5, 33.1, 31.5, 31.1.

HRMS m/z (ESI) calcd for $C_{20}H_{24}NOF_3Na$ $[M+Na]^+$ 374.1707, found 374.1706.

2-(4-Methoxyphenethyl)-*N*-methylaniline (5d)

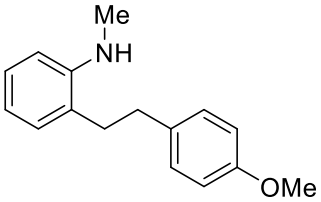

Following the general procedure using **1a** (66 mg, 0.3 mmol, 1 equiv.) and 4-vinylanisole **2f** (120 µL, 0.9 mmol, 3 equiv.), the residue was purified by flash chromatography on silica gel (Heptane/Ethyl Acetate = 90:10) to afford **5d** as a colorless oil in 75% yield (54 mg, 0.22 mmol).

^{1}H NMR (400 MHz, $CDCl_3$) δ (ppm) 7.27 – 7.23 (m, 2H), 7.20 – 7.14 (m, 1H), 7.12 – 7.07 (m, 2H), 7.01 (d, *J* = 7.4 Hz, 1H), 6.70 (t, *J* = 7.3 Hz, 1H), 6.64 (d, *J* = 8.0 Hz, 1H), 2.94 – 2.86 (m, 2H), 2.83 (s, 3H), 2.77 – 2.68 (m, 2H)

^{13}C NMR (101 MHz, $CDCl_3$) δ (ppm) 158.1, 147.0, 134.2, 129.4, 128.9, 127.5, 125.8, 117.2, 114.0, 109.9, 55.5, 34.4, 33.6, 31.1.

HRMS m/z (ESI) calcd for $C_{16}H_{19}NONa$ $[M+Na]^+$ 264.1358 found 264.1357.

2-(2,4-Dimethylphenethyl)-*N*-methylaniline (5e)

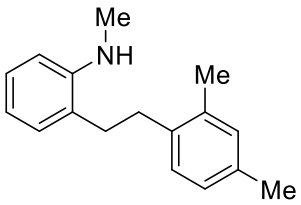

Following the general procedure using **1a** (66 mg, 0.3 mmol, 1 equiv.) and 2,4-dimethyl-styrene **2g** (131 µL, 0.9 mmol, 3 equiv.), the residue was purified by flash chromatography on silica gel (Heptane/Ethyl Acetate = 95:5) to afford **5e** as a colorless oil in 67% yield (48 mg, 0.20 mmol).

^{1}H NMR (400 MHz, $CDCl_3$) δ (ppm) 7.25 – 7.19 (m, 1H), 7.16 – 7.06 (m, 2H), 7.04 – 6.96 (m, 2H), 6.82 – 6.74 (m, 1H), 6.70 – 6.63 (m, 1H), 2.94 – 2.89 (m, 2H), 2.85 (s, 3H), 2.77 – 2.69 (m, 2H), 2.35 (s, 3H), 2.30 (s, 3H).

^{13}C NMR (101 MHz, $CDCl_3$) δ (ppm) 146.9, 137.1, 135.8, 135.7, 131.1, 129.2, 128.7, 127.4, 126.8, 125.9, 117.1, 109.8, 32.1, 32.3, 30.9, 20.9, 19.2.

HRMS m/z (ESI) calcd for $C_{17}H_{22}N$ $[M+H]^+$ 240.1746, found 240.1745.

2-(4-Fluorophenethyl)-*N*-methylaniline (5f)

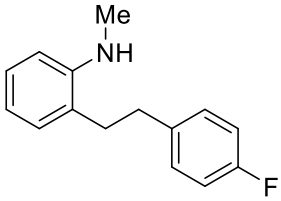

Following the general procedure using **1a** (66 mg, 0.3 mmol, 1 equiv.) and 4-fluorostyrene **2h** (99 µL, 0.9 mmol, 3 equiv.), the residue was purified by flash chromatography on silica gel (Heptane/Ethyl Acetate = 95:5) to afford **5f** as a colorless oil in 32% yield (22 mg, 0.09 mmol).

^{1}H NMR (400 MHz, $CDCl_3$) δ (ppm) 7.22 – 7.11 (m, 3H), 7.05 – 6.94 (m, 3H), 6.71 (t, *J* = 7.4 Hz, 1H), 6.65 (d, *J* = 8.0 Hz, 1H), 2.94 – 2.88 (m, 2H), 2.84 (s, 3H), 2.78 – 2.71 (m, 2H).

^{19}F NMR (376 MHz, $CDCl_3$) δ (ppm) -117.4.

^{13}C NMR (101 MHz, $CDCl_3$) δ (ppm) 161.5 (d, *J* = 243.7 Hz), 146.9, 137.6 (d, *J* = 3.3 Hz), 129.9 (d, *J* = 7.8 Hz), 128.9, 127.6, 125.3, 117.3, 115.3 (d, *J* = 21.2 Hz), 110.0, 34.3, 33.4, 31.0.

HRMS m/z (ESI) calcd for $C_{15}H_{17}NF$ $[M+H]^+$ 230.1339, found 230.1337.

2-(4-Chlorophenethyl)-*N*-methylaniline (5g)

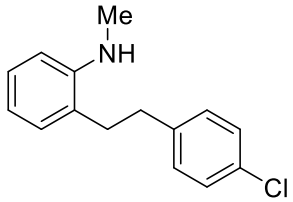

Following the general procedure using **1a** (66 mg, 0.3 mmol, 1 equiv.) and 4-chlorostyrene **2i** (108 µL, 0.9 mmol, 3 equiv.), the residue was purified by flash chromatography on silica gel (Heptane/Ethyl Acetate = 90:10) to afford **5g** as a colorless oil in 42% yield (31 mg, 0.17 mmol).

^{1}H NMR (400 MHz, $CDCl_3$) δ (ppm) 7.27 – 7.23 (m, 2H), 7.20 – 7.14 (m, 1H), 7.12 – 7.07 (m, 2H), 7.01 (d, *J* = 7.4 Hz, 1H), 6.70 (t, *J* = 7.3 Hz, 1H), 6.64 (d, *J* = 8.0 Hz, 1H), 2.94 – 2.86 (m, 2H), 2.83 (s, 3H), 2.77 – 2.68 (m, 2H).

^{13}C NMR (101 MHz, $CDCl_3$) δ (ppm) 146.7, 140.3, 131.8, 129.8, 128.8, 128.5, 127.5, 125.1, 117.2, 109.9, 34.3, 33.0, 30.9.

HRMS m/z (ESI) calcd for $C_{15}H_{17}NCl$ $[M+H]^+$ 246.1044, found 246.1045.

2.6.5. Procedure for C–H Bond Alkylation of Phosphanamine 1a for Preparation of 4a and Compound Characterization

***Tert*-butyl 3-(2-((diisopropylphosphaneyl)(methyl)amino)phenyl)propanoate (4a)**

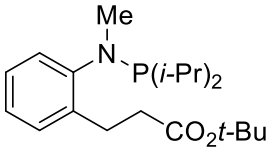

In a glovebox, an oven-dried Schlenk tube was charged with phosphanamine **1a** (66 mg, 0.3 mmol, 1 equiv.). The Schlenk tube was closed and removed from the glovebox. Under argon atmosphere, $[RhCl(COD)]_2$ (3 mg, 0.006 mmol, 2 mol%), toluene (1.5 mL), 2,2,6,6-tetramethylheptane-3,5-dione **L6** (3 µL, 0.012 mmol, 4 mol%) and *tert*-butyl acrylate **2a** (131 µL, 0.9 mmol, 3 equiv.) were added. The resulting mixture was stirred at 160 °C over 24 h. The residue was purified by flash chromatography on silica gel (Heptane/Ethyl Acetate = 70:30) to afford **4a** as a colorless oil in 21% yield (22 mg, 0.063 mmol).

^{1}H NMR (400 MHz, $CDCl_3$) δ (ppm) 7.20 (d, *J* = 7.9 Hz, 1H), 7.16 – 7.09 (m, 2H), 7.02 – 6.97 (m, 1H), 3.06 – 3.04 (m, 2H), 2.99 (d, *J* = 1.9 Hz, 3H), 2.56 – 2.52 (m, 2H), 2.10 (pd, *J* = 7.1, 2.7 Hz, 2H), 1.44 (s, 9H), 1.24 (dd, *J* = 11.8, 7.1 Hz, 6H), 1.12 (dd, *J* = 15.1, 7.0 Hz, 6H).

^{31}P{^{1}H} NMR (162 MHz, $CDCl_3$) δ (ppm) 79.8.

^{13}C NMR (101 MHz, $CDCl_3$) δ (ppm) 172.8, 151.7 (d, *J* = 17.3 Hz), 136.3 (d, *J* = 3.4 Hz), 126.6 (d, *J* = 7.3 Hz), 123.9, 80.2, 38.3 (d, *J* = 6.5 Hz), 36.8, 28.3, 27.4 (d, *J* = 7.1 Hz), 26.7, 26.6, 20.4 (d, *J* = 11.6 Hz), 19.8, 19.6.

2.6.6. Large Scale Reaction and Application to the Synthesis of Aripiprazole *N*-Methylated Analog

6-Methoxy-1-methyl-3,4-dihydroquinolin-2(1H)-one (3j)

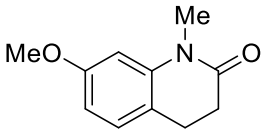

In a glovebox, an oven-dried Schlenk tube was charged with **1j** (1.27 g, 5 mmol, 1 equiv.) and distilled DMF (33 mL). Then, the Schlenk tube was closed and removed from the glovebox. Under argon atmosphere, $[RhCl(COD)]_2$ (25 mg, 0.05 mmol, 1 mol%), 2,2,6,6-tetramethylheptane-3,5-dione **L6** (27 µL, 0.1 mmol, 2 mol%), water (9 mL, 50 mmol, 10 equiv.) and *tert*-butyl acrylate (2 mL, 15 mmol, 3 equiv.) were added. The resulting mixture was stirred at 160 °C over 24 h. The crude product was purified by flash chromatography on silica gel (Heptane/Ethyl Acetate = 80:20) to afford **3j** in 57% yield (0.54 g, 2.85 mmol).

6-Hydroxy-1-methyl-3,4-dihydroquinolin-2(1H)-one (6)

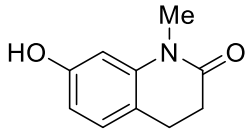

To a 0 °C solution of **3j** (0.54 g, 2.85 mmol, 1 equiv.) in DCM (10 mL) was added dropwise BBr_3 (1 M in DCM, 5.7 mL, 5.7 mmol, 2 equiv.) Then the

resulting mixture was slowly warmed up to room temperature and stirred over 14 h. The reaction mixture was concentrated under reduced pressure. The crude product was purified by flash chromatography (EtOAc/DCM/Hexanes = 1:1:1) to afford the product **6** as a yellow solid in 38% yield (0.19 g, 1.08 mmol). NMR datas were consistent with those in the literature.[19]

6-(4-Bromobutoxy)-1-methyl-3,4-dihydroquinolin-2(1H)-one (7)

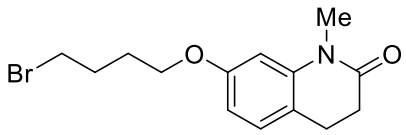

1,4-Dibromobutane (259 µL, 2.16 mmol, 2 equiv.) was added to a solution of **6** (0.19 g, 1.08 mmol, 1 equiv.) and potassium carbonate (135 mg, 1.96 mmol, 2 equiv.) in acetone (6 mL). The resulting mixture was refluxed over 6 h. After cooling to room temperature, the mixture was filtered, the solvent was evaporated under reduced pressure. The crude product was purified by flash column chromatography on silica gel (Heptane/EtOAc = 50:50) to afford **7** as a white solid in 56% yield (0.19 g, 0.60 mmol).
^{1}H NMR (400 MHz, $CDCl_3$) δ (ppm) 7.00 (d, *J* = 8.1 Hz, 1H), 6.57 – 6.43 (m, 2H), 3.96 (t, *J* = 6.0 Hz, 2H), 3.45 (t, *J* = 6.6 Hz, 2H), 3.28 (s, 3H), 2.83 – 2.74 (m, 2H), 2.66 – 2.47 (m, 2H), 2.11 – 1.98 (m, 2H), 1.98 – 1.83 (m, 2H).
^{13}C NMR (101 MHz, $CDCl_3$) δ (ppm) 170.5, 158.4, 141.6, 128.1, 118.4, 107.0, 102.9, 67.0, 33.4, 32.0, 29.5, 29.4, 27.9, 24.5.

7-(4-(4-(2,3-Dichlorophenyl)piperazin-1-yl)butoxy)-1-methyl-3,4-dihydroquinolin-2(1H)-one (8)

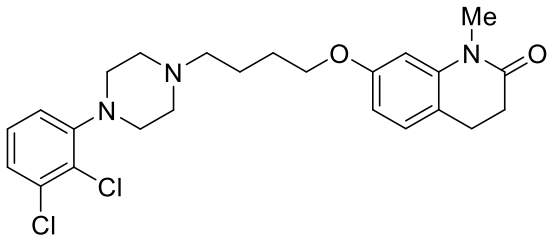

To a solution of **7** (0.19 g, 0.60 mmol, 1 equiv.) in acetonitrile (5 mL) was added potassium iodide (200 mg, 1.2 mmol, 2 equiv.). The mixture was refluxed at 85 °C over 30 min. Then the reaction was cooled to room temperature, triethylamine (167 µL, 1.2 mmol, 2 equiv.) and 1-(2,3-dichlorophenyl) piperazine hydrochloride (241 mg, 0.9 mmol, 1.5 equiv.) were added under stirring. The reaction mixture was refluxed at 85 °C over 8 h. After cooling to room temperature, the mixture was filtered, the solvent was evaporated under reduced pressure. The crude product was purified by flash chromatography on silica gel (EtOAc = 1) to afford **8** as a white solid in 70% yield (0.19 g, 0.42 mmol).

^{1}H NMR (400 MHz, $CDCl_3$) δ (ppm) 7.20 – 7.12 (m, 2H), 7.05 (d, *J* = 8.1 Hz, 1H), 6.97 (dd, *J* = 7.0, 2.6 Hz, 1H), 6.60 – 6.50 (m, 2H), 4.01 (t, *J* = 5.9 Hz, 2H), 3.33 (s, 3H), 3.19 – 3.09 (m, 4H), 2.90 – 2.80 (m, 2H), 2.67 – 2.59 (m, 4H), 1.92 – 1.74 (m, 8H).

^{13}C NMR (101 MHz, $CDCl_3$) δ (ppm) 170.8, 158.7, 150.9, 141.8, 134.3, 128.4, 128.3, 127.7, 125.1, 118.9, 118.6, 107.3, 103.1, 67.9, 58.2, 53.3, 50.7, 32.2, 29.7, 27.4, 24.8, 23.1.

2.6.7. Control and Deuterium Labelling Experiments

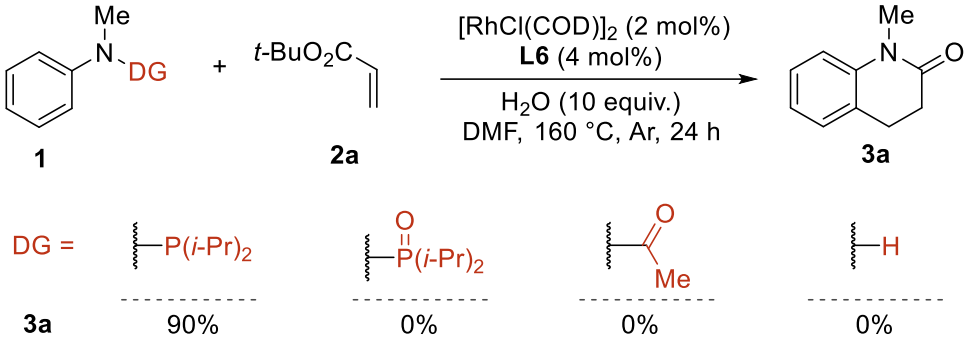

Scheme 2.5. Search of Potential Active Directing Groups.

Procedure: Under argon atmosphere, an oven-dried Schlenk tube was charged with starting material **1** (0.3 mmol, 1 equiv.), $[RhCl(COD)]_2$ (3 mg, 0.006 mmol, 2 mol%), distilled DMF (1.5 mL), 2,2,6,6-tetramethylheptane-3,5-dione **L6** (3 µL, 0.012 mmol, 4 mol%), water (54 µL, 3 mmol, 10 equiv.) and *tert*-butyl acrylate **2a** (131 µL, 0.9 mmol, 3 equiv.). The resulting mixture was stirred at 160 °C over 24 h. The crude product was then cooled down, diluted with ethyl acetate and injected in a calibrated GC-FID using *n*-dodecane (10 µL) as an internal standard to give the corresponding yields : t_R (min) 8.2 (*n*-dodecane), 10.7 (product **3a**).

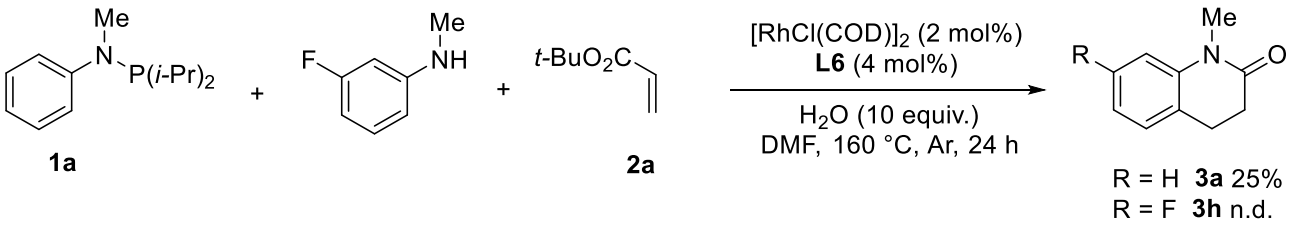

Scheme 2.6. Determination of Directing Group Scrambling.

Procedure: In a glovebox, an oven-dried Schlenk tube was charged with phosphanamine **1a** (66 mg, 0.3 mmol, 1 equiv.) and distilled DMF (1.5 mL). Then, the Schlenk tube was closed and removed from the glovebox. Under argon atmosphere, $[RhCl(COD)]_2$ (3 mg, 0.006 mmol, 2 mol%), 2,2,6,6-tetramethylheptane-3,5-dione **L6** (3 µL, 0.012 mmol, 4 mol%), water (54 µL, 3 mmol, 10 equiv.), 3-fluoro-*N*-methylaniline (40 µL, 0.3 mmol, 1 equiv.) and *tert*-butyl acrylate

2a (131 µL, 0.9 mmol, 3 equiv.) were added. The resulting mixture was stirred at 160 °C over 24 h. The crude product was then cooled down, diluted with ethyl acetate and injected in GC-MS.

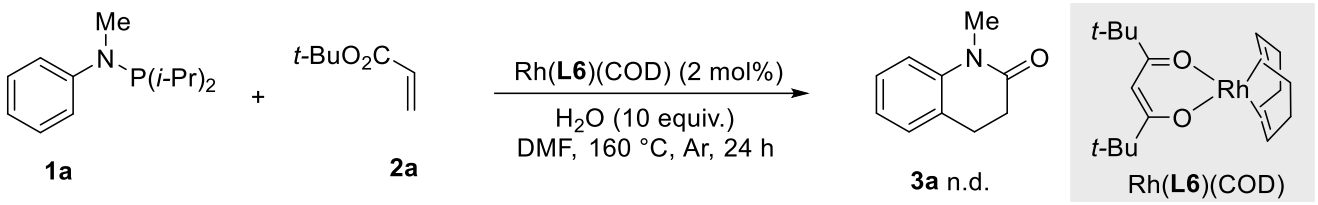

Scheme 2.7. Effect of Rh(**L6**)(COD) as Catalyst for the C–H Bond Alkylation – Amidation of Phosphanamine **1a**.

Procedure: In a glovebox, an oven-dried Schlenk tube was charged with phosphanamine **1a** (66 mg, 0.3 mmol, 1 equiv.) and distilled DMF (1.5 mL). Then, the Schlenk tube was closed and removed from the glovebox. Under argon atmosphere, Rh(**L6**)(COD) (2.5 mg, 0.006 mmol, 2 mol%), water (54 µL, 3 mmol, 10 equiv.) and *tert*-butyl acrylate **2a** (131 µL, 0.9 mmol, 3 equiv.) were added. The resulting mixture was stirred at 160 °C over 24 h. The crude product was then cooled down, diluted with ethyl acetate and injected in GC-MS.

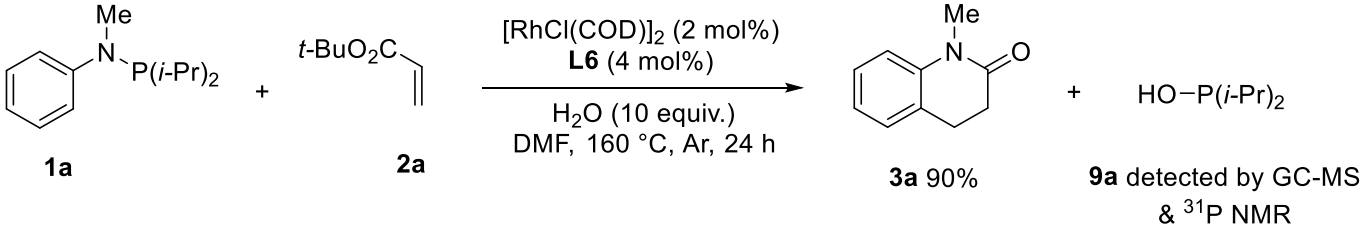

Scheme 2.8. Identification of Hydrodiisopropylphosphane as a By-product.

Procedure: In a glovebox, an oven-dried Schlenk tube was charged with phosphanamine **1a** (66 mg, 0.3 mmol, 1 equiv.) and distilled DMF (1.5 mL). Then, the Schlenk tube was closed and removed from the glovebox. Under argon atmosphere, $[RhCl(COD)]_2$ (3 mg, 0.006 mmol, 2 mol%), 2,2,6,6-tetramethylheptane-3,5-dione (3 µL, 0.012 mmol, 4 mol%), water (54 µL, 3 mmol, 10 equiv.), *tert*-butyl acrylate **2a** (131 µL, 0.9 mmol, 3 equiv.) were added. The resulting mixture was stirred at 160 °C over 24 h. The crude product was then cooled down, diluted with ethyl acetate and injected in GC-MS. Products were identified according to their retention time (t_R) and mass-to-charge ratio (m/z) : t_R (min) 5.9 (hydroxydiisopropylphosphane **9a**), 6.2 (*n*-dodecane), 9.2 (product **3a**).

Hydroxydiisopropylphosphane (9a)

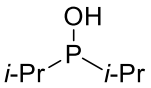

According to Zargarian's work,[20] hydroxydiisopropylphosphane was synthesized as followed. To a solution of chlorodiisopropylphosphine (318 µL, 2 mmol, 1 equiv.) in THF (5 mL) was added water (72 µL, 4 mmol, 2 equiv.). The resulting solution was stirred at room temperature over 2 h. Then Et_3N (245 µL, 2.2 mmol, 1.1 equiv.) was carefully added under stirring, followed by $MgSO_4$ and 5 mL of diethyl ether. The precipitate was filtered off by cannula filtration. The resulting filtrate was evaporated under reduced pressure to provide the pure product **9a** as a colorless liquid.

NMR datas were consistent with those in the literature. Mass-to-charge ratio (m/z = 134) was determined after GC-MS analysis.

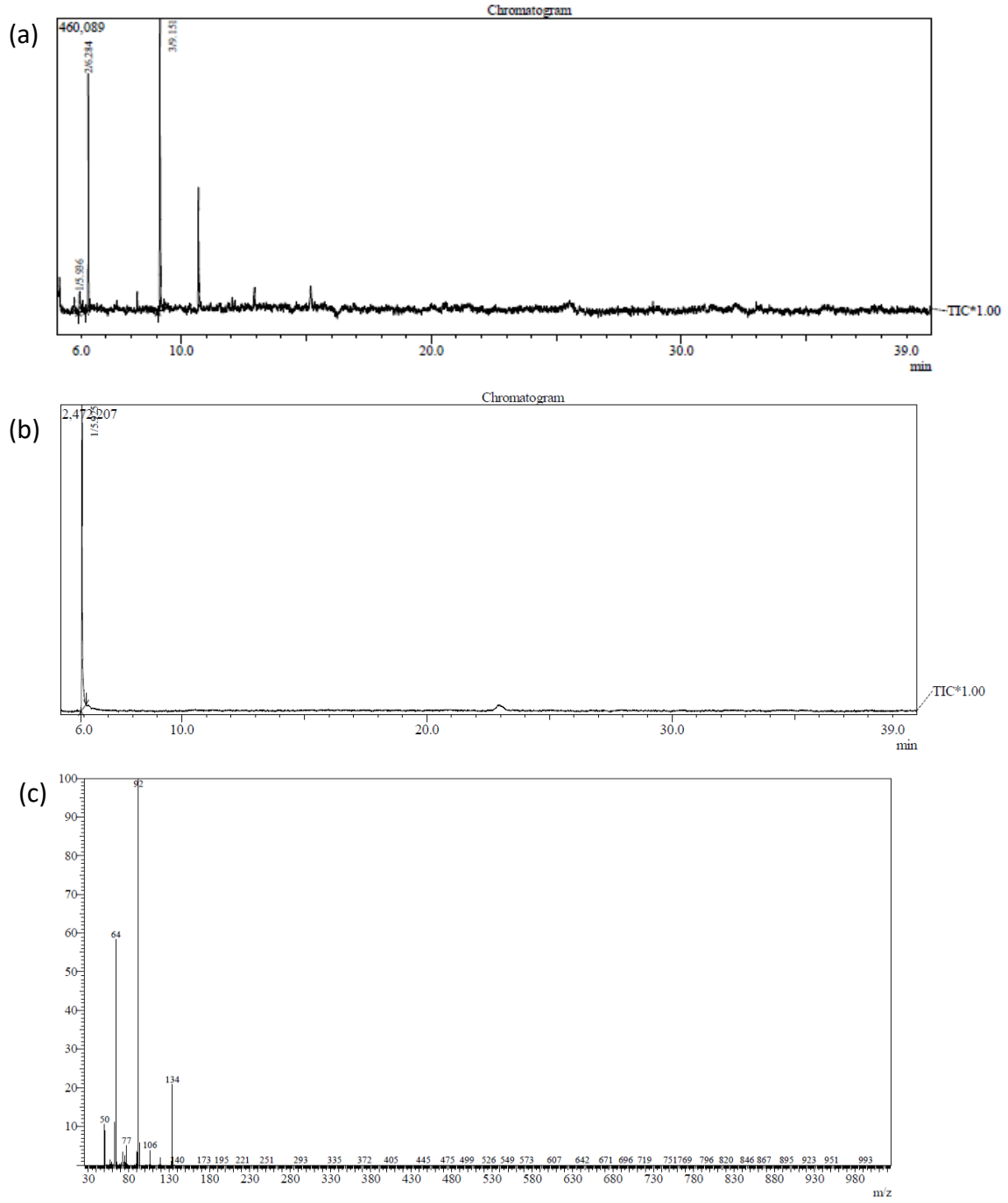

Figure 2.6. a) Gas Chromatogram of the Crude Mixture. b) Gas Chromatogram of Hydroxydiisopropylphosphane **9a**. c) Mass Spectrum of Hydroxydiisopropylphosphane **9a** (m/z = 134).

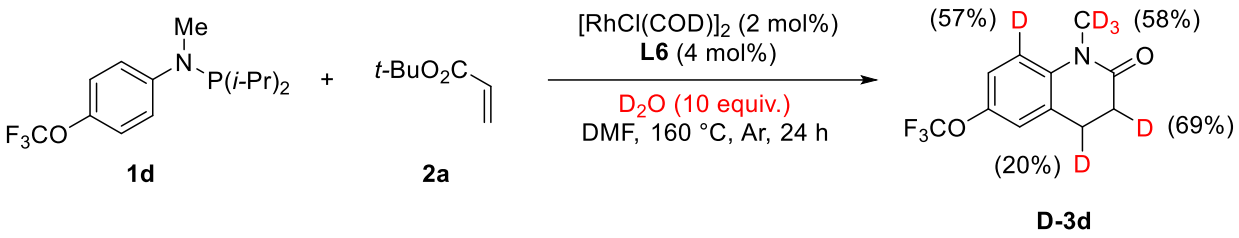

Scheme 2.9. H/D Exchange.

Procedure: In a glovebox, an oven-dried Schlenk tube was charged with phosphanamine **1d** (92 mg, 0.3 mmol, 1 equiv.) and distilled DMF (1.5 mL). The Schlenk tube was closed and removed from the glovebox. Under argon atmosphere, $[RhCl(COD)]_2$ (3 mg, 0.006 mmol, 2 mol%), 2,2,6,6-tetramethylheptane-3,5-dione **L6** (3 µL, 0.012 mmol, 4 mol%), deuterium oxide (54 µL, 3 mmol, 10 equiv.) and *tert*-butyl acrylate **2a** (131 µL, 0.9 mmol, 3 equiv.) were added. The resulting mixture was stirred at 160 °C over 24 h. the residue was purified by flash chromatography on silica gel (Heptane/Ethyl Acetate = 80:20) to afford **D-3d**.

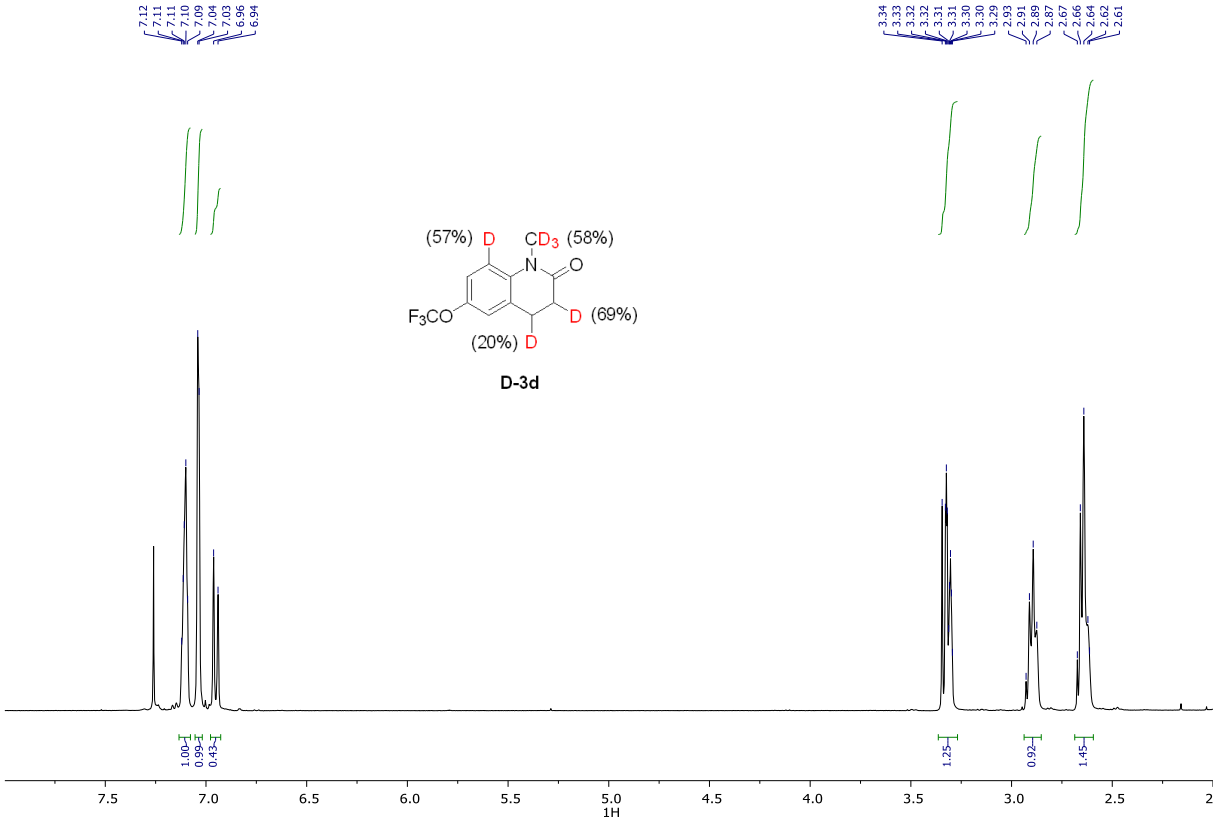

Figure 2.7. ^{1}H NMR Spectra of **D-3d**.

2.6.8. Kinetic Study

2.6.8.1 Kinetic Reaction Profile

Procedure: In a glovebox, a three-necked round bottom flask was charged with phosphanamine **1a** (88 mg, 0.4 mmol, 1 equiv.) and distilled DMF (2 mL). Then the flask was closed and removed from the glovebox. Under argon atmosphere, $[RhCl(COD)]_2$ (4 mg, 0.012 mmol, 2 mol%), 2,2,6,6-tetramethylheptane-3,5-dione **L6** (4 µL, 0.024 mmol, 4 mol%), water (72 µL, 4 mmol, 10 equiv.) and *tert*-butyl acrylate **2a** (174 µL, 1.2 mmol, 3 equiv.) were added. The reaction was initiated by placing the flask into a preheated bath at 160 °C. Reaction progress was followed by NMR spectroscopy analyses. The reaction was sampled by withdrawing 50 µL aliquots of the reaction solution, which was quenched with a solution of $CDCl_3$ (0.6 mL). Final concentrations of **1a** and **4a** were determined by ^{31}P NMR spectroscopy analysis using triphenylphosphine (0.038 mmol) as external standard. Final concentration of **3a** was determined by ^{1}H NMR spectroscopy analysis using dichloroethane (0.063 mmol) as external standard.

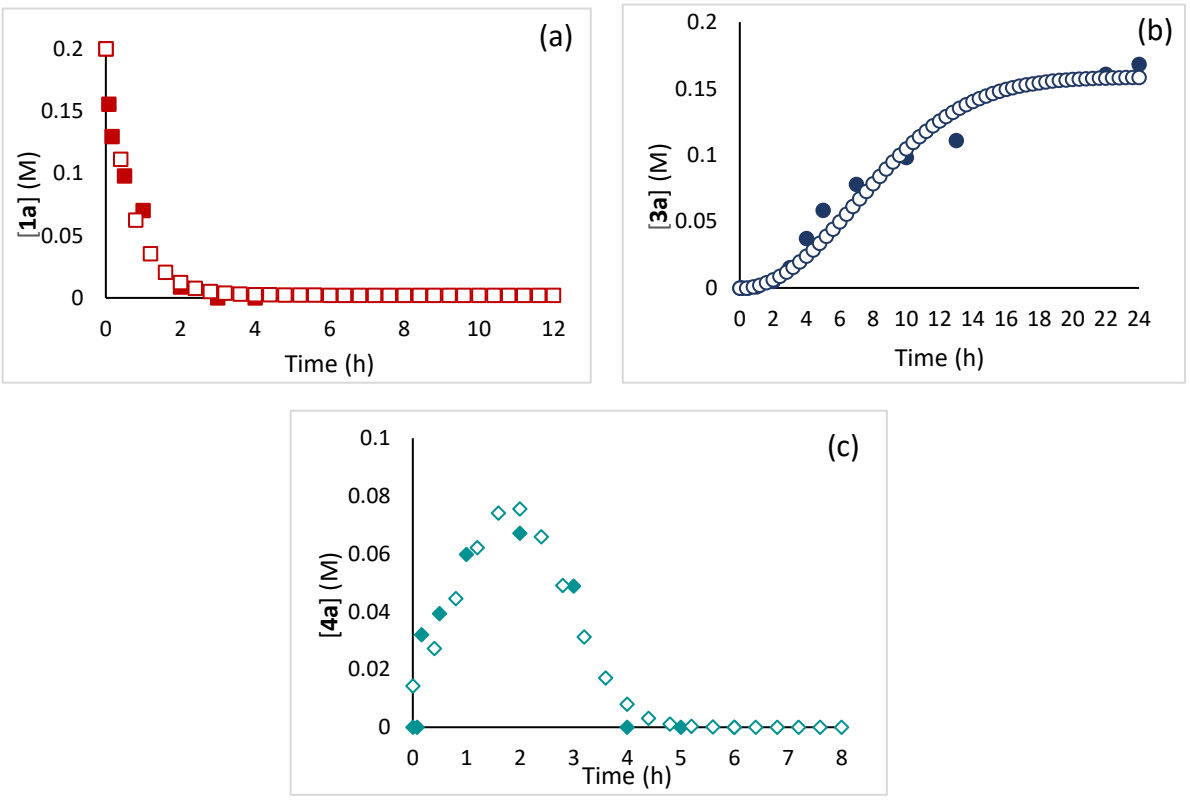

Figure 2.8. a) Consumption of Phosphanamine [**1a**] (M) *vs.* Time (h). Experimental datas are shown in red filled dots, fitting datas are shown in red empty dots and were obtained using exponential decay function. b) Formation of Final Product **3a** (M) *vs.* Time (h). Experimental

datas are shown in blue filled dots, fitting datas are shown in blue empty dots and were obtained using sigmoidal Boltzmann function. c) Formation and Consumption of Intermediate [**4a**] (M) *vs.* Time (h). Experimental datas are shown in green filled dots, fitting datas are shown in green empty dots and were obtained using Gaussian function.

2.6.8.2 Same "Excess" Experiments

In Reaction Progress Kinetic Analysis (RPKA), "excess" indicates the difference between the initial concentrations of the starting materials. A series of experiments were performed following the conditions in Table 2.5 with same "excess" of **1a** and **2a**.

Table 2.5. Reaction Conditions for the Same "Excess" Experiments.

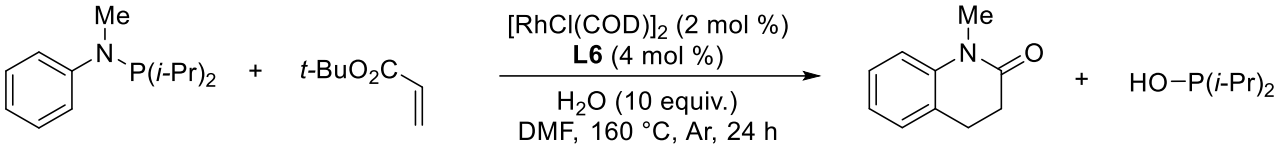

1a **2a** **3a** **9a**

Reaction	[**1a**]$_0$ (M)	[**2a**]$_0$ (M)	[**3a**]$_0$ (M)	[**9a**]$_0$ (M)
1	0.2	0.6	0	0
2	0.12	0.52	0	0
3	0.12	0.52	0.08	0
4	0.12	0.52	0	0.08

The results reveal that the same "excess" experiments with added product **3a** and **9a** (Reactions **3** and **4**) exhibit the same rate as the same "excess" experiment (Reaction **2**), providing evidence that no product inhibition occurred. Therefore, the lack of overlay between the standards conditions (Reaction **1**) and the time-adjusted same "excess" conditions (Reaction **2**) indicates that catalyst deactivation might occur.

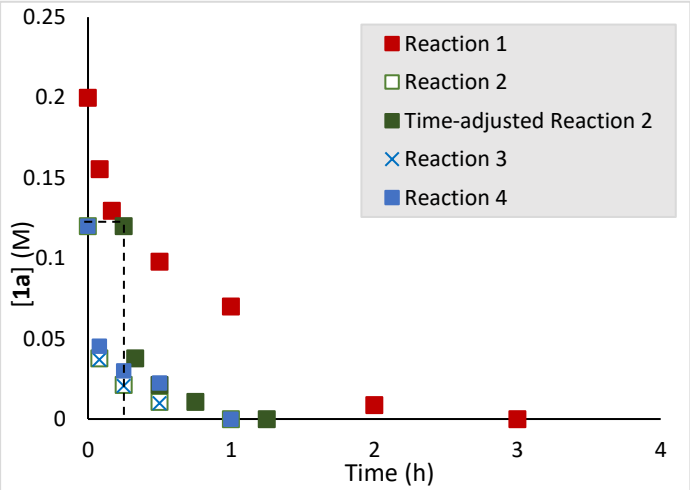

Figure 2.9. Same "Excess" Reaction Profile.

2.6.8.3 Effect of Water

Procedure: In a glovebox, a three-necked round bottom flask was charged with phosphanamine **1a** (88 mg, 0.4 mmol, 1 equiv.) and distilled DMF (2 mL). Then the flask was closed and removed from the glovebox. Under argon atmosphere, $[RhCl(COD)]_2$ (4 mg, 0.008 mmol, 2 mol%), 2,2,6,6-tetramethylheptane-3,5-dione **L6** (4 µL, 0.016 mmol, 4 mol%), water (0.4 mmol – 2 mmol – 4 mmol) and *tert*-butyl acrylate **2a** (174 µL, 1.2 mmol, 3 equiv.) were added. The reaction was initiated by placing the flask into a preheated bath at 160 °C. Reaction progress was followed by NMR spectroscopy analysis. The reaction was sampled by withdrawing 50 µL aliquots of the reaction solution, which was quenched with a solution of $CDCl_3$ (0.6 mL). Final concentrations of **1a** and **4a** were determined by ^{31}P NMR spectroscopy analysis using triphenylphosphine (0.038 mmol) as external standard. Final concentration of **3a** was determined by ^{1}H NMR spectroscopy analysis using dichloroethane (0.063 mmol) as external standard.

Table 2.6. Kinetic Data for Rate Dependance on Initial Concentration of Water.

Initial $[H_2O]$ (M)	Rate of **1a** consumption (M/h)	Rate of **3a** formation (M/h)
0.2	- 0.096	0.0019
1	- 0.097	0.0028
2	- 0.1	0.0072

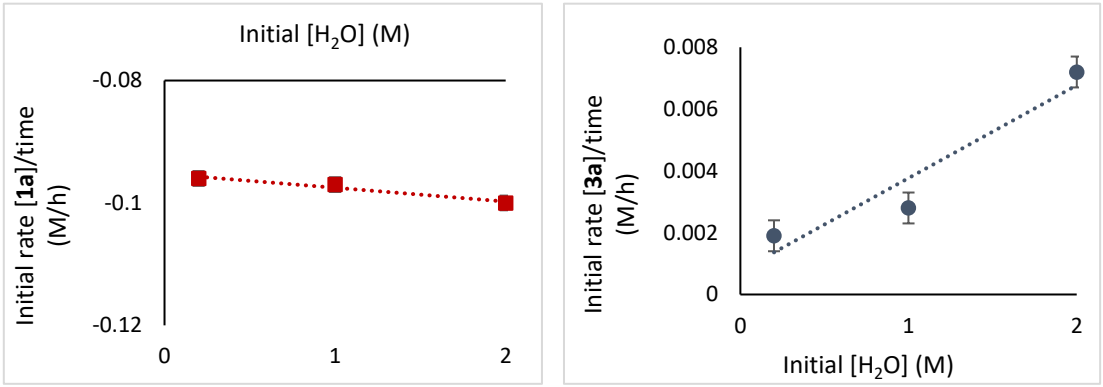

Figure 2.10. Kinetic Plot for Rate Dependance on Initial Concentration of Water.

2.6.8.4 Kinetic Order of Reagents

Procedure: In a glovebox, a three-necked round bottom flask was charged with phosphanamine **1a** (88 mg, 0.4 mmol, 1 equiv.) and distilled DMF (2 mL). Then the flask was closed and removed from the glovebox. Under argon atmosphere, $[RhCl(COD)]_2$ (0.004 mmol – 0.008 mmol – 0.012 mmol), 2,2,6,6-tetramethylheptane-3,5-dione **L6** (0.008 mmol – 0.016 mmol – 0.024 mmol), water (72 µL, 4 mmol, 10 equiv.) and *tert*-butyl acrylate **2a** (174 µL, 1.2 mmol, 3 equiv.) were added. The reaction was initiated by placing the flask into a preheated bath at 160 °C. Reaction progress was followed by NMR spectroscopy analysis. The reaction was sampled by withdrawing 50 µL aliquots of the reaction solution, which was quenched with a solution of $CDCl_3$ (0.6 mL). Final concentrations of **1a** and **4a** were determined by ^{31}P NMR spectroscopy analysis using triphenylphosphine (0.038 mmol) as external standard. Final concentration of **3a** was determined by ^{1}H NMR spectroscopy analysis using dichloroethane (0.063 mmol) as external standard.

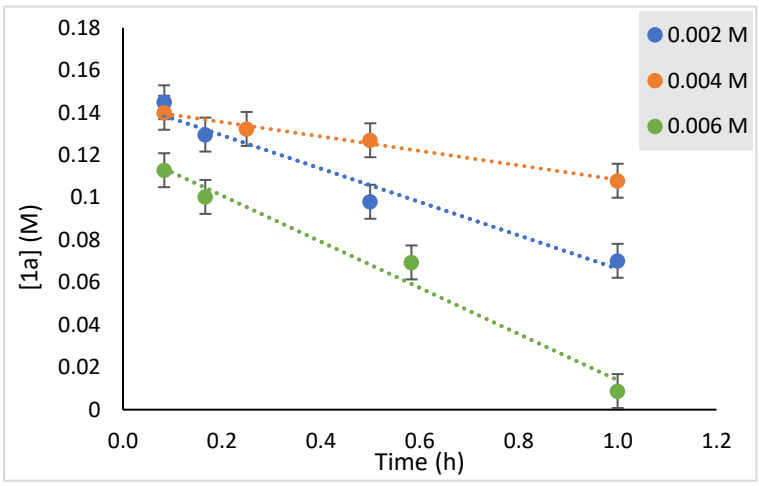

Figure 2.11. Kinetic Plot of Phosphanamine [**1a**] (M) *vs.* Time (h) for a Series of Initial Concentration of Rhodium.

Table 2.7. Kinetic Data for Rate Dependance on Initial Concentration of Rhodium.

Initial [Rh] (M)	Rate of **1a** consumption (M/h)
0.002	- 0.034
0.004	- 0.0787
0.006	- 0.1087

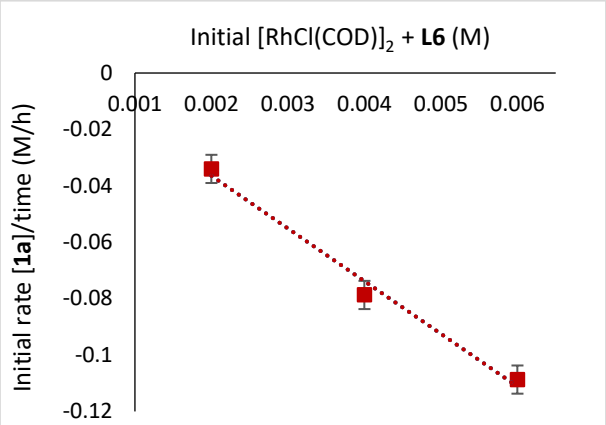

Figure 2.12. Kinetic Plot for Rate Dependance on Initial Concentration of Rhodium.

Procedure: In a glovebox, a three-necked round bottom flask was charged with phosphanamine **1a** (88 mg, 0.4 mmol, 1 equiv.) and distilled DMF (2 mL). Then the flask was closed and removed from the glovebox. Under argon atmosphere, $[RhCl(COD)]_2$ (4 mg, 0.008 mmol, 2 mol%), 2,2,6,6-tetramethylheptane-3,5-dione **L6** (4 µL, 0.016 mmol, 4 mol%), water (72 µL, 4 mmol, 10 equiv.) and *tert*-butyl acrylate **2a** (0.4 mmol – 0.8 mmol – 1.2 mmol – 2 mmol) were added. The reaction was initiated by placing the flask into a preheated bath at 160 °C. Reaction progress was followed by NMR spectroscopy analysis. The reaction was sampled by withdrawing 50 µL aliquots of the reaction solution, which was quenched with a solution of $CDCl_3$ (0.6 mL). Final concentrations of **1a** and **4a** were determined by ^{31}P NMR spectroscopy analysis using triphenylphosphine (0.038 mmol) as external standard. Final concentration of **3a** was determined by ^{1}H NMR spectroscopy analysis using dichloroethane (0.063 mmol) as external standard.

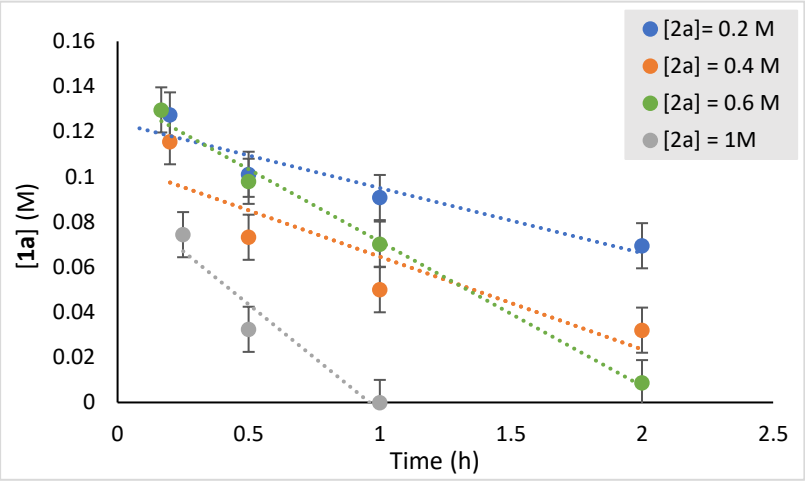

Figure 2.13. Kinetic Plot of [**1a**] (M) *vs.* Time (h) for a Series of Initial Concentration of *Tert*-butyl Acrylate **2a**.

Table 2.8. Kinetic Data for Rate Dependance on Initial Concentration of *Tert*-butyl Acrylate **2a**.

Initial [**2a**] (M)	Rate of **1a** consumption (M/h)
0.2	- 0.0288
0.4	- 0.0411
0.6	- 0.064
1	- 0.0942

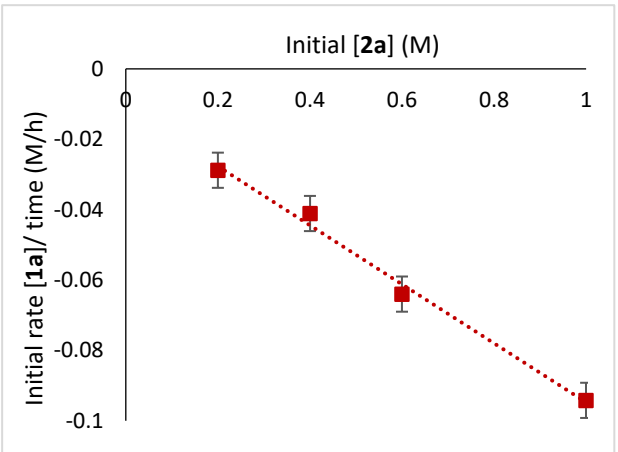

Figure 2.14. Kinetic Plot for Rate Dependance on Initial Concentration of *Tert*-butyl Acrylate **2a**.

Procedure: In a glovebox, a three-necked round bottom flask was charged with phosphanamine **1a** (0.1 mmol – 0.8 mmol) and distilled DMF (2 mL). Then the flask was closed and removed from the glovebox. Under argon atmosphere, $[RhCl(COD)]_2$ (4 mg, 0.008 mmol,

2 mol%), 2,2,6,6-tetramethylheptane-3,5-dione **L6** (4 µL, 0.016 mmol, 4 mol%), water (72 µL, 4 mmol, 10 equiv.) and *tert*-butyl acrylate **2a** (174 µL, 1.2 mmol, 3 equiv.) were added. The reaction was initiated by placing the flask into a preheated bath at 160 °C. Reaction progress was followed by NMR spectroscopy analysis. The reaction was sampled by withdrawing 50 µL aliquots of the reaction solution, which was quenched with a solution of $CDCl_3$ (0.6 mL). Final concentrations of **1a** and **4a** were determined by ^{31}P NMR spectroscopy analysis using triphenylphosphine (0.038 mmol) as external standard. Final concentration of **3a** was determined by ^{1}H NMR spectroscopy analysis using dichloroethane (0.063 mmol) as external standard.

Table 2.9. Kinetic Data for Rate Dependance on Initial Concentration of Phosphanamine **1a**.

Initial [**1a**] (M)	Rate of **1a** consumption (M/h)
0.05	- 0.0633
0.01	-0.0441
0.2	- 0.0309
0.4	- 0.029

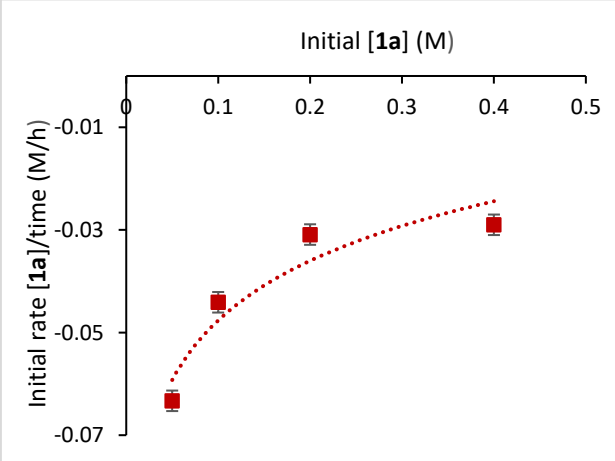

Figure 2.15. Kinetic Plot for Rate Dependance on Initial Concentration of Phosphanamine **1a**.

2.7. References

1. (a) Fischer, J.; Ganellin, C. R.; *Analogue-based drug discovery*, John Wiley & Sons., Weinheim, **2006**; (b) Sharma, R.; Yadav, R. K.; Sharma, R.; Sahu, N. K.; Jain, S.; Chaudhary, S. *Curr. Top. Med. Chem.* **2021**, *21*, 1538-1571.

2. (a) Cherest, M.; Lusinchi, X. *Tetrahedron Lett.* **1989**, *30*, 715-718; (b) Elliott, M. C.; Wordingham, S. V. *Synlett* **2004**, 0898-0900; (c) Li, K.; Foresee, L. N.; Tunge, J. A. *J. Org. Chem.* **2005**, *70*, 2881-2883.
3. (a) Wasa, M.; Yu., J. K. *J. Am. Chem. Soc.* **2008**, *130*, 14058-14059; (b) Zhang, L.; Sonaglia, L.; Stacey, J.; Lautens, M. *Org. Lett.* **2013**, *15*, 2128-2131; (c) Yan, J. -X.; Li, H.; Liu, X.-W.; Shi, J.-L.; Wang, X.; Shi, Z.-J. *Angew. Chem. Int. Ed.* **2014**, *53*, 4945-4949; (d) Li, B.; Park, Y.; Chang, S. *J. Am. Chem. Soc.* **2014**, *136*, 1125-1131; (e) Guan, M.; Pang, Y.; Zhang, J.; Zhao, Y. *Chem. Commun.* **2016**, *52*, 7043–7046; (f) Z Kuang, Z.; Li, B.; Song, Q. *Chem. Commun.* **2018**, *54*, 34–37; (g) Xiao, H.-Z.; Wang, W.-S.; Sun, Y.-S.; Luo, H.; Li, B.-W.; Wang, X.-D.; Lin, W.-L.; Luo, F.-X. *Org. Lett.* **2019**, *21*, 1668-1671.
4. (a) Hurst, T. E.; Taylor, R. J. K. *Chem. Eur. J.* **2014**, *20*, 14063-14073; (b) Bai, Q.-F.; Jin, C.; He, J.-Y.; Feng, G. *Org. Lett.* **2018**, *20*, 2172-2175; (c) Cheng, H.; Lam, T.-L.; Liu, Y.; Tang, Z.; Che, C.-M. *Angew. Chem. Int. Ed.* **2021**, *60*, 1383-1389; (d) Liu, Z.; Zhong, S.; Ji, X.; Deng, G.-J.; Huang, H. *Org. Lett.* **2022**, *24*, 349-353.
5. (a) Loh, T.-P.; Wei, L.-L. *Synlett* **1998**, *1*, 975-976; (b) Munro-Leighton, C.; Blue, E. D.; Gunnoe, T. B. *J. Am. Chem. Soc.* **2006**, *128*, 1446-1447; (c) De, K.; Legros, J.; Crousse, B.; Bonnet-Delpon, D. *J. Org. Chem.* **2009**, *74*, 6260-6265.
6. Wu, J.; Xiang, S.; Zeng, J.; Leow, M.; Liu, X.-W. *Org. Lett.* **2015**, *17*, 222-225.
7. Liu, X.; Hii, K. K. (Mimi). *J. Org. Chem.* **2011**, *76*, 8022-8026.
8. Kim, J.; Park, S.-W.; Baik, M.-H.; Chang, S. *J. Am. Chem. Soc.* **2015**, *137*, 13448-13451.
9. (a) Shelby, Q.; Kataoka, N.; Mann, G.; Hartwig, J. *J. Am. Chem. Soc.* **2000**, *122*, 10718-10719; (b) Qiu, X.; Wang, M.; Zhao, Y.; Shi, Z. *Angew. Chem. Int. Ed.* **2017**, *56*, 7233-7237; (c) Luo, X.; Yuan, J.; Yue, C.-D.; Zhang, Z.-Y.; Chen, J.; Yu, G.-A.; Che, C.-M. *Org. Lett.* **2018**, *20*, 1810-1814; (d) Qiu, X.; Deng, H.; Zhao, Y.; Shi, Z. *Sci. Adv.* **2018**, *4*, eaau6468; (e) Fukuda, K.; Iwasawa, N.; Takaya, J. *Angew. Chem. Int. Ed.* **2019**, *58*, 2850-2853; (f) Li, J.-W.; Wang, L.-N.; Li, M.; Tang, P.-T.; Luo, X.-P.; Kurmoo, M.; Liu, Y.-J.; Zeng, M.-H. *Org. Lett.* **2019**, *21*, 2885-2889; (g) Wang, D.; Zhao, Y.; Yuan, C.; Wen, J.; Zhao, Y.; Shi, Z. *Angew. Chem. Int. Ed.* **2019**, *58*, 12529-12533; (h) Wen, J.; Wang, D.; Qian, J.; Wang, D.; Zhu, C.; Zhao, Y.; Shi, Z. *Angew. Chem. Int. Ed.* **2019**, *58*, 2078-2082; (i) Wright, S. E.; Richardson-Solorzano, S.; Stewart, T. N.; Miller, C. D.; Morris, K. C.; Daley, C. J. A.; Clark, T. B. *Angew. Chem. Int. Ed.* **2019**, *58*, 2834-2838; (j) Dong, B.; Qian, J.; Li, M.; Wang, Z.-J.; Wang, M.; Wang, D.; Yuan, C.; Han, Y.; Zhao, Y.; Shi, Z. *Sci. Adv.* **2020**, *6*, eabd1378; (k) Homma, Y.; Fukuda, K.; Iwasawa, N.; Takaya, J. *Chem. Commun.* **2020**, *56*, 10710-10713; (l) Li, G.; An, J.; Jia, C.; Yan, B.; Zhong, L.; Wang, J.; Yang, S. *Org. Lett.* **2020**, *22*, 9450-9455;

(m) Luo, H.; Wang, D.; Wang, M.; Shi, Z. *Synlett* **2020**, *33*, 351-356; (n) Wen, J.; Dong, B.; Zhu, J.; Zhao, Y.; Shi, Z. *Angew. Chem. Int. Ed.* **2020**, *59*, 10909-10912; (o) Zhang, Z.; Cordier, M.; Dixneuf, P. H.; Soulé, J.-F. *Org. Lett.* **2020**, *22*, 5936-5940; (p) Zhang, Z.-Y.; Zhang, X.; Yuan, J.; Yue, C.-D.; Meng, S.; Chen, J.; Yu, G.-A.; Che, C.-M. *Chem. Eur. J.* **2020**, *26*, 5037-5050; (q) Komuro, T.; Asagami, J.; Higashi, H.; Sato, K.; Hashimoto, H.; Tobita, H. *Organometallics* **2021**, *40*, 3113-3123; (r) Li, M.; Tao, J.-Y.; Wang, L.-N.; Li, J.-W.; Liu, Y.-J.; Zeng, M.-H. *J. Org. Chem.* **2021**, *86*, 11915-11925; (s) Wang, L.-N.; Tang, P.-T.; Li, M.; Li, J.-W.; Liu, Y.-J.; Zeng, M.-H. *Adv. Synth. Catal.* **2021**, *363*, 2843-2849; (t) Xu, H.-B.; Chen, Y.-J.; Chai, X.-Y.; Yang, J.-H.; Xu, Y.-J.; Dong, L. *Org. Lett.* **2021**, *23*, 2052-2056; (u) Zhang, N.-J.; Ma, W.-T.; Li, J.-W.; Liu, Y.-J.; Zeng, M.-H. *Asian J. Org. Chem.* **2021**, *10*, 1113-1116; (v) Fu, Y.; Chen, C.-H.; Huang, M.-G.; Tao, J.-Y.; Peng, X.; Xu, H.-B.; Liu, Y.-J.; Zeng, M.-H. *ACS Catal.* **2022**, *12*, 5036-5047; (w) Ma, W.-T.; Huang, M.-G.; Fu, Y.; Wang, Z.-H.; Tao, J.-Y.; Li, J.-W.; Liu, Y.-J.; Zeng, M.-H. *Chem. Commun.* **2022**, *58*, 7152-7155; (x) Wang, D.; Li, M.; Shuang, C.; Liang, Y.; Zhao, Y.; Wang, M.; Shi, Z. *Nat. Commun.* **2022**, *13*, 2934.

10. (a) Qiu, X.; Wang, P.; Wang, D.; Wang, M.; Yuan, Y.; Shi, Z. *Angew. Chem. Int. Ed.* **2019**, *58*, 1504-1508; (b) Borah, A. J.; Shi, Z. *J. Am. Chem. Soc.* **2018**, *140*, 6062-6066.
11. (a) Zhang, Z.; Roisnel, T.; Dixneuf, P. H.; Soulé, J.-F. *Angew. Chem. Int. Ed.* **2019**, *58*, 14110-14114; (b) Li, J.-W.; Wang, L.-N.; Li, M.; Tang, P.-T.; Zhang, N.-J.; Li, T.; Luo, X.-P.; Kurmoo, M.; Liu, Y.-J.; Zeng, M.-H. *Org. Lett.* **2020**, *22*, 1331-1335; (c) Wang, D.; Dong, B.; Wang, Y.; Qian, J.; Zhu, J.; Zhao, Y.; Shi, Z. *Nat. Commun.* **2019**, *10*, 3539.
12. (a) Davies, D. L.; Donald, S. M. A.; Macgregor, S. A. *J. Am. Chem. Soc.* **2005**, *127*, 13754-13755; (b) Colby, D. A.; Bergman, R. G.; Ellman, J. A. *Chem. Rev.* **2010**, *110*, 624-655.
13. Reaction with 1,1-diisopropyl-*N*-phenylphosphanamine with **2a** results in *N*-addition reaction.
14. (a) Grady, M. A.; Gasperoni, T. L.; Kirkpatrick, P. *Nat. Rev. Drug Discovery* **2003**, *2*, 427-428; (b) Ozdemir, V.; Fourie, J.; Ozdener, F. *Curr. Opin. Investig. Drugs* **2002**, *3*, 113-120.
15. Kowalski, P.; Jaskowska, J.; Majka, Z. *Mini-Rev. Org. Chem.* **2012**, *9*, 374-380.
16. Bonacorsi Jr, S. J.; Waller, S. C.; Kent Rinehart, J. *J. Label. Compd. Radiopharm.* **2006**, *49*, 1-9.
17. (a) Bedford, R. B.; Coles, S. J.; Hursthouse, M. B.; Limmert, M. E. *Angew. Chem. Int. Ed.* **2003**, *42*, 112-114; (b) Bedford, R. B.; Betham, M.; Caffyn, A. J. M.; Charmant, J. P. H.; Lewis-Alleyne, L. C.; Long, P. D.; Polo-Cerón, D.; Prashar, S. *Chem. Commun.* **2008**, 990-992.
18. Stemmler, R. T.; Bolm, C. *Adv. Synth. Catal.* **2007**, *349*, 1185–1198.

19. Chen, Y.; Turlik, A.; Newhouse, T. R. *J. Am. Chem. Soc.* **2016**, *138*, 1166–1169.
20. Mangin, L. P.; Michaud, G.; Zargarian, D. *Organometallics* **2020**, *39*, 4006–4018.

Chapter 3. Merging C–H Bond Activation and Rearrangements in Rh(III)-Catalysis : *N*-Heterocycle Synthesis from Nitroarenes and Alkynes

3.1. Introduction

Nitrogen-containing heterocycles are essential to life science since they are abundant in nature, existing as subunits in several natural products and more than half of prescribed drugs contain an *N*-heterocycle backbone.[1] Moreover, they also found diverse applications in materials sciences.[2] Therefore, their formations, manipulations, and diversifications represent a significant stake for chemical companies, and the discovery of novel synthetic approaches fulfilling modern reaction ideals of green chemistry is still an important challenge, especially starting from the low-functionalized materials. Since the pioneer work by Fagnou and co-workers on Rh(III)-catalyzed C−H bond annulation of acetanilides with alkynes for the synthesis of indoles,[3] several *N*-directed C−H bond annulation protocols have been developed for straightforward access to *N*-heterocycles.[4] However, the conditions often required stochiometric amount of oxidant. An external oxidant-free alternative consists of merging C−H bond functionalization with *O*-atom transfer (OAT) − proved that the directing group holds an N−O bond − then, the resulting intermediate can undergo rearrangements to roll *N*-heterocycles in a one-pot cascade process (Figure 3.1-a). This strategy was initially reported by Li and co-workers using quinoline-*N*-oxides, albeit the reaction stopped after the *O*-atom transfer (Figure 3.1-b).[5] Shortly later, Cp*Rh(III)-catalyzed one-pot cascade of C−H bond functionalization – OAT − rearrangement were implemented to prepare indolyl scaffolds from arylnitrones (Figure 3.1-c),[6] indoles from arylnitrones (Figure 3.1-d),[7] or from amine-*N*-oxides (Figure 3.1-e).[8] Although the high efficiency of these methods for the direct synthesis of *N*-heterocycles, all require the pre-installation of the oxidizing directing group (N−O bond) using hazardous reagents.[9] Nitroarenes constitute abundant feedstocks of *N*-containing molecules as they are readily prepared by nitration of arenes.[10] Despite a few examples of C−H bond functionalizations of nitroarenes,[11] NO_2 group had never been considered as a suitable oxidizing directing group to develop redox-neutral coupling reactions yet. Therefore, we planned to use, for the first time, nitroarenes in Cp*Rh(III)-catalyzed one-pot cascade of C−H bond functionalization – OAT – rearrangement(s) (Figure 3.1-f). The advantage of this approach is to employ naturally occurring NO_2 as oxidizing directing group. Moreover, the OAT should deliver nitrosoarene intermediates, which are very reactive and undergo unpredictable rearrangements toward *N*-heterocycles.[12] In contrast to previous methods to generate nitrosoarenes which employ reductants, our strategy is redox-neutral. This cascade approach led us to discover a novel synthesis of oxindoles. In retrospect to the realization of this unpredictable endeavor, we also optimized the catalyst design, investigate the scope of the reaction and thoughtfully studied the reaction mechanism.

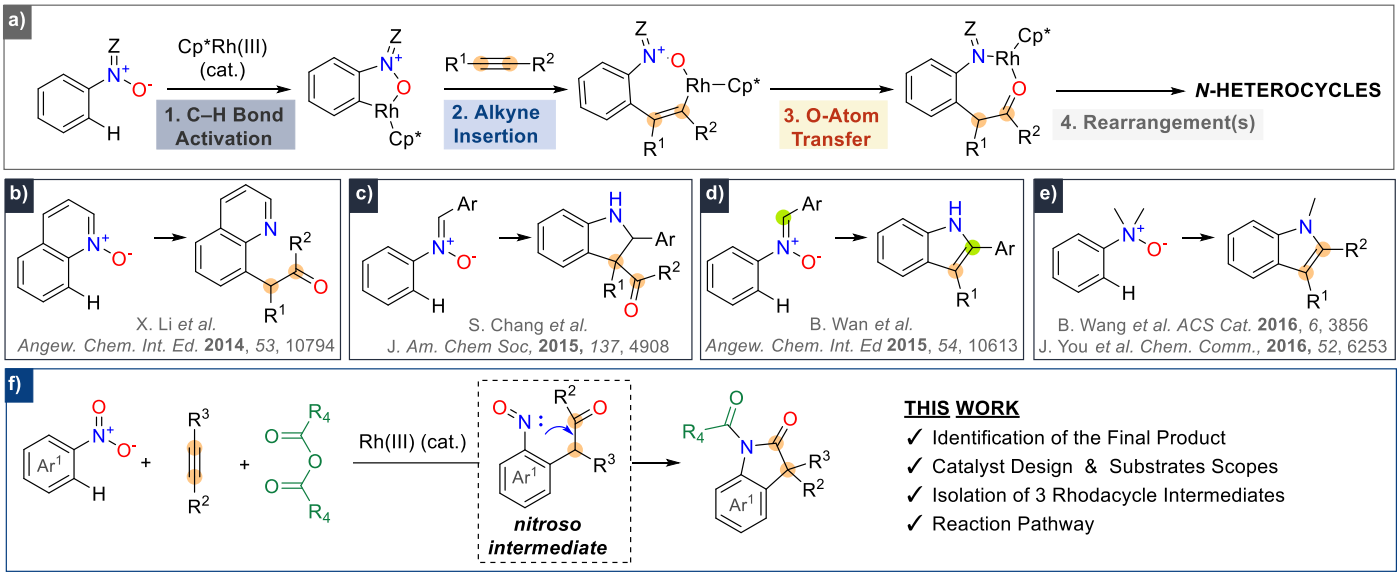

Scheme 3.1. Merge of Rh(III)-Catalyzed C–H Bond Activation, *O*-Atom Transfer and Rearrangements.

3.2. Results and Discussion

3.2.1. Optimization of the Reaction Conditions

We began our studies on Rh-catalyzed C–H bond activation by reacting nitrobenzene with 1-diphenylacetylene in the presence of $[Cp^*RhCl_2]_2$ in DCE at 120 °C. Surprisingly, we observed the unexpected formation of oxindole **1** in 41% yield that was formed upon *ortho*-C–H bond annulation of nitrobenzene *via* multi-step reaction: twofold reduction of NO_2, migration of alkyne phenyl group, and *N*-acylation (Table 3.1, entry 1). The structure of **1** was secured by X-ray analysis. This class of oxindoles containing an α-carbonyl quaternary center was widely recognized as valuable synthetic intermediates, forming the core of numerous natural products and drugs, which often required several consecutive reactions.[13] A solvent screen revealed DCE to be essential for the reaction outcomes, whereas most of the common additives employed in C–H bond functionalization had deleterious effects. Following the seminal work of Rovis,[14] Tanaka,[15] and Cramer[16] on modification of Cp ligand to improve the selectivity and performance in Rh(III) catalysis in other reactions, we decided to evaluate an array of $[Cp^RRhCl_2]_2$ catalyst precursors (Table 3.1). Electron-deficient $[Cp^ERhCl_2]_2$ was inactive for this transformation (Table 3.1, entry 2).[17] Rh(III) complex surrounded by Cp^{iPr}* ligand – exhibiting a similar disc-shape and electronic nature than Cp*– [14] gave the desired product **1** in a similar yield (Table 3.1, entry 3). We next prepared a set of Rh(III) complexes holding C_5Me_4-Ar ligand exhibiting an elliptical-shape. The presence of substituents at the *para* position on the aryl group affects the redox potentials predictably, decreasing in the order of

[CF_3 (-1.21), H (-1.24), and OMe (-1.25)] which is consistent with an increase in electron density of the rhodium center. Increasing the electron density of the Cp ring resulted in an improvement of the yields [Cp^{TFT}*Rh (10%) < Cp^{Ph}*Rh (25%) < Cp^{MP}*Rh (55%)] (Table 3.1, entries 4-6). Subsequently, we prepared two novel [C_5Me_4-ArRh$Cl_2]_2$ with Ar = 3,4-dimethoxyphenyl (DMP) and 3,4,5-trimethoxyphenyl (TMP). Incorporating additional methoxy substituents affects the electronic nature slightly, but their multiplication leads to a bulkier system. Both complexes displayed higher reactivity, and the best result was obtained with [Cp^{TMP}*Rh$Cl_2]_2$, allowing the formation of **1** in 72% isolated yield (Table 3.1, entries 7 and 8). No reaction occurred without Rh(III) catalyst (Table 3.1, entry 9). Similar to the C–H bond arylation of nitroarenes,[11a] the use of a large excess of nitrobenzene (10 equivalents) is required (Table 3.1, entry 10), but most of the nitrobenzene (70-85%) can be recovered by purification on column chromatography after the reaction.

Table 3.1. Optimization : Nature of Cp-Ligand.

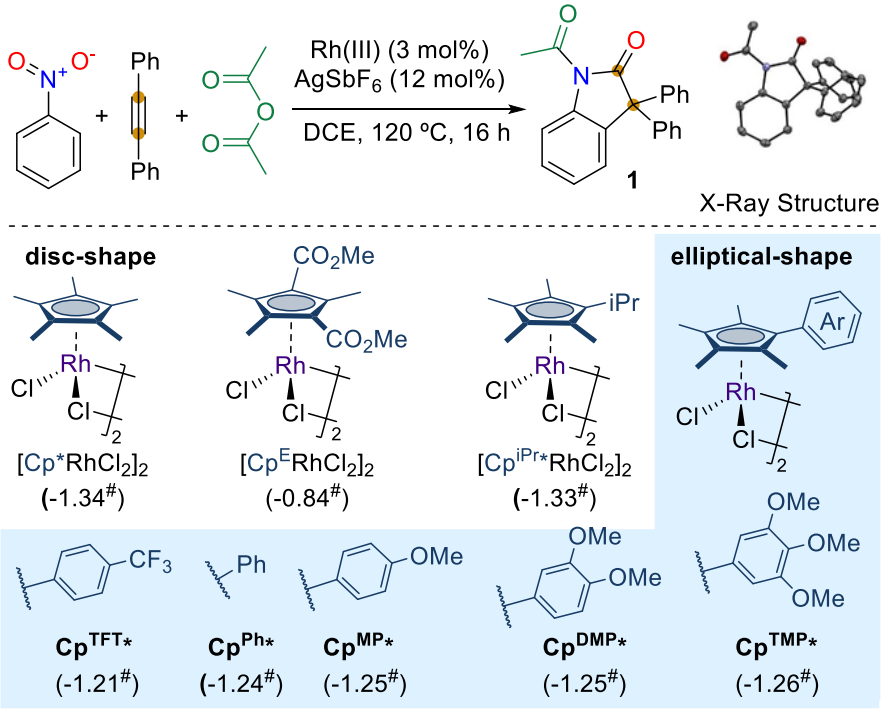

= E(Rh^{III}/Rh^{II}) (V *vs*. Cp_2Fe)

Entry	$[Cp^RRhCl_2]_2$	Conv.(%)[a]	Yield **1** (%)[a]
1	$[Cp^*RhCl_2]_2$	100	41
2	$[Cp^ERhCl_2]_2$	0	0
3	$[Cp^{iPr}*RhCl_2]_2$	100	42
4	$[Cp^{TFT}*RhCl_2]_2$	67	10
5	$[Cp^{Ph}*RhCl_2]_2$	100	25
6	$[Cp^{MP}*RhCl_2]_2$	100	55
7	$[Cp^{DMP}*RhCl_2]_2$	100	64
8	$[Cp^{TMP}*RhCl_2]_2$	100	79 (72)
9	–	0	0
10[b]	$[Cp^{TMP}*RhCl_2]_2$	100	45

Reaction conditions: $[Cp^RRhCl_2]_2$ (3 mol%), $AgSbF_6$ (12 mol%), nitrobenzene (5 mmol), diphenylacetylene (0.5 mmol), and acetic anhydride (2 mmol) in 1,2-dichloroethane (DCE, 2 mL) at 120 °C. [a]Determined by GC-analysis using *n*-dodecane as internal standard, conversion is based on diphenylacetylene consumption; isolated yield is shown in parentheses. [b]Nitrobenzene (2.5 mmol).

3.2.2. Scope of the Reaction

With the optimized conditions in hand using $[Cp^{TMP}*RhCl_2]_2$, the scope of nitroarene, alkyne, and anhydride partners was evaluated. We first subjected 12 different nitroarenes, adorned with various functional groups with different substitution patterns, to this C−H bond alkenylation – *O*-atom transfer – [1,2]-aryl shift cascade reaction (Scheme 3.2). Halides (i.e., F, Cl, Br, I) at the *para*-position of the nitro group were well tolerated and delivered the corresponding products in good to moderate yields (**2**-**5**). *Para*- or *meta*-nitrotoluene reacted to afford oxindoles **6** and **7** in 48% and 58% yield, respectively; while *ortho*-nitrotoluene did not react (**9**). The reaction was regioselective with *meta*-substituted nitroarenes (R = Me or Ph), affording the products resulting from activating the less hindered C6−H bond (**7**, **8**). From 5 equivalents of methyl 2-methyl-5-nitrobenzoate, corresponding oxindoles **10** was isolated in 64% yield. From disubstituted nitroarenes at *para*- and *meta*-positions, the corresponding products were obtained in good yields as single regiosiomers (**11**, **12**). Interestingly, when the *meta* substituent is an F atom, the reaction occurred at its adjacent C−H bond (**12**). The electronically enhanced *ortho*-to-fluorine selectivity is a common feature observed in C−H bond functionalizations involving a CMD mechanism.[18] Reaction with 3,4,5-trifluoronitrobenzene gave an excellent yield (**13**). Propionic, valeric, and isovaleric anhydrides gave the corresponding products **14**-**16** in good yields.

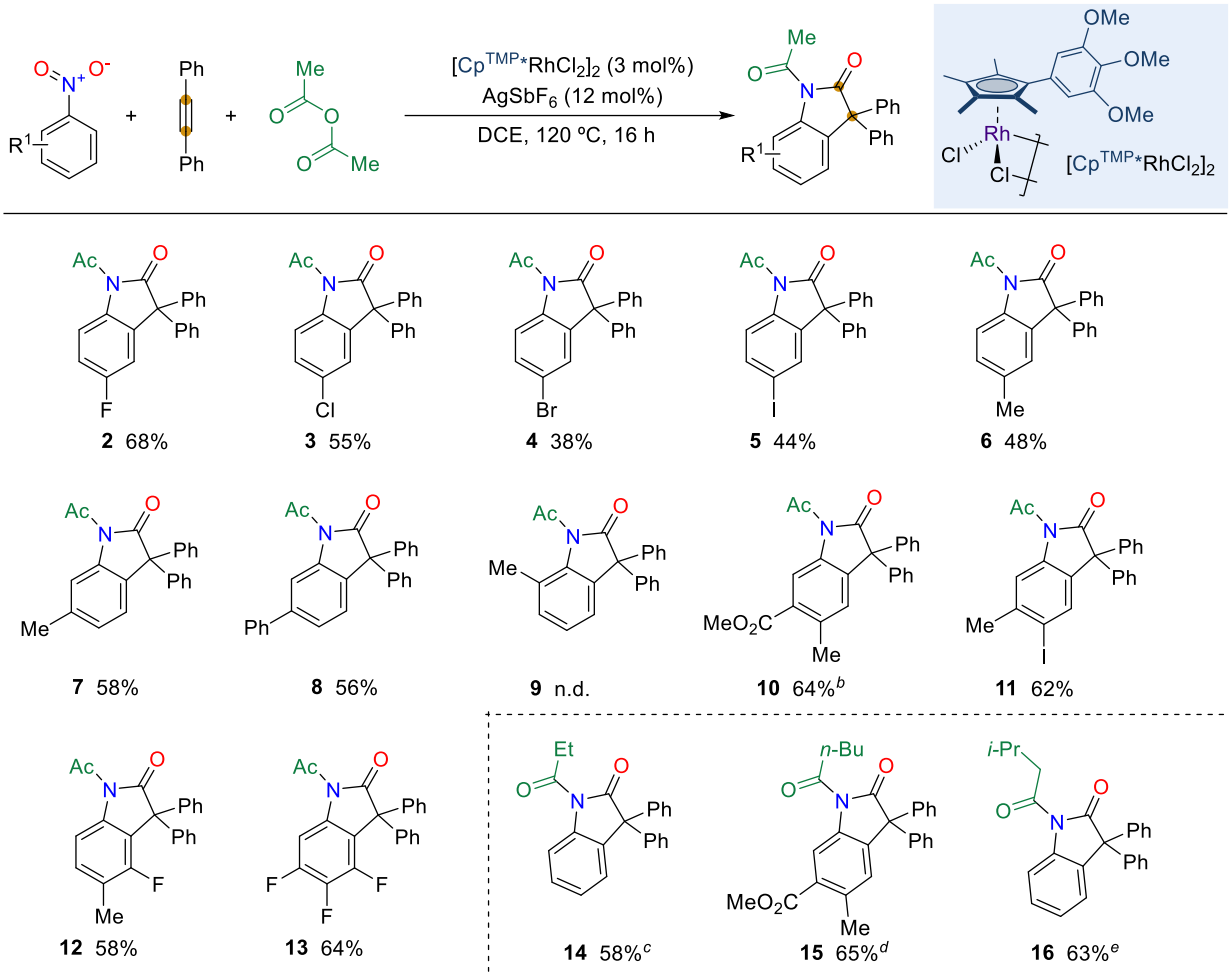

Reaction conditions: nitroarene (5 mmol), diphenylacetylene (0.5 mmol), and acetic anhydride (2 mmol), $[Cp^{TMP}*RhCl_2]_2$ (3 mol%), $AgSbF_6$ (12 mol%), DCE (2 mL) at 120 °C, 16 h. [b]Nitroarene (2.5 mmol). [c]From propionic anhydride. [d]From valeric anhydride. [e]From isovaleric anhydride.

Scheme 3.2. Scope of Nitroarenes and Anhydrides Partners.

A broad range of 1,2-diaryl alkynes was readily converted to the corresponding oxindole products in modest to good yields (Scheme 3.3). The reaction conditions were compatible with a variety of functional groups such as bromo (**17**, **18**), chloro (**19**), fluoro (**20**), trifluoromethyl (**21**), and alkyl (**22**, **23**). The reaction outcomes are not affected by the substitution patterns of the aryl group as a fluor-atom at the *meta*-position (**24**, **25**) or a chloro-atom at the *ortho*-position (**26**) atom were well tolerated. It should be noted that the [1,2]-aryl shift took place with complete retention of the regioselectivity of the migrated aryl group. We next explored this transformation with 1,2-diaryl alkynes containing two different aryl groups to form oxindoles with an α-carbonyl quaternary stereogenic center. Again, the reaction tolerated a wide range of functional group such as F, Cl, I, CO_2Et, Me, and OMe affording the oxindoles **27**-**32** in 50-65% yields.

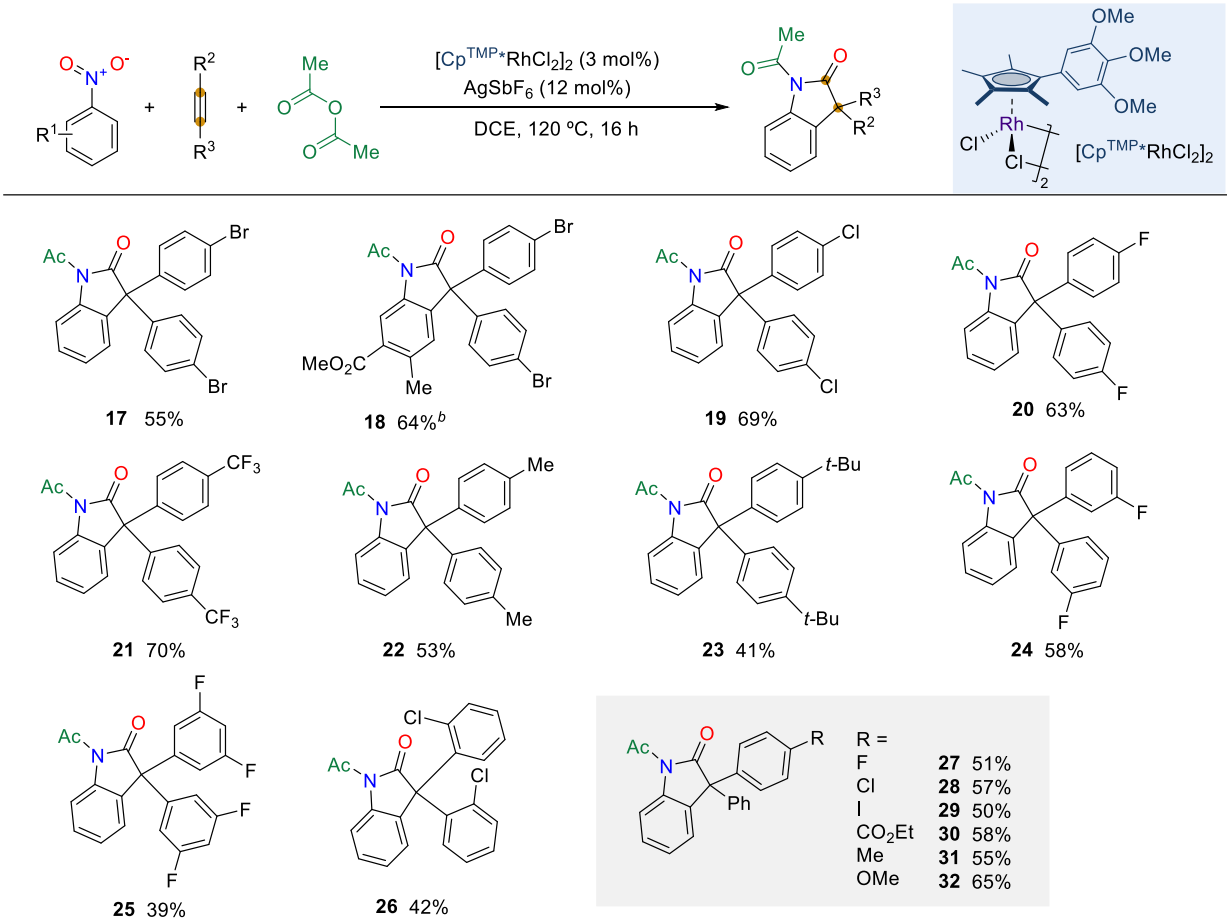

Reaction conditions: nitroarene (5 mmol), diarylacetylene (0.5 mmol), and acetic anhydride (2 mmol), $[Cp^{TMP}*RhCl_2]_2$ (3 mol%), $AgSbF_6$ (12 mol%), DCE (2 mL) at 120 °C, 16 h. [b]Nitroarene (2.5 mmol).

Scheme 3.3. Scope of Alkynes Partners.

3.2.3. Post-Functionalizations

In addition, to further illustrate the synthetic value of this novel reaction, we investigated the reduction of amide groups (Scheme 3.4). In the presence of $LiAlH_4$, the only reduction of the acetyl group was observed, affording the indolin-2-one **33** in 97% yield. While compound **1** was fully reduced using borane−tetrahydrofuran to deliver **34** in 80% yield. These 3,3-disubstituted indolines − which are architectures embedded in many complex alkaloids or key building blocks − are now easy to prepare from nitrobenzene in only two steps, where formerly multi-step synthesis was necessary.[19] Due to the strongly electron-withdrawing nature of the nitro group, the main limitation of our novel cascade reaction is the incompatibility with electron-poor nitroarenes because of an unfavorable C−H bond activation.[11] To improve the diversity of structure accessible through this methodology, we performed post-functionalization of iodo-substituted oxindoles. Firstly a formyl group was introduced through Rh(III)-catalyzed hydroformylation affording oxindole **35** in 75% yield. Pd-

catalyzed cyanation with $Zn(CN)_2$ as coupling reagent allowed to prepare 5-nitril-substituted oxindole **36** in 70% yield. Finally, we also succeeded to prepare alkynyl-substitued oxindole **37** through Pd/Cu-catalyzed Sonogashira reaction with phenyl acetylene in 85% yield.

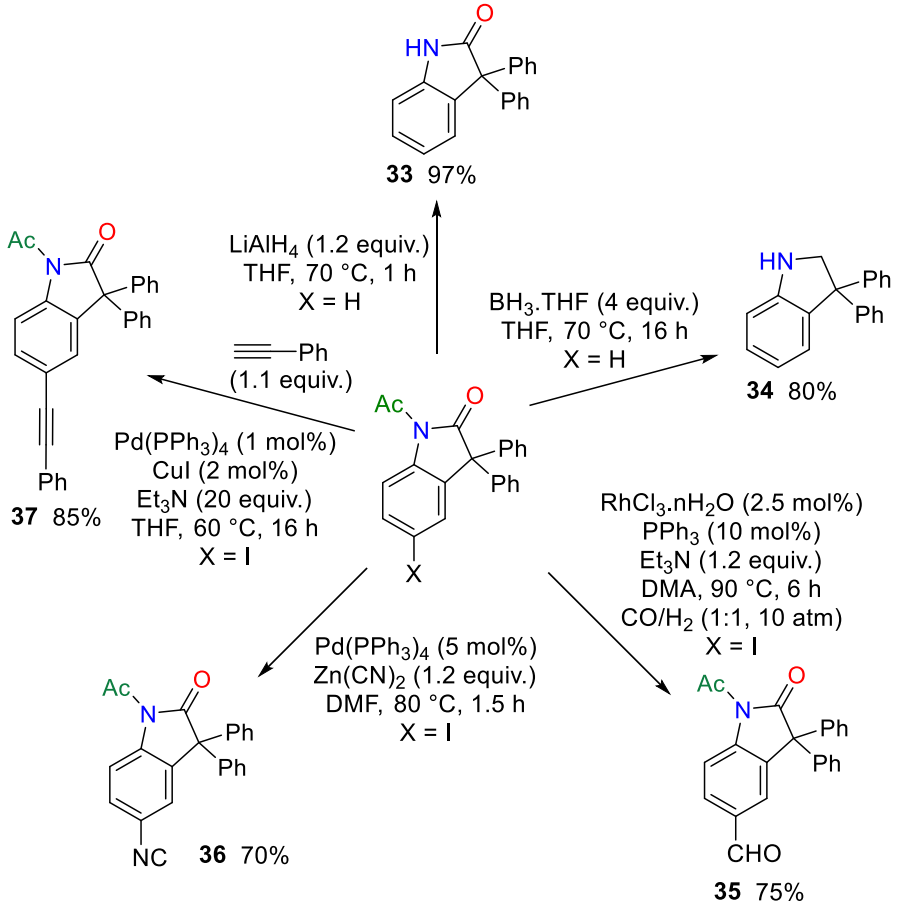

Scheme 3.4. Access to Molecular Diversity through Post-Functionalizations.

3.3. Mechanistic Study

In order to get insight into this unpredictable reaction, mechanistic experiments were conducted. Significant kinetic isotope effects (KIE 3.5 or 2.6) with both $[Cp^{TMP}*RhCl_2]_2$ and $[Cp*RhCl_2]$ support that the C–H bond cleavage corresponds to the rate determining step of the catalytic cycle (Scheme 3.5).

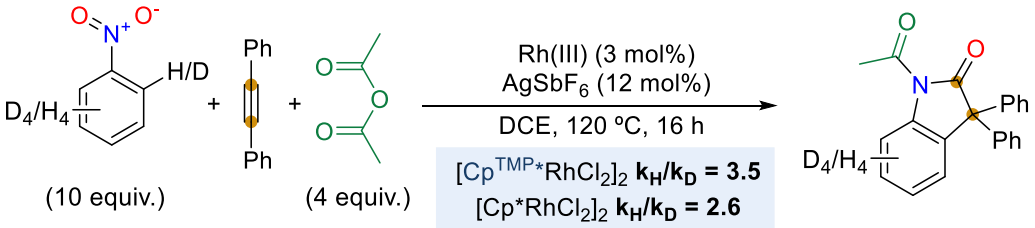

Scheme 3.5. Kinetic Isotope Effects (KIE) with $[Cp^{TMP}*RhCl_2]_2$ and $[Cp*RhCl_2]_2$.

Next, we decided to map the reaction by capturing potential rhodacycles and studying their reactivity (Figure 3.1). Our attempts to isolate a cyclometalated Rh(III) intermediate from a stoichiometric reaction between nitrobenzene and $[Cp^{TMP}*RhCl_2]_2$ in the presence or not of $AgSbF_6$ and acetate sources failed. However, cyclometalated Rh(III) **38a** has been prepared by transmetalation from 2-nitrophenylmercurial.[20] The reaction between **38a** and 1-diphenylacetylene with $AgSbF_6$ in DCE at room temperature afforded Rh(III) η^3-benzyl complex **39a**. This 18 e^- complex **39a** was fully characterized by NMR spectroscopies, mainly the exchange η^3-benzyl unit was observed by NOESY experiments. This intermediate **39a** results from the alkyne insertion into Rh−C bond followed by *O*-atom transfer. When we tried to get some crystal for X-ray analysis, **39a** spontaneously evolved into **40**. We, therefore, repeated the experiments with $[Cp*RhCl_2]_2$. Successfully, the Rh(III) η^3-benzyl complex **39b** was obtained as single crystals and analyzed by X-ray experiments, demonstrating that *O*-atom transfer has proceeded to give the formal hydration of alkyne among with coordinated nitrosobenzene. When this reaction was conducted at 80 °C, Rh(III) complex **40** was isolated by crystallization in good yield and was fully characterized, including by X-ray structure. This intermediate **40** is formed *via* the N−Rh bond insertion into the carbonyl group followed by a migration of the phenyl ring at the *meso*-position of the nitrobenzene ring. Finally, the reaction from **38a** or **40** in the presence of Ac_2O at 120 °C furnished the desired product **1**. Combined with the detection of 2-chloroacetaldehyde by GC-analysis, these results suggest that the second N−O bond cleavage occurred through *O*-alkylation with 1,2-dichloroethane followed by a hydride-shift.[21]

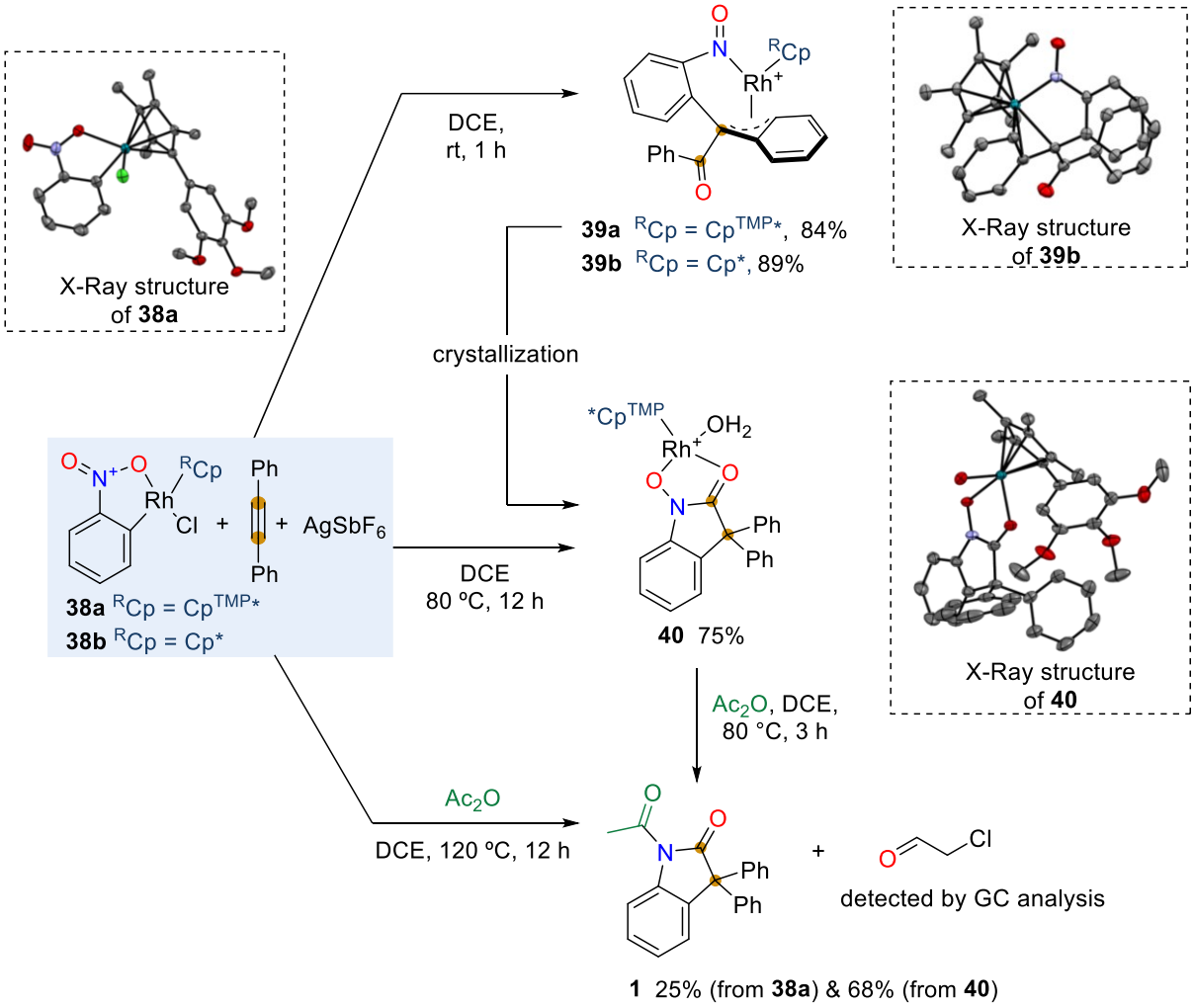

Scheme 3.5. Reaction Mapping through Isolation and Reactivities of Intermediates.

3.4. Proposed Mechanism

Based on these experiments and literature known mechanisms of Rh(III)-catalyzed C−H bond activation and *O*-atom transfer,[5-8] we propose the following catalytic cycle for Rh(III)-catalyzed C−H bond activation with migrations of nitroarenes with alkynes (Figure 3.2). The catalytically active species **A** is generated from $[Cp^{TMP}*RhCl_2]_2$ and $AgSbF_6$ in the presence of Ac_2O by chloride abstraction and ligand exchange. Nitro coordinates to the metal center, and rhodacycle **B** is formed by C−H bond cleavage with the release of AcOH, probably *via* a CMD mechanism. Alkyne associates with the metal center (**C**) and inserts into the Rh−C bond to give seven-member rhodacycle **D**. Then, an *O*-atom transfer occurred to afford the isolable η^3-benzyl nitroso complex **H**. The reaction may proceed through a reductive elimination affording cationic heterocycle **F** and Rh(I) followed by oxidative addition of the N−O bond to generate the O-bond Rh(III)-enolate intermediate **G,** which prefers to adopt the C-enolate form (**H**) displaying a η^3-benzyl coordination mode. Thus, the nucleophilic attack of the nitroso group

to the carbonyl group (shown by grey arrows) leads to the intermediate **I**. In analogy to semipinacol rearrangement,[22] a 1,2-aryl shift (shown by grey arrows) affords the isolable *N*-oxido Rh(III) complex **J**. The helicoidal-shape of Cp^{TMP}* might favor the nucleophilic attack since **39a** is consensually involved into **40** at room temperature, while **39b** with disc-shaped Cp* is stable. Finally, in the presence of 1,2-dichloroethane and Ac_2O, acylated indolinone **1** is formed in a non-catalyzed pathway along with the regeneration of the active catalytic species.

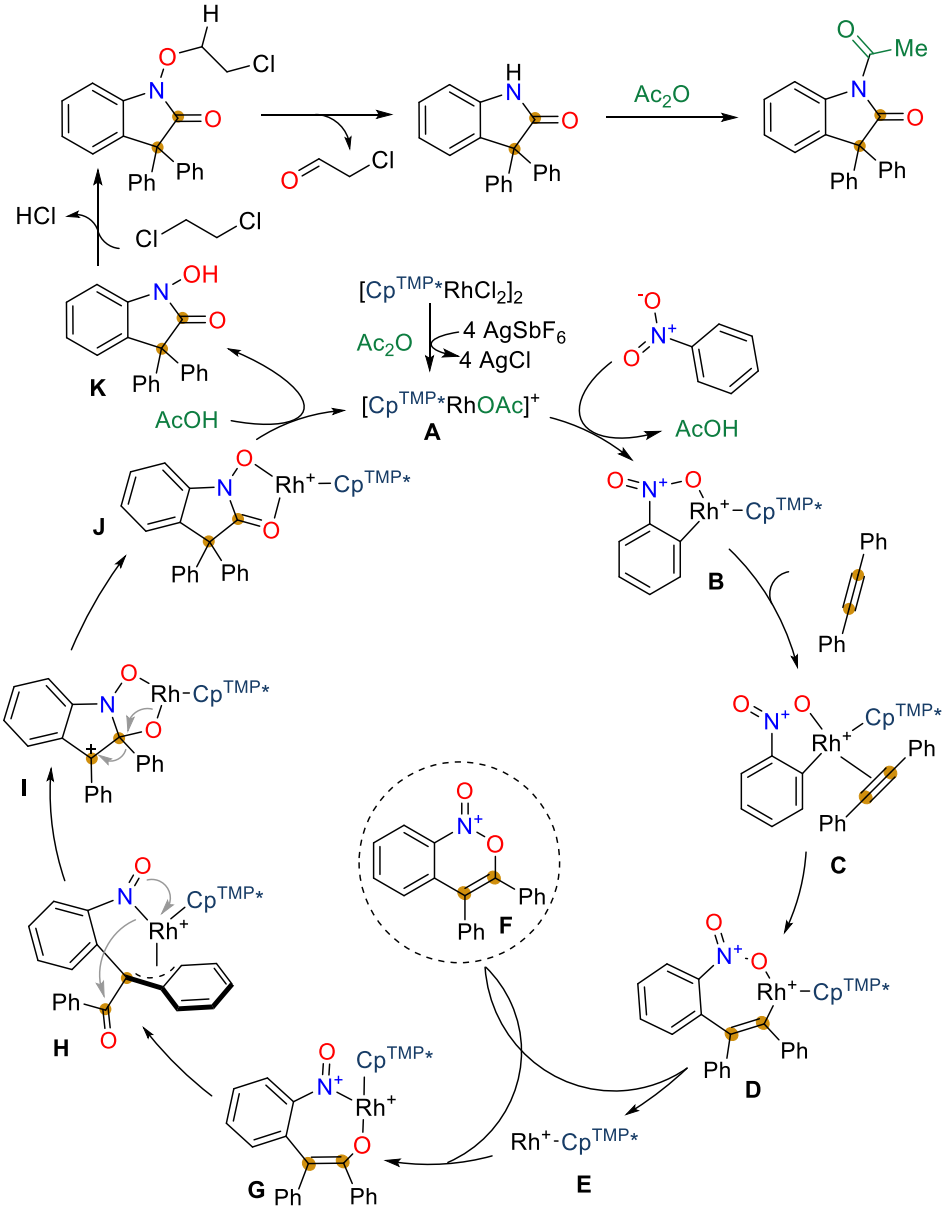

Figure 3.2. Proposed Mechanism.

3.5. Conclusion

In conclusion, we have developed a highly selective three-components protocol for the construction of oxindole derivatives with the formation of a quaternary center at the C3 position merely from nitroarenes and alkynes through Rh(III)-catalyzed one-pot cascade of C−H bond activation − *O*-atom transfer − [1,2]-aryl shift − deoxygenation − acylation. The reaction proceeds under redox-neutral conditions and tolerates a wide range of common functional groups. To improve the reactivity, we designed a new ligand, namely $Cp^{TMP}*$. Its resulting Rh(III) complex combines an electron-rich character required for C−H activation − or *O*-atom transfer − with a helicoidal shape to favor the nucleophilic character of the coordinated nitroso group. The reaction pathway has been rationalized by capturing and fully analyzing three Rh(III) intermediates. This unique strategy generating nitrosoarenes from nitroarenes will pave the way to explore further their reactivities in the presence of other coupling partners for the quest of novel cascade transformations to expend the chemical space of *N*-heterocycles.

3.6. Experimental Data

3.6.1. General Information

All reactions were carried out under argon atmosphere with standard Schlenk techniques or set up in a glovebox (Mbraun, MB10-Compact). All reagents were obtained from commercial sources and used as supplied unless stated otherwise. Acetic anhydride was distilled under argon before use. DCE and nitrobenzene were distilled with CaH_2 under argon. ^1H NMR spectra were recorded on Bruker AV III 400 MHz spectrometer fitted with a BBFO probe or Bruker AV III HD 500 MHz spectrometer fitted with a BBFO probe. Chemical shifts (δ) were reported in parts per million relatives to residual chloroform (7.26 ppm for ^1H; 77.16 ppm for ^{13}C), methylene chloride (5.32 ppm for ^1H; 54.00 ppm for ^{13}C) or dimethyl sulfoxide (2.50 ppm for ^1H; 39.52 ppm for ^{13}C). Coupling constants were reported in Hertz.

^1H NMR assignment abbreviations were the following: singlet (s), doublet (d), triplet (t), quartet (q), doublet of doublets (dd), doublet of triplets (dt), doublet of doublet of doublets (ddd), multiplet (m) and broad (br). ^{13}C NMR spectra were recorded at 101 MHz on the same spectrometer and reported in ppm. ^{19}F NMR spectra were recorded at 376 MHz on the same spectrometer and reported in ppm.

GC analyses were performed with a gas chromatograph (GC-2014 Shimadzu) instrument equipped with a capillary column (UptibondTM UB5P- 5% phenyl-95% dimethyl polysiloxane), which was coupled to a flame ionization detector (FID). The following GC conditions were

used: flow rate (77.7 kPa, N_2), Inject (250 °C), Detect. (280 °C), Int. T. (50 °C), Int. T. (2 min), Rate (20 °C /min), Fin. T. (280 °C), Fin. T. (20 min).

Mass spectroscopy were recorded on a Waters Q-Tof 2 mass spectrometer or a Bruker Ultraflex III mass spectrometer at the corresponding facilities of the CRMPO, Centre Régional de Mesures Physiques de l'Ouest, Université de Rennes 1.

Column chromatography was carried out on a Teledyne ISCO CombiFlash NextGen 300 using FlashPure silica flash columns (4, 12, 25 g; 35–45 µm). Substrates were purified using heptane and EtOAc on a gradient of 100:0 to 0:100 with flow rates of 13 – 400 mL/min depending on the size of column and ΔRf.

Cyclopentadienyl ligands Cp^E,[15] Cp^{iPr}*,[23] Cp^{Ph}*,[23] Cp^{MP}*,[14] rhodium(III) complexes $[Cp^ERhCl_2]_2$,[15] $[Cp^{iPr}$*$RhCl_2]_2$,[14] $[Cp^{Ph}$*$RhCl_2]_2$,[14] $[Cp^{MP}$*$RhCl_2]_2$,[14], alkynes 1,2-bis(4-chlorophenyl)ethyne,[24] 1,2-bis(4-fluorophenyl)ethyne,[24] 1,2-bis(4-(trifluoromethyl)phenyl)ethyne,[24] 1,2-bis(2-chlorophenyl)ethyne,[24] 1,2-di-*p*-tolylethyne,[25] 1,2-bis(3-fluorophenyl)ethyne,[25] 1,2-bis(4-(tert-butyl)phenyl)ethyne,[26] 1,2-bis(3,5-difluorophenyl)ethyne,[27] 1-fluoro-4-(phenylethynyl)benzene,[28] 1-iodo-4-(phenylethynyl)benzene,[29] 1-chloro-4-(phenylethynyl)benzene,[30] ethyl 4-(phenylethynyl)benzoate,[30] 1-methoxy-4-(phenylethynyl)benzene,[30] and 1-methyl-4-(phenylethynyl)benzene,[31] were already reported and prepared according to the literature.

3.6.2. Optimization of the Reaction Conditions

Procedure: In a glovebox, an oven-dried Schlenk tube was charged with $[Cp^*RhCl_2]_2$ (9.3 mg, 0.015 mmol, 3 mol%), $AgSbF_6$ (20 mg, 0.06 mmol, 12 mol%), diphenylacetylene (90 mg, 0.5 mmol, 1 equiv.), acetic anhydride (187 µL, 2 mmol, 4 equiv.)**,** nitrobenzene (512 µL, 5 mmol, 10 equiv.), the additives and solvent (2 mL). The Schlenk tube was closed and removed from the glovebox. The resulting mixture was stirred overnight at 120 °C unless stated otherwise. The crude product was then cooled down, diluted with ethyl acetate and injected in a calibrated GC-FID using *n*-dodecane (20 µL) as internal standard to give the corresponding yields. Conversion was based on diphenylacetylene consumption: t_R (min) 8.2 (*n*-dodecane), 11.5 (diphenylacetylene), 16.6 (product **1**).

Table 3.2. Screening of Solvents (GC Yields)

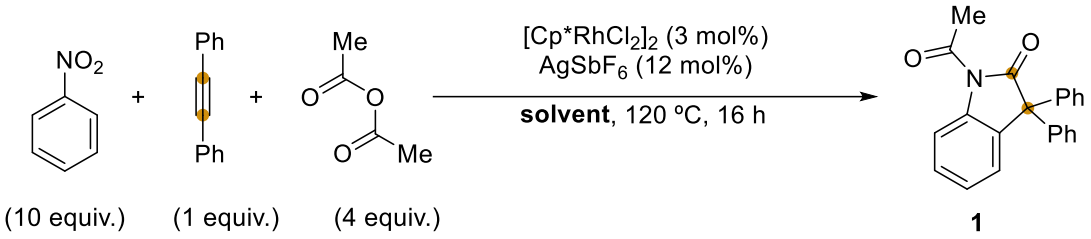

Entry	Solvent	Conversion (%)	Yield **1** (%)
1	DCE	100	41
2	Dioxane	100	18[a]
3	AcOH	0	0
4	DMA	0	0[a]
5	Ethoxyethanol	72	0
6	DMF	72	0[a]
7	HFIP	100	9
8	Dimethyl carbonate	100	26
9	Toluene	100	12[a]
10	1,2-Dichloropropane	69	5
11	Dioxane/DCE (1:1)	100	20

[a]Reactions were carried out at 160 °C.

Table 3.3. Screening of Additives (GC Yields)

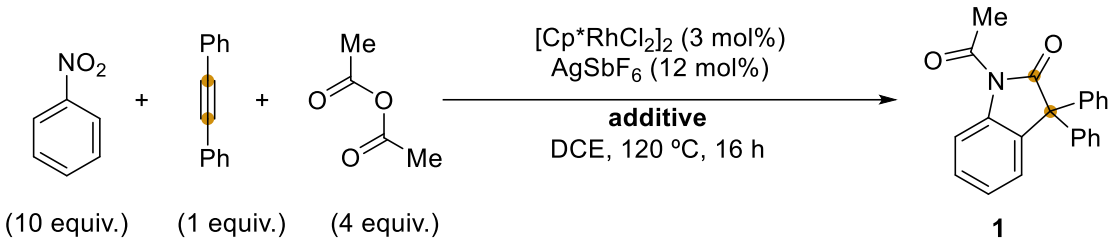

Entry	Additive	Conversion (%)	Yield **1** (%)
1	-	100	41
2	AcOH (10 mol%)	100	40
3	AcOH (40 mol%)	100	40
4	AcOH (2 equiv.)	100	35
5	PivOH (10 mol%)	100	38
6	AdCOOH (10 mol%)	100	40
7	AgOAc (10 mol%)	100	41
8	$AgNO_3$ (10 mol%)	100	27
9	$AgClO_4$ (10 mol%)	100	18
10	AgOPiv (10 mol%)	100	42
11	AgOAd (10 mol%)	100	42
12	$Cu(OAc)_2$ (20 mol%)	100	43
13	$Cu(OAc)_2$ (1 equiv.)	100	44
14	PPh_3 (25 mol%)	55	3
15	Zn (2 equiv.)	95	traces
16	$PhSiH_3$ (2 equiv.)	0	0
17	$Mo(CO)_6$ (2 equiv.)	33	0
18	KOAc (20 mol%)	0	0
19	CsF (1 equiv.)	33	0
20	H_2O (2.5 equiv.)	100	40
21	H_2O (5 equiv.)	72	traces

3.6.3. Synthesis of Novel Cyclopentadienyl Proligands (Cp^RH), Rhodium Complexes $[Cp^RRhCl_2]_2$ and their Characterizations

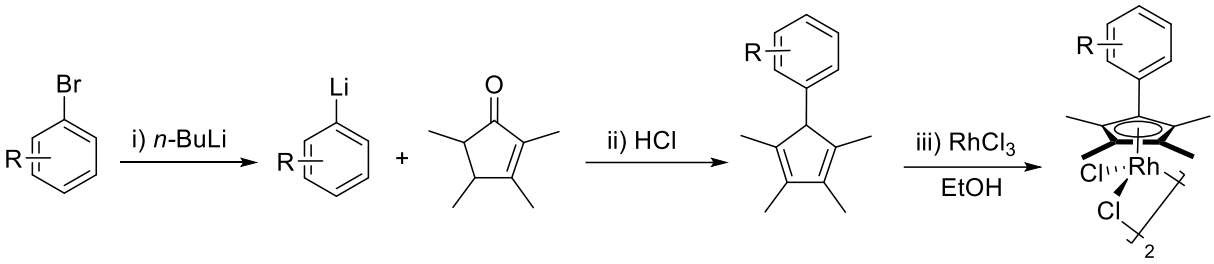

Scheme 3.6. Synthesis of Rhodium Complexes $[Cp^RRhCl_2]_2$.

1-(3,4-Dimethoxyphenyl)-2,3,4,5-tetramethylcyclopentadienyl (Cp^{DMP}*H)

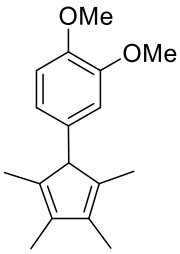

The organolithium reagent was prepared from 4-bromoveratrole (1.2 mL, 8.4 mmol, 1.2 equiv.) and a solution of *n*-BuLi (1.1 M in hexanes, 7.6 mL, 8.4 mmol, 1.2 equiv.) in anhydrous Et_2O (30 mL) under argon at -78 °C. The solution was stirred over 30 min then cannulated to a cooled mixture of 2,3,4,5-tetramethyl-2-cyclopentenone (1 mL, 7 mmol, 1 equiv.) in anhydrous Et_2O (10 mL) at -78 °C. The resultant mixture was stirred over 15 min then warmed up to room temperature and stirred overnight.

The reaction was quenched with water (5 mL) at 0 °C and 2 N HCl aq. (10 mL) was added to dissolve all inhomogeneities. The aqueous layer was extracted with Et_2O (10 mL x3). The combined organic layers were dried over $MgSO_4$ and concentrated under reduced pressure. The product was obtained in 28% yield as a yellow oil and directly used for the next step.

^{1}H NMR (400 MHz, $CDCl_3$) δ (ppm) 6.94 – 6.85 (m, 2H), 6.81 – 6.75 (m, 1H), 4.00 – 3.75 (m, 6H), 3.14 (dt, *J* = 7.7, 1.7 Hz, 1H), 2.02 (d, *J* = 1.8 Hz, 3H), 1.92 (s, 3H), 1.86 (s, 3H), 1.56 (s, 3H).

Dichloro[1-(3,4-Dimethoxyphenyl)-2,3,4,5-tetramethylcyclopentadienyl]rhodium (III),dimer $[Cp^{DMP}*RhCl_2]_2$

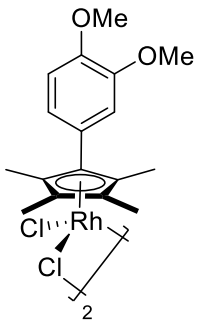

To a solution of **Cp^{DMP}H***(296 mg, 1.15 mmol, 1.2 equiv.) in EtOH absolute (8 mL) was added $RhCl_3.nH_2O$ (200 mg, 0.95 mmol, 1 equiv.). The resulting mixture was stirred at 85 °C under an argon atmosphere over 3 days. The solvent was removed under reduced pressure. After purification on silica column using dichloromethane as eluent, the rhodium complex was obtained in 34% yield as an orange solid.

^{1}H NMR (400 MHz, $CDCl_3$) δ (ppm) 7.53 (d, *J* = 2.0 Hz, 1H), 7.04 (m, 1H), 6.88 – 6.85 (m, 1H), 3.94 (s, 3H), 3.89 (s, 3H), 1.71 (s, 6H), 1.70 (s, 6H).

^{13}C NMR (101 MHz, $CDCl_3$) δ (ppm) 149.6, 148.9, 122.4, 120.6, 114.6, 111.1, 100.2 (d, *J* = 8.4 Hz), 93.4 (d, *J* = 9.0 Hz), 56.5, 56.0, 10.8, 9.7.

HRMS m/z (MALDI) calcd for $C_{34}H_{42}O_4Cl_3Rh_2$ $[M\text{-}Cl]^+$ 825.0253 found 825.0257.

1-(3,4,5-Trimethoxyphenyl)-2,3,4,5-tetramethylcyclopentadienyl ($Cp^{TMP}H^*$)

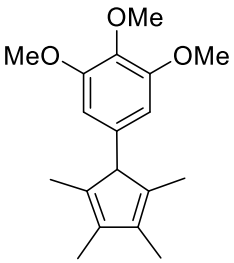

The organolithium reagent was prepared from 5-bromo-1,2,3-trimethoxybenzene (2 g, 8.4 mmol, 1.2 equiv.) and a solution of *n*-BuLi (1.1 M in hexanes, 7.6 mL, 8.4 mmol, 1.2 equiv.) in anhydrous THF (30 mL) under argon at -78 °C. The solution was stirred over 30 min and then cannulated to a cooled mixture of 2,3,4,5-tetramethyl-2-cyclopentenone (1 mL, 7 mmol, 1 equiv.) in anhydrous THF (10 mL) at -78 °C. The resultant mixture was stirred over 15 min then warmed up to room temperature and stirred overnight. The reaction was quenched with water (5 mL) at 0 °C and 2 N HCl aq. (10 mL) was added to dissolve all inhomogeneities. The aqueous layer was extracted with Et_2O (10 mL x3). The combined organic layers were dried over $MgSO_4$ and concentrated under reduced pressure. The product was obtained in 70% yield as a yellow oil and directly used for the next step.

^{1}H NMR (400 MHz, $CDCl_3$) δ (ppm) 6.43 (s, 2H), 3.86 (d, *J* = 1.3 Hz, 9H), 1.69 (s, 12H).

Dichloro[1-(3,4,5-Trimethoxyphenyl)-2,3,4,5-tetramethylcyclopentadienyl] rhodium (III) dimer $[Cp^{TMP}*RhCl_2]_2$

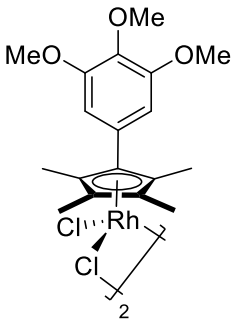

To a solution of **$Cp^{TMP}H^*$** (332 mg, 1.15 mmol, 1.2 equiv.) in EtOH absolute (8 mL) was added $RhCl_3.nH_2O$ (200 mg, 0.95 mmol, 1 equiv.). The resulting mixture was stirred at 85 °C under an argon atmosphere over 3 days. The resulting precipitate was filtered and rinsed with cold ethanol and pentane to obtain the corresponding rhodium complex in 42% yield as an orange solid. Crystals suitable for X-ray diffraction were grown by slow diffusion of pentane into a dichloromethane solution of the rhodium complex.

^{1}H NMR (400 MHz, $CDCl_3$) δ (ppm) 6.99 (s, 2H), 3.87 (s, 9H), 1.72 (s, 6H), 1.70 (s, 6H).

^{13}C NMR (101 MHz, $CDCl_3$) δ (ppm) 153.2, 138.5, 123.6, 108.0, 100.9 (d, *J* = 8.5 Hz), 93.5 (d, *J* = 9.0 Hz), 60.9, 56.6, 10.8, 9.7.

HRMS m/z (MALDI) calcd for $C_{36}H_{46}O_6Cl_3Rh_2$ $[M\text{-}Cl]^+$ 885.0465 found 885.0468.

1-(4-Trifluorotoluene)-2,3,4,5-tetramethylcyclopentadienyl ($Cp^{TFT}H^*$)

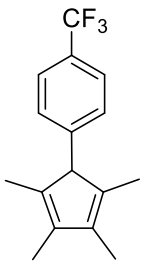

The organolithium reagent was prepared from 4-bromobenzotrifluoride (1.2 mL, 8.4 mmol, 1.2 equiv.) and a solution of *n*-BuLi (1.1 M in hexanes, 7.6 mL, 8.4 mmol, 1.2 equiv.) in anhydrous THF (30 mL) under argon at -78 °C. The solution was stirred over 30 min and then cannulated to a cooled mixture of 2,3,4,5-tetramethyl-2-cyclopentenone (1 mL, 7 mmol, 1 equiv.) in anhydrous THF (10 mL) at -78 °C. The resultant mixture was stirred over 15 min then warmed up to room temperature and stirred overnight.

The reaction was quenched with water (5 mL) at 0 °C and 2 N HCl aq. (10 mL) was added to dissolve all inhomogeneities. The aqueous layer was extracted with Et_2O (10 mL x3). The combined organic layers were dried over $MgSO_4$ and concentrated under reduced pressure. The product was obtained in 50% yield as yellow oil and directly used for the next step.

^{1}H NMR (400 MHz, $CDCl_3$) δ (ppm) 7.59 (d, *J* = 8.2 Hz, 2H), 7.36 – 7.30 (m, 2H), 3.30 – 3.16 (m, 1H), 2.05 (s, 3H), 1.94 (s, H), 1.87 (s, 3H), 0.96 (d, *J* = 7.7 Hz, 3H).

^{19}F NMR (376 MHz, $CDCl_3$) δ (ppm) -62.2.

Dichloro[1-(4-Trifluorotoluene)-2,3,4,5-tetramethylcyclopentadienyl]rhodium (III), dimer $[Cp^{TFT}*RhCl_2]_2$

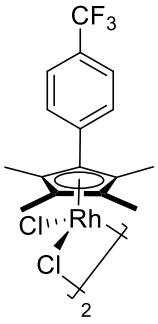

To a solution of **$Cp^{TFT}H^*$** (306 mg, 1.15 mmol, 1.2 equiv.) in EtOH absolute (8 mL) was added $RhCl_3.nH_2O$ (200 mg, 0.95 mmol, 1 equiv.). The resulting mixture was stirred at 85 °C under an argon atmosphere over 3 days. The resulting precipitate was filtered and rinsed with cold ethanol and pentane to obtain the corresponding rhodium complex in 40% yield as an orange solid. Crystals suitable for X-ray diffraction were grown by slow diffusion of pentane into a dichloromethane solution of the rhodium complex.

^{1}H NMR (400 MHz, $CDCl_3$) δ (ppm) 7.83 (d, *J* = 8.0 Hz, 2H), 7.68 – 7.62 (m, 2H), 1.73 (s, 6H), 1.67 (s, 6H).

^{19}F NMR (376 MHz, $CDCl_3$) δ (ppm) -62.9.

^{13}C NMR (101 MHz $CDCl_3$) δ (ppm) 132.5, 131.4, 131.1, 125.8 (q, *J* = 3.5 Hz), 124.1 (d, *J* = 272.7 Hz), 100.8 (d, *J* = 8.5 Hz), 94.2 (d, *J* = 9.0 Hz), 89.2 (d, *J* = 9.9 Hz)., 10.7, 9.7.

HRMS m/z (MALDI) calcd for $C_{32}H_{32}F_6Cl_3Rh_2$ $[M\text{-}Cl]^+$ 840.9578 found 840.9680.

General Procedure for Measuring Redox Potentials of Rhodium Complexes $[Cp^RRhCl_2]_2$: Peak potentials (Ep) were measured relative to Fc^+/Fc as reference and obtained by square wave voltammetry and cyclic voltammetry. Measurements were performed on complexes

$[Cp^{R}RhCl_2]_2$ at nominal concentrations of 0.005 M in degassed dimethylformamide using a 0.10 M solution of $[n\text{-}Bu_4N][PF_6]$ as the electrolyte, with a carbon glass working electrode, a Pt wire as auxiliary electrode, and a Ag wire as reference electrode at a scan rate of 250 $mV.s^{-1}$.

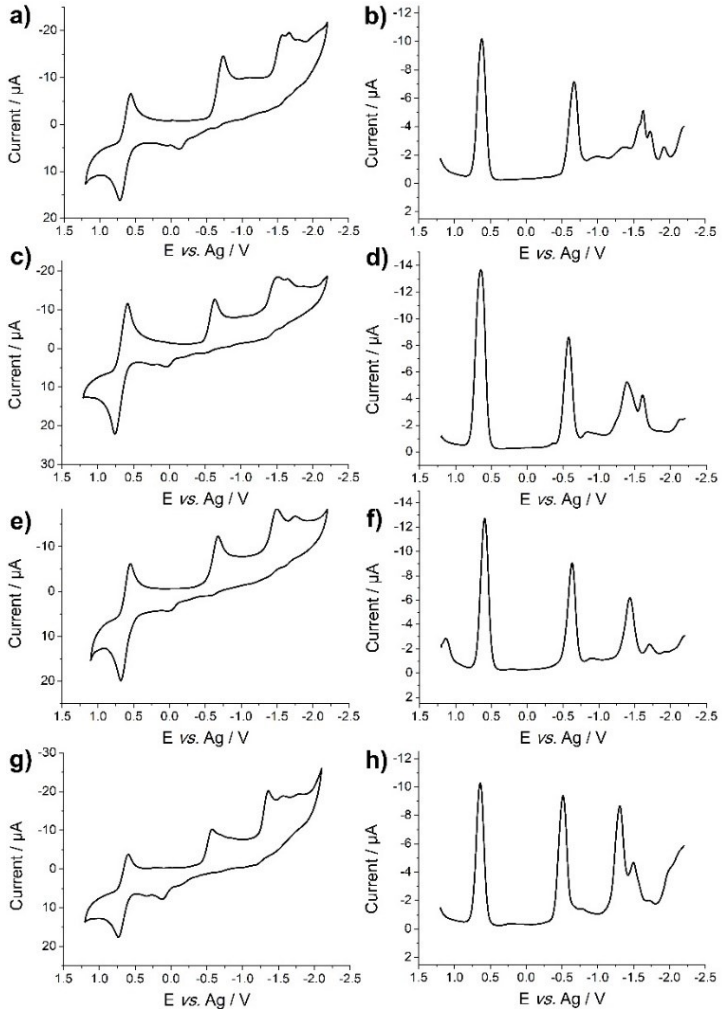

Figure 3.3. **a**) Cyclic Voltammogram of $[Cp^*RhCl_2]_2$. **b**) Square Wave Voltammogram of $[Cp^*RhCl_2]_2$. **c**) Cyclic Voltammogram of $[Cp^{DMP}*RhCl_2]_2$. **d**) Square Wave Voltammogram of $[Cp^{DMP}*RhCl_2]_2$. **e**) Cyclic Voltammogram of $[Cp^{TMP}*RhCl_2]_2$. **f**) Square Wave Voltammogram of $[Cp^{TMP}*RhCl_2]_2$. **g**) Cyclic Voltammogram of $[Cp^{TFT}*RhCl_2]_2$. **h**) Square Wave Voltammogram of $[Cp^{TFT}*RhCl_2]_2$.

3.6.4. Representative Procedure for the Synthesis of 1-32 and Compounds Characterization

Procedure: In a glovebox, an oven-dried 15 mL Schlenk tube was charged with $[Cp^{TMP}*RhCl_2]_2$ (13.8 mg, 0.015 mmol, 3 mol%) $AgSbF_6$ (20 mg, 0.06 mmol, 12 mol%), alkyne (0.5 mmol, 1 equiv.), anhydride (2 mmol, 4 equiv.), nitroarene (5 mmol, 10 equiv.) and DCE (2 mL). The Schlenk tube was closed and removed from the glovebox. The resulting mixture was stirred at

120 °C overnight. The solvent was removed under vacuo and the crude product was purified on flash chromatography using heptane and ethyl acetate as eluents to provide the pure products.

1-Acetyl-3,3-diphenylindolin-2-one (1)

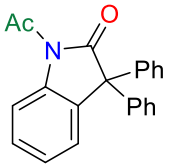

Following the general procedure using nitrobenzene (512 µL, 5 mmol, 10 equiv.), diphenylacetylene (90 mg, 0.5 mmol, 1 equiv.) and acetic anhydride (187 µL, 2 mmol, 4 equiv.), the residue was purified by flash chromatography on silica gel (Heptane/Ethyl Acetate = 95:5) to afford **1** as a pale yellow solid in 72% yield (118 mg, 0.3 mmol). Crystals suitable for X-ray diffraction were grown by slow diffusion of pentane into a dichloromethane solution of **1**.

^{1}H NMR (400 MHz, $CDCl_3$) δ (ppm) 8.43 – 8.29 (m, 1H), 7.46 – 7.20 (m, 13H), 2.74 (s, 3H).

^{13}C NMR (101 MHz, $CDCl_3$) δ (ppm) 178.8, 171.2, 141.5, 139.5, 132.1, 128.8, 128.7, 128.6, 127.9, 126.1, 125.6, 117.0, 63.2, 26.9.

HRMS m/z (ESI) calcd for $C_{22}H_{17}NO_2Na$ $[M+Na]^+$ 350.1151, found 350.1151.

1-Acetyl-5-fluoro-3,3-diphenylindolin-2-one (2)

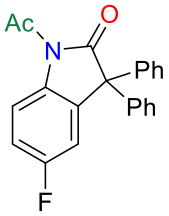

Following the general procedure using 1-fluoro-4-nitrobenzene (530 µL, 5 mmol, 10 equiv.), diphenylacetylene (90 mg, 0.5 mmol, 1 equiv.) and acetic anhydride (187 µL, 2 mmol, 4 equiv.), the residue was purified by flash chromatography on silica gel (Heptane/Ethyl Acetate = 95:5) to afford **2** as a yellow solid in 68% yield (117 mg, 0.34 mmol).

^{1}H NMR (400 MHz, $CDCl_3$) δ (ppm) 8.34 (dd, *J* = 9.0, 4.8 Hz, 1H), 7.40 – 7.29 (m, 6H), 7.24 – 7.12 (m, 4H), 7.06 (td, *J* = 8.9, 2.8 Hz, 1H), 6.93 (dd, *J* = 7.9, 2.8 Hz, 1H), 2.70 (s, 3H).

^{19}F{^{1}H} NMR (376 MHz, $CDCl_3$) δ (ppm) -115.6.

^{13}C NMR (101 MHz, $CDCl_3$) δ (ppm) 178.4, 171.0, 160.4 (d, *J* = 245.4 Hz), 140.9, 135.5 (d, *J* = 2.5 Hz), 134.1 (d, *J* = 8.1 Hz), 128.9, 128.5, 128.2, 118.5 (d, *J* = 7.9 Hz), 115.5 (d, *J* = 22.7 Hz), 113.4 (d, *J* = 24.6 Hz), 63.3, 26.8.

HRMS m/z (ESI) calcd for $C_{22}H_{16}NO_2FNa$ $[M+Na]^+$ 368.1057, found 368.1057.

1-Acetyl-5-chloro-3,3-diphenylindolin-2-one (3)

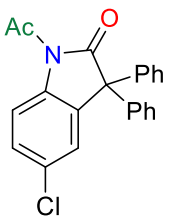

Following the general procedure using 1-chloro-nitrobenzene (788 mg, 5 mmol, 10 equiv.), diphenylacetylene (90 mg, 0.5 mmol, 1 equiv.) and acetic anhydride (187 µL, 2 mmol, 4 equiv.), the residue was purified by flash

chromatography on silica gel (Heptane/Ethyl Acetate = 95:5) to afford **3** as a yellow solid in 55% yield (99 mg, 0.28 mmol).

^{1}H NMR (400 MHz, $CDCl_3$) δ (ppm) 8.31 (d, *J* = 8.8 Hz, 1H), 7.40 – 7.26 (m, 7H), 7.25 – 7.15 (m, 5H), 2.70 (s, 3H).

13C NMR (101 MHz, $CDCl_3$) δ (ppm) 178.1, 171.0, 140.8, 138.0, 133.9, 131.0, 129.7, 128.9, 128.2, 126.2, 125.1, 118.3, 63.2, 26.9.

HRMS m/z (ESI) calcd for $C_{22}H_{16}NO_2ClNa$ $[M+Na]^+$ 384.0762, found 384.0762.

1-Acetyl-5-bromo-3,3-diphenylindolin-2-one (4)

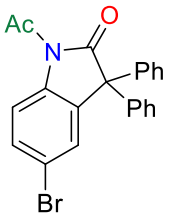

Following the general procedure using 1-bromo-4-nitrobenzene (1010 mg, 5 mmol, 10 equiv.), diphenylacetylene (90 mg, 0.3 mmol, 1 equiv.) and acetic anhydride (187 µL, 2 mmol, 4 equiv.), the residue was purified by flash chromatography on silica gel (Heptane/Ethyl Acetate = 95:5) to afford **4** as a yellow solid in 38% yield (77 mg, 0.19 mmol).

^{1}H NMR (400 MHz, $CDCl_3$) δ (ppm) 8.24 (d, *J* = 8.7 Hz, 1H), 7.52 – 7.45 (m, 1H), 7.39 – 7.30 (m, 7H), 7.23 – 7.12 (m, 4H), 2.69 (s, 3H).

^{13}C NMR (101 MHz, $CDCl_3$) δ (ppm) 178.1, 171.0, 140.8, 138.5, 134.2, 131.9, 129.0, 128.9, 128.5, 128.2, 118.7, 118.6, 63.1, 26.9.

HRMS m/z (ESI) calcd for $C_{22}H_{16}NO_2BrNa$ $[M+Na]^+$ 428.0256, found 428.0253.

1-Acetyl-5-iodo-3,3-diphenylindolin-2-one (5)

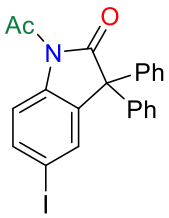

Following the general procedure using 1-iodo-4-nitrobenzene (1245 mg, 5 mmol, 10 equiv.), diphenylacetylene (90 mg, 0.5 mmol, 1 equiv.) and acetic anhydride (187 µL, 2 mmol, 4 equiv.), the residue was purified by flash chromatography on silica gel (Heptane/Ethyl Acetate = 98:2) to afford **5** as a yellow solid in 44% yield (100 mg, 0.22 mmol).

^{1}H NMR (400 MHz, $CDCl_3$) δ (ppm) 8.12 (d, *J* = 8.6 Hz, 1H), 7.69 (m, 1H), 7.50 (m, 1H), 7.36 – 7.31 (m, 6H), 7.22 – 7.16 (m, 4H), 2.69 (s, 3H).

^{13}C NMR (101 MHz, $CDCl_3$) δ (ppm) 177.9, 171.0, 140.8, 139.2, 137.9, 134.7, 134.4, 128.9, 128.5, 128.2, 119.0, 89.3, 63.0, 26.9.

HRMS m/z (ESI) calcd for $C_{22}H_{16}NO_2INa$ $[M+Na]^+$ 476.0118, found 476.0119.

1-Acetyl-5-methyl-3,3-diphenylindolin-2-one (6)

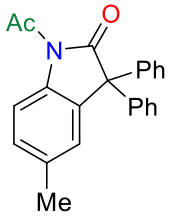

Following the general procedure using 4-nitrotoluene (685 mg, 5 mmol, 10 equiv.), diphenylacetylene (90 mg, 0.5 mmol, 1 equiv.) and acetic anhydride (187 µL, 2 mmol, 4 equiv.), the residue was purified by flash chromatography on silica gel (Heptane/Ethyl Acetate = 95:5) to afford **6** as a yellow solid in 48% yield (82 mg, 0.24 mmol).

^{1}H NMR (400 MHz, $CDCl_3$) δ (ppm) 8.22 (d, *J* = 8.3 Hz, 1H), 7.42 – 7.29 (m, 6H), 7.29 – 7.20 (m, 4H), 7.21 – 7.09 (m, 1H), 7.01 (s, 1H), 2.70 (s, 3H), 2.33 (s, 3H).

^{13}C NMR (101 MHz, $CDCl_3$) δ (ppm) 179.0, 171.1, 141.6, 137.2, 135.3, 132.1, 129.4, 128.7, 128.7, 127.8, 126.5, 116.8, 63.3, 26.9, 21.4.

HRMS m/z (ESI) calcd for $C_{23}H_{19}NO_2Na$ $[M+Na]^+$ 364.1308, found 364.1308.

1-Acetyl-6-methyl-3,3-diphenylindolin-2-one (7)

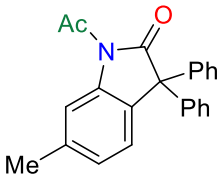

Following the general procedure using 3-nitrotoluene (433 µL, 5 mmol, 10 equiv.), diphenylacetylene (90 mg, 0.5 mmol, 1 equiv.) and acetic anhydride (187 µL, 2 mmol, 4 equiv.), the residue was purified by flash chromatography on silica gel (Heptane/Ethyl Acetate = 95:5) to afford **7** as a yellow solid in 58% yield (99 mg, 0.29 mmol).

^{1}H NMR (400 MHz, $CDCl_3$) δ (ppm) 8.26 (s, 1H), 7.40 – 7.32 (m, 7H), 7.30 – 7.24 (m, 4H), 7.18 – 7.06 (m, 2H), 2.75 (s, 3H), 2.46 (s, 3H).

^{13}C NMR (101 MHz, $CDCl_3$) δ (ppm) 179.1, 171.2, 141.7, 139.4, 138.9, 129.2, 128.7, 128.6, 127.8, 126.2, 125.7, 117.5, 63.0, 26.9, 22.0.

HRMS m/z (ESI) calcd for $C_{23}H_{19}NO_2Na$ $[M+Na]^+$ 364.1308, found 364.1308.

1-Acetyl-3,3,4-triphenylindolin-2-one (8)

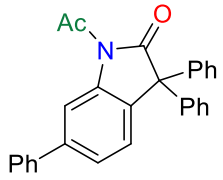

Following the general procedure using 3-nitrobiphenyl (997 mg, 5 mmol, 10 equiv.), diphenylacetylene (90 mg, 0.5 mmol, 1 equiv.) and acetic anhydride (187 µL, 2 mmol, 4 equiv.), the residue was purified by flash chromatography on silica gel (Heptane/Ethyl Acetate = 95:5) to afford **8** as a yellow solid in 58% yield (117 mg, 0.29 mmol).

^{1}H NMR (400 MHz, $CDCl_3$) δ (ppm) 8.62 (d, *J* = 1.7 Hz, 1H), 7.65 – 7.60 (m, 2H), 7.48 – 7.42 (m, 3H), 7.41 – 7.31 (m, 7H), 7.30 – 7.23 (m, 5H), 2.73 (s, 3H).

^{13}C NMR (101 MHz, $CDCl_3$) δ (ppm) 179.0, 171.3, 142.2, 141.5, 140.8, 140.0, 131.0, 129.0, 128.8, 128.6, 128.0, 127.8, 127.5, 126.2, 124.5, 115.8, 63.1, 27.1.

HRMS m/z (ESI) calcd for $C_{28}H_{21}NO_2Na$ $[M+Na]^+$ 426.1464, found 426.1461.

Methyl 1-acetyl-5-methyl-2-oxo-3,3-diphenylindoline-6-carboxylate (10)

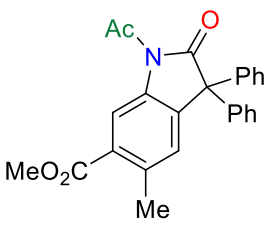

Following the general procedure using methyl 2-methyl-5-nitrobenzoate (488 mg, 2.5 mmol, 5 equiv.), diphenylacetylene (90 mg, 0.5 mmol, 1 equiv.) and acetic anhydride (187 µL, 2 mmol, 4 equiv.), the residue was purified by flash chromatography on silica gel (Heptane/Ethyl Acetate = 90:10) to afford **10** as a yellow solid in 64% yield (128 mg, 0.32 mmol).

^{1}H NMR (400 MHz, $CDCl_3$) δ (ppm) 8.84 (s, 1H), 7.36 – 7.28 (m, 6H), 7.26 – 7.14 (m, 4H), 7.08 (s, 1H), 3.92 (s, 3H), 2.71 (s, 3H), 2.56 (s, 3H)

^{13}C NMR (101 MHz, $CDCl_3$) δ (ppm) 178.3, 170.9, 167.6, 140.8, 137.8, 137.4, 135.8, 130.1, 128.9, 128.8, 128.6, 128.1, 118.6, 63.3, 52.3, 26.8, 21.7.

HRMS m/z (ESI) calcd for $C_{25}H_{21}NO_4Na$ $[M+Na]^+$ 422.1362, found 422.1362.

1-Acetyl-5-iodo-6-methyl-3,3-diphenylindolin-2-one (11)

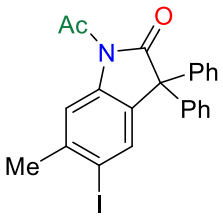

Following the general procedure using 2-iodo-5-nitrotoluene (1315 mg, 5 mmol, 10 equiv.), diphenylacetylene (90 mg, 0.5 mmol, 1 equiv.) and acetic anhydride (187 µL, 2 mmol, 4 equiv.), the residue was purified by flash chromatography on silica gel (Heptane/Ethyl Acetate = 97:3) to afford **11** as a yellow solid in 62% yield (145 mg, 0.31 mmol).

^{1}H NMR (400 MHz, $CDCl_3$) δ (ppm) 8.29 (s, 1H), 7.59 (s, 1H), 7.35 – 7.30 (m, 6H), 7.23 – 7.17 (m, 4H), 2.69 (s, 3H), 2.49 (s, 3H).

^{13}C NMR (101 MHz, $CDCl_3$) δ (ppm) 178.3, 171.1, 142.2, 141.1, 139.8, 135.8, 131.6, 128.9, 128.5, 128.1, 118.1, 96.1, 62.7, 28.9, 27.0

HRMS m/z (ESI) calcd for $C_{23}H_{18}NO_2INa$ $[M+Na]^+$ 490.0274, found 490.0273.

1-Acetyl-4-fluoro-5-methyl-3,3-diphenylindolin-2-one (12)

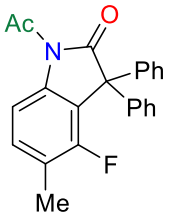

Following the general procedure using 1-fluoro-2-methyl-5-nitrobenzene (775 mg, 5 mmol, 10 equiv.), diphenylacetylene (90 mg, 0.5 mmol, 1 equiv.) and acetic anhydride (187 µL, 2 mmol, 4 equiv.), the residue was purified by flash chromatography on silica gel (Heptane/Ethyl Acetate = 95:5) to afford **12** as a yellow solid in 58% yield (104 mg, 0.29 mmol).

^{1}H NMR (400 MHz, $CDCl_3$) δ (ppm) 8.06 (d, *J* = 8.3 Hz, 1H), 7.37 – 7.30 (m, 6H), 7.30 – 7.24 (m, 4H), 7.25 – 7.18 (m, 1H), 2.70 (s, 3H), 2.24 (s, 3H).

^{19}F{^{1}H} NMR (376 MHz, $CDCl_3$) δ -117.7.

^{13}C NMR (101 MHz, $CDCl_3$) δ (ppm) 178.4, 171.0, 156.9 (d, *J* = 248.5 Hz), 139.4, 138.4 (d, *J* = 7.3 Hz), 132.0 (d, *J* = 5.6 Hz), 128.8, 128.6, 128.1, 122.7 (d, *J* = 16.5 Hz), 118.7 (d, *J* = 18.8 Hz), 112.7 (d, *J* = 4.0 Hz), 62.9 (d, *J* = 2.3 Hz), 26.9, 14.4 (d, *J* = 3.5 Hz).

HRMS m/z (ESI) calcd for $C_{23}H_{18}NO_2FNa$ $[M+Na]^+$ 382.1214, found 382.1216.

1-Acetyl-4,5,6-trifluoro-3,3-diphenylindolin-2-one (13)

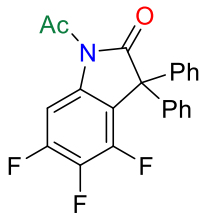

Following the general procedure using 1,2,3-trifluoro-5-nitrobenzene (583 µL, 5 mmol, 10 equiv.), diphenylacetylene (90 mg, 0.5 mmol, 1 equiv.) and acetic anhydride (187 µL, 2 mmol, 4 equiv.), the residue was purified by flash chromatography on silica gel (Heptane/Ethyl Acetate = 95:5) to afford **13** as a yellow solid in 64% yield (122 mg, 0.32 mmol).

^{1}H NMR (400 MHz, $CDCl_3$) δ (ppm) 8.26 – 8.01 (m, 1H), 7.38 – 7.33 (m, 5H), 7.26 – 7.21 (m, 5H), 2.69 (s, 3H).

^{19}F{^{1}H} NMR (376 MHz, $CDCl_3$) δ (ppm) -131.2 (dd, *J* = 20.6, 8.0 Hz), -134.5 (dd, *J* = 21.7, 8.0 Hz), -163.1 – -163.3 (m).

^{13}C NMR (101 MHz, $CDCl_3$) δ (ppm) 177.4, 170.9, 151.4 (ddd, *J* = 249.1, 10.4, 3.7 Hz), 147.7 (ddd, *J* = 253.5, 12.0, 4.5 Hz), 147.6, 138.5, 138.2 (dt, *J* = 250.2, 15.7 Hz), 128.9, 128.5, 128.3, 116.1 (dd, *J* = 14.2, 4.1 Hz), 103.0 (dd, *J* = 25.1, 3.7 Hz), 62.7, 26.8.

HRMS m/z (ESI) calcd for $C_{22}H_{14}NO_2F_3Na$ $[M+Na]^+$ 404.0868, found 404.0868.

3,3-Diphenyl-1-propionylindolin-2-one (14)

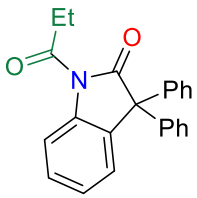

Following the general procedure using nitrobenzene (512 µL, 5 mmol, 10 equiv.), diphenylacetylene (90 mg, 0.5 mmol, 1 equiv.) and propionic anhydride (258 µL, 2 mmol, 4 equiv.), the residue was purified by flash chromatography on silica gel (Heptane/Ethyl Acetate = 97:3) to afford **14** as a yellow solid in 58% yield (99 mg, 0.29 mmol).

^{1}H NMR (400 MHz, $CDCl_3$) δ (ppm) 8.35 (d, *J* = 8.2 Hz, 1H), 7.39 – 7.27 (m, 7H), 7.25 – 7.17 (m, 6H), 3.12 (q, *J* = 7.2 Hz, 2H), 1.23 (t, *J* = 7.3 Hz, 3H).

^{13}C NMR (101 MHz, $CDCl_3$) δ (ppm) 178.8, 175.3, 141.6, 139.7, 132.3, 128.8, 128.7, 128.7, 127.9, 126.1, 125.5, 117.0, 63.3, 32.2, 8.5.

HRMS m/z (ESI) calcd for $C_{23}H_{19}NO_2Na$ $[M+Na]^+$ 364.1308, found 364.1307.

Methyl 5-methyl-2-oxo-1-pentanoyl-3,3-diphenylindoline-6-carboxylate (15)

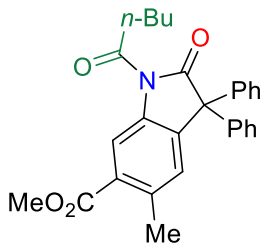

Following the general procedure using methyl 2-methyl-5-nitrobenzoate (488 mg, 2.5 mmol, 5 equiv.), diphenylacetylene (90 mg, 0.5 mmol, 1 equiv.) and valeric anhydride (393 µL, 2 mmol, 4 equiv.), the residue was purified by flash chromatography on silica gel (Heptane/Ethyl Acetate = 95:5) to afford **15** as a yellow solid in 65% yield (143 mg, 0.33 mmol).

^{1}H NMR (400 MHz, $CDCl_3$) δ (ppm) 8.84 (s, 1H), 7.36 – 7.27 (m, 6H), 7.24 – 7.14 (m, 4H), 7.05 (s, 1H), 3.90 (s, 3H), 3.09 (t, *J* = 7.5 Hz, 2H), 2.55 (s, 3H), 1.70 (p, *J* = 7.5 Hz, 2H), 1.40 (dq, *J* = 14.8, 7.4 Hz, 2H), 0.93 (t, *J* = 7.3 Hz, 3H).

^{13}C NMR (101 MHz, $CDCl_3$) δ (ppm) 178.2, 174.4, 167.6, 140.9, 137.7, 137.6, 135.9, 130.0, 128.9, 128.8, 128.6, 128.1, 118.6, 63.3, 52.2, 38.3, 26.4, 22.4, 21.7, 14.0.

HRMS m/z (ESI) calcd for $C_{28}H_{27}NO_4Na$ $[M+Na]^+$ 464.1832, found 464.1834.

1-(3-Methylbutanoyl)-3,3-diphenylindolin-2-one (16)

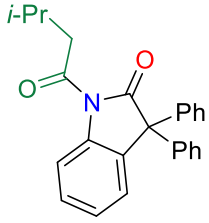

Following the general procedure using nitrobenzene (512 µL, 5 mmol, 10 equiv.), diphenylacetylene (90 mg, 0.5 mmol, 1 equiv.) and isovaleric anhydride (398 µL, 2 mmol, 4 equiv.), the residue was purified by flash chromatography on silica gel (Heptane/Ethyl Acetate = 99:1) to afford **16** as a yellow solid in 63% yield (116 mg, 0.32 mmol).

^{1}H NMR (400 MHz, $CDCl_3$) δ (ppm) 8.37 (d, *J* = 8.2 Hz, 1H), 7.40 – 7.33 (m, 7H), 7.31 – 7.12 (m, 6H), 3.03 (d, *J* = 6.8 Hz, 2H), 2.28 (dt, *J* = 13.4, 6.7 Hz, 1H), 1.04 (d, *J* = 6.7 Hz, 6H).

^{13}C NMR (101 MHz, $CDCl_3$) δ (ppm) 178.7, 173.9, 141.6, 139.7, 132.2, 128.8, 128.7, 128.6, 127.8, 126.1, 125.5, 117.0, 63.3, 47.1, 25.1, 22.7.

HRMS m/z (ESI) calcd for $C_{25}H_{23}NO_2Na$ $[M+Na]^+$ 392.1621, found 392.1623.

1-Acetyl-3,3-bis(4-bromophenyl)indolin-2-one (17)

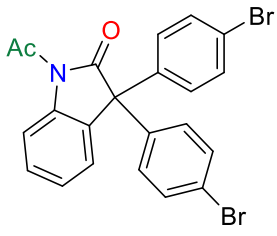

Following the general procedure using nitrobenzene (512 µL, 5 mmol, 10 equiv.), 1,2-bis(4-bromophenyl)ethyne (168 mg, 0.5 mmol, 1 equiv.) and acetic anhydride (187 µL, 2 mmol, 4 equiv.), the residue was purified by flash chromatography on silica gel (Heptane/Ethyl Acetate = 98:2) to afford **17** as a yellow solid in 55% yield (267 mg, 0.28 mmol).

^{1}H NMR (400 MHz, $CDCl_3$) δ (ppm) 8.33 (d, *J* = 8.2 Hz, 1H), 7.47 – 7.42 (m, 4H), 7.42 – 7.35 (m, 1H), 7.28 – 7.20 (m, 1H), 7.17 – 7.13 (m, 1H), 7.10 – 7.02 (m, 4H), 2.69 (s, 3H).

^{13}C NMR (101 MHz, $CDCl_3$) δ (ppm) 178.1, 171.0, 140.0, 139.4, 132.0, 131.0, 130.3, 129.3, 125.9, 125.8, 122.5, 117.3, 62.3, 26.9.

HRMS m/z (ESI) calcd for $C_{22}H_{15}NO_2Br_2Na$ $[M+Na]^+$ 505.9361, found 505.9357.

Methyl 1-acetyl-3,3-bis(4-bromophenyl)-5-methyl-2-oxoindoline-6-carboxylate (18)

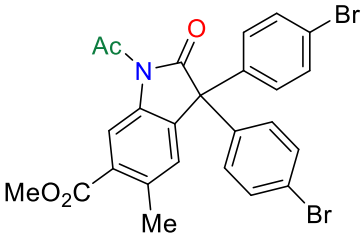

Following the general procedure using methyl 2-methyl-5-nitrobenzoate (488 mg, 2.5 mmol, 5 equiv.), 1,2-bis(4-bromophenyl)ethyne (168 mg, 0.5 mmol, 1 equiv.) and acetic anhydride (187 µL, 2 mmol, 4 equiv.), the residue was purified by flash chromatography on silica gel (Heptane/Ethyl Acetate = 98:2) to afford **18** as a yellow solid in 64% yield (178 mg, 0.32 mmol).

^{1}H NMR (400 MHz, $CDCl_3$) δ (ppm) 8.81 (s, 1H), 7.47 – 7.45 (m, 4H), 7.07 – 7.04 (m, 4H), 7.00 (s, 1H), 3.92 (s, 3H), 2.69 (s, 3H), 2.56 (s, 3H).

^{13}C NMR (101 MHz, $CDCl_3$) δ (ppm) 177.6, 170.7, 167.4, 139.4, 138.0, 137.3, 134.5, 132.2, 130.6, 130.2, 128.6, 122.8, 118.8, 62.4, 52.3, 26.8, 21.7.

HRMS m/z (ESI) calcd for $C_{25}H_{19}NO_4Br_2Na$ $[M+Na]^+$ 577.9573, found 577.9572.

1-Acetyl-3,3-bis(4-chlorophenyl)indolin-2-one (19)

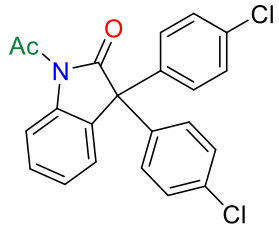

Following the general procedure using nitrobenzene (512 µL, 5 mmol, 10 equiv.), 1,2-bis(4-chlorophenyl)ethyne (123 mg, 0.5 mmol, 1 equiv.) and acetic anhydride (187 µL, 2 mmol, 4 equiv.), the residue was purified by flash chromatography on silica gel (Heptane/Ethyl Acetate = 98:2) to afford **19** as a yellow solid in 69% yield (137 mg, 0.35 mmol).

^{1}H NMR (400 MHz, $CDCl_3$) δ (ppm) 8.34 (d, *J* = 8.2 Hz, 1H), 7.42 – 7.36 (m, 1H), 7.32 – 7.27 (m, 4H), 7.27 – 7.22 (m, 1H), 7.18 – 7.11 (m, 5H), 2.69 (s, 3H).

^{13}C NMR (101 MHz, $CDCl_3$) δ (ppm) 178.2, 171.0, 139.6, 139.4, 134.3, 131.2, 129.9, 129.3, 129.1, 125.9, 125.8, 117.3, 62.2, 26.9.

HRMS m/z (ESI) calcd for $C_{22}H_{15}NO_2Cl_2Na$ $[M+Na]^+$ 418.0372, found 418.0375.

1-Acetyl-3,3-bis(4-fluorophenyl)indolin-2-one (20)

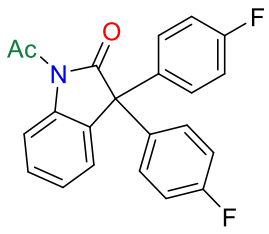

Following the general procedure using nitrobenzene (512 µL, 5 mmol, 10 equiv.), 1,2-bis(4-fluorophenyl)ethyne (107 mg, 0.5 mmol, 1 equiv.) and acetic anhydride (187 µL, 2 mmol, 4 equiv.), the residue was purified by flash chromatography on silica gel (Heptane/Ethyl Acetate = 98:2) to afford **20** as a yellow solid in 63% yield (114 mg, 0.32 mmol).

^{1}H NMR (400 MHz, $CDCl_3$) δ (ppm) 8.34 (d, *J* = 8.2 Hz, 1H), 7.41 – 7.35 (m, 1H), 7.28 – 7.22 (m, 1H), 7.22 – 7.14 (m, 5H), 7.05 – 6.96 (m, 4H), 2.70 (s, 3H).

^{19}F{^{1}H} NMR (376 MHz, $CDCl_3$) δ (ppm) -114.0.

^{13}C NMR (101 MHz, $CDCl_3$) δ (ppm) 178.7, 171.1, 162.4 (d, *J* = 248.1 Hz), 138.4, 137.1 (d, *J* = 3.3 Hz), 130.4, 130.3 (d, *J* = 8.3 Hz), 129.1, 125.8 (d, *J* = 7.6 Hz), 117.2, 115.9, 115.7, 61.9, 26.9.

HRMS m/z (ESI) calcd for $C_{22}H_{15}NO_2F_2Na$ $[M+Na]^+$ 386.0963, found 386.0962.

1-Acetyl-3,3-bis(4-(trifluoromethyl)phenyl)indolin-2-one (21)

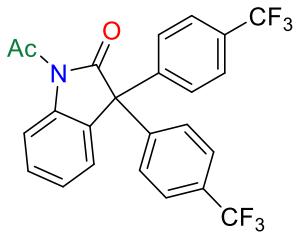

Following the general procedure using nitrobenzene (512 µL, 5 mmol, 10 equiv.), 1,2-bis(4-(trifluoromethyl)phenyl)ethyne (157 mg, 0.5 mmol, 1 equiv.) and acetic anhydride (187 µL, 2 mmol, 4 equiv.), the residue was purified by flash chromatography on silica gel (Heptane/Ethyl Acetate = 98:2) to afford **21** as a yellow solid in 70% yield (162 mg, 0.35 mmol).

^{1}H NMR (400 MHz, $CDCl_3$) δ (ppm) 8.37 (d, *J* = 8.2 Hz, 1H), 7.62 – 7.57 (m, 4H), 7.45 – 7.39 (m, 1H), 7.36 – 7.31 (m, 4H), 7.30 – 7.26 (m, 1H), 7.21 – 7.11 (m, 1H), 2.71 (s, 3H).

^{19}F{^{1}H} NMR (376 MHz, $CDCl_3$) δ (ppm) -62.8.

^{13}C NMR (400 MHz, $CDCl_3$) δ (ppm) 177.6, 170.9, 144.7, 139.6, 130.7, 130.4, 129.7, 129.0, 126.0-125.9 (m), 125.9, 125.8, 124.0 (q, *J* = 272.7 Hz), 117.5, 63.0, 27.0.

HRMS m/z (ESI) calcd for $C_{24}H_{15}NO_2F_6Na$ $[M+Na]^+$ 486.0899, found 486.0902.

1-Acetyl-3,3-di-p-tolylindolin-2-one (22)

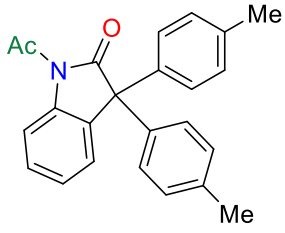

Following the general procedure using nitrobenzene (512 µL, 5 mmol, 10 equiv.), 1,2-di-*p*-tolylethyne (100 mg, 0.5 mmol, 1 equiv.) and acetic anhydride (187 µL, 2 mmol, 4 equiv.), the residue was purified by flash chromatography on silica gel (Heptane/Ethyl Acetate = 98:2) to afford **22** as a yellow solid in 53% yield (94 mg, 0.27 mmol).

^{1}H NMR (400 MHz, $CDCl_3$) δ (ppm) 8.33 (d, *J* = 8.2 Hz, 1H), 7.39 – 7.32 (m, 1H), 7.25 – 7.18 (m, 2H), 7.15 – 7.06 (m, 8H), 2.70 (s, 3H), 2.33 (s, 6H).

^{13}C NMR (101 MHz, $CDCl_3$) δ (ppm) 179.1, 171.3, 139.4, 138.6, 137.6, 132.5, 129.4, 128.6, 128.5, 125.9, 125.5, 116.9, 62.6, 27.0, 21.2.

HRMS m/z (ESI) calcd for $C_{24}H_{21}NO_2Na$ $[M+Na]^+$ 378.1465, found 378.1465.

1-Acetyl-3,3-bis(4-(tert-butyl)phenyl)indolin-2-one (23)

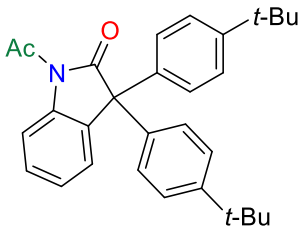

Following the general procedure using nitrobenzene (512 µL, 5 mmol, 10 equiv.), 1,2-bis(4-(*tert*-butyl)phenyl)ethyne (145 mg, 0.5 mmol, 1 equiv.) and acetic anhydride (187 µL, 2 mmol, 4 equiv.), the residue was purified by flash chromatography on silica gel (Heptane/Ethyl Acetate = 98:2) to afford **23** as a yellow solid in 41% yield (90 mg, 0.21 mmol).

^{1}H NMR (400 MHz, $CDCl_3$) δ (ppm) 8.32 (d, *J* = 8.2 Hz, 1H), 7.35 – 7.29 (m, 5H), 7.24 – 7.20 (m, 2H), 7.16 – 7.09 (m, 4H), 2.70 (s, 3H), 1.29 (s, 18H).

^{13}C NMR (101 MHz, $CDCl_3$) δ (ppm) 179.2, 171.3, 150.7, 139.5, 138.4, 132.6, 128.6, 128.2, 126.1, 125.6, 125.5, 116.9, 62.5, 34.6, 31.4, 27.0.

HRMS m/z (ESI) calcd for $C_{30}H_{33}NO_2Na$ $[M+Na]^+$ 462.2404, found 462.2404.

1-Acetyl-3,3-bis(3-fluorophenyl)indolin-2-one (24)

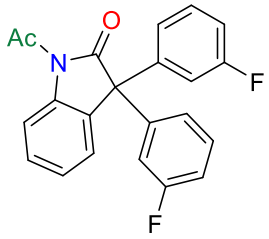

Following the general procedure using nitrobenzene (512 µL, 5 mmol, 10 equiv.), 1,2-bis(3-fluorophenyl)ethyne (107 mg, 0.5 mmol, 1 equiv.) and acetic anhydride (187 µL, 2 mmol, 4 equiv.), the residue was purified by flash chromatography on silica gel (Heptane/Ethyl Acetate = 95:5) to afford **24** as a yellow solid in 58% yield (105 mg, 0.29 mmol).

^{1}H NMR (400 MHz, $CDCl_3$) δ (ppm) 8.35 (d, *J* = 8.2 Hz, 1H), 7.43 – 7.37 (m, 1H), 7.34 – 7.19 (m, 4H), 7.05 – 6.99 (m, 4H), 6.96 – 6.91 (m, 2H), 2.71 (s, 3H).

^{19}F{^{1}H} NMR (376 MHz, $CDCl_3$) δ (ppm) -111.4.

^{13}C NMR (101 MHz, $CDCl_3$) δ (ppm) 177.8, 171.0, 162.9 (d, *J* = 247.3 Hz), 143.2 (d, *J* = 7.0 Hz), 139.5, 130.9, 130.4 (d, *J* = 8.3 Hz), 129.4, 125.9 (d, *J* = 8.6 Hz), 124.3 (d, *J* = 2.9 Hz), 117.2, 115.9 (d, *J* = 23.2 Hz), 115.2 (d, *J* = 21.0 Hz), 62.6 (t, *J* = 1.9 Hz), 26.9.

HRMS m/z (ESI) calcd for $C_{22}H_{15}NO_2F_2Na$ $[M+Na]^+$ 386.0963, found 386.0961.

1-Acetyl-3,3-bis(3,5-difluorophenyl)indolin-2-one (25)

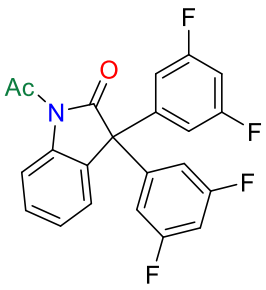

Following the general procedure using nitrobenzene (512 µL, 5 mmol, 10 equiv.), 1,2-bis(3,5-difluorophenyl)ethyne (125 mg, 0.5 mmol, 1 equiv.) and acetic anhydride (187 µL, 2 mmol, 4 equiv.), the residue was purified by flash chromatography on silica gel (Heptane/Ethyl Acetate = 95:5) to afford **25** as a yellow solid in 39% yield (78 mg, 0.20 mmol).

^{1}H NMR (400 MHz, $CDCl_3$) δ (ppm) 8.35 (d, *J* = 8.2 Hz, 1H), 7.47 – 7.40 (m, 1H), 7.29 (td, *J* = 7.6, 1.1 Hz, 1H), 7.23 – 7.16 (m, 1H), 6.85 – 6.69 (m, 6H), 2.71 (s, 3H).

^{19}F{^{1}H} NMR (376 MHz, $CDCl_3$) δ (ppm) -107.7.

^{13}C NMR (101 MHz, $CDCl_3$) δ (ppm) 176.8, 170.8, 163.2 (dd, *J* = 250.1, 12.8 Hz), 143.8 (t, *J* = 8.9 Hz), 139.5, 130.0, 129.7, 125.9 (d, *J* = 33.7 Hz), 117.5, 112.1, 111.9 (d, *J* = 11.6 Hz), 111.8, 104.2 (t, *J* = 25.2 Hz), 26.9.

HRMS m/z (ESI) calcd for $C_{22}H_{13}NO_2F_4Na$ $[M+Na]^+$ 422.0774, found 422.0772.

1-Acetyl-3,3-bis(2-chlorophenyl)indolin-2-one (26)

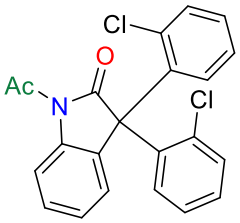

Following the general procedure using nitrobenzene (512 µL, 5 mmol, 10 equiv.), 1,2-bis(2-chlorophenyl)ethyne (123 mg, 0.5 mmol, 1 equiv.) and acetic anhydride (187 µL, 2 mmol, 4 equiv.), the residue was purified by flash chromatography on silica gel (Heptane/Ethyl Acetate = 98:2) to afford **26** as a yellow solid in 42% yield (83 mg, 0.21 mmol).

^{1}H NMR (400 MHz, $CDCl_3$) δ (ppm) 8.35 (d, *J* = 8.2 Hz, 1H), 7.43 – 7.37 (m, 1H), 7.34 – 7.19 (m, 4H), 7.05 – 6.99 (m, 4H), 6.96 – 6.91 (m, 2H), 2.71 (s, 3H).

^{13}C NMR (101 MHz, $CDCl_3$) δ (ppm) 175.7, 171.6, 139.8, 136.9, 131.5, 130.4, 129.9, 129.5, 129.1, 127.3, 126.9, 126.1, 125.8, 116.7, 62.9, 27.1.

HRMS m/z (ESI) calcd for $C_{22}H_{15}NO_2Cl_2Na$ $[M+Na]^+$ 418.0372, found 418.0367.

1-Acetyl-3-(4-fluorophenyl)-3-phenylindolin-2-one (27)

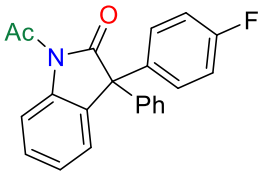

Following the general procedure using nitrobenzene (512 µL, 5 mmol, 10 equiv.), 1-fluoro-4-(phenylethynyl)benzene (98 mg, 0.5 mmol, 1 equiv.) and acetic anhydride (187 µL, 2 mmol, 4 equiv.), the residue was purified by flash chromatography on silica gel (Heptane/Ethyl Acetate = 95:5) to afford **27** as a yellow solid in 51% yield (88 mg, 0.21 mmol).

^{1}H NMR (400 MHz, $CDCl_3$) δ (ppm) 8.31 (d, *J* = 8.2 Hz, 1H), 7.38 – 7.25 (m, 4H), 7.22 – 7.14 (m, 6H), 7.02 – 6.94 (m, 2H), 2.67 (s, 3H).

^{19}F{^{1}H} NMR (376 MHz, $CDCl_3$) δ (ppm) -114.3.

^{13}C NMR (101 MHz, $CDCl_3$) δ (ppm) 178.8, 171.1, 162.4 (d, *J* = 247.8 Hz), 141.5, 139.4, 137.1 (d, *J* = 3.3 Hz), 131., 130.5 (d, *J* = 8.1 Hz), 129.0, 128.9, 128.4, 128.0, 126.0, 125.7, 117.1, 115.6 (d, *J* = 21.6 Hz), 62.6, 27.0.

HRMS m/z (ESI) calcd for $C_{22}H_{16}NO_2FNa$ $[M+Na]^+$ 368.1057, found 368.1057.

1-Acetyl-3-(4-iodophenyl)-3-phenylindolin-2-one (28)

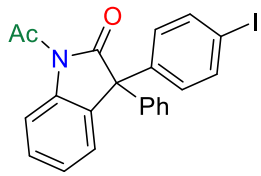

Following the general procedure using nitrobenzene (512 µL, 5 mmol, 10 equiv.), 1-iodo-4-(phenylethynyl)benzene (152 mg, 0.5 mmol, 1 equiv.) and acetic anhydride (187 µL, 2 mmol, 4 equiv.), the residue was purified by flash chromatography on silica gel (Heptane/Ethyl Acetate = 95:5) to afford **28** as a yellow solid in 50% yield (113 mg, 0.25 mmol).

^{1}H NMR (400 MHz, $CDCl_3$) δ (ppm) 8.34 (d, *J* = 8.2 Hz, 1H), 7.69 – 7.62 (m, 2H), 7.42 – 7.29 (m, 4H), 7.27 – 7.14 (m, 5H), 6.99 – 6.94 (m, 2H), 2.70 (s, 3H).

^{13}C NMR (101 MHz, $CDCl_3$) δ (ppm) 178.4, 171.1, 141.2, 141.0, 139.5, 137.9, 131.5, 130.6, 129.1, 128.9, 128.5, 128.1, 125.9, 125.7, 117.1, 94.0, 62.9, 27.0.

HRMS m/z (ESI) calcd for $C_{22}H_{16}NO_2INa$ $[M+Na]^+$ 476.0118, found 476.0119.

1-Acetyl-3-(4-chlorophenyl)-3-phenylindolin-2-one (29)

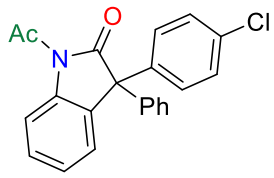

Following the general procedure using nitrobenzene (512 µL, 5 mmol, 10 equiv.), 1-chloro-4-(phenylethynyl)benzene (106 mg, 0.5 mmol, 1 equiv.) and acetic anhydride (187 µL, 2 mmol, 4 equiv.), the residue was purified by flash chromatography on silica gel (Heptane/Ethyl Acetate = 95:5) to afford **29** as a yellow solid in 48% yield (87 mg, 0.24 mmol).

^{1}H NMR (400 MHz, $CDCl_3$) δ (ppm) 8.34 (d, *J* = 8.2 Hz, 1H), 7.40 – 7.35 (m, 1H), 7.34 – 7.27 (m, 5H), 7.25 – 7.15 (m, 6H), 2.70 (s, 3H).

^{13}C NMR (101 MHz, $CDCl_3$) δ (ppm) 178.5, 171.1, 141.2, 139.9, 139.5, 134.1, 131.7, 130.1, 129.1, 128.9, 128.9, 128.5, 128.1, 125.9, 125.7, 117.2, 62.7, 27.0.

HRMS m/z (ESI) calcd for $C_{22}H_{16}NO_2ClNa$ $[M+Na]^+$ 384.0767, found 384.0766.

1-Acetyl-3-phenyl-3-(p-tolyl)indolin-2-one (30)

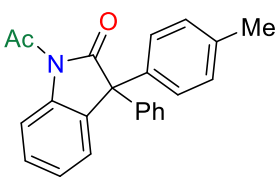

Following the general procedure using nitrobenzene (512 µL, 5 mmol, 10 equiv.), 1-methyl-4-(phenylethynyl)benzene (96 mg, 0.5 mmol, 1 equiv.) and acetic anhydride (187 µL, 2 mmol, 4 equiv.), the residue was purified by flash chromatography on silica gel (Heptane/Ethyl Acetate = 95:5) to afford **30** as a yellow solid in 48% yield (82 mg, 0.24 mmol).

^{1}H NMR (400 MHz, $CDCl_3$) δ (ppm) 8.35 (d, *J* = 8.2 Hz, 1H), 7.39 – 7.29 (m, 4H), 7.26 – 7.21 (m, 4H), 7.16 – 7.09 (m, 4H), 2.71 (s, 3H), 2.34 (s, 3H).

^{13}C NMR (101 MHz, $CDCl_3$) δ (ppm) 179.0, 171.2, 141.6, 139.5, 138.5, 137.7, 132.3, 129.4, 128.7, 128.6, 128.5, 127.8, 126.0, 125.6, 123.6, 117.0, 62.9, 27.0, 21.2.

HRMS m/z (ESI) calcd for $C_{23}H_{19}NO_2Na$ $[M+Na]^+$ 364.1308, found 364.1309.

Ethyl 4-(1-acetyl-2-oxo-3-phenylindolin-3-yl)benzoate (31)

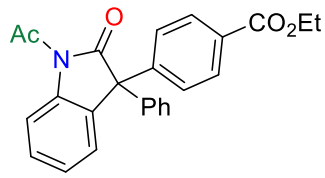

Following the general procedure using nitrobenzene (512 µL, 5 mmol, 10 equiv.), ethyl 4-(phenylethynyl)benzoate (125 mg, 0.5 mmol, 1 equiv.) and acetic anhydride (187 µL, 2 mmol, 4 equiv.), the residue was purified by flash chromatography on silica gel (Heptane/Ethyl Acetate = 95:5) to afford **31** as a yellow solid in 40% yield (80 mg, 0.20 mmol).

^{1}H NMR (400 MHz, $CDCl_3$) δ (ppm) 8.34 (d, *J* = 8.2 Hz, 1H), 7.99 (d, *J* = 8.2 Hz, 1H), 7.41 – 7.36 (m, 1H), 7.34 – 7.28 (m, 5H), 7.25 – 7.17 (m, 4H), 4.36 (q, *J* = 7.1 Hz, 2H), 2.70 (s, 3H), 1.37 (t, *J* = 7.1 Hz, 3H).

^{13}C NMR (101 MHz, $CDCl_3$) δ (ppm) 178.2, 171.0, 166.1, 146.2, 140.8, 139.4, 131.3, 130.0, 129.8, 129.0, 128.8, 128.7, 128.5, 128.4, 128.0, 125.9, 125.6, 117.0, 63.1, 61.1, 26.8, 14.3.

HRMS m/z (ESI) calcd $C_{25}H_{21}NO_4Na$ $[M+Na]^+$ 422.1363, found 422.1365.

1-Acetyl-3-(4-methoxyphenyl)-3-phenylindolin-2-one (32)

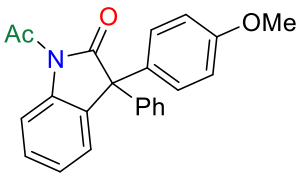

Following the general procedure using nitrobenzene (512 µL, 5 mmol, 10 equiv.), 1-methoxy-4-(phenylethynyl)benzene (104 mg, 0.5 mmol, 1 equiv.) and acetic anhydride (187 µL, 2 mmol, 4 equiv.), the residue was purified by flash chromatography on silica gel (Heptane/Ethyl Acetate = 95:5) to afford **32** as a yellow solid in 50% yield (88 mg, 0.25 mmol).

^{1}H NMR (400 MHz, $CDCl_3$) δ (ppm) 8.33 (d, *J* = 8.2 Hz, 1H), 7.39 – 7.27 (m, 4H), 7.24 – 7.11 (m, 6H), 6.85 (d, *J* = 8.9 Hz, 2H), 3.79 (s, 3H), 2.70 (s, 3H).

^{13}C NMR (101 MHz, $CDCl_3$) δ (ppm) 179.1, 171.2, 159.3, 141.9, 139.4, 133.2, 132.5, 129.9, 128.7, 128.5, 127.8, 126.0, 125.6, 117.0, 114.1, 62.5, 55.4, 26.9.

HRMS m/z (ESI) calcd $C_{23}H_{19}NO_3Na$ $[M+Na]^+$ 380.1262, found 364.1261.

3.6.5. Post-Functionalizations and Compounds Characterization

3,3-Diphenylindolin-2-one (33)

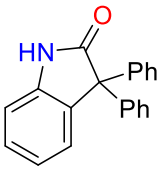

Under argon atmosphere, a solution of **1** (50 mg, 0.15 mmol, 1 equiv.) in THF was added to a solution of $LiAlH_4$ (7 mg, 0.18 mmol, 1.2 equiv.) in THF (2 mL). The resulting mixture was stirred at 70 °C over 1 h. Then, the reaction was cooled down to 0 °C and water (1 mL) was added. The aqueous layer was washed with dichloromethane (3 mL x3) and the combined organic layers were filtered and dried over $MgSO_4$ and concentrated in vacuo. The product **33** was obtained in 97% yield as an orange solid (42 mg, 0.145 mmol).

^{1}H NMR (400 MHz, $CDCl_3$) δ (ppm) 9.15 (s, 1H), 7.34 – 7.28 (m, 10H), 7.25 – 7.21 (m, 2H), 7.11 – 7.05 (m, 1H), 7.01 – 6.96 (m, 1H).

^{13}C NMR (101 MHz, $CDCl_3$) δ (ppm) 180.4, 141.8, 140.4, 133.7, 128.6, 128.6, 128.4, 127.5, 126.4, 122.9, 110.6, 63.2.

HRMS m/z (ESI) calcd for $C_{20}H_{15}NONa$ $[M+Na]^+$ 308.1045, found 308.1044.

3,3-Diphenylindoline (34)

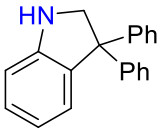

To a solution of **1** (50 mg, 0.15 mmol, 1 equiv.) in THF was added a solution of 1M borane-THF complex in THF (0.18 mL, 0.60 mmol, 4 equiv.) at 0 °C. The resultant mixture was heated to reflux and stirred overnight. Then, the reaction was cooled down to 0 °C and MeOH (3mL) was added followed by 2 N HCl aq. (3 mL). The mixture was refluxed over 2 h then cooled to room temperature and concentrated. The reaction was treated with dichloromethane (10 mL) and water (10 mL) and the aqueous layer was washed with dichloromethane (10 mL x3). The combined organic layers were filtered and dried over $MgSO_4$ and concentrated in vacuo. The product **34** was obtained in 80% yield as a brown oil (33 mg, 0.12 mmol).

^{1}H NMR (400 MHz, $CDCl_3$) δ (ppm) 7.33 – 7.21 (m, 11H), 7.16 – 7.09 (m, 2H), 6.87 – 6.79 (m, 2H), 4.16 (s, 2H).

^{13}C NMR (101 MHz, $CDCl_3$) δ (ppm) 149.7, 146.5, 128.6, 128.3, 128.2, 127.5, 126.5, 126.3, 120.0, 111.3, 62.4, 59.6.

HRMS m/z (ESI) calcd for $C_{20}H_{18}N$ $[M+H]^+$ 272.1433, found 272.1431.

1-Acetyl-2-oxo-3,3-diphenylindoline-6-carbaldehyde (35)

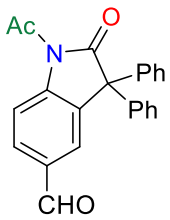

To a stainless-steel autoclave was added 1-acetyl-5-iodo-3,3-diphenylindolin-2-one **5** (50 mg, 0.1 mmol, 1 equiv.), $RhCl_3.3H_2O$ (0.6 mg, 0.0025 mmol, 2.5 mol%), PPh_3 (2.8 mg, 0.01 mmol, 10 mol%), NEt_3 (18 µL, 0.12 mmol, 1.2 equiv.) and DMA (0.5 mL). The autoclave was screwed up and charged with CO/H_2 (1:1, 10 atm) and transferred to an oil bath at 90 °C. After 6 h, the autoclave was cooled down in ice and the gas vented. Then 2 mL of DCM was added to the mixture followed by 5 mL of water. The organic layer was extracted with water (5 mL x3), dried over $MgSO_4$ and concentrated. The residue was purified by flash chromatography on silica gel (Heptane/Ethyl Acetate = 80:20) to afford **35** in 75% yield (26 mg, 0.075 mmol) as a yellow solid.

^{1}H NMR (400 MHz, $CDCl_3$) δ (ppm) 9.45 (s, 1H), 8.02 (d, *J* = 8.4 Hz, 1H), 7.40 (dd, *J* = 8.4, 1.8 Hz, 1H), 7.26 (d, *J* = 1.8 Hz, 1H), 6.91 – 6.79 (m, 6H), 6.76 – 6.66 (m, 4H), 2.23 (s, 3H).

^{13}C NMR (101 MHz, $CDCl_3$) δ (ppm) 191.0, 178.4, 171.2, 144.3, 140.6, 133.9, 133.4, 132.3, 129.0, 128.5, 128.3, 126.4, 117.2, 62.9, 27.0.

HRMS m/z (ESI) calcd for $C_{23}H_{17}NO_3Na$ $[M+Na]^+$ 378.1101, found 378.1101.

1-Acetyl-2-oxo-3,3-diphenylindoline-6-carbonitrile (36)

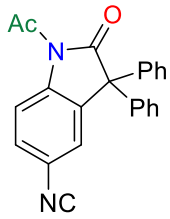

To an oven-dried 15 mL Schlenk tube was added 1-acetyl-5-iodo-3,3-diphenylindolin-2-one **5** (50 mg, 0.1 mmol, 1 equiv.), $Zn(CN)_2$ (14 mg, 0.12 mmol, 1.2 equiv.), $Pd(PPh_3)_4$ (5.7 mg, 0.005 mmol, 5 mol%), and DMF (0.5 mL). The resulting mixture was stirred at 80 °C over 90 min. Then 3 mL of water was added and the aqueous layer was extracted with EtOAc (5 mL x3). The organic layers were combined, dried over $MgSO_4$ and concentrated. The residue was purified by flash chromatography on silica gel (Heptane/Ethyl Acetate = 80:20) to afford **36** in 70% yield as a white solid (25 mg, 0.07 mmol).

^{1}H NMR (400 MHz, $CDCl_3$) δ (ppm) 8.46 (d, *J* = 8.5 Hz, 1H), 7.68 (dd, *J* = 8.5, 1.8 Hz, 1H), 7.49 (d, *J* = 1.7 Hz, 1H), 7.40 – 7.32 (m, 6H), 7.21 – 7.13 (m, 4H), 2.72 (s, 3H).

^{13}C NMR (101 MHz, $CDCl_3$) δ (ppm) 177.7, 171.1, 142.9, 140.2, 133.5, 133.4, 129.7, 129.1, 128.5, 128.4, 118.5, 117.7, 109.3, 62.9, 26.9.

HRMS m/z (ESI) calcd for $C_{23}H_{16}N_2O_2Na$ $[M+Na]^+$ 375.1104, found 375.1104.

1-Acetyl-3,3-diphenyl-6-(phenylethynyl)indolin-2-one (37)

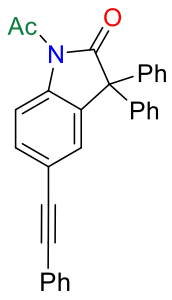

To an oven-dried 15 mL Schlenk tube was added added 1-acetyl-5-iodo-3,3-diphenylindolin-2-one (50 mg, 0.1 mmol, 1 equiv.), $Pd(PPh_3)_4$ (1.3 mg, 0.001 mmol, 1 mol%), CuI (0.5 mg, 0.002 mmol, 2 mol%), NEt_3 (325 µL, 2 mmol, 20 equiv.), phenylacetylene (12 µL, 0.11 mmol, 1.1 equiv.) and THF (0.5 mL). The resulting mixture was stirred at 50 °C overnight. Then 3 mL of water was added and the aqueous layer was extracted with EtOAc (5 mL x3). The organic layers were combined, dried over $MgSO_4$ and concentrated. The residue was purified by flash chromatography on silica gel (Heptane/Ethyl Acetate = 90:10) to afford **37** in 85% yield as a yellow solid (36 mg, 0.085 mmol).

^{1}H NMR (400 MHz, $CDCl_3$) δ (ppm) 8.34 (d, *J* = 8.5 Hz, 1H), 7.55 (dd, *J* = 8.5, 1.8 Hz, 1H), 7.53 – 7.47 (m, 2H), 7.39 – 7.30 (m, 11H), 7.26 – 7.20 (m, 3H), 2.71 (s, 3H).

^{13}C NMR (101 MHz, $CDCl_3$) δ (ppm) 178.6, 171.1, 141.0, 139.2, 132.5, 132.4, 131.7, 129.1, 128.9, 128.6, 128.6, 128.5, 128.1, 123.1, 120.6, 117.1, 89.9, 88.9, 63.1, 26.9.

HRMS m/z (ESI) calcd for $C_{30}H_{21}NO_2Na$ $[M+Na]^+$ 450.1470, found 450.1471.

3.6.6. Mechanistic Studies

3.6.6.1 Reaction Mapping by Search of Potential Intermediates

Procedure: In a glovebox, an oven-dried 15 mL Schlenk tube was charged with $[Cp^{TMP}*RhCl_2]_2$ (5.5 mg, 0.006 mmol, 3 mol%), $AgSbF_6$ (8 mg, 0.024 mmol, 12 mol%), diphenylacetylene (36 mg, 0.2 mmol, 1 equiv.), acetic anhydride (76 µL, 0.8 mmol, 4 equiv.)**,** the "reduced" nitroarene (2 mmol, 10 equiv.) and DCE (1 mL). The Schlenk tube was closed and removed from the glovebox. The resulting mixture was stirred at 120 °C overnight under argon.

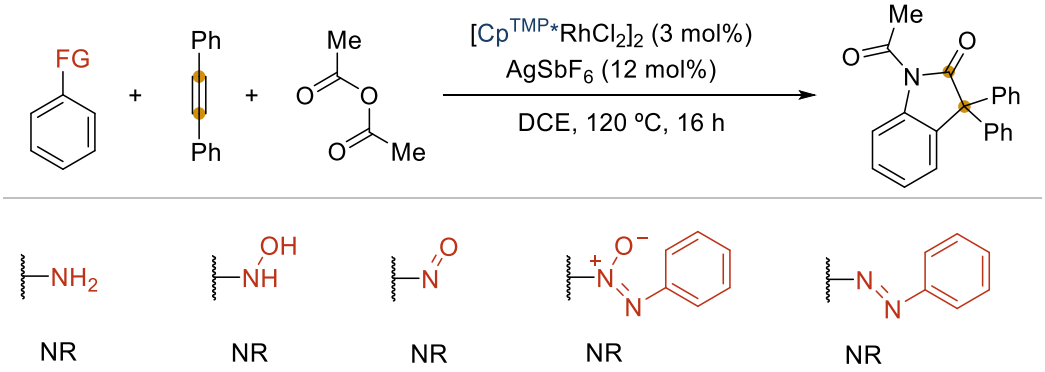

Scheme 3.7. Search of Potential Intermediates.

3.6.6.2 Kinetic Isotopic Effect Experiment

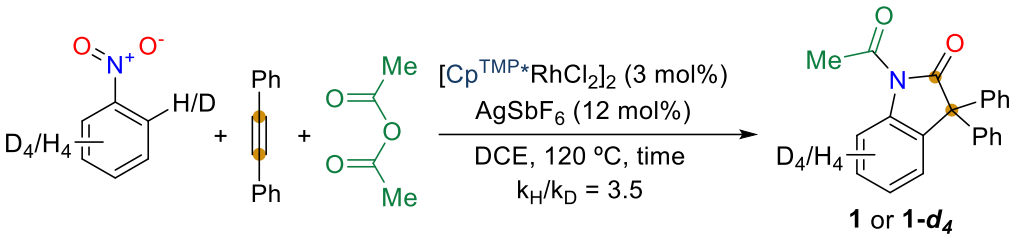

Scheme 3.8. KIE Experiment with $[Cp^{TMP}*RhCl_2]_2$.

The kinetic isotope effect (KIE) was determined by measuring the initial rates of the reactions. 4 Reactions with nitrobenzene and 4 reactions with nitrobenzene-d_5 were stopped at 5, 10, 15 and 20 minutes.

Procedure: In a glovebox, an oven-dried 15 mL Schlenk tube was charged with $[Cp^{TMP}*RhCl_2]_2$ (16.5 mg, 0.018 mmol, 3 mol%), $AgSbF_6$ (24 mg, 0.072 mmol, 12 mol%), diphenylacetylene (108 mg, 0.6 mmol, 1 equiv.), acetic anhydride (228 µL, 2.4 mmol, 4 equiv.), nitrobenzene or nitrobenzene-d_5 (6 mmol, 10 equiv.), *n*-dodecane (60 µL) and DCE (2.4 mL). The resulting solution was split in 4 Schlenk tubes (0.15 M). The Schlenk tubes were closed and removed from the glovebox. The resulting mixture was stirred at 120 °C for the indicated time. The crude product was then cooled down, diluted with methanol and ethyl acetate and injected in a calibrated GC-FID using *n*-dodecane as internal standard to give the concentration (mol/L). A KIE value of $k_H/k_D = 3.5$ was obtained.

Table 3.4. Time(min) and Concentration(mol/L) of **1** and **1-*d*$_5$**.

Time (min)	Concentration **1** (mol/L)	Concentration **1-*d*$_5$** (mol/L)
5	0.015	0
10	0.071	0.012
15	0.097	0.020
20	0.112	0.046

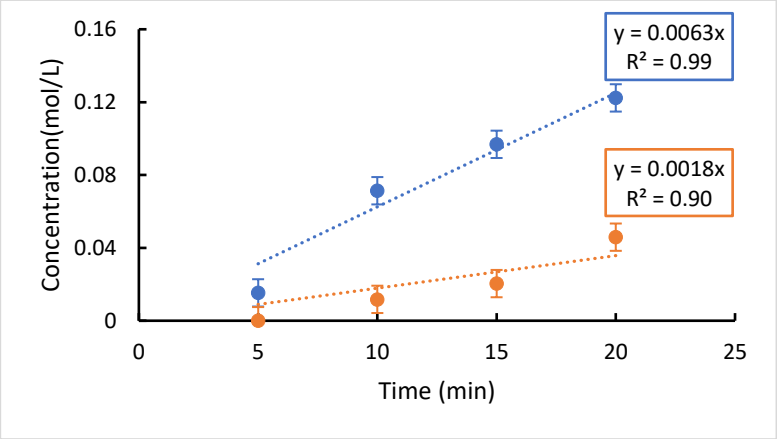

Figure 3.4. Initial Rates of the Reactions with Nitrobenzene and Nitrobenzene-d_5 Using $[Cp^{TMP}*RhCl_2]_2$ as catalyst.

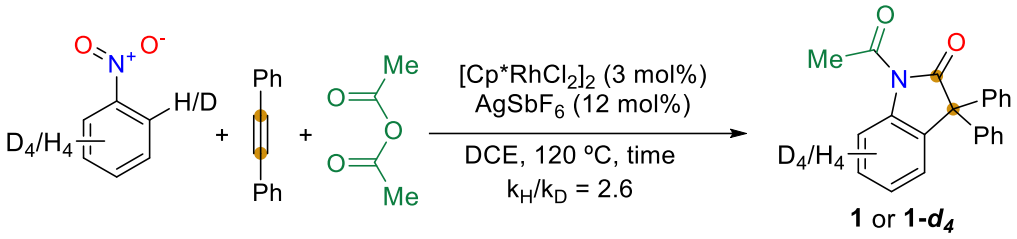

Scheme 3.9. KIE Experiment with $[Cp*RhCl_2]_2$.

The kinetic isotope effect (KIE) was determined by measuring the initial rates of the reactions. 4 Reactions with nitrobenzene and 4 reactions with nitrobenzene-d_5 were stopped at 15, 20, 30 and 60 minutes.

Procedure: In a glovebox, an oven-dried 15 mL Schlenk tube was charged with $[Cp*RhCl_2]_2$ (10.8 mg, 0.018 mmol, 3 mol%), $AgSbF_6$ (24 mg, 0.072 mmol, 12 mol%), diphenylacetylene (108 mg, 0.6 mmol, 1 equiv.), acetic anhydride (228 µL, 2.4 mmol, 4 equiv.), nitrobenzene or nitrobenzene-d_5 (6 mmol, 10 equiv.), *n*-dodecane (60 µL) and DCE (2.4 mL). The resulting solution was split in 4 Schlenk tubes (0.15 M). The Schlenk tubes were closed and removed from the glovebox. The resulting mixture was stirred at 120 °C for the indicated time. The crude product was then cooled down, diluted with methanol and ethyl acetate and injected in a calibrated GC-FID using *n*-dodecane as internal standard to give the concentration (mol/L). A KIE value of $k_H/k_D = 2.6$ was obtained.

Table 3.5. Time(min) and Concentration(mol/L) of **1** and **1-d_5**.

Time (min)	Concentration **1** (mol/L)	Concentration **1-d_5** (mol/L)
5	0.045	0.005
10	0.061	0.035
15	0.122	0.051
20	0.168	0.066

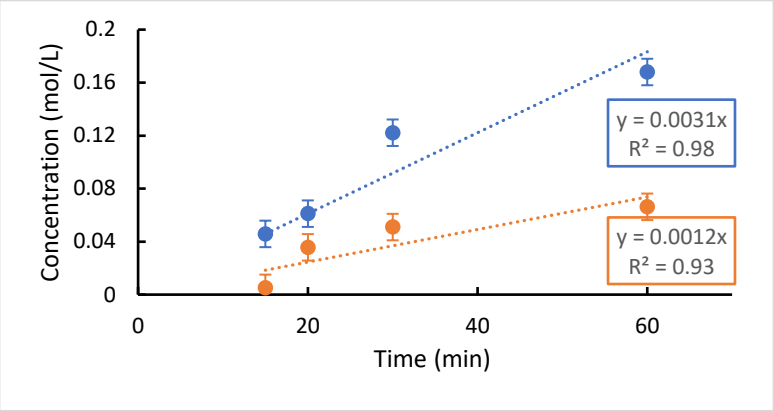

Figure 3.5. Initial Rates of the Reactions with Nitrobenzene and Nitrobenzene-d_5 Using $[Cp^*RhCl_2]_2$ as catalyst.

3.6.6.3 Reaction Mapping Through Isolation of Intermediates

The synthesis of the cyclometalated rhodium complex was inspired by the work of Abad.[20]

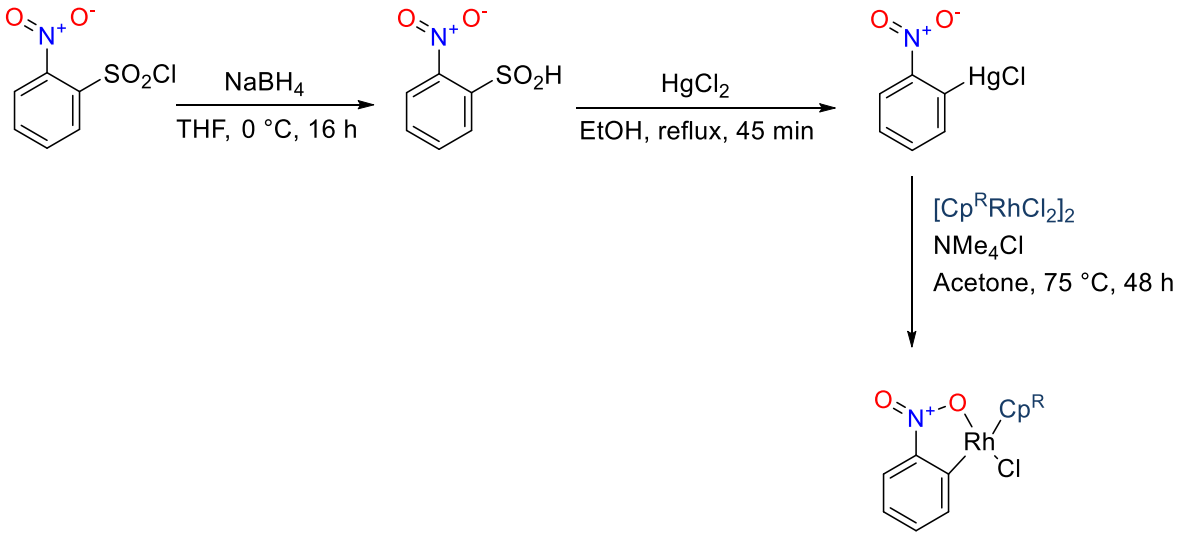

Scheme 3.10. Synthesis of the Cyclometalated Rhodium Complex.

2-Nitrobenzene sulfinic acid

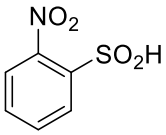

To a solution of 2-nitrobenzenesulfonyl chloride (1.220 g, 5.5 mmol, 1 equiv.) in THF (30 mL) was added $NaBH_4$ (1 g, 27.5 mmol, 5 equiv.) in portions at 0 °C. The reaction mixture was stirred overnight at 0 °C. Then, water (10 mL) was added followed by HCl aq. until the pH was adjusted to 1. The resulting mixture was extracted with chloroform (20 mL x3). The organic layers were combined, washed with brine and dried over $MgSO_4$, filtered and evaporated. The product was obtained in 81% yield and directly used for the next step without purification. The NMR datas were consistent with those of the literature.[32]

^{1}H NMR (400 MHz, DMSO-*d_6*) δ (ppm) 8.22 (d, *J* = 8.1 Hz, 1H), 8.15 – 8.03 (m, 1H), 8.04 – 7.96 (m, 1H), 7.87 – 7.74 (m, 1H).

^{13}C NMR (101 MHz, DMSO-*d_6*) δ (ppm) 145.9, 144.6, 134.9, 132.5, 125.3, 125.0.

2-Nitrophenylmercury chloride

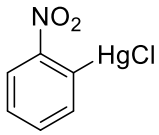

According to the literature,[33] the 2-nitrophenylmercury chloride was synthesized as followed. To a solution of mercury chloride (2 g, 7.4 mmol, 2 equiv.) in EtOH 50% (14 mL) was added a solution of 2-nitrobenzene sulfinic acid (700 mg, 3.7 mmol, 1 equiv.) in EtOH (7 mL). The resultant mixture was refluxed over 45 min. Then the precipitate was extracted with boiling acetone and filtered. The solution was evaporated and the residue was recrystallized in EtOH/H_2O (95:5). Colorless crystals were obtained in 39% yield.

^{1}H NMR (400 MHz, DMSO-*d_6*) δ (ppm) 8.25 – 8.15 (m, 1H), 7.84 – 7.72 (m, 2H), 7.57 – 7.47 (m, 1H).

^{13}C NMR (101 MHz, DMSO-*d_6*) δ (ppm) 152.6, 147.1, 138.2, 134.5, 128.9, 124.1.

Cyclometalated rhodium complex 38a

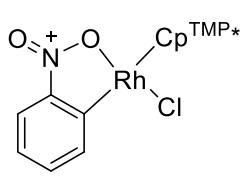

In a glovebox, to an oven-dried Schlenk tube was added $[Cp^{TMP}*RhCl_2]_2$ (276 mg, 0.3 mmol, 1 equiv.) followed by 2-nitrophenylmercury chloride (214 mg, 0.6 mmol, 2 equiv.), NMe_4Cl (145 mg, 1.4 mmol, 4.7 equiv.) and acetone (6 mL). The Schlenk tube was closed and removed from the glovebox. The reaction was heated at 75 °C over 48 h. The solvent was removed under vacuo then water (10 mL) was added and the residue was extracted with dichloromethane (10 mL x3). The organic layers were combined, dried over $MgSO_4$, filtered and evaporated. The product was purified by silica column using dichloromethane/MeOH (98:2) as eluents and

obtained in 85% yield as a dark brown solid. Single crystals of X-ray were obtained by slow diffusion of pentane into a toluene solution of **38a**.

^{1}H NMR (400 MHz, CD_2Cl_2) δ (ppm) 7.83 (dd, *J* = 15.2, 7.8 Hz, 2H), 7.51 (t, *J* = 7.9 Hz, 1H), 7.17 (t, *J* = 7.7 Hz, 1H), 6.69 (s, 2H), 3.79 (s, 3H), 3.73 (s, 6H), 1.83 (s, 3H), 1.81 (s, 3H), 1.71 (s, 3H), 1.67 (s, 3H).

^{13}C NMR (101 MHz, CD_2Cl_2) δ (ppm) 177.3 (d, *J* = 32.8 Hz), 153.8, 150.0 (br), 138.7 (br), 137.6, 136.3, 126.2, 125.2 (d, *J* = 5.8 Hz), 108.3, 105.3 (d, *J* = 6.3 Hz), 102.7 (d, *J* = 6.8 Hz), 96.8 (d, *J* = 7.1 Hz), 96.2 (d, *J* = 8.4 Hz), 94.7 (d, *J* = 7.5 Hz), 61.0, 56.7, 10.8, 9.8, 9.7, 9.0.

HRMS m/z (MALDI) calcd for $C_{24}H_{27}NO_5Rh$ $[M\text{-}Cl]^+$ 512.0939, found 512.0950.

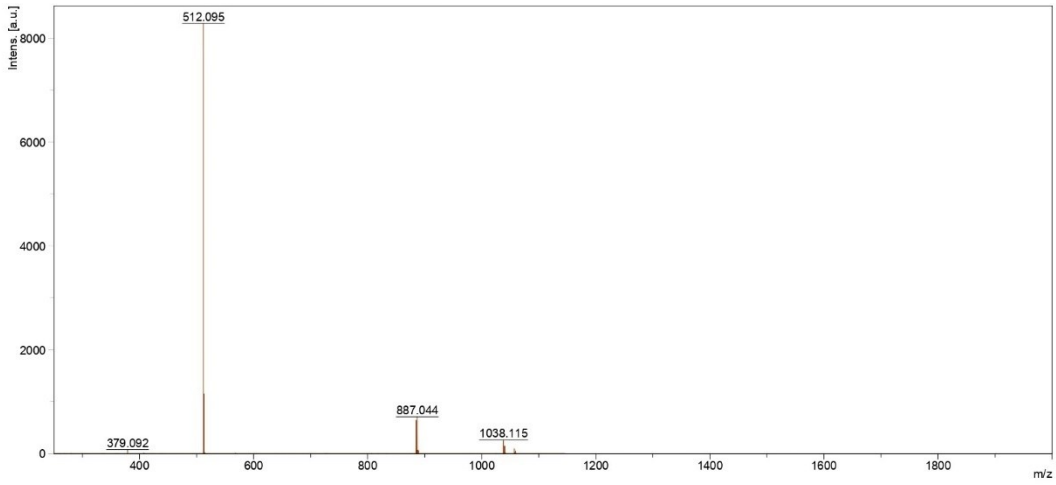

Figure 3.6. High Resolution Mass Spectroscopy of **38a**.

Cyclometalated rhodium complex 38b

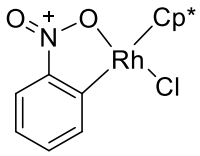

Using slightly modified Abad's method,[20] in a glovebox, to an oven-dried Schlenk tube was added $[Cp^*RhCl_2]_2$ (200 mg, 0.3 mmol, 1 equiv.), 2-nitrophenylmercury chloride (214 mg, 0.6 mmol, 2 equiv.), NMe_4Cl (145 mg, 1.4 mmol, 4.7 equiv.) and acetone (6 mL). The reaction was heated at 75 °C over 48 h. The solvent was removed under vacuo then water (10 mL) was added and the residue was extracted with dichloromethane (10 mL x3). The organic layers were combined, dried over $MgSO_4$, filtered and evaporated. The product was purified by silica column using dichloromethane as eluent and obtained in 42% yield as a brown solid.

^{1}H NMR (400 MHz, CD_2Cl_2) δ (ppm) 7.90 (dd, *J* = 7.7, 1.3 Hz, 1H), 7.84 (dd, *J* = 8.2, 1.3 Hz, 1H), 7.55 (td, *J* = 7.4, 1.3 Hz, 1H), 7.17 (ddd, *J* = 8.2, 7.0, 1.2 Hz, 1H), 1.71 (s, 15H).

^{13}C NMR (101 MHz, CD_2Cl_2) δ (ppm) 177.6 (d, *J* = 33.0 Hz), 150.1 (br), 137.6, 136.0 (d, *J* = 1,7 Hz), 125.1, 124.9, 97.3 (d, *J* = 7.3 Hz), 9.6.

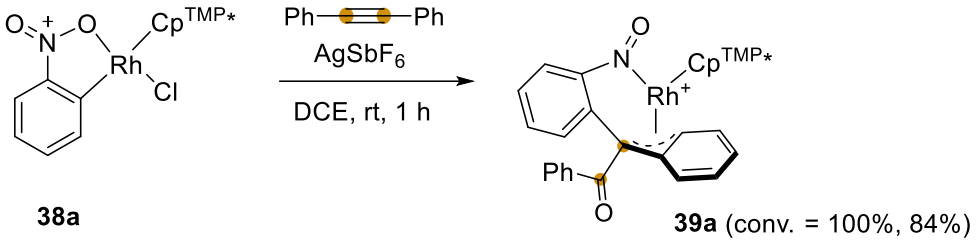

Scheme 3.11. Synthesis of Rhodium Complex **39a**.

Procedure: In a glovebox, to a 5 mL vial was added **38a** (15 mg, 0.027 mmol, 1 equiv.), diphenylacetylene (4.9 mg, 0.027 mg, 1 equiv.), $AgSbF_6$ (9.4 mg, 0.027 mmol, 1 equiv.) and DCE (1 mL). The reaction was stirred at room temperature over 1 h in the glovebox. The crude solution was directly used for NMR analyses using a capillary of CD_2Cl_2 and a Young NMR tube. **39a** was obtained with 100% conversion and 84% isolated yield.

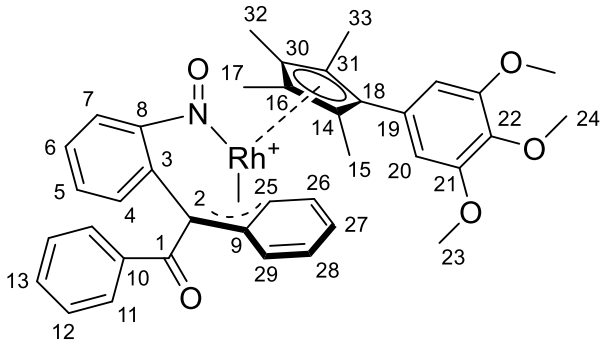

^{1}H NMR (400 MHz, CD_2Cl_2) δ (ppm) 9.09 (d, *J* = 8.8 Hz, 1H), 7.78 (t, *J* = 7.4 Hz, 1H), 7.73 (t, *J* = 7.8 Hz, 1H), 7.48 – 7.37 (m, 3H), 7.28 – 7.14 (m, 8H), 7.12 – 7.01 (m, 4H), 6.22 (s, 2H), 4.95 (d, *J* = 7.2 Hz, 1H), 3.79 (s, 3H), 3.73 (s, 6H), 1.54 (s, 3H), 1.16 (s, 3H), 0.72 (s, 3H), 0.52 (s, 3H).
^{13}C NMR (101 MHz, CD_2Cl_2) δ (ppm) 197.5, 170.7 (d, *J* = 4.9 Hz), 153.5, 148.7, 139.6, 139.6, 139.2, 133.6, 132.5, 132.1, 131.9, 130.8, 129.6, 129.4, 128., 128.4, 128.3, 128.3, 123.0, 114.5, 109.2 (br), 108.1, 107.6 (d, *J* = 6.6 Hz), 105.3 (d, *J* = 5.3 Hz), 104.3 (d, *J* = 7.3 Hz), 97.7 (d, *J* = 4.1 Hz), 93.6 (d, *J* = 6.3 Hz), 77.1, 60.4, 56.2, 8.8, 6.4, 6.0, 5.3.
HRMS m/z (ESI) calcd for $C_{38}H_{37}NO_5Rh$ $[M]^+$ 690.1721, found 690.1718.

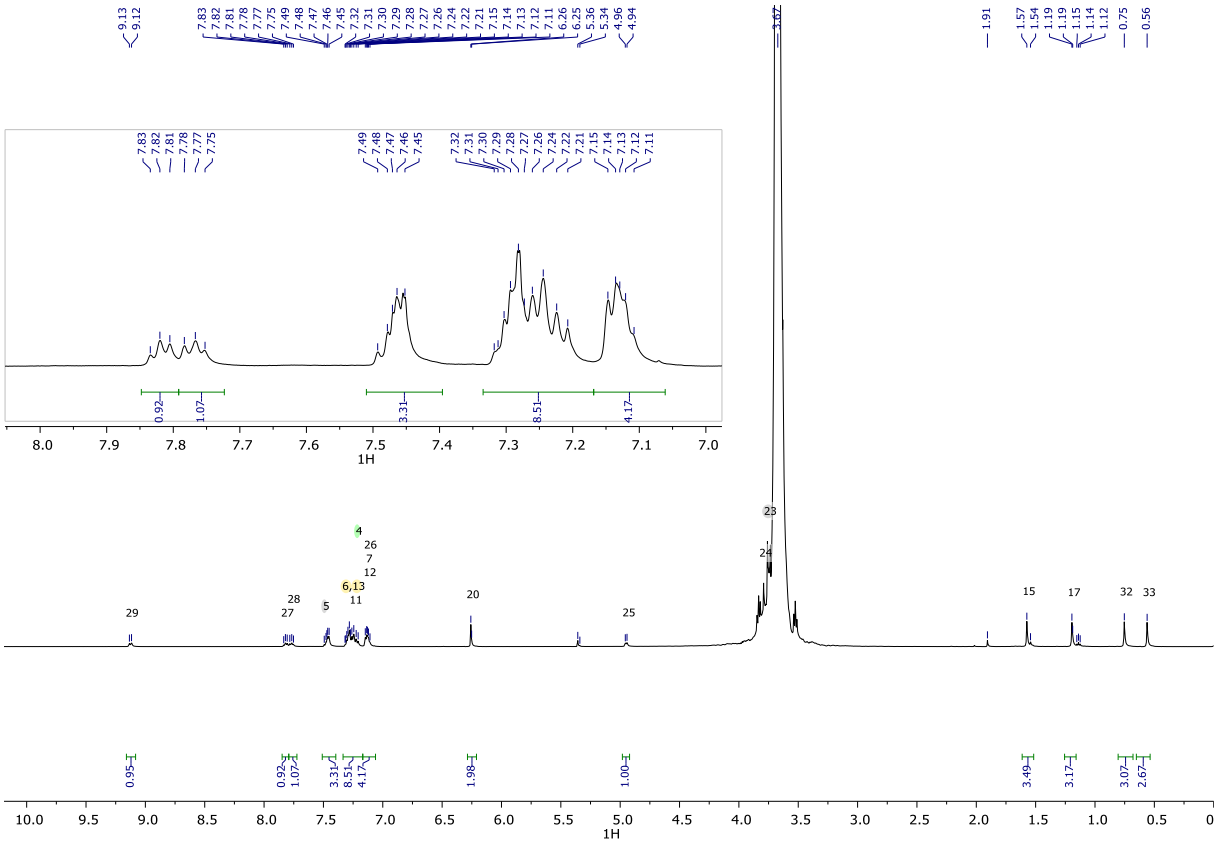

Figure 3.7. ^{1}H NMR Spectra of **39a**.

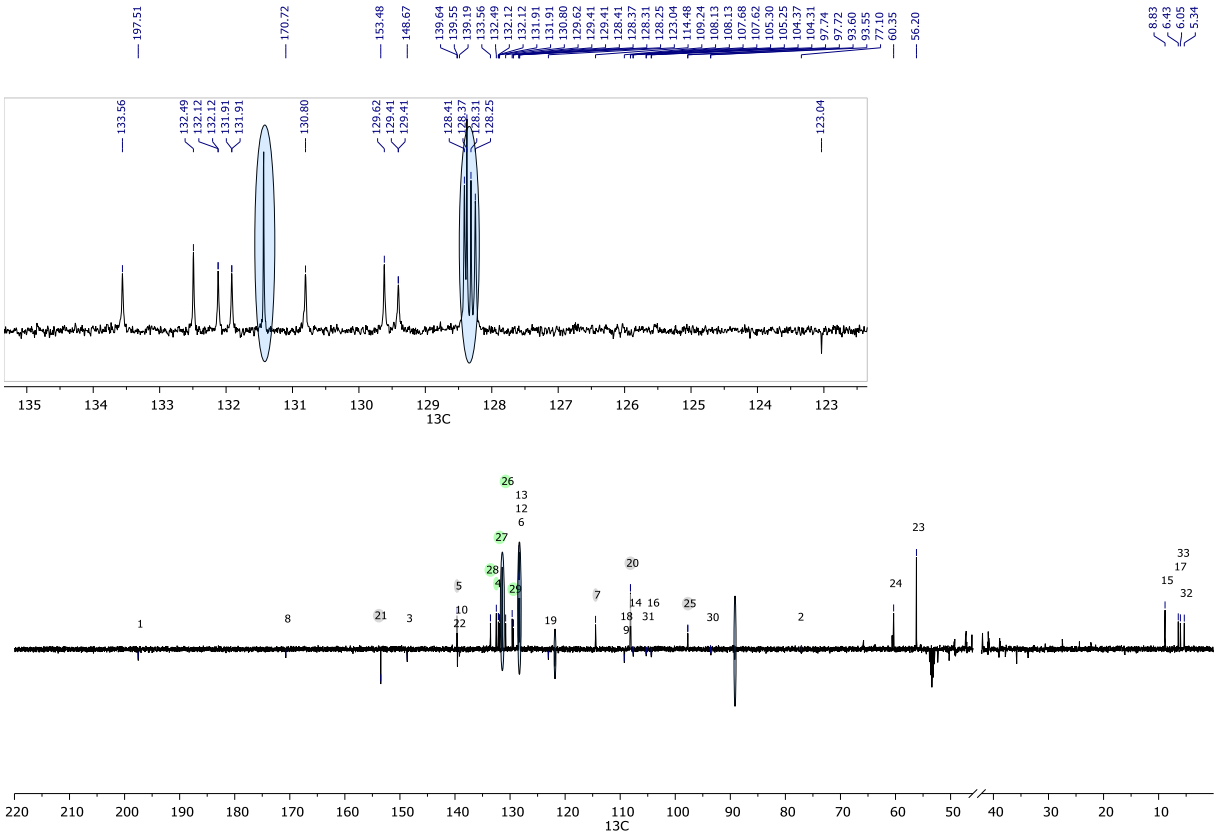

Figure 3.8. JMod Experiment of **39a**. (Highlighted in Blue: Excess of Diphenylacetylene)

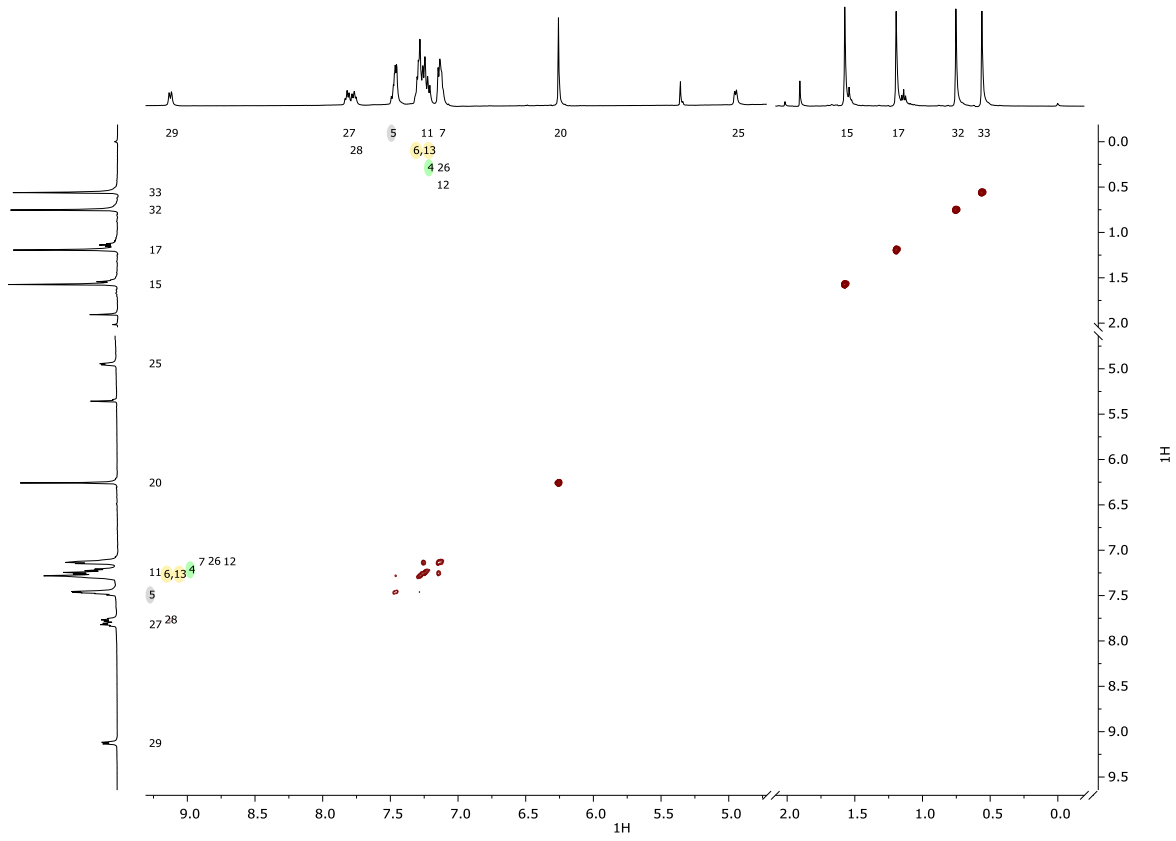

Figure 3.9. COSY Experiment of **39a**.

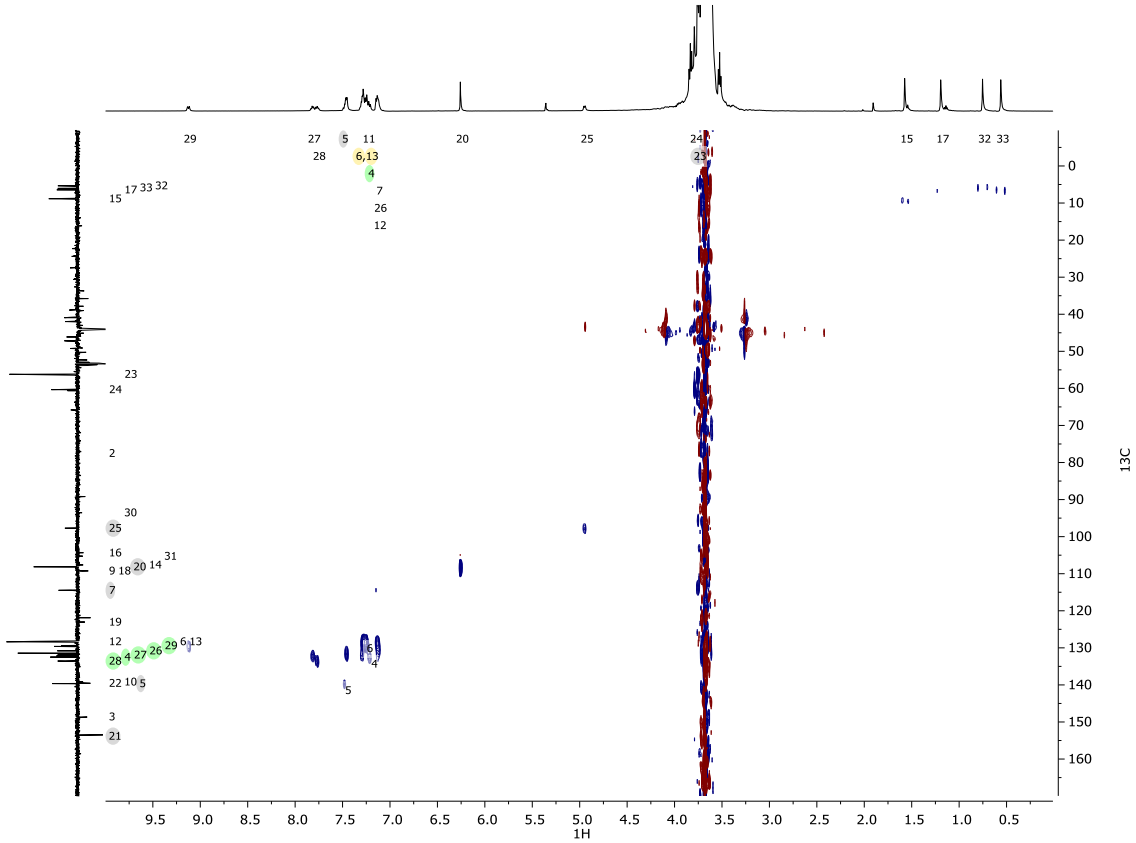

Figure 3.10. HSQC Experiment of **39a**.

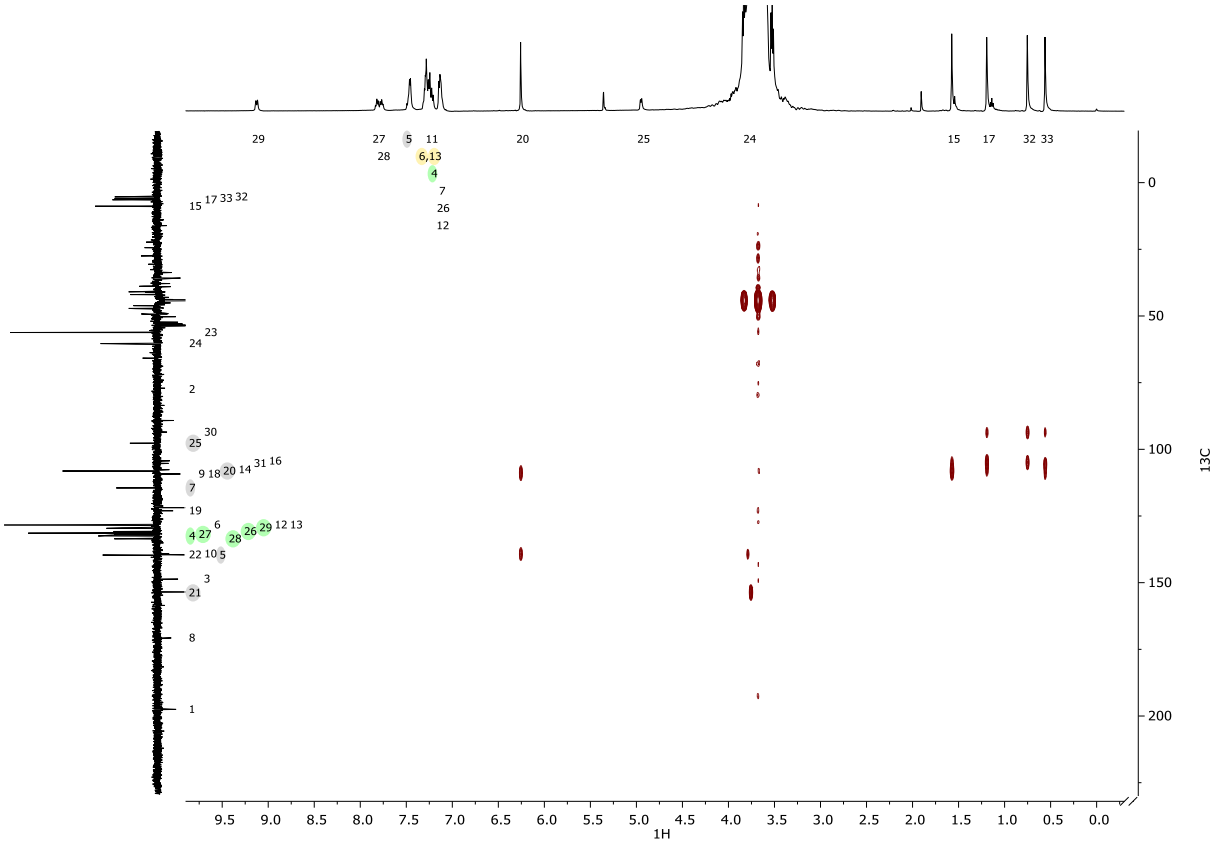

Figure 3.11. HMBC Experiment of **39a**.

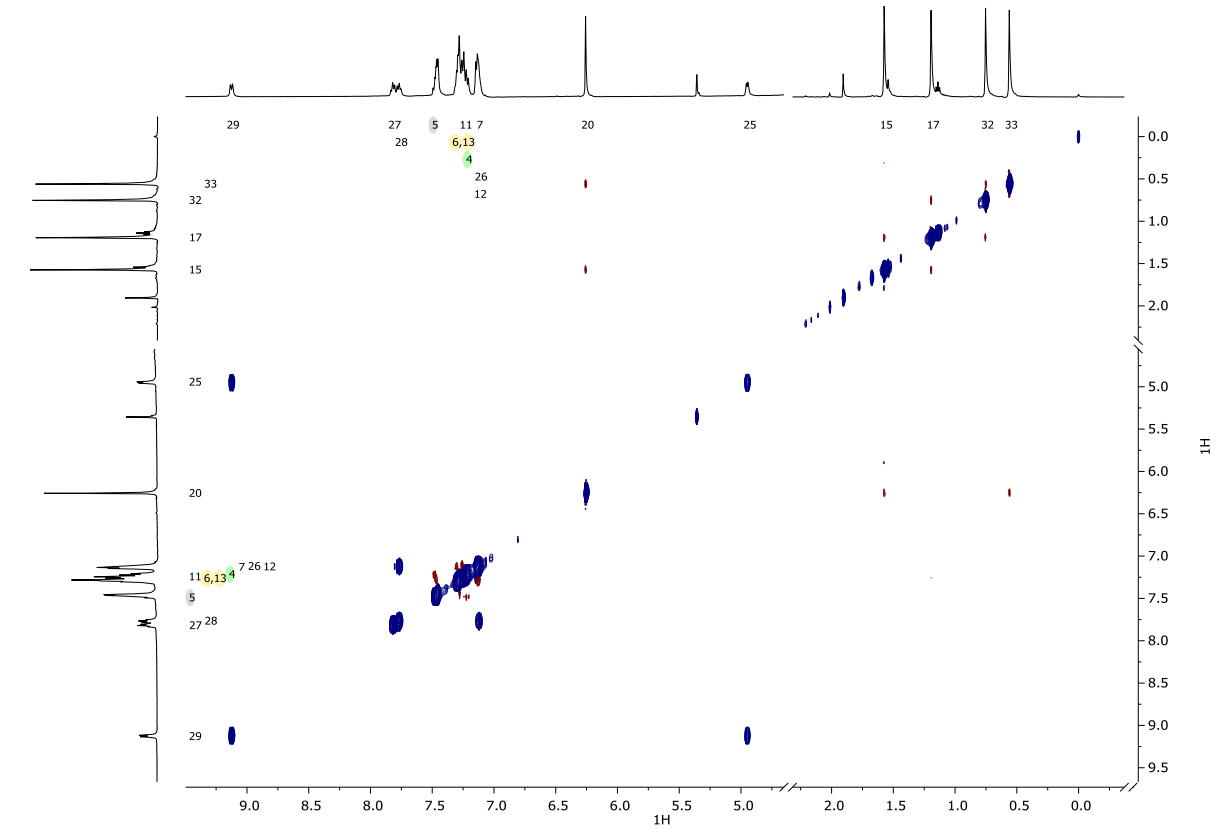

Figure 3.12. NOESY Experiment of **39a**.

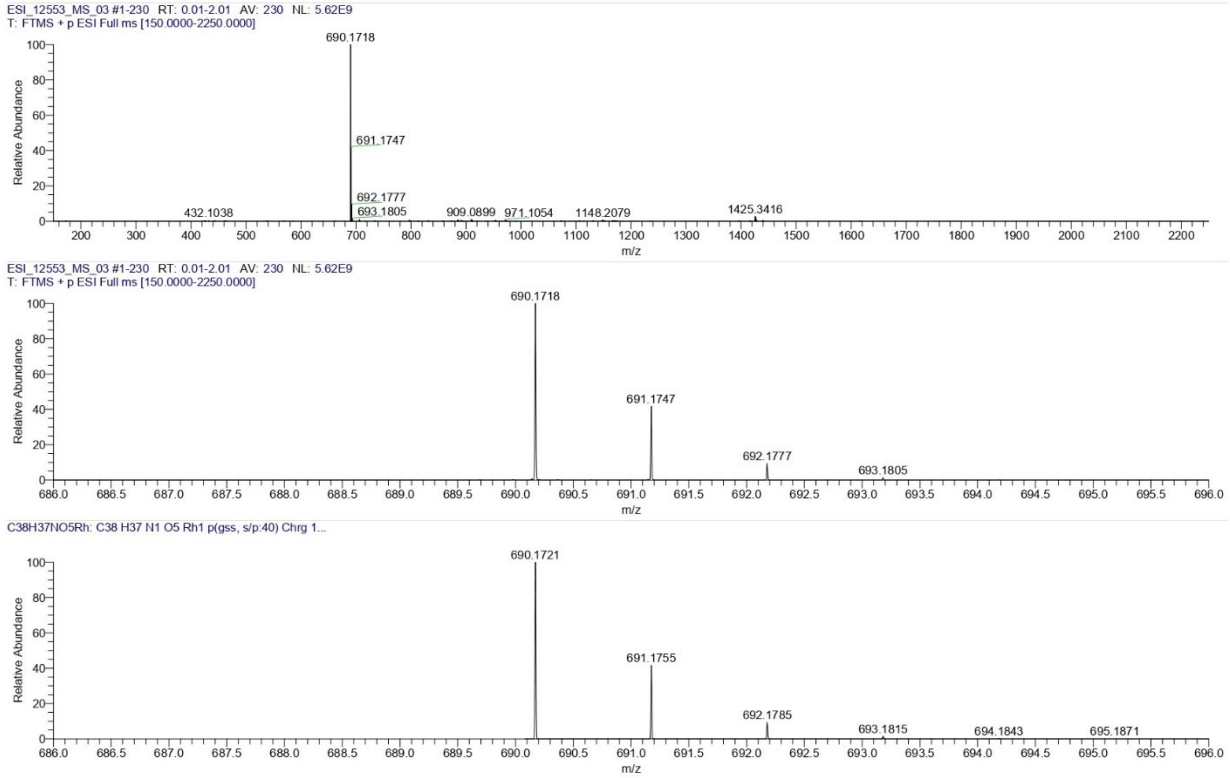

Figure 3.13. High Resolution Mass Spectroscopy of **39a**.

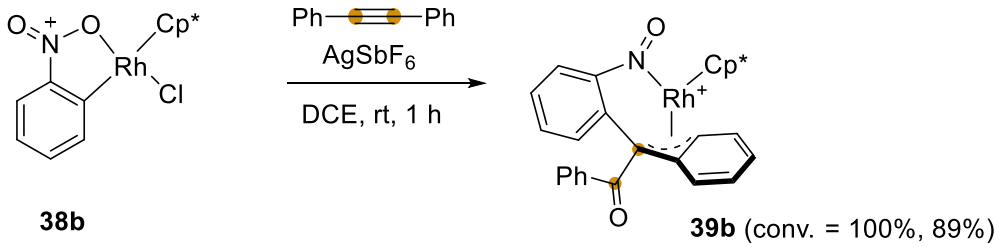

38b

39b (conv. = 100%, 89%)

Scheme 3.12. Synthesis of Rhodium Complex **39b**.

Procedure: In a glovebox, to a 5 mL vial was added **38b** (15 mg, 0.027 mmol, 1 equiv.), diphenylacetylene (4.9 mg, 0.027 mg, 1 equiv.), $AgSbF_6$ (9.4 mg, 0.027 mmol, 1 equiv.) and DCE (1 mL). The reaction was stirred at room temperature over 1 h. The sample was removed from the glovebox and the crude solution was concentrated under vacuo and used for NMR analyses using CD_2Cl_2 as deuterated solvent. **39b** was obtained with 100% conversion and 89% isolated yield. Single crystals of X-ray were obtained by slow diffusion of pentane into a DCE solution of **39b**.

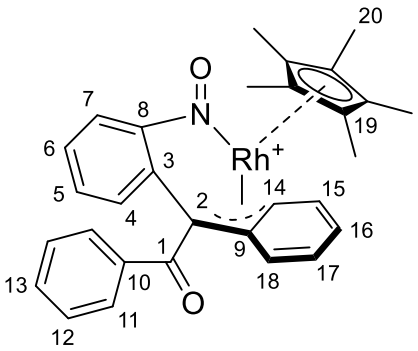

^{1}H NMR (400 MHz, CD_2Cl_2) δ (ppm) 9.15 (d, *J* = 8.7 Hz, 1H), 7.94 (t, *J* = 7.3 Hz, 1H), 7.91 – 7.86 (m, 1H), 7.57 – 7.52 (m, 1H), 7.40 – 7.34 (m, 1H), 7.33 – 7.17 (m, 8H), 4.94 (d, *J* = 8.6 Hz, 1H), 1.19 (s, 15H).

^{13}C NMR (101 MHz, CD_2Cl_2) δ (ppm) 197.3, 171.5 (d, *J* = 4.9 Hz), 148.8, 139.8, 139.6, 133.6, 132.5, 132.1, 131.9, 131.4, 129.7, 129.1, 128.5, 128.2, 114.5, 109.9 (d, *J* = 3.5 Hz), 102.7 (d, *J* = 6.4 Hz), 96.5 (d, *J* = 3.1 Hz), 77.5 (d, *J* = 13,0 Hz), 6.5.

HRMS m/z (ESI) calcd for $C_{30}H_{29}NO_2Rh$ $[M]^+$ 538.1248, found 538.1250.

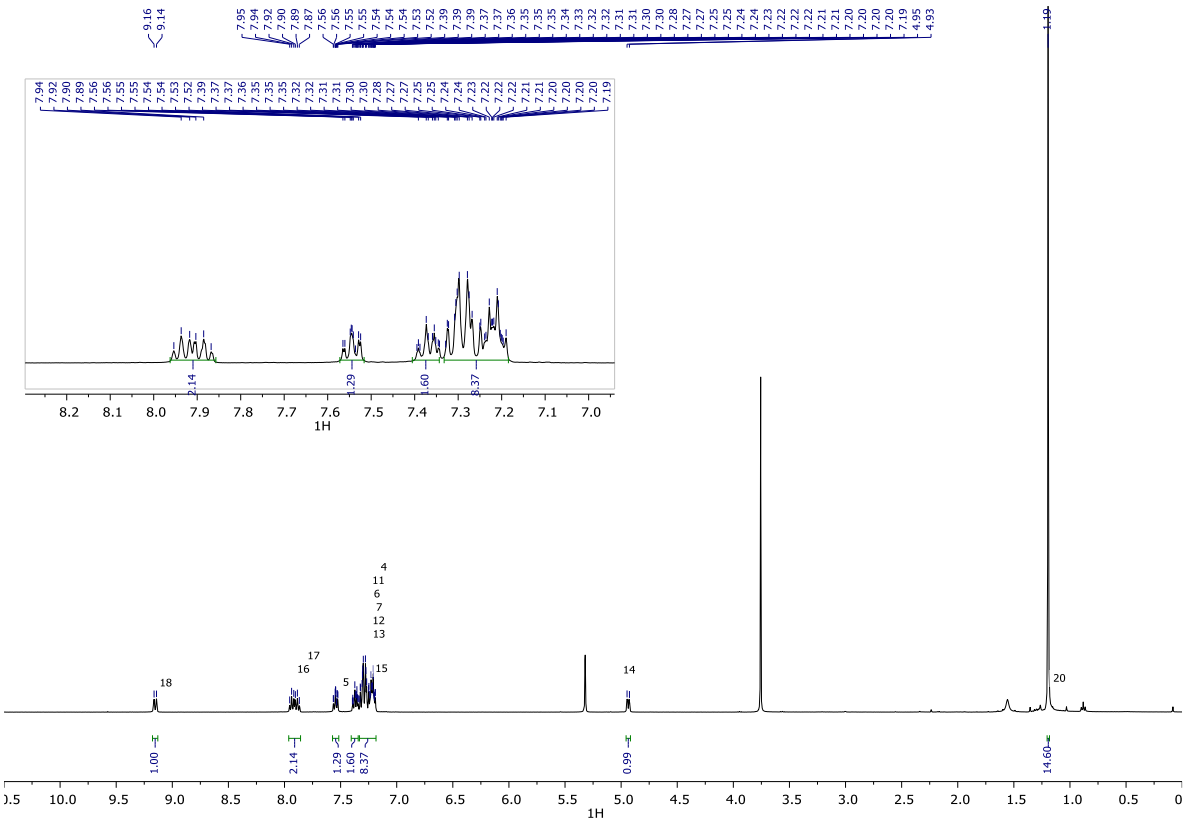

Figure 3.14. ^{1}H NMR Spectra of **39b**.

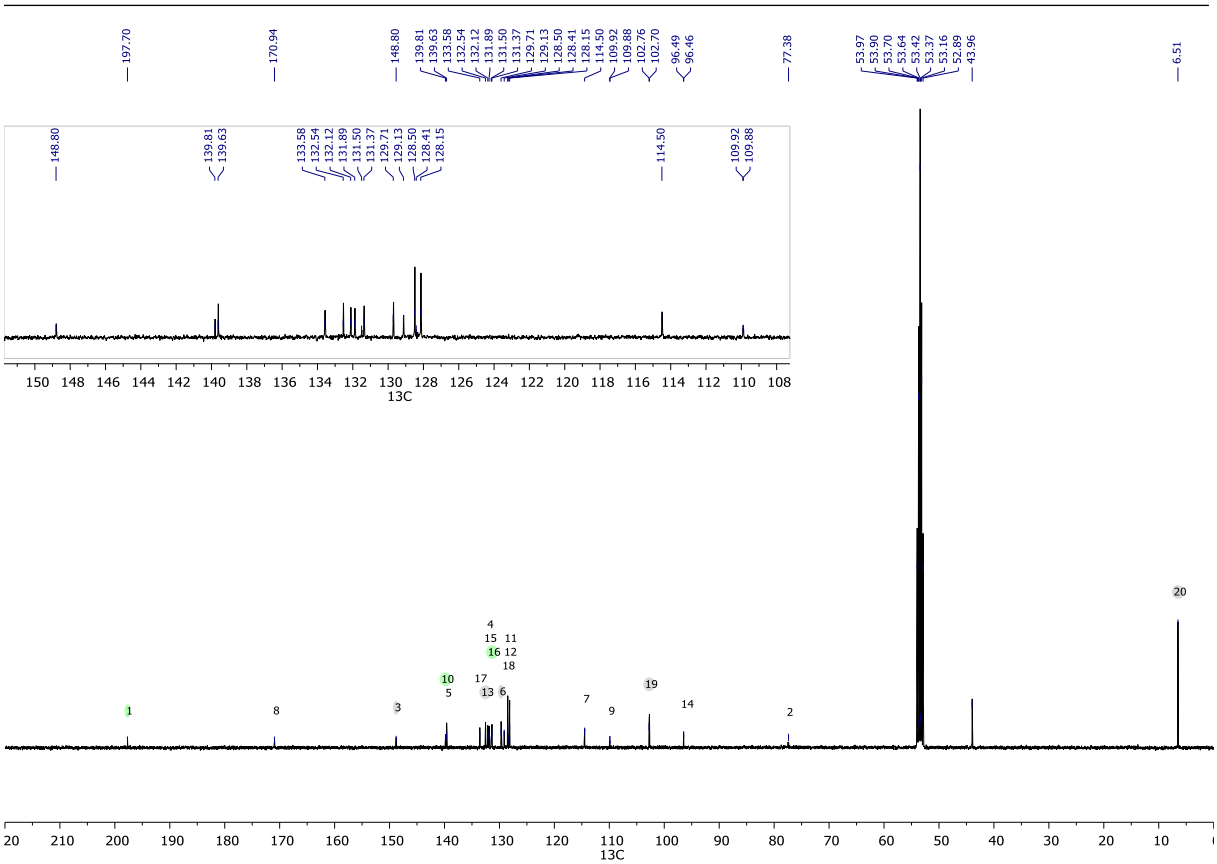

Figure 3.15. ^{13}C NMR Spectra of **39b**.

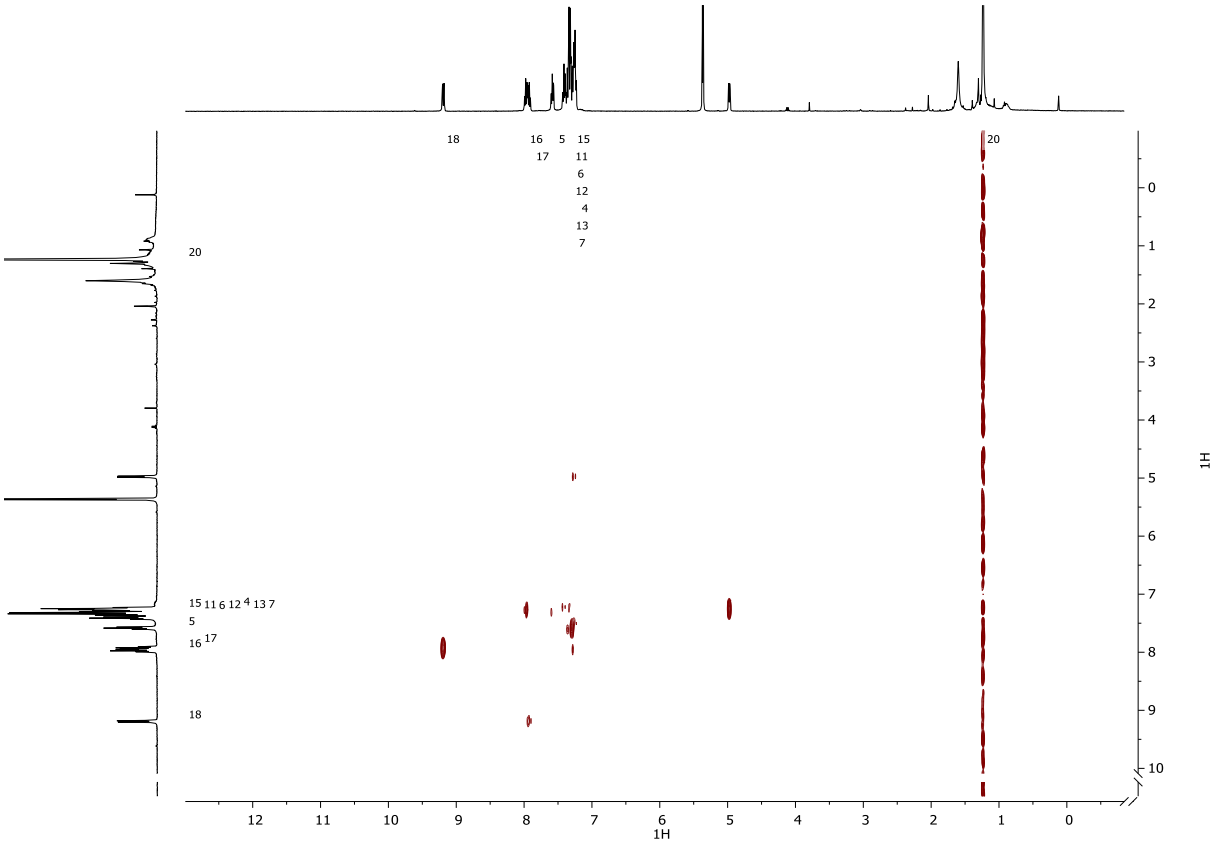

Figure 3.16. COSY Experiment of **39b**.

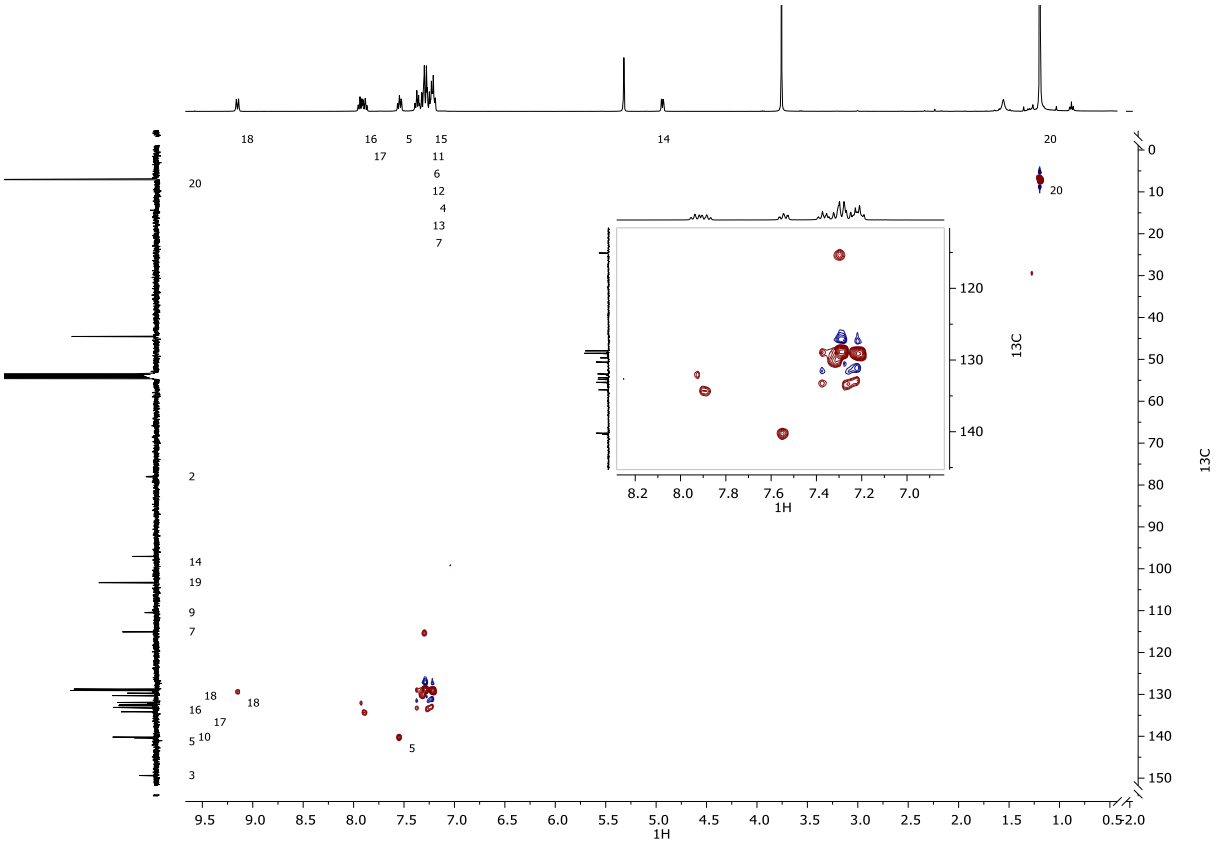

Figure 3.17. HSQC Experiment of **39b**.

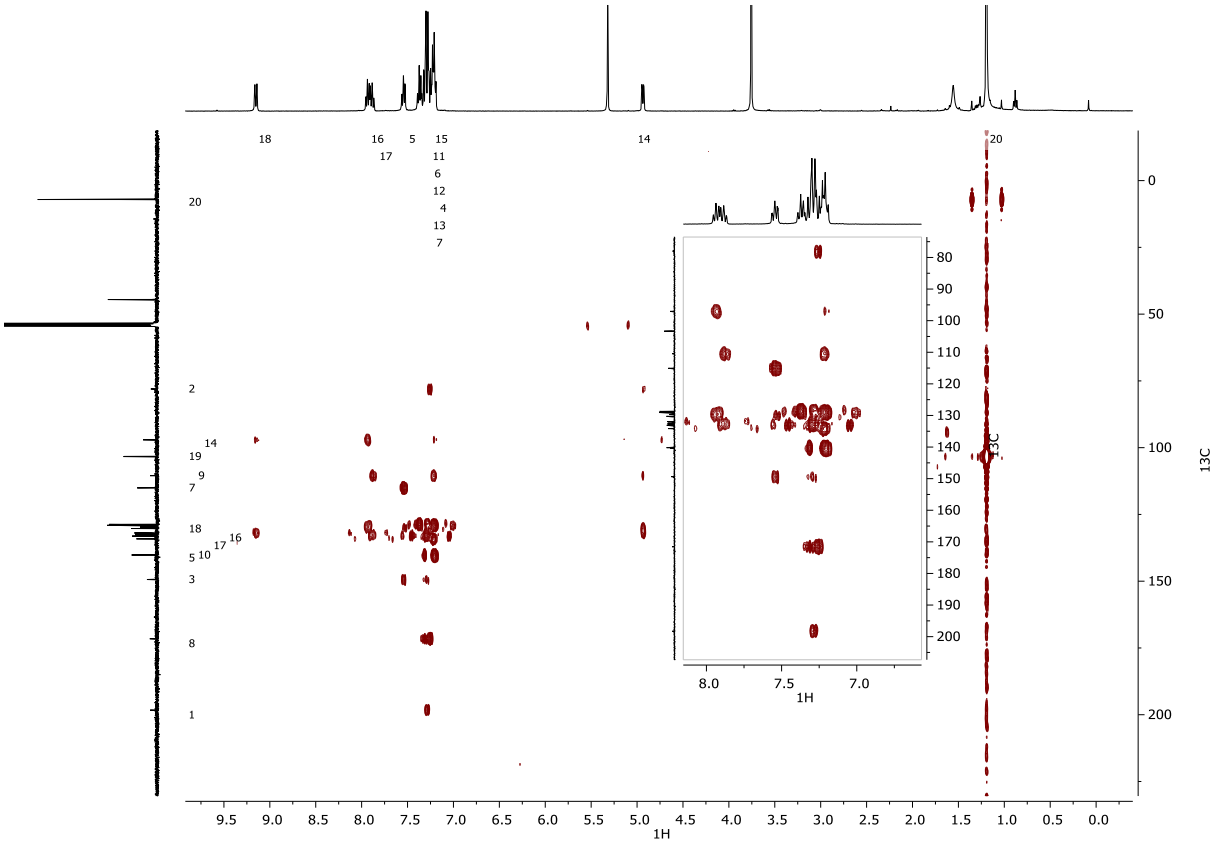

Figure 3.18. HMBC Experiment of **39b**.

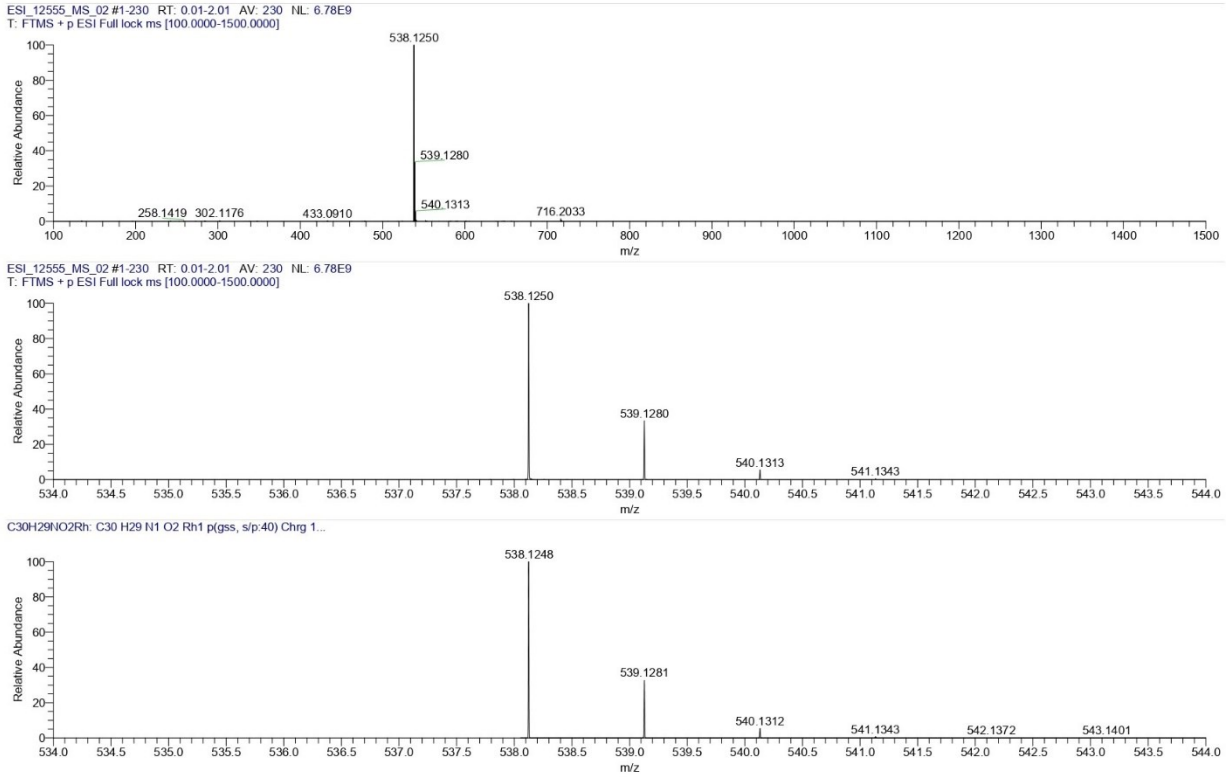

Figure 3.19. High Resolution Mass Spectroscopy of **39b**.

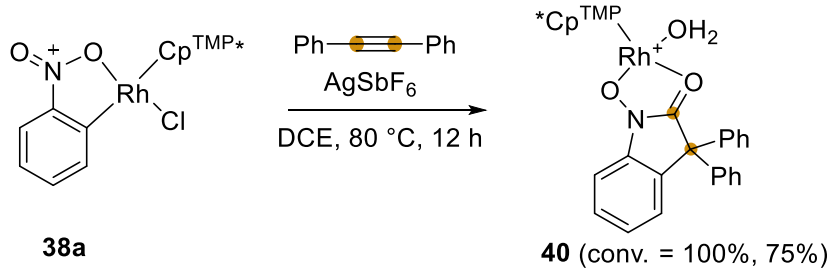

38a **40** (conv. = 100%, 75%)

Scheme 3.13. Synthesis of the Intermediate Rhodium Complex **40**.

Procedure: In a glovebox, to a 5 mL vial was added **38a** (15 mg, 0.027 mmol, 1 equiv.), diphenylacetylene (4.9 mg, 0.027 mmol, 1 equiv.), $AgSbF_6$ (9.4 mg, 0.027 mmol, 1 equiv.) and DCE (1 mL). The reaction was stirred at 80 °C over 12 h. The sample was removed from the glovebox and the crude solution was concentrated under vacuo and used for NMR analyses using CD_2Cl_2 as deuterated solvent. **40** was obtained with 100% conversion and 75% isolated yield. Single crystals of X-ray were obtained by slow diffusion of pentane into a chloroform solution of **40**. The coordination of water occurred during the recrystallization process.

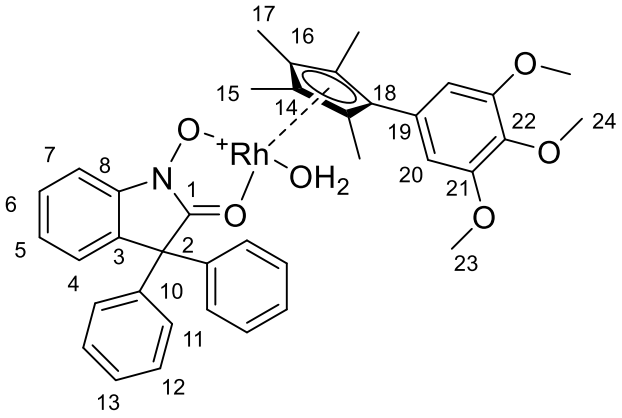

^{1}H NMR (400 MHz, CD_2Cl_2) δ (ppm) 7.49 – 7.42 (m, 1H), 7.39 (d, *J* = 7.7 Hz, 1H), 7.30-7.33 (m, 9H), 7.10 (d, *J* = 7.4 Hz, 4H), 6.99 (s, 2H), 3.84 (s, 3H), 3.75 (s, 6H), 1.91 (s, 6H), 1.85 (s, 6H).

^{13}C NMR (101 MHz, CD_2Cl_2) δ (ppm) 175.4, 154.5, 140.0, 139.3, 139.1, 135.5, 129.7, 129.4,128.9, 128.5, 126.9, 126.5, 122.5, 110.8, 107, 6, 99.6 (d, *J* = 9.0 Hz), 96.3 (br), 96.0 (br), 61.0, 60.7, 56.7, 10.9, 10.0.

HRMS m/z (ESI) calcd for $C_{38}H_{37}NO_5Rh$ $[M\text{-}H_2O]^+$ 690.1721, found 690.1721.

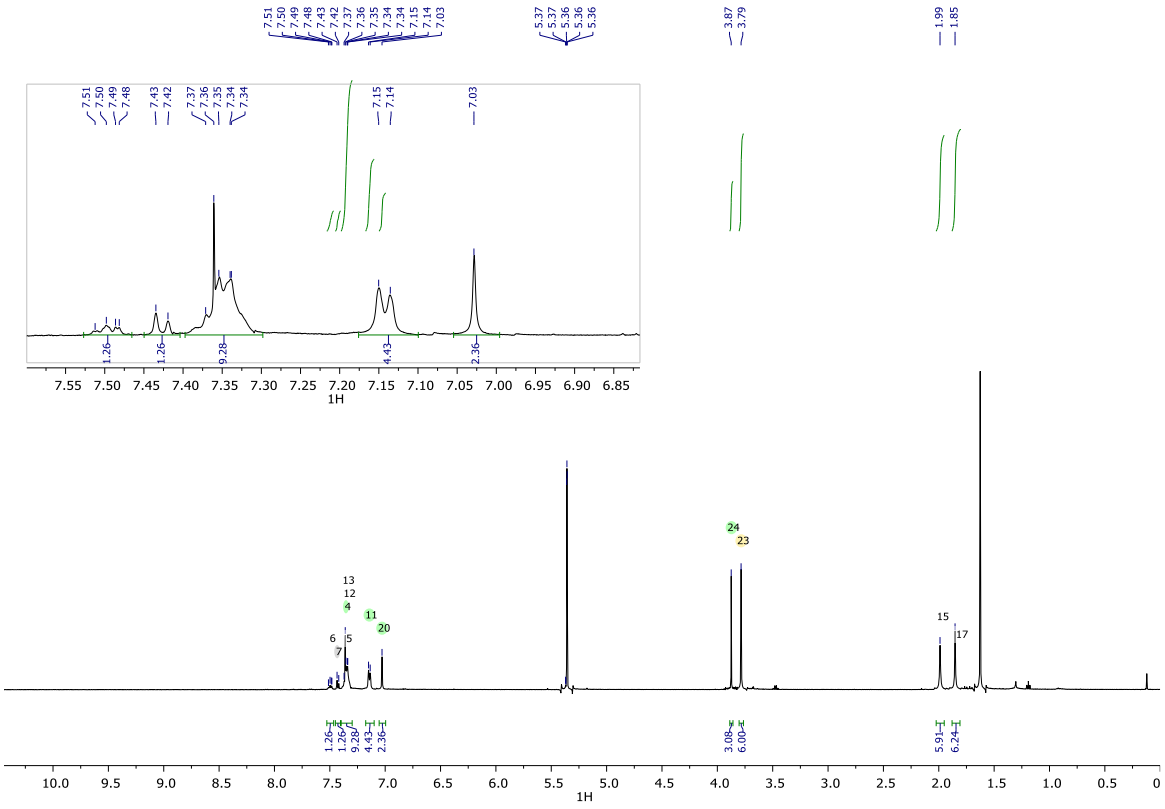

Figure 3.20. ^{1}H Spectra of **40**.

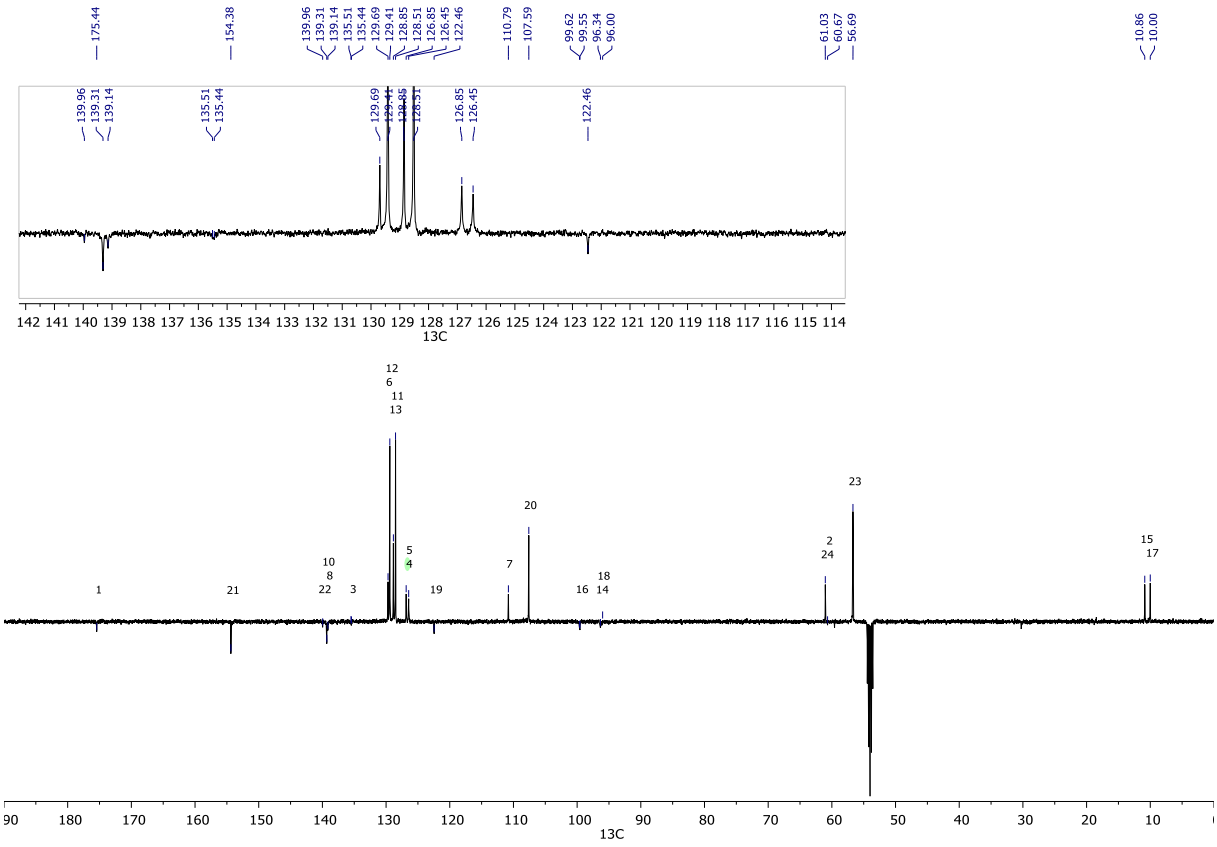

Figure 3.21. Jmod Experiment of **40**.

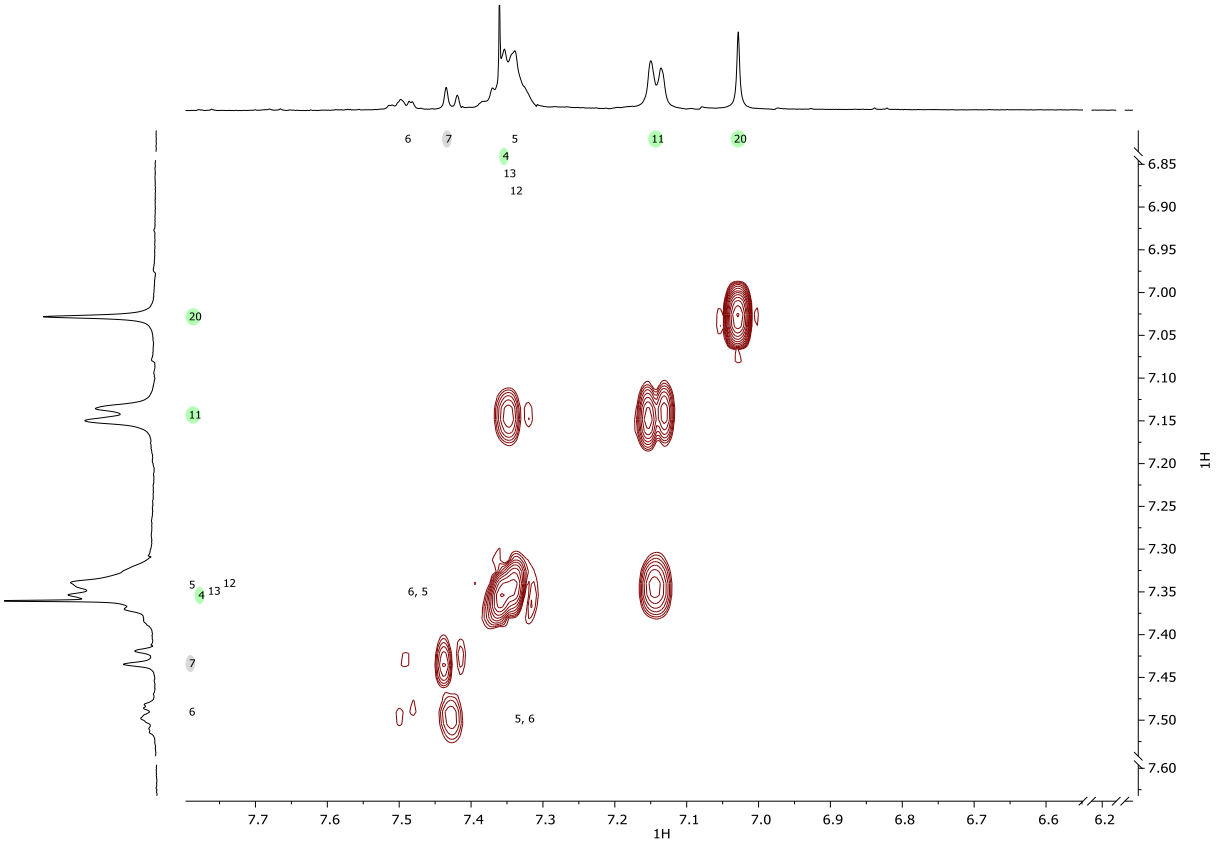

Figure 3.22. COSY Experiment of **40**.

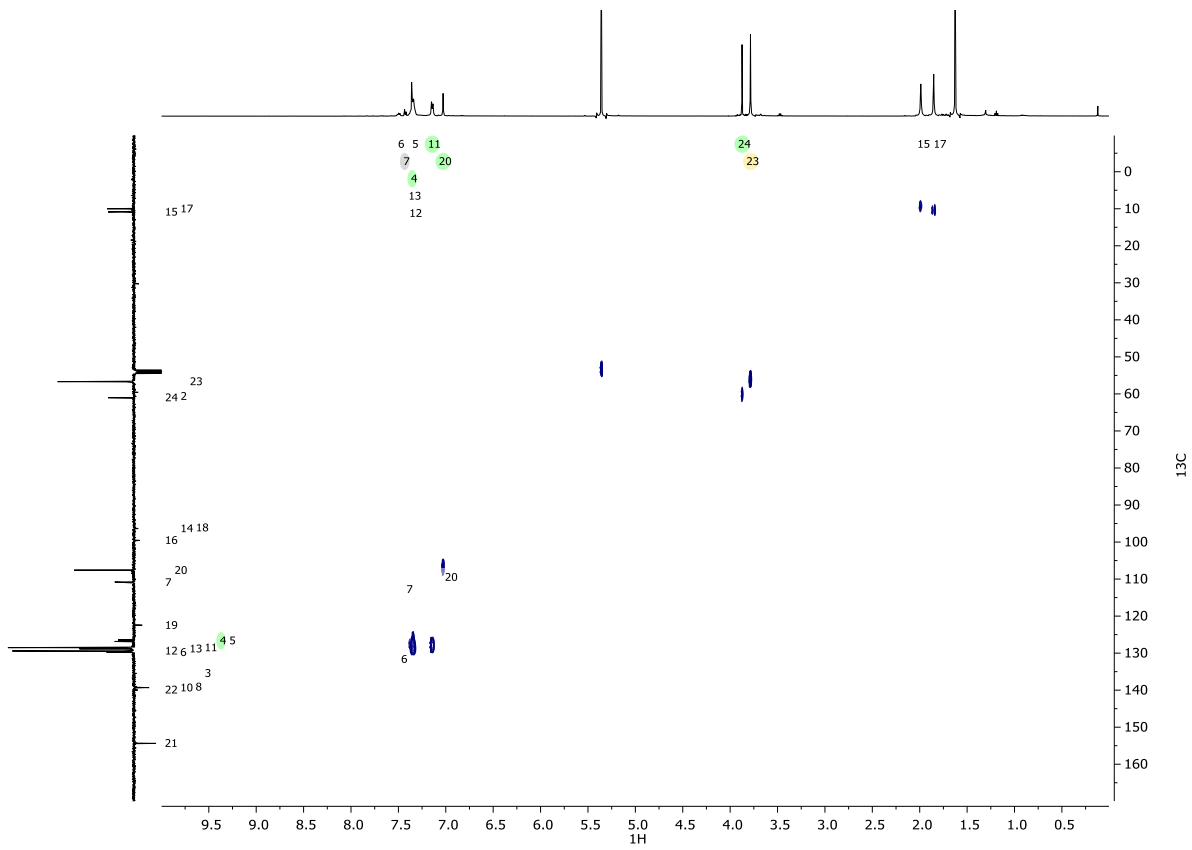

Figure 3.23. HSQC Experiment of **40**.

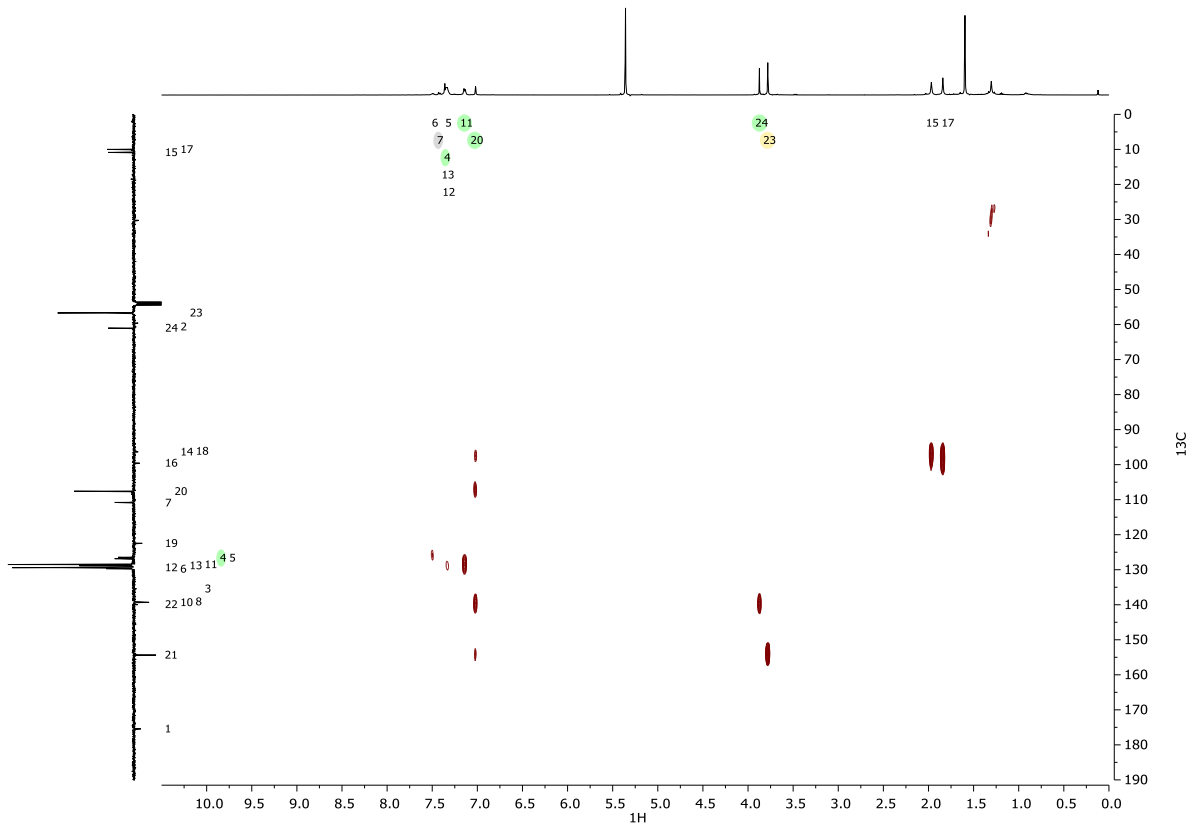

Figure 3.24. HMBC Experiment of **40**.

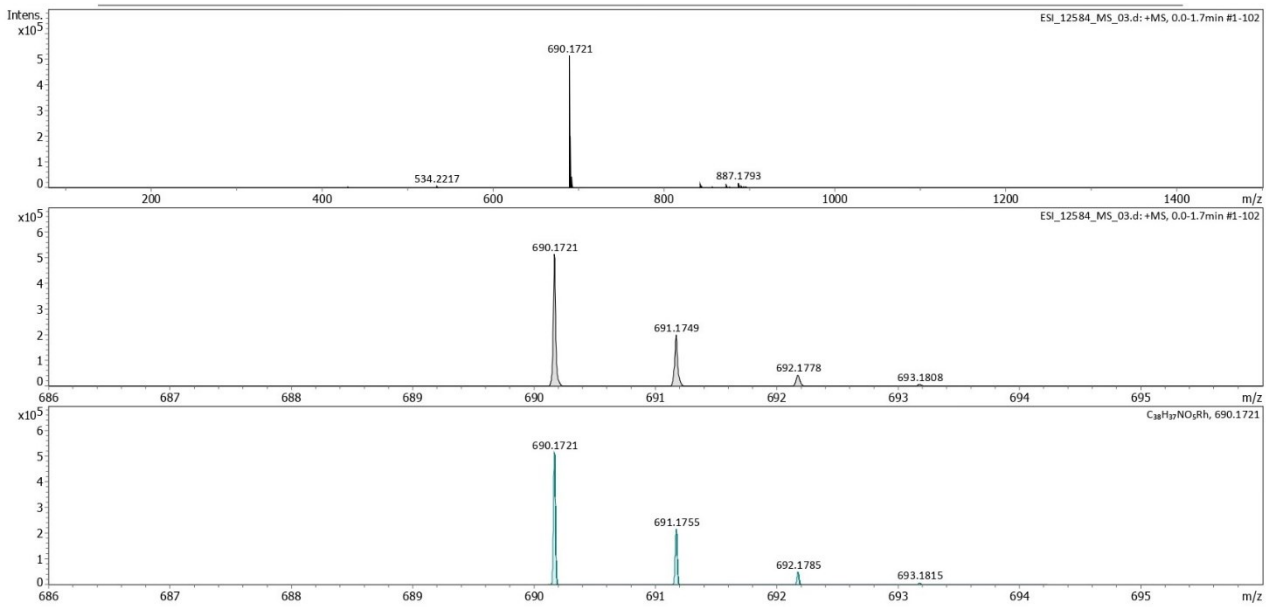

Figure 3.25. High Resolution Mass Spectroscopy of **40**.

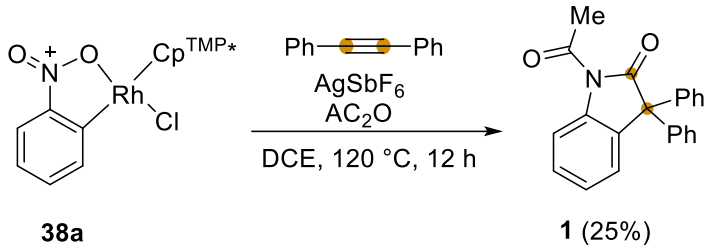

38a **1** (25%)

Scheme 3.14. Synthesis of the Product **1** Starting from Rhodium Complex **31a**.

Procedure: In a glovebox, to a dried Schlenk tube was added **38a** (15 mg, 0.027 mmol, 1 equiv.), diphenylacetylene (4.9 mg, 0.027 mg, 1 equiv.), $AgSbF_6$ (9.4 mg, 0.027 mmol, 1 equiv.), acetic anhydride (2.6 µL, 0.027 mmol, 1 equiv.) and DCE (1 mL). The Schlenk tube was closed and removed from the glovebox. The reaction was stirred at 120 °C over 12 h. **1** was obtained in 25% yield. The yield was determined by GC-FID using *n*-dodecane as internal standard.

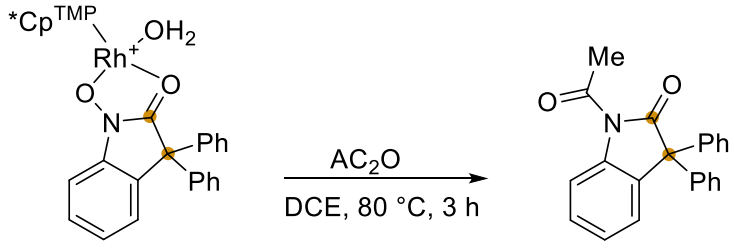

40 **1** (68%)

Scheme 3.15. Synthesis of the Product **1** Starting from Rhodium Complex **40**.

Procedure: In a glovebox, to a dried Schlenk tube was added **40** (15 mg, 0.021 mmol, 1 equiv.), acetic anhydride (2 µL, 0.021 mmol, 1 equiv.) and DCE (1 mL). The Schlenk tube was closed and removed from the glovebox. The reaction was stirred at 80 °C over 3 h. **1** was obtained in 68% yield. The yield was determined by GC-FID using *n*-dodecane as internal standard.

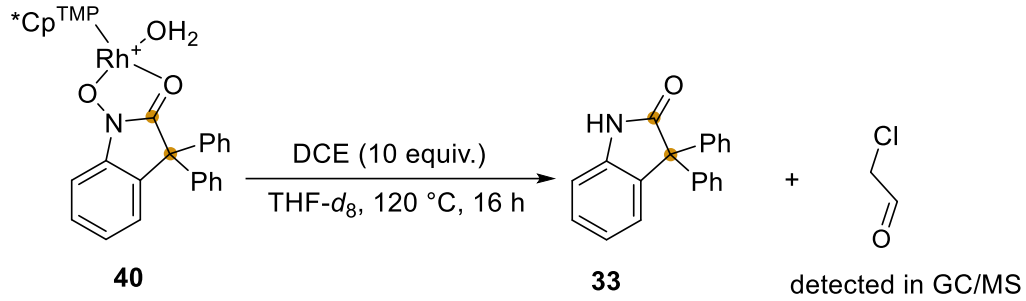

Scheme 3.16. Synthesis of the Product **33** Starting from Rhodium Complex **40**.

Procedure: In a glovebox, to a dried Young tube NMR was added **40** (15 mg, 0.021 mmol, 1 equiv.), THF-d_8 (1 mL) and DCE (17 µL, 0.21 mmol, 10 equiv.). The tube was sealed, removed from the glovebox and stirred at 120 °C over 16 h. Products were identified according to their retention time: t_R (min) 12.1 (2-chloroacetaldehyde), 40.5 (product **33**).

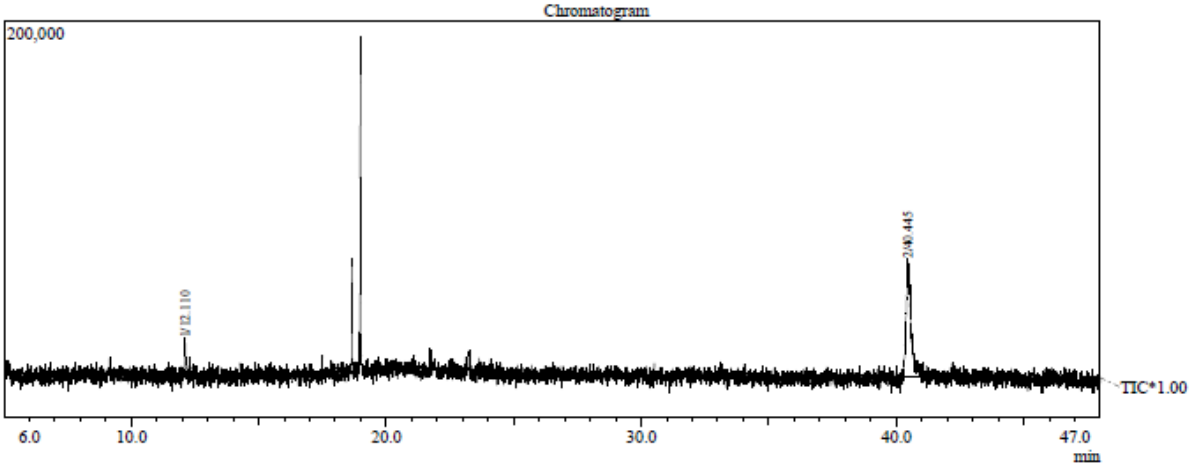

Figure 3.26. Gas Chromatogram of the Crude Mixture of **33** and 2-Chloroacetaldehyde.

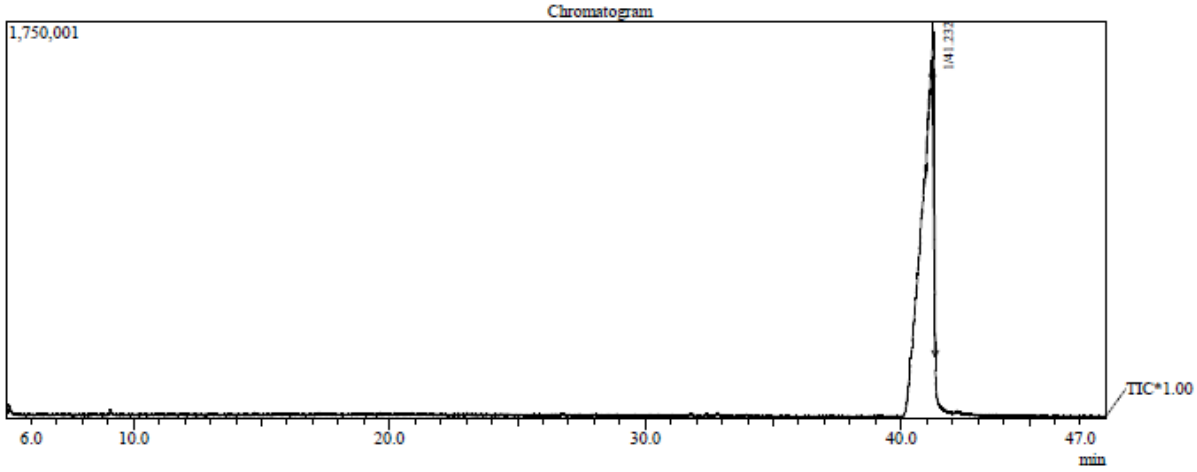

Figure 3.27. Gas Chromatogram of **33**.

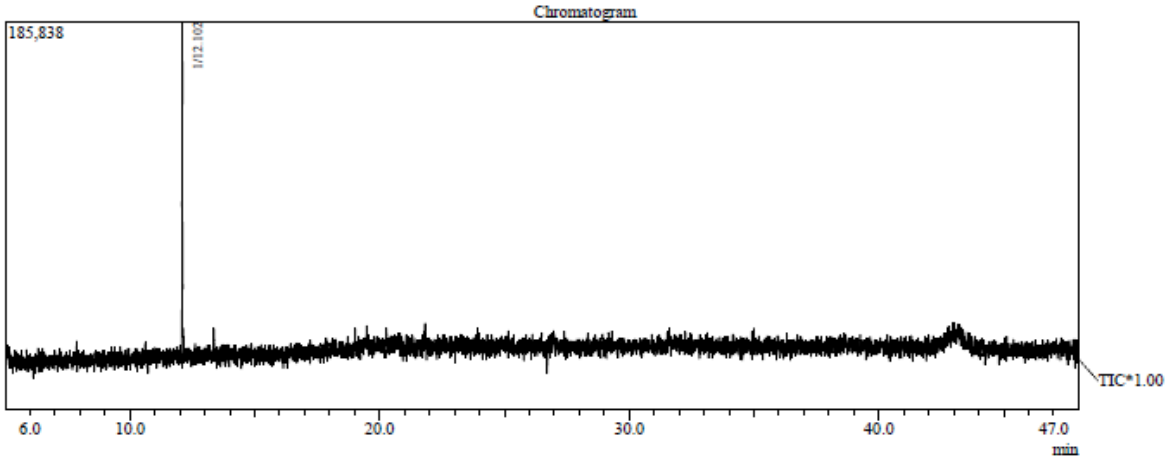

Figure 3.28. Gas Chromatogram of 2-Chloroacetaldehyde.

3.6.7. X-Ray Crystallographic Datas

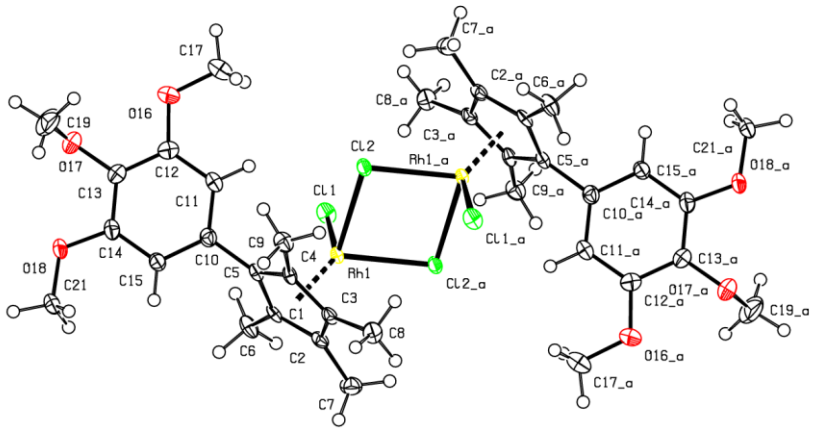

Table 3.6. Crystal Data and Structure for **$[Cp^{TMP}*RhCl_2]_2$** (CCDC2108501).

Empirical formula	$C_{38}H_{50}Cl_8O_6Rh_2$
Extended formula	$C_{36}H_{46}Cl_4O_6Rh_2$, $2(CH_2Cl_2)$
Formula weight	1092.20 g/mol
Temperature	150(2) K
Radiation type	Mo-Ka
Wavelength	0.71073 Å
Crystal system, space group	monoclinic, P $2_{1/c}$
Unit cell dimensions	a = 13.4424(7) Å
b = 8.7468(4) Å	
c = 20.0034(10) Å	
b = 106.961(2) °	
Volume	2249.66(19) $Å^3$
Z, Calculated density	2, 1.612 g/ cm^{-3}
Absorption coefficient	1.251 mm^{-1}
F(000)	1104
Crystal size	0.330 x 0.260 x 0.210 mm
Crystal color	orange
Crystal description	prism
Diffractometer	APEXII Kappa-CCD diffractometer
θ range for data collection	2.560 to 27.515 °
(sinθ/λ)max ($Å^{-1}$)	0.650
h_{min}, h_{max}	-17, 11
k_{min}, k_{max}	-10, 11
l_{min}, l_{max}	-25, 24
Reflections collected / unique	15629 / 5160 [$^aR(int) = 0.0377$]
Reflections [I > 2σ]	4255
Completeness to θ_{max}	0.996
Absorption correction type	multi-scan
Max. and min. transmission	0.769, 0.702
Refinement method	Full-matrix least-squares on F^2
H-atom treatment	H-atom parameters constrained
Data / restraints / parameters	5160 / 0 / 251
Goodness-of-fit	1.051
Final R indices [I>2σ]	$R_1 = 0.0351$, $wR_2 = 0.0924$
R indices (all data)	$R_1 = 0.0477$, $wR_2 = 0.1016$
Largest diff. peak and hole	0.937 and -1.209 e.$Å^{-3}$

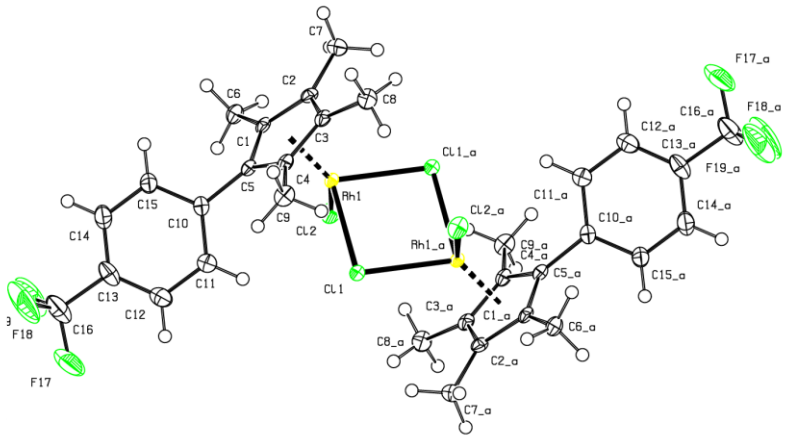

Table 3.7. Crystal Data and Structure for **$[Cp^{TFT}*RhCl_2]_2$** (CCDC2108500).

Empirical formula	$C_{32}H_{32}Cl_4O_6F_6Rh_2$
Formula weight	878.19 g/mol
Temperature	150(2) K
Radiation type	Mo-Ka
Wavelength	0.71073 Å
Crystal system, space group	monoclinic, P $2_{1/c}$
Unit cell dimensions	a = 13.1042(12) Å
b = 20.2106(16) Å	
c = 8.5987(7) Å	
b = 109.070(4) °	
Volume	2152.3(3) $Å^3$
Z, Calculated density	2, 1.355 g/ cm^{-3}
Absorption coefficient	1.058 mm^{-1}
F(000)	872
Crystal size	0.580 x 0.300 x 0.090 mm
Crystal color	orange
Crystal description	board
Diffractometer	APEXII Kappa-CCD diffractometer
θ range for data collection	1.928 to 27.531°
(sinθ/λ)max ($Å^{-1}$)	0.650
h_{min}, h_{max}	-17, 11
k_{min}, k_{max}	-26, 25
l_{min}, l_{max}	-10, 11
Reflections collected / unique	15770 / 4939 [^{a}R(int) = 0.0310]
Reflections [I > 2σ]	4127
Completeness to $θ_{max}$	0.994
Absorption correction type	multi-scan
Max. and min. transmission	0.909, 0.737
Refinement method	Full-matrix least-squares on F^2

H-atom treatment	H-atom parameters constrained
Data / restraints / parameters	4939 / 0 / 203
Goodness-of-fit	1.034
Final R indices [I>2σ]	R_1 = 0.0300, wR_2 = 0.0770
R indices (all data)	R_1 = 0.0388, wR_2 = 0.0821
Largest diff. peak and hole	0.761 and -0.716 e.Å^{-3}

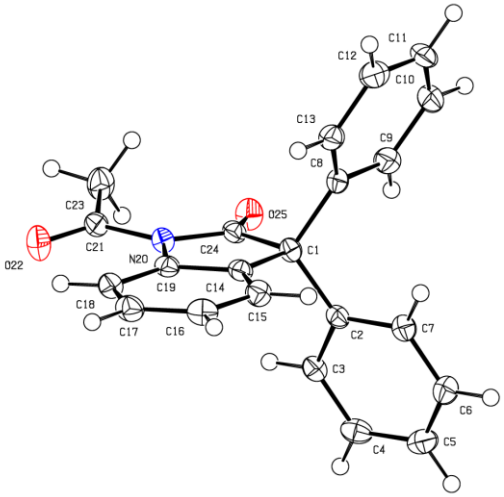

Table 3.8. Crystal Data and Structure for **1** (CCDC2108502).

Empirical formula	$C_{22}H_{17}NO_2$
Formula weight	327.36 g/mol
Temperature	150(2) K
Radiation type	Mo-Ka
Wavelength	0.71073 Å
Crystal system, space group	triclinic, P 1
Unit cell dimensions	a = 8.5179(9) Å
b = 9.3436(9) Å	
c = 11.3934(11)Å	
a = 91.577(3) °	
b = 96.312(4) °	
γ = 114.317(3) °	
Volume	818.66(14) Å^3
Z, Calculated density	2, 1.328 g/ cm^{-3}
Absorption coefficient	0.085 mm^{-1}
F(000)	344
Crystal size	0.450 x 0.310 x 0.240 mm
Crystal color	colorless
Crystal description	prism
Diffractometer	APEXII Kappa-CCD (Bruker-AXS)

θ range for data collection	2.400 to 27.518 °
(sinθ/λ)max ($Å^{-1}$)	0.650
h_{min}, h_{max}	-9, 11
k_{min}, k_{max}	-12, 10
l_{min}, l_{max}	-11, 14
Reflections collected / unique	7906 / 3680 [^{a}R(int) = 0.0215]
Reflections [I > 2σ]	2937
Completeness to θ_{max}	0.975
Absorption correction type	multi-scan
Max. and min. transmission	0.980, 0.905
Refinement method	Full-matrix least-squares on F^2
H-atom treatment	H-atom parameters constrained
Data / restraints / parameters	3680 / 0 / 227
Goodness-of-fit	1.025
Final R indices [I>2σ]	R_1 = 0.0395, wR_2 = 0.0937
R indices (all data)	R_1 = 0.0534, wR_2 = 0.1033
Largest diff. peak and hole	0.309 and -0.223 e.$Å^{-3}$

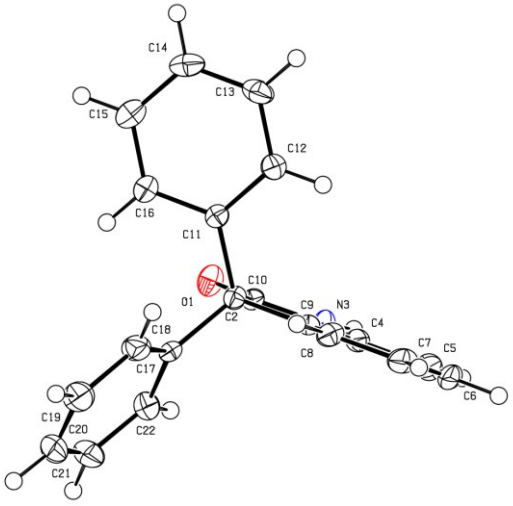

Table 3.9. Crystal Data and Structure for **33** (CCDC2108503).

Empirical formula	$C_{20}H_{15}NO$
Formula weight	285.33 g/mol
Temperature	150(2) K
Radiation type	Mo-Ka
Wavelength	0.71073 Å
Crystal system, space group	monoclinic, P $2_{1/c}$
Unit cell dimensions	a = 8.6609(13) Å
b = 21.515(3) Å	
c = 8.9271(13) Å	

b = 117.830(5) °	
Volume	1471.1(4) $Å^3$
Z, Calculated density	4, 1.288 g/ cm^{-3}
Absorption coefficient	0.079 mm^{-1}
F(000)	600
Crystal size	0.430 x 0.140 x 0.040 mm
Crystal color	colorless
Diffractometer	D8 VENTURE Bruker AXS diffractometer
θ range for data collection	3.201 to 27.435 °
h_{min}, h_{max}	-11, 11
k_{min}, k_{max}	-25, 27
l_{min}, l_{max}	-10, 11
Reflections collected / unique	13622 / 3340 [^{a}R(int) = 0.0555]
Reflections [I > 2σ]	2649
Completeness to $θ_{max}$	0.996
Absorption correction type	multi-scan
Max. and min. transmission	0.997 , 0.831
Refinement method	Full-matrix least-squares on F^2
H-atom treatment	H-atom parameters constrained
Data / restraints / parameters	3340 / 0 / 202
Goodness-of-fit	1.261
Final R indices [I>2σ]	R1 = 0.0905, wR2 = 0.1923
R indices (all data)	R1 = 0.1125, wR2 = 0.2005
Largest diff. peak and hole	0.435 and -0.295 e.$Å^{-3}$

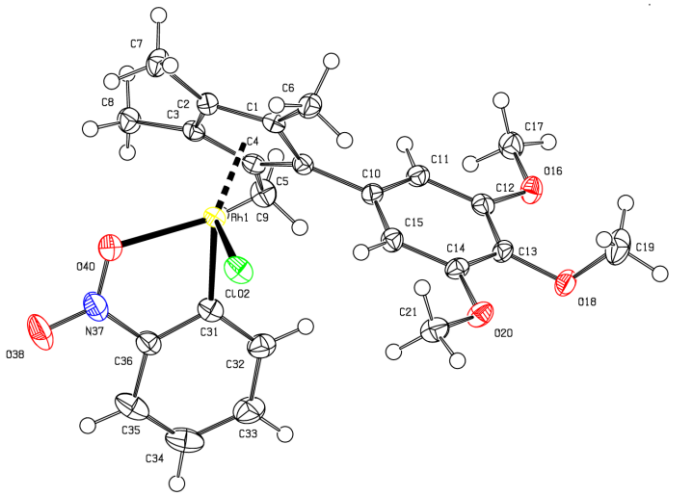

Table 3.10. Crystal Data and Structure for **38a** (CCDC2108504)

Empirical formula	$C_{24}H_{27}ClNO_5Rh$
Formula weight	547.82 g/mol
Temperature	150(2) K

Radiation type	Mo-Ka
Wavelength	0.71073 Å
Crystal system, space group	triclinic, P 1
Unit cell dimensions	a = 7.6846(9) Å
b = 10.5534(10) Å	
c = 17.5685(19) Å	
a = 81.605(3) °	
b = 83.090(4) °	
γ = 69.238(3) °	
Volume	1314.4(2) $Å^3$
Z, Calculated density	2, 1.384 g/ cm^{-3}
Absorption coefficient	0.783 mm^{-1}
F(000)	560
Crystal size	0.310 x 0.170 x 0.040 mm
Crystal color	brown
Crystal description	board
Diffractometer	APEXII Kappa-CCD (Bruker-AXS)
θ range for data collection	1.175 to 27.490 °
(sinθ/λ)max ($Å^{-1}$)	0.649
h_{min}, h_{max}	-9, 9
k_{min}, k_{max}	-9, 13
l_{min}, l_{max}	-22, 22
Reflections collected / unique	21236 / 5964 [^{a}R(int) = 0.0380]
Reflections [I > 2σ]	5143
Completeness to $θ_{max}$	0.990
Absorption correction type	multi-scan
Max. and min. transmission	0.969, 0.7882
Refinement method	Full-matrix least-squares on F^2
H-atom treatment	H-atom parameters constrained
Data / restraints / parameters	5964 / 0 / 296
Goodness-of-fit	0.989
Final R indices [I>2σ]	R_1 = 0.0341, wR_2 = 0.0859
R indices (all data)	R_1 = 0.0425, wR_2 = 0.0911
Largest diff. peak and hole	1.217 and -0.834 e.$Å^{-3}$

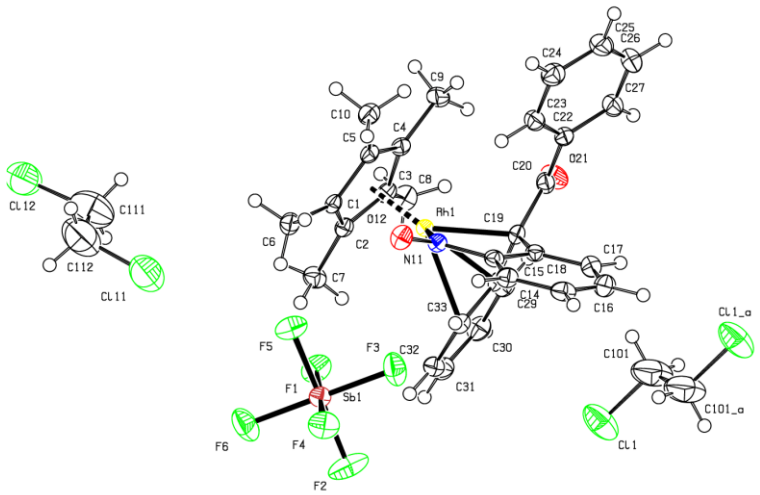

Table 3.11. Crystal Data and Structure for **39b** (CCDC2108506)

Empirical formula	$C_{33}H_{35}Cl_3F_6NO_2RhSb$
Extended formula	$C_{30}H_{29}NO_2Rh$, F_6Sb, 1.5 ($C_2H_4Cl_2$)
Formula weight	922.63 g/mol
Temperature	150(2) K
Radiation type	Mo-Ka
Wavelength	0.71073 Å
Crystal system, space group	triclinic, P 1
Unit cell dimensions	a = 8.8335(10) Å
b = 13.5040(14) Å	
c = 16.1483(18) Å	
a = 68.632(3) °	
b = 76.854(3) °	
γ = 80.257(3) °	
Volume	1738.9(3) $Å^3$
Z, Calculated density	2, 1.762 g/ cm^{-3}
Absorption coefficient	1.546 mm^{-1}
F(000)	914
Crystal size	0.720 x 0.120 x 0.030 mm
Crystal color	brown
Crystal description	board
Diffractometer	APEXII Kappa-CCD (Bruker-AXS)
θ range for data collection	2.378 to 27.506 °
(sinθ/λ)max ($Å^{-1}$)	0.650
h_{min}, h_{max}	-10, 11
k_{min}, k_{max}	-17, 14
l_{min}, l_{max}	-20, 20
Reflections collected / unique	27932 / 7935 [^{a}R(int) = 0.0369]

Reflections [I > 2σ]	6266
Completeness to θ_{max}	0.993
Absorption correction type	multi-scan
Max. and min. transmission	0.955, 0.821
Refinement method	Full-matrix least-squares on F^2
H-atom treatment	H-atom parameters constrained
Data / restraints / parameters	7935 / 0 / 429
Goodness-of-fit	1.014
Final R indices [I>2σ]	R_1 = 0.0338, wR_2 = 0.0788
R indices (all data)	R_1 = 0.0494, wR_2 = 0.0870
Largest diff. peak and hole	0.938 and -1.282 e.Å^{-3}

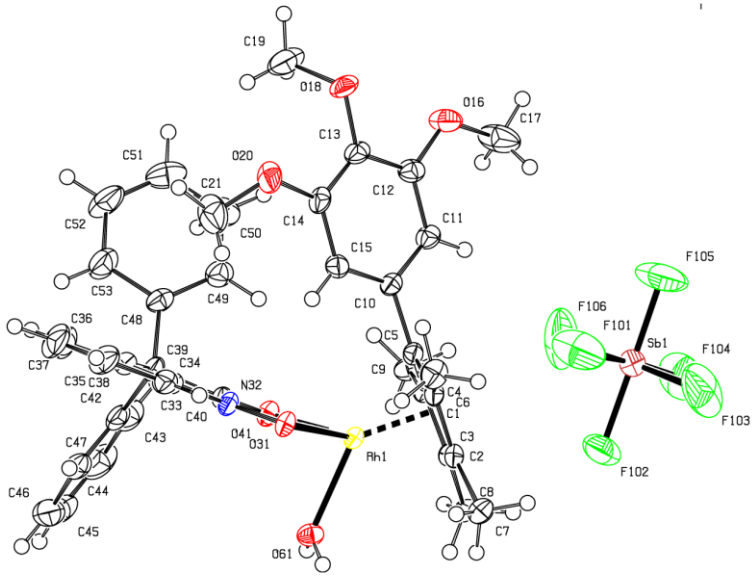

Table 3.12. Crystal Data and Structure for **40** (CCDC2108507)

Empirical formula	$C_{38}H_{39}F_6NO_6RhSb$
Extended formula	$C_{38}H_{39}NO_6Rh$, F_6Sb
Formula weight	944.36 g/mol
Temperature	150(2) K
Radiation type	Mo-Ka
Wavelength	0.71073 Å
Crystal system, space group	monoclinic, P $2_{1/c}$
Unit cell dimensions	a = 14.9385(10) Å
b = 16.1802(11) Å	
c = 18.7410(12) Å	
b = 108.800(3) °	
Volume	4288.2(5) Å^3
Z, Calculated density	4, 1.463 g/ cm^{-3}
Absorption coefficient	1.082 mm^{-1}
F(000)	1888

Crystal size	0.360 x 0.240 x 0.110 mm
Crystal color	yellow
Crystal description	plate
Diffractometer	APEXII Kappa-CCD (Bruker-AXS)
θ range for data collection	1.703 to 27.498 °
$(\sin\theta/\lambda)_{max}$ (Å^{-1})	0.650
h_{min}, h_{max}	-19, 15
k_{min}, k_{max}	-20, 21
l_{min}, l_{max}	-22, 24
Reflections collected / unique	30736 / 9802 [^{a}R(int) = 0.0262]
Reflections [I > 2σ]	7974
Completeness to θ_{max}	0.996
Absorption correction type	multi-scan
Max. and min. transmission	0.888, 0.755
Refinement method	Full-matrix least-squares on F^2
H-atom treatment	H-atom parameters treated by a mixture of independent and constrained refinement
Data / restraints / parameters	9802 / 0 / 491
Goodness-of-fit	1.004
Final R indices [I>2σ]	R_1 = 0.0297, wR_2 = 0.0709
R indices (all data)	R_1 = 0.0422, wR_2 = 0.0769
Largest diff. peak and hole	0.609 and -0.558 e.Å^{-3}

3.7. References

1. Heravi, M. M.; Zadsirjan, V. *RSC Adv.* **2020**, *10*, 44247-44311.
2. Chen, D.; Su, S.-J.; Cao, Y. *J. Mat. Chem. C.* **2014**, *2*, 9565-9578.
3. (a) Stuart, D. R.; Bertrand-Laperle, M.; Burgess, K. M. N.; Fagnou, K. *J. Am. Chem. Soc.* **2008**, *130*, 16474-16475; (b) Stuart, D. R.; Alsabeh, P.; Kuhn, M.; Fagnou, K., *J. Am. Chem. Soc.* **2010**, *132*, 18326-18339; (c) Huestis, M. P.; Chan, L.; Stuart, D. R.; Fagnou, K. *Angew. Chem. Int. Ed.* **2011**, *50*, 1338-1341.
4. For selected examples on Rh(III)-catalyzed C–H bond annulation, see: (a) Su, Y.; Zhao, M.; Han, K.; Song, G.; Li, X. *Org. Lett.* **2010**, *12*, 5462-5465; (b) Wang, C.; Sun, H.; Fang, Y.; Huang, Y. *Angew. Chem. Int. Ed.* **2013**, *52*, 5795-5798; (c) Zhao, D.; Shi, Z.; Glorius, F. *Angew. Chem. Int. Ed.* **2013**, *52*, 12426-12429; (d) Liu, B.; Song, C.; Sun, C.; Zhou, S.; Zhu, J. *J. Am. Chem. Soc.* **2013**, *135*, 16625-16631; (e) Yang, Y.; Wang, X.; Li, Y.; Zhou, B. *Angew. Chem. Int. Ed.* **2015**, *54*, 15400-15404; (f) Li, X.; Li, X.; Jiao, N. *J. Am. Chem. Soc.* **2015**, *137*, 9246-9249; (g) Font, M.; Cendón, B.; Seoane, A.; Mascareñas, J. L.; Gulías, M. *Angew. Chem. Int. Ed.* **2018**, *57*, 8255-8259; (h) Özkaya, B.; Bub, C. L.; Patureau, F. W. *Chem.*

Commun. **2020**, *56*, 13185-13188; (i) Singh, A.; Shukla, R. K.; Volla, C. M. R. *Chem. Sci.* **2022**, *13*, 2043-2049.

5. Zhang, X.; Qi, Z.; Li, X. *Angew. Chem. Int. Ed.* **2014**, *53*, 10794-10798.
6. Dateer, R. B.; Chang, S. *J. Am. Chem. Soc.* **2015**, *137*, 4908-4911.
7. Yan, H.; Wang, H.; Li, X.; Xin, X.; Wang, C.; Wan, B. *Angew. Chem. Int. Ed.* **2015**, *54*, 10613-10617.
8. (a) Li, B.; Xu, H.; Wang, H.; Wang, B. *ACS Catal.* **2016**, *6*, 3856-3862; (b) Huang, X.; Liang, W.; Shi, Y.; You, J. *Chem. Commun.* **2016**, *52*, 6253-6256.
9. Palav, A.; Misal, B.; Ernolla, A.; Parab, V.; Waske, P.; Khandekar, D.; Chaudhary, V.; Chaturbhuj, G. *Org. Process Res. Dev.* **2019**, *23*, 244-251.
10. (a) Greish, A. *Rus. Chem. J.* **2004**, *48*, 92-104; (b) Yan, G.; Yang, M. *Org. Biomol. Chem.* **2013**, *11*, 2554-2566; (c) Koskin, A. P.; Mishakov, I. V.; Vedyagin, A. A. *Resour. Technol.* **2016**, *2*, 118-125; (d) Calvo, R.; Zhang, K.; Passera, A.; Katayev, D. *Nat. Commun.* **2019**, *10*, 3410.
11. (a) Caron, L.; Campeau, L.-C.; Fagnou, K. *Org. Lett.* **2008**, *10*, 4533-4536; (b) Tan, E.; Montesinos-Magraner, M.; García-Morales, C.; Mayans, J. G.; Echavarren, A. M. *Chem. Sci.* **2021**, *12*, 14731-14739.
12. For selected examples of formation and reactivities of nitrosoarenes, see: (a) Jana, N.; Zhou, F.; Driver, T. G. *J. Am. Chem. Soc.* **2015**, *137*, 6738-6741; (b) Shevlin, M.; Guan, X.; Driver, T. G. *ACS Catal.* **2017**, *7*, 5518-5522; (c) Zhou, F.; Wang, D.-S.; Guan, X.; Driver, T. G. *Angew. Chem. Int. Ed.* **2017**, *56*, 4530-4534; (d) Ford, R. L.; Alt, I.; Jana, N.; Driver, T. G. *Org. Lett.* **2019**, *21*, 8827-8831, (e) Shimizu, H.; Yoshinaga, K.; Yokoshima, S. *Org. Lett.* **2021**, *23*, 2704-2709.
13. For selected examples to prepare oxindoles, see: (a) Overman, L. E.; Poon, D. J. *Angew. Chem. Int. Ed.* **1997**, *36*, 518-521; (b) Ashimori, A.; Bachand, B.; Calter, M. A.; Govek, S. P.; Overman, L. E.; Poon, D. J. *J. Am. Chem. Soc.* **1998**, *120*, 6488-6499; (c) Marti, C.; Carreira, Erick M. *Eur. J. Org. Chem.* **2003**, 2209-2219; (d) Galliford, C. V.; Scheidt, K. A. *Angew. Chem. Int. Ed.* **2007**, *46*, 8748-8758; (e) Duguet, N.; Slawin, A. M. Z.; Smith, A. D. *Org. Lett.* **2009**, *11*, 3858-3861; (f) Çelebi-Ölçüm, N.; Lam, Y.-h.; Richmond, E.; Ling, K. B.; Smith, A. D.; Houk, K. N. *Angew. Chem. Int. Ed.* **2011**, *50*, 11478-11482.
14. Piou, T.; Romanov-Michailidis, F.; Romanova-Michaelides, M.; Jackson, K. E.; Semakul, N.; Taggart, T. D.; Newell, B. S.; Rithner, C. D.; Paton, R. S.; Rovis, T. *J. Am. Chem. Soc.* **2017**, *139*, 1296-1310.
15. Shibata, Y.; Tanaka, K. *Angew. Chem. Int. Ed.* **2011**, *50*, 10917-10921.
16. Wodrich, M. D.; Ye, B.; Gonthier, J. F.; Corminboeuf, C.; Cramer, N. *Chem. Eur. J.* **2014**, *20*, 15409-15418.

17. The electronic properties can be estimated from the redox potentials of Rh complexes.
18. For the F effect in C–H bond functionalization, see: (a) Lafrance, M.; Rowley, C. N.; Woo, T. K.; Fagnou, K. *J. Am. Chem. Soc.* **2006**, *128*, 8754-8756; (b) Yan, T.; Zhao, L.; He, M.; Soulé, J.-F.; Bruneau, C.; Doucet, H. *Adv. Synth. Catal.* **2014**, *356*, 1586-1596; (c) He, M.; Soulé, J.-F.; Doucet, H. *Chem. Cat. Chem.* **2015**, *7*, 2130-2140; (d) Obligacion, J. V.; Bezdek, M. J.; Chirik, P. J. *J. Am. Chem. Soc.* **2017**, *139*, 2825-2832; (e) Boyaala, R.; Touzani, R.; Roisnel, T.; Dorcet, V.; Caytan, E.; Jacquemin, D.; Boixel, J.; Guerchais, V.; Doucet, H.; Soulé, J.-F. *ACS Catal.* **2019**, *9*, 1320-1328.
19. (a) Bariwal, J.; Voskressensky, L. G.; Van der Eycken, E. V. *Chem. Soc. Rev.* **2018**, *47*, 3831-3848; (b) Pradhan, S.; De, P. B.; Shah, T. A.; Punniyamurthy, T. *Chem. Asian J.* **2020**, *15*, 4184-4198.
20. Vicente, J.; Abad, J. A.; Lahoz, F. J.; Plou, F. J. *J. Chem. Soc., Dalton Trans.* **1990**, 1459-1462.
21. Lee, B. H.; Biswas, A.; Miller, M. J. *J. Org. Chem.* **1986**, *51*, 106-109.
22. Delayre, B.; Wang, Q.; Zhu, J. *ACS Cent. Sci.* **2021**, *7*, 559-569.
23. Morris, D. M.; McGeagh, M.; De Peña, D.; Merola, J. S. *Polyhedron* **2014**, *84*, 120–135.
24. Mio, M. J.; Kopel, L. C.; Braun, J. B.; Gadzikwa, T. L.; Hull, K. L.; Brisbois, R. G.; Markworth, C. J.; Grieco, P. A. *Org. Lett.* **2002**, *4,* 3199–3202.
25. Jia, X.; Petrone, D. A.; Lautens, M. *Angew. Chem. Int. Ed.* **2012**, *51*, 9870–9872.
26. Kumar, A.; Tadigoppula, N. *Org. Lett.* **2021**, *23*, 8–12.
27. Jones, D. J.; Purushothaman, B.; Ji, S.; Holmes, A. B.; Wong, W. W. H. *Chem. Commun.* **2012**, *48*, 8066–8068.
28. Wilson, K. L.; Kennedy, A. R.; Murray, J.; Greatrex, B.; Jamieson, C.; Watson, A. J. B. *Beilstein J. Org. Chem.* **2016**, *12*, 2005–2011.
29. Yang, J.; Chen, M.; Ma, J.; Huang, W.; Zhu, H.; Huang, Y.; Wang, W. *J. Mater. Chem. C.* **2015**, *39*, 10074–10078.
30. Miao, Y.; Dupé, A.; Bruneau, C.; Fischmeister, C. *Eur. J. Org. Chem.* **2014**, *23,* 5071–5077
31. Gu, S.; Chen, W. *Organometallics* **2009**, *28*, 909–914.
32. Aizawa, K.; Nakagawa, H.; Matuso, K.; Kawai, K.; Ieda, N.; Suzuki, T.; Miyata, N. *Bioorg. Med. Chem. Lett.* **2013**, *1,* 2340–2343.
33. Kitching, W.; Glenn, M. *Sci. Synth.* **2004**, *1*,133–301.

Chapter 4. Rh(III)/Ag(I)-Catalyzed *ortho*-Heteroarylation of Amide at Room-Temperature *via* C–H/C–H Bonds Couplings

4.1. Introduction

Aryl-heteroarenes are important scaffolds since they are widely found in biological compounds, pharmaceuticals, and organic materials.[1] Therefore, developing new synthetic routes has raised attention in the organic synthesis community. Although cross-coupling reactions are still mainly used, direct C−H bond activation/functionalization has emerged as a powerful tool in a viewpoint of step- and atom- economy.[2] Over the years, different groups reported many examples of *ortho*-C−H arylation of heteroarenes using transition metal catalysts such as Pd, Rh, Ir, Ru, Cu or Ni.[3-10] Despite meaningful advances in the field, these methodologies often involve harsh reaction conditions with elevated temperatures (over 120 °C) due to the low reactivity of C−H bonds which might limit the scope of functional groups. Moreover, haloarenes are often involved as arylating sources, and/or significant excess of the coupling partner is required. Therefore, developing milder conditions to perform double C−H bond activation is highly desirable because, expressively, only "H_2" is generated as "waste".

In 2012, Glorius and co-workers reported the twofold Rh(III)-catalyzed C−H bond functionalization between benzamides and bromoarenes providing an efficient pathway to form aryl-aryl bond.[11] This strategy was extended to heteroarenes although the scope of coupling partners remains narrow (Scheme 4.1-a).[12] On the other hand, You and co-workers succeeded in developing the C2-arylation of heteroarenes through Rh(III)-catalyzed oxidative C−H/C−H cross-coupling reactions with *N*-heteroaryl arenes as aryl sources. The reaction is operative with a wide range of directing groups such as quinoline, pyridine, pyrimidine, pyrazole[13], pivalamido group[14], oxime ether group[15] and *N*-nitroso group.[16] Later on, the same group put efforts into the development of an efficient method using $[Cp^*IrCl_2]_2$ as the catalyst to undergo *ortho*-C−H bond heteroarylation of arenes with 16 directing groups ranging from primary to tertiary amides, oxime ether, *N*-heteroaryl to ketones and enamides.[17] In this work, $[Cp^*RhCl_2]_2$ was also employed in comparative studies and could undergo C−H bond activation between arenes and thiophenes derivatives, although high temperature was required (Scheme 4.1-b). The same year, Larrosa and co-workers reported the first example of Pd/Ag-mediated C−H activation of benzo[*b*]thiophenes with aryl-iodide under mild conditions.[18] This methodology proved to be efficient at near room temperature with a switch of the regioselectivity on benzo[*b*]thiophenes depending on Pd catalyst loading. At a low concentration of Pd, silver salts carry out the C−H activation in the C2 position of benzo[*b*]thiophenes, whereas the C3 selective C−H activation occurred with higher loading of Pd catalyst (Scheme 4.1-c). Inspired by these strategies, we envisioned the regioselective C−H

heteroarylation of benzamide under mild conditions using Rh(III) as catalyst in presence of silver salts. Following the previous works by Rovis[19], Tanaka[20] and Cramer[21] on the modification of Cp ligand to boost the catalytic activities of Rh(III) complexes in C–H bond activation, we also wanted to compare the catalytic activities of an array of $[Cp^{R}RhCl_2]_2$ complexes in such C–H/C–H bond couplings. In contrast with the previous methodologies employing benzamide as a directing group, this reaction proceeds at room temperature in the presence of Rh(III) complex as catalyst and silver salts to generate aryl-heteroarene scaffolds (Scheme 4.1-d). Furthermore, the reduction of secondary amide to a primary amide was examined for Cu-catalyzed C−H/N−H coupling to access more sophisticated *N*-heterocycles.[22]

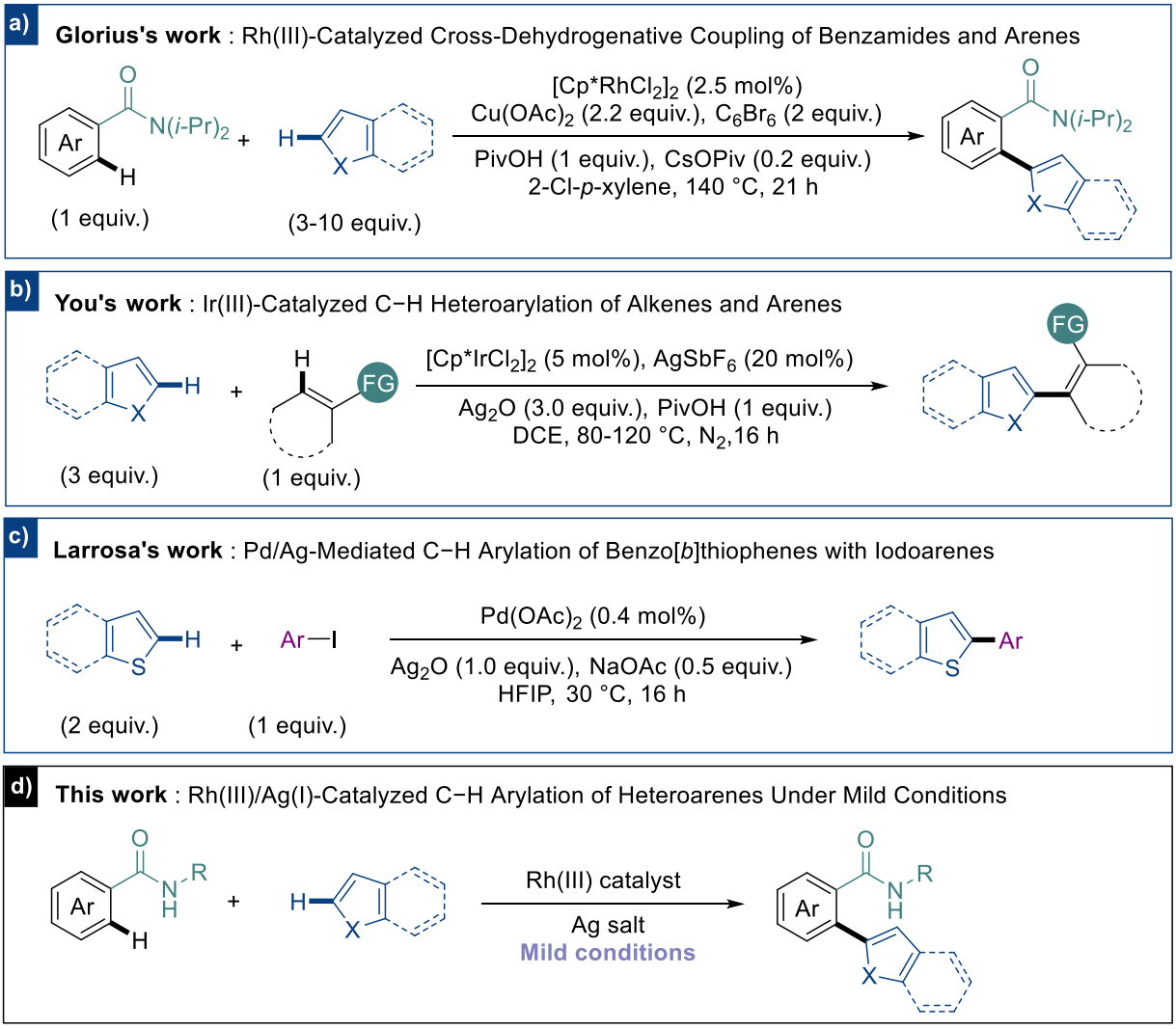

Scheme 4.1. Aryl-Heteroaryl Synthesis.

4.2. Results and Discussion

4.2.1. Optimization of the Reaction Conditions

N-*tert*-butyl benzamide **1a** and benzo[*b*]thiophene **2a** were selected as model substrates to begin our investigation. We evaluated the conditions using $[Cp^*RhCl_2]_2$ as the catalyst, 2 equivalents of Ag_2O as oxidant, and 0.5 equivalents of $Zn(OTf)_2$ as an additive in THF/HFIP under an argon atmosphere. The reaction was carried out at 100 °C over 24 h and provided the desired compound **3a** as a single regioisomer in 86% yield (Table 4.1, entry 1). Although satisfactory yield was obtained at 100 °C, we evaluated a series of Rh(III) catalysts using milder conditions. Indeed, the nature of the cyclopentadienyl ligand can highly impact the regioselectivity and the reactivity of C−H activation reactions, as demonstrated by our group and others.[23–27] The reaction was repeated with $[Cp^*RhCl_2]_2$ at 35 °C generating the desired product in 10% yield (Table 4.1, entry 2). Next, isopropylcyclopentadienyl ligand (Cp^{iPr}*) was employed and presented similar reactivity to Cp* (Table 4.1, entry 3). We evaluated the reaction employing the electron-deficient Cp^E ligand, which showed poor reactivity providing a 1:2 mixture of **3a** and **3a'** in 13% yield (Table 4.1, entry 4). Cyclohexyl-fused cyclopentadienyl ligand (Cp^{Cy}) reacted poorly providing **3a** in only 12% yield with a low conversion of the starting materials (Table 4.1, entry 5). Next, we evaluated a set of elliptical-shaped cyclopentadienyl ligands we had previously developed. A bulkier system can be provided by incorporating different substituents on the aryl ring and electron density can be tuned. As a result, a combination of these two parameters can lead to better reactivity. We evaluated the reactivity of an electron-withdrawing group on the aryl ring of the cyclopentadienyl ligand. Trifluorotoluene cyclopentadienyl ligand (Cp^{TFT}*) provided product **3a** in modest yield (Table 4.1, entry 6). Methoxyphenyl cyclopentadienyl ligand (Cp^{MP}*) increased the reactivity to 38% yield (Table 4.1, entry 7). The best result was obtained with trimethoxyphenyl cyclopentadienyl ligand (Cp^{TMP}*), allowing the formation of **3a** in 55% yield (Table 4.1, entry 8). With these promising results, we continued our investigation by screening the reaction conditions. It was noticed that the reaction could occur in THF with a slightly lower yield. This could be explained by the fact that HFIP might improve the solubility of $Zn(OTf)_2$. A more prolonged reaction time resulted in a complete conversion of the starting materials, and the desired product **3a** was successfully obtained in 80% isolated yield after 40 h hours of reaction only in HFIP (Table 4.1, entry 9).

Table 4.1. Influence of Cyclopentadienyl Ligands on the Reaction.

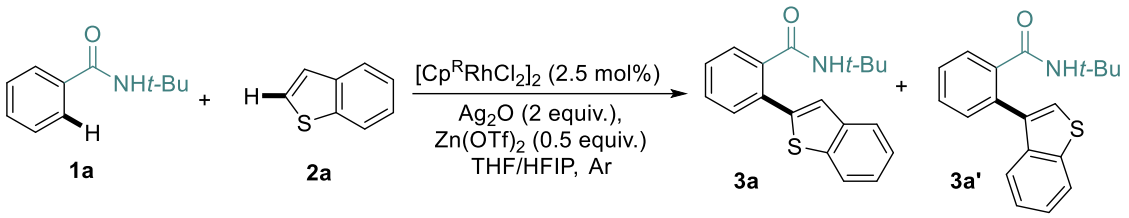

Entry	Cp^R	T°(C)	Time (h)	Yield **3a** (%)
1	Cp*	100	24	86
2	Cp*	35	24	10
3	Cp^{iPr}*	35	24	12
4	Cp^E	35	24	13[a]
5	Cp^{Cy}	35	24	12
6	Cp^{TFT}*	35	24	15
7	Cp^{MP}*	35	24	38
8	Cp^{TMP}*	35	24	55
9	Cp^{TMP}*	35	40	83 (80)[b]

Reaction conditions: **1a** (35.4 mg, 0.2 mmol, 1 equiv.), **2a** (32.2 mg, 0.24 mmol, 1.2 equiv.), Rh(III) cat. (0.005 mmol, 2.5 mol%), Ag_2O (92.6 mg, 0.4 mmol, 2 equiv.), $Zn(OTf)_2$ (36.3 mg, 0.1 mmol, 0.5 equiv.) in THF/HFIP (0.2 mL, 1:1). Yields were determined by ^1H NMR analysis using iodomethane as an internal standard. [a]Mixture of **3a** and **3a'** in 1:2 ratio. [b]Reaction was set up in HFIP. Isolated Yield is shown in parentheses.

4.2.2. Control Experiments

Control experiments were done to investigate the role of silver salt and additive. First, it was noted that the silver was primordial to roll out the reaction. No product was detected in the absence of silver oxide under argon or oxygen atmosphere (Table 4.2, entries 2 and 3). Replacing silver oxide with copper acetate failed to provide the desired compound **3a** (Table

4.2, entry 4). A 1:1 mixture of C2 and C3-arylated benzo[*b*]thiophenes **3a** and **3a'** was observed when the number of equivalents of silver oxide decreased from 2 equivalents to 0.2 equivalents with a significant drop of the reactivity (Table 4.2, entry 5). Then, several silver salts were tested, revealing that silver oxide was the most efficient. Silver carbonate also promoted the reaction, albeit in a lower yield (Table 4.2, entry 6). However, no product was detected in the presence of silver triflate (Table 4.2, entry 7). No conversion was observed when the reaction was carried out without $Zn(OTf)_2$ (Table 4.2, entry 8). When $Cu(OTf)_2$ was employed as an additive, a very low reactivity was observed (Table 4.2, entry 9).

Table 4.2. Control Experiments of Ag/OTf sources.

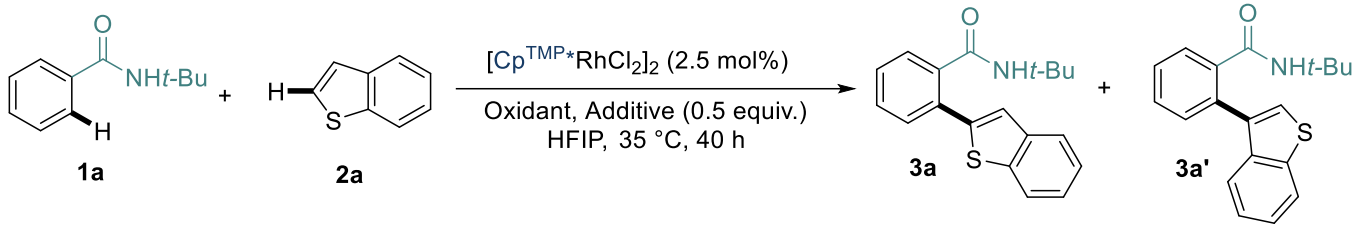

Entry	Oxidant (n equiv.)	Additive	Yield **3a** (%)
1	Ag_2O (2)	$Zn(OTf)_2$	83
2	-	$Zn(OTf)_2$	n.d.
3	O_2	$Zn(OTf)_2$	n.d.
4	$Cu(OAc)_2$ (2)	$Zn(OTf)_2$	n.d.
5	Ag_2O (0.2)	$Zn(OTf)_2$	16[a]
6	Ag_2CO_3 (2)	$Zn(OTf)_2$	45
7	AgOTf (2)	-	n.d.
8	Ag_2O (2)	-	n.d.
9	Ag_2O (2)	$Cu(OTf)_2$	8

Reaction conditions: **1** (0.2 mmol, 1 equiv.), **2** (0.24 mmol, 1.2 equiv.), $[Cp^{TMP}*RhCl_2]_2$ (4.6 mg, 0.005 mmol, 2.5 mol%), oxidant, additive, in HFIP at 35 °C. Yields were determined by ^1H NMR analysis using iodomethane as an internal standard. [a]Mixture of **3a** and **3a'** in 1:1 ratio.

4.2.3. Scope of the Reaction

With the optimized conditions in hand, we explored the scope of the reaction. Firstly, we investigated the reactivity of different functionalized benzamides (Scheme 4.2). Different amides were examined to undergo the C−H activation at the C2-position of benzo[*b*]thiophene. Benzamides holding a long aliphatic *N*-substituent (*N*-Hex or *N*-Dec) provided desired products **3b** and **3c** in 62% and 55% yield, respectively. Reaction from *N*-(2-methoxyethyl)benzamide afforded α-arylated benzo[*b*]thiophene **3d** in 70% yield. The reaction performed from *N*-(cyclohexylmethyl)benzamide delivered the desired product **3e** in 72% yield. *N*-benzyl benzamide is also a suitable coupling partner for this C–H/C–H bond coupling as **3f** was isolated in 75% yield. Next, the substituent effect on the aryl group of *N*-(*tert*-butyl)benzamide was examinated. *Para*-decorated benzamides with electron-rich groups such as methoxy or methyl were well tolerated providing the corresponding products **3g** and **3h** in 88% and 85% yield. Benzamide bearing halogen atoms such as bromine and chlorine at the *para*-position also reacted to give the desired products **3i** and **3j** with high regioselectivity in good yields. Interestingly, the C−Br and C−Cl bonds did not react under these conditions, allowing further Pd-catalyzed cross-coupling reactions to access a broader molecular diversity. *N*-(*tert*-butyl)benzamide with a methyl substituent at the *meta*-position also showed a good reactivity giving **3k** in 75% yield. Notably, the C−H bond activation only occurred at the less sterically hindered position without generating other regioisomers. *Ortho*-substituted benzamides with methyl and fluorine are also tolerated giving the corresponding products **3l** and **3m** in moderate yields. A lower conversion was observed due to the steric hindrance of functional group at the *ortho*-position. Unfortunately, *N*-(*tert*-butyl)-2-iodobenzamide was not compatible for the reaction as the insertion into the carbon-halogen bond proceeded faster. Reaction from 2,4-difluorobenzamide afforded the compound **3n** as a single regioisomer in 66% yield.

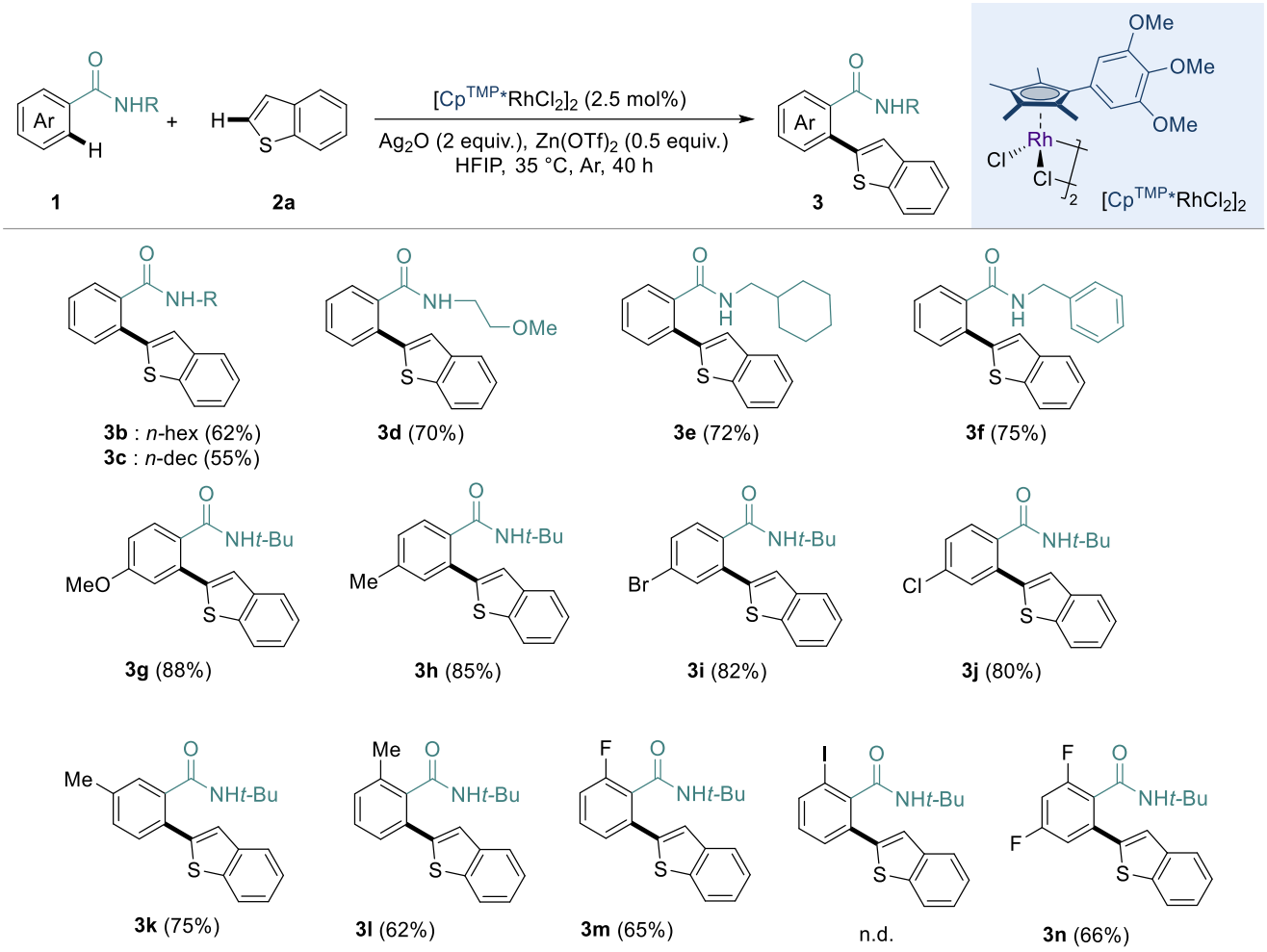

Reaction conditions: **1** (0.3 mmol, 1 equiv.), **2a** (48.3 mg, 0.36 mmol, 1.2 equiv.), $[Cp^{TMP*}RhCl_2]_2$ (6.9 mg, 0.0075 mmol, 2.5 mol%), Ag_2O (139.0 mg, 0.6 mmol, 2 equiv.), $Zn(OTf)_2$ (54.5 mg, 0.15 mmol, 0.5 equiv.) in HFIP (0.3 mL) at 35 °C.

Scheme 4.2. Scope of Benzamides in Rh(III)/Ag(I)-Catalyzed C–H Arylation of Heteroarenes Under Mild Conditions.

Next, we turned our attention to the scope of the heteroarene partners. 2-Substituted thiophenes reacted at the C5-position providing the corresponding products in high yields. The reaction was compatible with several functional group such as methyl affording **3o** in 78% yield. Electron-withdrawing cyano group was investigated and provided **3p** in 62% yield. Ketone and ester functions were suitable for the reaction giving **3q** and **3r** in 78% and 80% yields. 2,3-Di-substituted thiophenes with methyl ester and methyl/chloride substituents smoothly reacted to provide **3s** and **3t** in high yields. 2-Acetyl-3-chlorothiophene provided the corresponding bi(hetero)aryl compound **3u** in 85% yield. Finally, the *ortho*-heteroarylation of benzamide with furan afforded the corresponding compound **3v** in 65% yield.

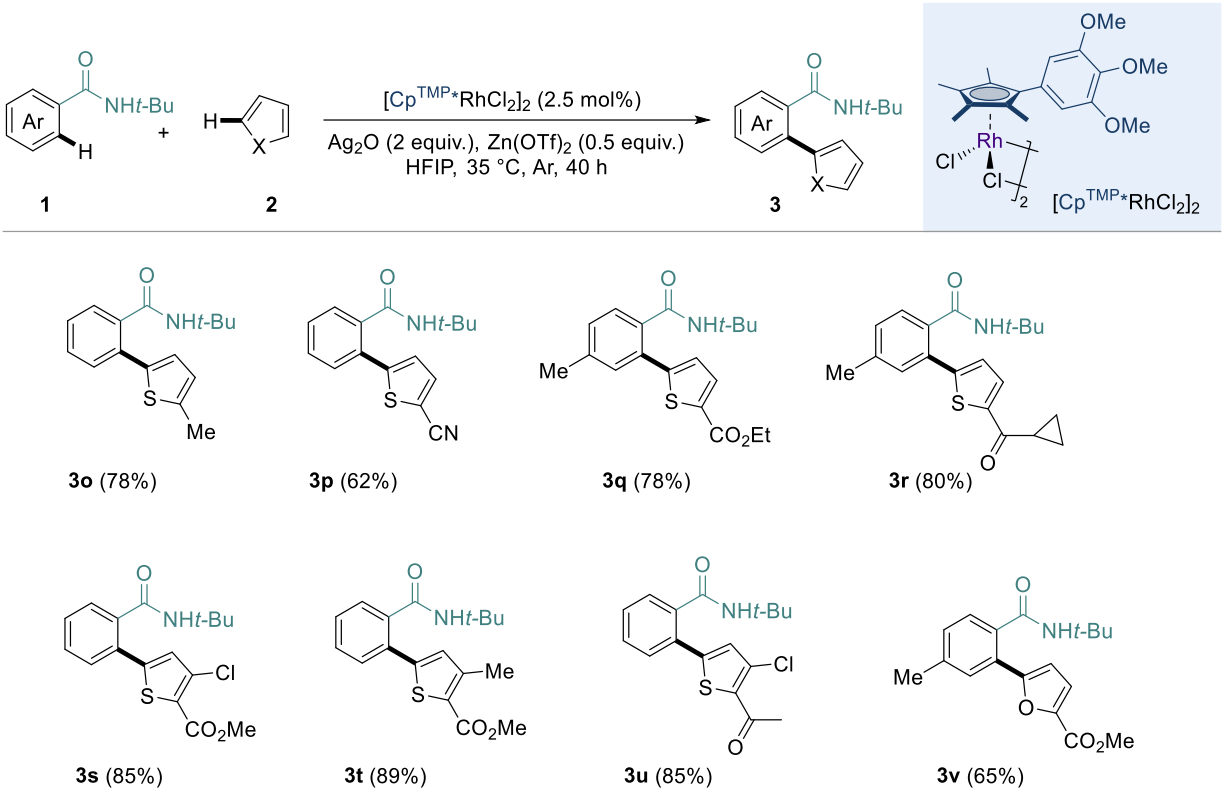

Reaction conditions: **1** (0.3 mmol, 1 equiv.), **2** (0.36 mmol, 1.2 equiv.), $[Cp^{TMP}*RhCl_2]_2$ (6.9 mg, 0.0075 mmol, 2.5 mol%), Ag_2O (139.0 mg, 0.6 mmol, 2 equiv.), $Zn(OTf)_2$ (54.5 mg, 0.15 mmol, 0.5 equiv.) in HFIP (0.3 mL) at 35 °C.

Scheme 4.3. Scope of Heteroarenes in Rh(III)/Ag(I)-Catalyzed C–H Heteroarylation of Benzamides Under Mild Conditions.

4.2.4. Access to 3,4-Fused Isoquinolin-1-*(2H)*-one Scaffold

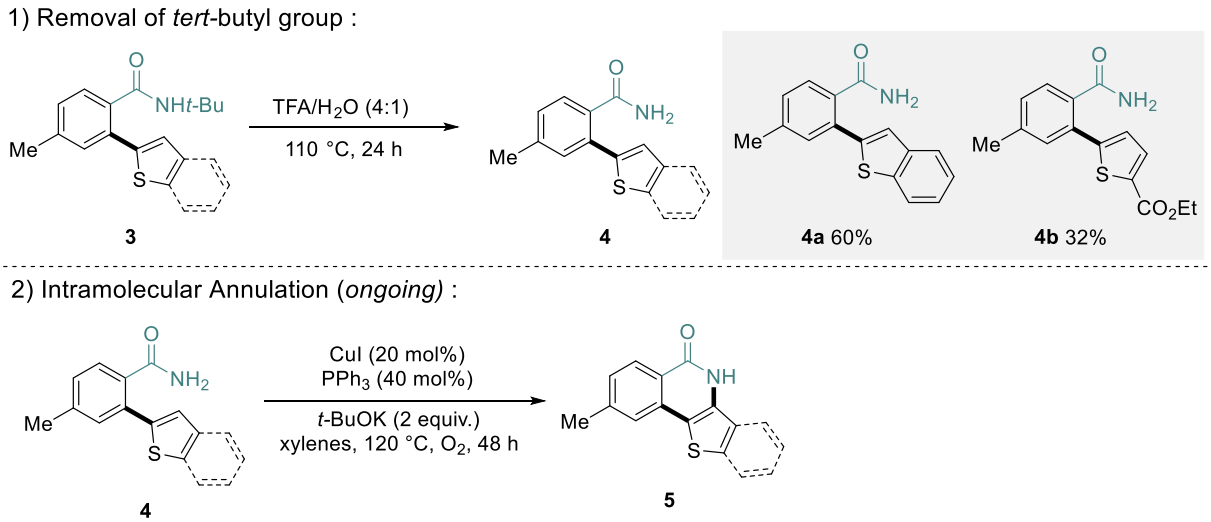

Scheme 4.4. Synthetic Transformations.

To highlight the synthetic value of this novel reaction, we conducted post-functionalization to access 3,4-fused isoquinolin-1-(*2H*)-one scaffold (Scheme 4.4). These motifs can be found in many applications as precursors for materials such as solar cells or building blocks in biologically active compounds.[28] Primary amides can be obtained in moderate yields after removal of the *tert*-butyl group in the presence of trifluoroacetic acid at 110 °C. Intramolecular C3−H/N−H coupling reaction is currently ongoing using CuI (20 mol%) as catalyst associated with PPh_3 (40 mol%) as a ligand in the presence of *t*-BuOK (2 equivalents) as the base in xylenes to deliver the desired 3,4-fused isoquinolin-1-*2H*-one derivatives.

4.3. Proposed Mechanism

We propose the following mechanism based on our observations and previous literature on Rh(III) catalyzed C−H heteroarylation[16,29] and the role of Ag(I) for C–H bond activation (Figure 4.1).[30] First, the active catalytic specie [Cp^{TMP}*Rh(III)] complex **I** is formed in presence of $Zn(OTf)_2$. Then, the carbonyl group of the benzamide derivative **1** coordinates to the Rh center to form the neutral five-membered rhodacycle complex **II** after C−H bond cleavage *via* a concerted metalation – deprotonation (CMD) mechanism with the release of HOTf. In the meantime, Ag promoted the C–H bond cleavage of the heteroarene **2** giving the Ag-heteroarene intermediate **III,** which can undergo transmetalation at [Cp^{TMP*}Rh(III)] to form complex **IV**. Finally, the Rh(III)Cp^{TMP}* complex **IV** release the desired product **3** after reductive elimination followed by reoxidation of the Rh(I)Cp^{TMP}* specie **V** by Ag(I) salts.

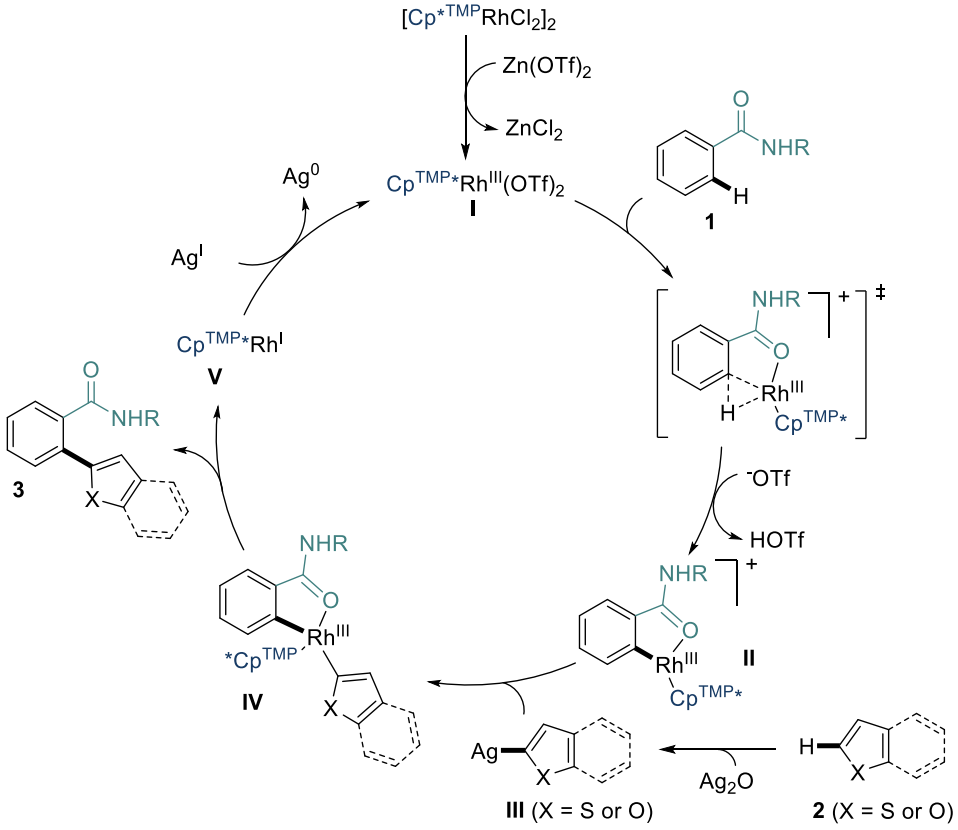

Figure 4.1. Proposed Mechanism Pathway.

4.4. Conclusion

In summary, we have developed an novel Rh(III)/Ag(I)-catalyzed twofold C–H bond functionalization between benzamides and heteroarenes. Different secondary amides could undergo the arylation of benzo[*b*]thiophene derivatives, thiophenes, and furans. The electron-rich elliptical-shaped $[Cp^{TMP}*RhCl_2]_2$ complex smoothly provides bi-heteroaryl compounds under mild conditions at near room temperature in the presence of Ag_2O and $Zn(OTf)_2$. A broad scope of substrates was achieved with good functional group tolerance at the *para-, meta-* and *ortho*-positions on benzamides. Mono- and di-substituted thiophenes and furans were also suitable for the reactions. Mechanistic studies and deuterium labeling experiments will be proceeded to disclose the mechanism pathway. Ongoing work seeks to apply this methodology for new Rh(III) C–H bond activation and annulation reactions.

4.5. Experimental Data

4.5.1. General Information

All reactions were carried out under argon atmosphere with standard Schlenk techniques. All reagents were obtained from commercial sources and used as supplied unless stated otherwise. ^{1}H NMR spectra were recorded on Bruker AV III 400 MHz spectrometer fitted with a BBFO probe. Chemical shifts (δ) were reported in parts per million relatives to residual chloroform (7.26 ppm for ^{1}H, 77.16 ppm for ^{13}C). Coupling constants were reported in Hertz. ^{1}H NMR assignment abbreviations were the following: broad singlet (bs), singlet (s), doublet (d), triplet (t), quartet (q), doublet of doublets (dd), doublet of triplets (dt), multiplet (m). ^{13}C NMR spectra were recorded at 101 MHz on the same spectrometer and reported in ppm. ^{19}F NMR spectra were recorded at 376 MHz on the same spectrometer and reported in ppm.

Column chromatography was carried out on a Teledyne ISCO CombiFlash NextGen 300 using FlashPure silica flash columns (4, 12, 25 g; 35–45 µm). Substrates were purified using petroleum ether and ethyl acetate on a gradient of 100:0 to 0:100 with flow rates of 13 – 400 mL/min depending on the size of column and ΔRf.

Cyclopentadienyl ligands Cp^{MP}*,[19] Cp^{Cy},[19] Cp^{E},[20] Cp^{iPr}*,[31] Cp^{TFT}*,[32] Cp^{DMP}*,[32] rhodium(III) complexes $[Cp^{MP}*RhCl_2]_2$,[19] $[Cp^{Cy}RhCl_2]_2$,[19] $[Cp^{E}RhCl_2]_2$,[2] $[Cp^{iPr}*RhCl_2]_2$,[31] $[Cp^{TFT}*RhCl_2]_2$,[32] $[Cp^{DMP}*RhCl_2]_2$,[32] were already reported and prepared according to the literature.

4.5.2. General Procedure for the Synthesis of Benzamides Derivatives 1a-1m and Compounds Characterization

Procedure: A 100 mL round-bottom flask was charged with CH_2Cl_2 (10 mL), Et_3N (1 mL, 7 mmol, 1.4 equiv.) and amine (6 mmol, 1.2 equiv.). Then the reaction was cooled to 0 °C. Benzoyl chloride (5 mmol, 1 equiv.) was added dropwise and the reaction was allowed to warm up to room temperature and stirred over 8 h. The reaction mixture was quenched with 10 mL of 1 N HCl and was extracted with CH_2Cl_2 (10 mL x 3). The organic layers were combined, dried over $MgSO_4$ and concentrated to provide the product. Benzamides derivatives were used directly without purification.

***N*-(*Tert*-butyl)benzamide (1a)**

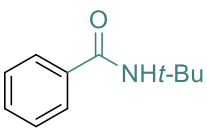

Following the general procedure using benzoyl chloride (0.6 mL, 5 mmol, 1 equiv.) and *tert*-butylamine (0.63 mL, 6 mmol, 1.2 equiv.), the product was directly used without purification.

^{1}H NMR (400 MHz, $CDCl_3$) δ (ppm) 7.72 – 7.69 (m, 2H), 7.46 – 7.35 (m, 3H), 5.99 (bs, 1H), 1.46 (s, 9H).

^{13}C NMR (101 MHz, $CDCl_3$) δ (ppm) 167.0, 136.0, 131.1, 128.5, 126.8, 51.7, 29.0.

***N*-Hexylbenzamide (1b)**

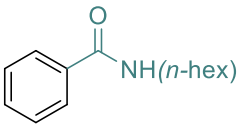

Following the general procedure using benzoyl chloride (0.6 mL, 5 mmol, 1 equiv.) and *n*-hexylamine (0.8 mL, 6 mmol, 1.2 equiv.), the product was directly used without purification.

^{1}H NMR (400 MHz, $CDCl_3$) δ (ppm) 7.77 – 7.74 (m, 2H), 7.44 – 7.39 (m, 1H), 7.36 – 7.31 (m, 2H), 6.76 (bs, 1H), 3.39 – 3.34 (m, 2H), 1.59 – 1.51 (m, 2H), 1.34 – 1.23 (m, 6H), 0.86 – 0.83 (m, 3H).

^{13}C NMR (101 MHz, $CDCl_3$) δ (ppm) 167.7, 134.9, 131.2, 128.4, 127.0, 40.2, 31.5, 29.6, 26.7, 22.6, 14.0.

***N*-Decylbenzamide (1c)**

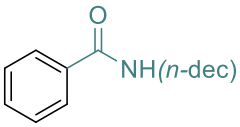

Following the general procedure using benzoyl chloride (0.6 mL, 5 mmol, 1 equiv.) and *n*-decylamine (1.2 mL, 6 mmol, 1.2 equiv.), the product was directly used without purification.

^{1}H NMR (400 MHz, $CDCl_3$) δ (ppm) 7.77 – 7.75 (m, 2H), 7.46 – 7.40 (m, 1H), 7.39 – 7.36 (m, 2H), 6.44 (bs, 1H), 3.44 – 3.39 (m, 2H), 1.62 – 1.55 (m, 2H), 1.32 – 1.25 (m, 14H), 0.87 (t, *J* = 6.7 Hz, 3H).

^{13}C NMR (101 MHz, $CDCl_3$) δ (ppm) 167.7, 135.0, 131.3, 128.5, 127.0, 40.2, 32.0, 29.8, 29.6, 29.6, 29.4, 29.4, 27.1, 22.8, 14.2.

***N*-(2-Methoxyethyl)benzamide (1d)**

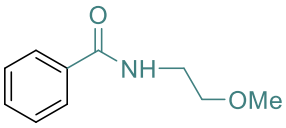

Following the general procedure using benzoyl chloride (0.6 mL, 5 mmol, 1 equiv.) and 2-methoxyethylamine (0.52 mL, 6 mmol, 1.2 equiv.), the product was directly used without purification.

^{1}H NMR (400 MHz, $CDCl_3$) δ (ppm) 7.75 – 7.72 (m, 2H), 7.42 – 7.38 (m, 1H), 7.34 – 7.30 (m, 2H), 6.95 (bs, 1H), 3.58 – 3.54 (m, 2H), 3.49 – 3.46 (m, 2H), 3.29 (s, 3H).

^{13}C NMR (101 MHz, $CDCl_3$) δ (ppm) 167.6, 134.4, 131.3, 128.4, 127.0, 71.1, 58.6, 39.6.

_N_-(Cyclohexylmethyl)benzamide (1e)

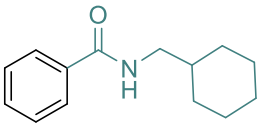

Following the general procedure using benzoyl chloride (0.6 mL, 5 mmol, 1 equiv.) and cyclohexanemethylamine (0.78 mL, 6 mmol, 1.2 equiv.), the product was directly used without purification.

^{1}H NMR (400 MHz, $CDCl_3$) δ (ppm) 7.77 – 7.75 (m, 2H), 7.44 – 7.40 (m, 1H), 7.37 – 7.32 (m, 2H), 6.76 (bs, 1H), 3.24 – 3.21 (m, 2H), 1.756 – 1.60 (m, 5H), 1.57 – 1.50 (m, 1H), 1.24 – 1.09 (m, 3H), 0.98 – 0.88 (m, 2H).

^{13}C NMR (101 MHz, $CDCl_3$) δ (ppm) 167.7, 134.9, 131.2, 128.4, 127.0, 46.3, 38.0, 30.9, 26.4, 25.8.

_N_-(_Tert_-butyl)-4-methylbenzamide (1g)

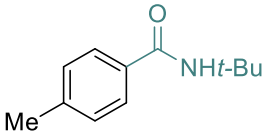

Following the general procedure using *p*-toluoyl chloride (0.67 mL, 5 mmol, 1 equiv.) and *tert*-butylamine (0.63 mL, 6 mmol, 1.2 equiv.), the product was directly used without purification.

^{1}H NMR (400 MHz, $CDCl_3$) δ (ppm) 7.59 (d, *J* = 8.2 Hz, 2H), 7.15 (d, *J* = 7.8 Hz, 2H), 6.00 (bs, 1H), 2.33 (s, 3H), 1.43 (s, 9H).

^{13}C NMR (101 MHz, $CDCl_3$) δ (ppm) 166.9, 141.3, 133.1, 129.1, 126.7, 51.5, 28.9, 21.4.

4-Bromo-_N_-(_tert_-butyl)benzamide (1h)

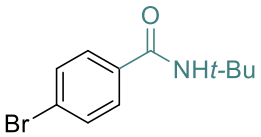

Following general procedure using 4-bromobenzoyl chloride (1 g, 5 mmol, 1 equiv.) and *tert*-butylamine (0.63 mL, 6 mmol, 1.2 equiv.), the product was directly used without purification.

^{1}H NMR (400 MHz, $CDCl_3$) δ (ppm) 7.57 – 7.49 (m, 4H), 5.96 (bs, 1H), 1.44 (s, 9H).

^{13}C NMR (101 MHz, $CzDCl_3$) δ (ppm) 166.0, 134.9, 131.7, 128.5, 125.7, 51.9, 28.9.

4-Chloro-_N_-(_tert_-butyl)benzamide (1i)

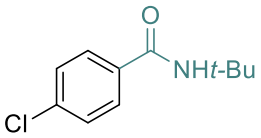

Following the general procedure using 4-chlorobenzoyl chloride (0.64 mL, 5 mmol, 1 equiv.) and *tert*-butylamine (0.63 mL, 6 mmol, 1.2 equiv.), the product was directly used without purification.

^{1}H NMR (400 MHz, $CDCl_3$) δ (ppm) 7.65 – 7.62 (m, 2H), 7.36 – 7.32 (m, 2H), 5.96 (bs, 1H), 1.45 (s, 9H).

^{13}C NMR (101 MHz, $CDCl_3$) δ (ppm) 165.9, 137.3, 134.4, 128.7, 128.3, 51.9, 28.9.

***N*-(*Tert*-butyl)-4-methoxybenzamide (1j)**

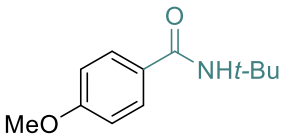

Following the general procedure using 4-methoxybenzoyl chloride (0.67 mL, 5 mmol, 1 equiv.) and *tert*-butylamine (0.63 mL, 6 mmol, 1.2 equiv.), the product was directly used without purification.

^{1}H NMR (400 MHz, $CDCl_3$) δ (ppm) 7.67 – 7.65 (m, 2H), 6.87 – 6.83 (m, 2H), 5.93 (bs, 1H), 3.79 (s, 3H), 1.43 (s, 9H).

^{13}C NMR (101 MHz, $CzDCl_3$) δ (ppm) 166.5, 161.9, 128.5, 128.3, 113.6, 55.4, 51.5, 29.0.

***N*-(*Tert*-butyl)-3-methylbenzamide (1k)**

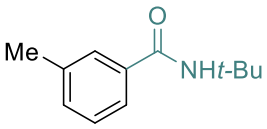

Following the general procedure using *m*-toluoyl chloride (0.66 mL, 5 mmol, 1 equiv.) and *tert*-butylamine (0.63 mL, 6 mmol, 1.2 equiv.), the product was directly used without purification.

^{1}H NMR (400 MHz, $CDCl_3$) δ (ppm) 7.52 (s, 1H), 7.48 – 7.46 (m, 1H), 7.25 – 7.23 (m, 1H), 5.99 (bs, 1H), 2.35 (s, 3H), 1.45 (s, 9H).

^{13}C NMR (101 MHz, $CDCl_3$) δ (ppm) 167.2, 138.3, 136.0, 131.8, 128.3, 127.5, 123.7, 51.6, 28.9, 21.4.

***N*-(*Tert*-butyl)-2-methylbenzamide (1l)**

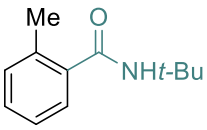

Following the general procedure using *o*-toluoyl chloride (0.65 mL, 5 mmol, 1 equiv.) and *tert*-butylamine (0.63 mL, 6 mmol, 1.2 equiv.), the product was directly used without purification.

^{1}H NMR (400 MHz, $CDCl_3$) δ (ppm) 7.31 – 7.24 (m, 2H), 7.19 – 7.14 (m, 2H), 5.62 (bs, 1H), 2.40 (s, 3H), 1.43 (s, 9H).

^{13}C NMR (101 MHz, $CDCl_3$) δ (ppm) 169.7, 138.0, 135.4, 130.8, 129.4, 126.5, 125.6, 51.7, 28.9, 19.6.

***N*-(*Tert*-butyl)-2-fluorobenzamide (1m)**

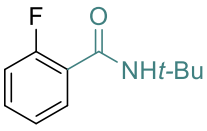

Following the general procedure using 2-fluorobenzoyl chloride (0.60 mL, 5 mmol, 1 equiv.) and *tert*-butylamine (0.63 mL, 6 mmol, 1.2 equiv.), the product was directly used without purification.

^{1}H NMR (400 MHz, $CDCl_3$) δ (ppm) 8.07 – 8.03 (m, 1H), 7.45 – 7.40 (m, 1H), 7.26 – 7.22 (m, 1H), 7.11 – 7.06 (m, 1H), 6.58 (bs, 1H), 1.47 (s, 9H).

^{19}F{^{1}H} NMR (376 MHz, $CDCl_3$) δ (ppm) -113.9.

^{13}C NMR (101 MHz, $CDCl_3$) δ (ppm) 162.4 (d, *J* = 3.3 Hz), 160.5 (d, *J* = 244.5 Hz), 132.9 (d, *J* = 9.3 Hz), 131.9, 124.8 (d, *J* = 3.0 Hz), 122.4 (d, *J* = 11.7 Hz), 116.0 (d, *J* = 25.5 Hz), 51.9, 29.0.

***N*-(*Tert*-butyl)-2,4-difluorobenzamide (1n)**

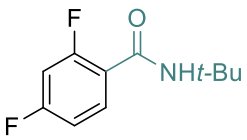

Following the general procedure using 2,4-difluorobenzoyl chloride (0.61 mL, 5 mmol, 1 equiv.) and *tert*-butylamine (0.63 mL, 6 mmol, 1.2 equiv.), the product was directly used without purification.

^{1}H NMR (400 MHz, $CDCl_3$) δ (ppm) 7.99 – 7.93 (m, 1H), 6.90 – 6.85 (m, 1H), 6.77 – 6.71 (m, 1H), 6.45 (d, *J* = 12.2 Hz, 1H), 1.38 (s, 9H).

^{19}F{^{1}H} NMR (376 MHz, $CDCl_3$) δ (ppm) -105.2 (d, *J* = 10.5 Hz), -109.5 (d, *J* = 10.8 Hz).

^{13}C NMR (101 MHz, $CDCl_3$) δ (ppm) 164.4 (dd, *J* = 254.3, 12.9 Hz), 161.4 (d, *J* = 3.8 Hz), 160.6 (dd, *J* = 248.5, 12.2 Hz), 133.4 (dd, *J* = 10.1, 3.9 Hz), 118.9 (dd, *J* = 12.2, 3.8 Hz), 112.1 (dd, *J* = 21.2, 3.4 Hz), 104.0 (dd, *J* = 29.3, 25.8 Hz), 51.8, 28.8.

4.5.3. General Procedure for the Rh(III)/Ag(I)-Catalyzed *ortho*-Heteroarylation of Amide and Compounds 3a-3r Characterization

Procedure: An oven-dried Schlenk tube was charged with $[Cp^{TMP}*RhCl_2]_2$ (6.9 mg, 0.0075 mmol, 2.5 mol%), Ag_2O (139.0 mg, 0.6 mmol, 2 equiv.), $Zn(OTf)_2$ (54.5 mg, 0.15 mmol, 0.5 equiv.), benzamide derivative **1** (0.3 mmol, 1 equiv.), heteroarene **2** (0.36 mmol, 1.2 equiv) and HFIP (0.3 mL) under argon atmosphere. The resulting mixture was stirred at 35 °C over 40 h. The solution was filtered through a plug of celite and washed with CH_2Cl_2 (5 mL). The filtrate was concentrated and purified by flash chromatography on silica gel using petroleum ether and ethyl acetate to provide the pure products.

2-(Benzo[*b*]thiophen-2-yl)-*N*-(*tert*-butyl)benzamide (3a)

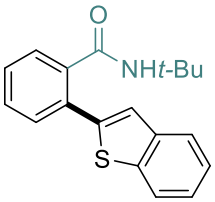

Following the general procedure using *N*-(*tert*-butyl)benzamide **1a** (53.1 mg, 0.3 mmol, 1 equiv.) and benzo[*b*]thiophene **2a** (48.3 mg, 0.36 mmol, 1.2 equiv.), the product was purified by flash chromatography on silica gel (Petroleum ether/Ethyl acetate = 80:20) to afford **3a** as a white solid in 83% yield (77 mg, 0.25 mmol).

^{1}H NMR (400 MHz, $CDCl_3$) δ (ppm) 7.83 (d, *J* = 7.8 Hz, 1H), 7.75 (d, *J* = 7.4 Hz, 1H), 7.64 – 7.58 (m, 1H), 7.56 – 7.48 (m, 1H), 7.47 – 7.33 (m, 5H), 5.45 (bs, 1H), 1.17 (s, 9H).

^{13}C NMR (101 MHz, $CDCl_3$) δ (ppm) 168.5, 141.3, 140.3, 140.1, 137.9, 131.6, 130.5, 129.7, 128.6, 124.8, 124.7, 124.0, 123.9, 122.2, 51.7, 28.4.

2-(Benzo[*b*]thiophen-3-yl)-*N*-(*tert*-butyl)benzamide (3a')

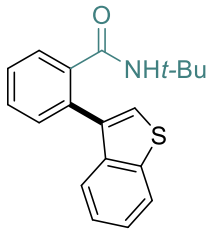

According to You's work,[27] **3a'** was prepared as followed. An over-dried Schlenk tube was charged with $[Cp^*RhCl_2]_2$ (4.6 mg, 0.0075 mmol, 2.5 mol%), $Cu(OAc)_2$ (10.9 mg, 0.9 mmol, 20 mol%), $Zn(OTf)_2$ (54.5 mg, 0.15 mmol, 0.5 equiv.), *N*-(*tert*-butyl)benzamide **1a** (53.1 mg, 0.3 mmol, 1 equiv.) and benzo[*b*]thiophene **2a** (48 mg, 0.36 mmol, 1.2 equiv.) and THF/HFIP (0.3 mL, 1:1) under oxygen atmosphere. The resulting mixture was stirred at 110 °C over 24 h. The solution was filtered through a plug of celite and washed with CH_2Cl_2 (5 mL). The filtrate was concentrated and purified by flash chromatography on silica gel (Petroleum ether/Ethyl acetate = 80:20) to afford **3a'** as a white solid in 32% yield (29.6 mg, 0.096 mmol). NMR datas were consistent with the literature.

^{1}H NMR (400 MHz, $CDCl_3$) δ (ppm) 7.93 – 7.89 (m, 2H), 7.56 – 7.54 (m, 1H), 7.52 – 7.49 (m, 2H),200 7.42 (s, 1H), 7.41 – 7.33 (m, 3H), 5.20 (bs, 1H), 0.80 (s, 9H).

^{13}C NMR (101 MHz, $CDCl_3$) δ (ppm) 167.4, 139.9, 138.9, 137.5, 137.0, 132.7, 130.9, 130.4, 129.5, 128.7, 125.1, 125.0, 124.1, 123.2, 122.8, 51.0, 28.0.

2-(Benzo[*b*]thiophen-2-yl)-*N*-hexylbenzamide (3b)

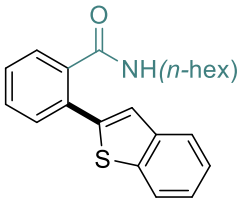

Following the general procedure using *N*-hexylbenzamide **1b** (61.6 mg, 0.3 mmol, 1 equiv.) and benzo[*b*]thiophene **2a** (48.3 mg, 0.36 mmol, 1.2 equiv.), the product was purified by flash chromatography on silica gel (Petroleum ether/Ethyl acetate = 80:20) to afford **3b** as a brown solid in 62% yield (63 mg, 0.19 mmol).

^{1}H NMR (400 MHz, $CDCl_3$) δ (ppm) 7.83 – 7.81 (m, 1H), 7.77 – 7.75 (m, 1H), 7.62 – 7.59 (m, 1H), 7.55 – 7.53 (m, 1H), 7.47 – 7.31 (m, 5H), 5.64 (bs, 1H), 3.24 – 3.19 (m, 2H), 1.24 – 1.16 (m, 2H), 1.06 – 1.00 (m, 2H), 0.97 – 0.84 (m, 4H), 0.76 (t, *J* = 7.0 Hz, 3H).

^{13}C NMR (101 MHz, $CDCl_3$) δ (ppm) 169.3, 141.2, 140.2, 136.9, 131.7, 130.6, 129.8, 128.5, 128.4, 126.85, 124.6, 124.6, 123.8, 123.6, 122.1, 40.0, 31.3, 29.0, 26.4, 22.3, 13.9.

2-(Benzo[*b*]thiophen-2-yl)-*N*-decylbenzamide (3c)

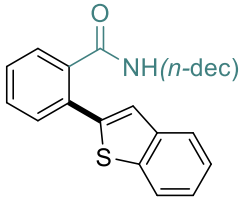

Following the general procedure using *N*-decylbenzamide **1c** (78.4 mg, 0.3 mmol, 1 equiv.) and benzo[*b*]thiophene **2a** (48.3 mg, 0.36 mmol, 1.2 equiv.), the product was purified by flash chromatography on silica gel (Petroleum ether/Ethyl acetate = 80:20) to afford **3c** as a brown solid in 55% yield (65 mg, 0.17 mmol).

^{1}H NMR (400 MHz, $CDCl_3$) δ (ppm) 7.83 – 7.81 (m, 1H), 7.77 – 7.75 (m, 1H), 7.62 – 7.60 (m, 1H), 7.55 – 7.53 (m, 1H), 7.48 – 7.31 (m, 5H), 5.62 (bs, 1H), 3.25 – 3.21 (m, 2H), 1.30 – 1.11 (m, 10H), 1.02 – 0.94 (m, 6H), 0.89 (t, *J* = 7.0 Hz, 3H).

^{13}C NMR (101 MHz, $CDCl_3$) δ (ppm) 169.3, 141.2, 140.2, 140.2, 136.9, 131.6, 130.6, 129.8, 128.6, 128.5, 124.6, 124.6, 123.8, 123.6, 122.1, 40.0, 31.9, 29.5, 29.3, 29.3, 29.2, 29.0, 26.8, 22.7, 14.1.

2-(Benzo[*b*]thiophen-2-yl)-*N*-(2-methoxyethyl)benzamide (3d)

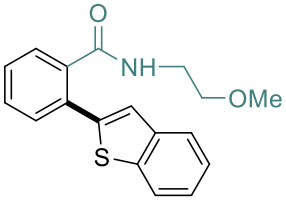

Following the general procedure using *N*-(2-methoxyethyl) benzamide **1d** (53.8 mg, 0.3 mmol, 1 equiv.) and benzo[*b*]thiophene **2a** (48.3 mg, 0.36 mmol, 1.2 equiv.), the product was purified by flash chromatography on silica gel (Petroleum ether/Ethyl acetate = 50:50) to afford **3d** as a white solid in 70% yield (65 mg, 0.21 mmol).

^{1}H NMR (400 MHz, $CDCl_3$) δ (ppm) 7.81 (d, *J* = 8.5 Hz, 1H), 7.62 – 7.60 (m, 1H), 7.53 – 7.51 (m, 1H), 7.47 – 7.29 (m, 6H), 6.10 (bs, 1H), 3.43 – 3.39 (m, 2H), 3.13 (t, *J* = 5.2 Hz, 2H), 2.82 (s, 3H).

^{13}C NMR (101 MHz, $CDCl_3$) δ (ppm) 169.2, 141.4, 140.2, 136.6, 131.4, 130.7, 129.9, 128.6, 128.5, 127.0, 124.6, 124.5, 123.8, 123.5, 122.1, 70.5, 58.2, 39.5.

2-(Benzo[*b*]thiophen-2-yl)-*N*-(cyclohexylmethyl)benzamide (3e)

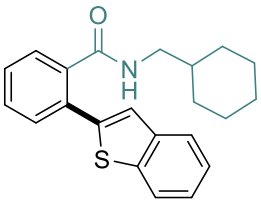

Following the general procedure using *N*-(cyclohexylmethyl)benzamide **1e** (65.1 mg, 0.3 mmol, 1 equiv.) and benzo[*b*]thiophene **2a** (48.3 mg, 0.36 mmol, 1.2 equiv.), the product was purified by flash chromatography on silica gel (Petroleum ether/Ethyl acetate = 80:20) to afford **3e** as a white solid in 72% yield (76 mg, 0.22 mmol).

^{1}H NMR (400 MHz, $CDCl_3$) δ (ppm) 7.82 (d, *J* = 7.7 Hz, 1H), 7.76 (d, *J* = 7.2 Hz, 1H), 7.62 – 7.60 (m, 1H), 7.53 – 7.51 (m, 1H), 7.47 – 7.30 (m, 5H), 5.70 (bs, 1H), 3.06 (t, *J* = 6.4 Hz, 2H), 1.47 – 1.37 (m, 3H), 1.32 – 1.26 (m, 2H), 1.21 – 1.12 (m, 1H), 0.91 – 0.79 (m, 3H), 0.66 – 0.56 (m, 2H).

^{13}C NMR (101 MHz, $CDCl_3$) δ (ppm) 169.3, 141.2, 140.3, 140.2, 137.0, 131.6, 130.7, 129.8, 128.6, 128.5, 124.7, 124.6, 123.9, 123.7, 122.1, 46.2, 37.4, 30.7, 26.1, 25.5.

2-(Benzo[*b*]thiophen-2-yl)-*N*-benzylbenzamide (3f)

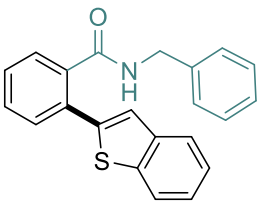

Following the general procedure using *N*-benzylamide **1f** (63.0 mg, 0.3 mmol, 1 equiv.) and benzo[*b*]thiophene **2a** (48.3 mg, 0.36 mmol, 1.2 equiv.), the product was purified by flash chromatography on silica gel (Petroleum ether/Ethyl acetate = 80:20) to afford **3f** as white solid in 75% yield (72 mg, 0.23 mmol).

^{1}H NMR (400 MHz, $CDCl_3$) δ (ppm) 7.87 – 7.79 (m, 4H), 7.62 – 7.58 (m, 4H), 7.52 – 7.50 (m, 1H), 7.42 – 7.37 (m, 5H), 5.84 (bs, 1H), 4.30 (d, *J* = 5.8 Hz, 2H).

^{13}C NMR (101 MHz, $CDCl_3$) δ (ppm) 168.1, 140.6, 140.3, 140.3, 137.0, 136.1, 132.9, 130.5, 129.2, 128.2, 127.4, 127.2, 124.6, 124.6, 124.3, 124.2, 122.0, 43.8.

2-(Benzo[*b*]thiophen-2-yl)-*N*-(*tert*-butyl)-4-methoxybenzamide (3g)

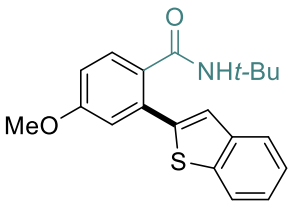

Following the general procedure using *N*-(*tert*-butyl)-4-methoxybenzamide **1j** (62.2 mg, 0.3 mmol, 1 equiv.) and benzo[*b*]thiophene **2a** (48.3 mg, 0.36 mmol, 1.2 equiv.), the product was purified by flash chromatography on silica gel (Petroleum ether/Ethyl acetate = 80:20) to afford **3g** as a white solid in 88% yield (90 mg, 0.26 mmol).

^{1}H NMR (400 MHz, $CDCl_3$) δ (ppm) 7.85 – 7.82 (m, 1H), 7.77 – 7.75 (m, 1H), 7.64 (d, *J* = 8.5 Hz, 1H), 7.40 – 7.32 (m, 3H), 7.00 (d, *J* = 2.6 Hz, 1H), 6.94 (dd, *J* = 8.6, 2.6 Hz, 1H), 5.39 (s, 1H), 3.84 (s, 3H), 1.13 (s, 9H).

^{13}C NMR (101 MHz, $CzDCl_3$) δ (ppm) 167.9, 160.2, 141.3, 140.1, 140.0, 133.2, 130.6, 130.4, 124.8, 124.6, 124.0, 123.7, 122.1, 115.7, 114.1, 55.5, 51.4, 28.3.

2-(Benzo[*b*]thiophen-2-yl)-*N*-(*tert*-butyl)-4-methylbenzamide (3h)

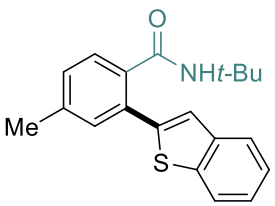

Following the general procedure using *N*-(*tert*-butyl)-4-methylbenzamide **1g** (57.4 mg, 0.3 mmol, 1 equiv.) and benzo[*b*]thiophene **2a** (48.3 mg, 0.36 mmol, 1.2 equiv.), the product was purified by flash chromatography on silica gel (Petroleum ether/Ethyl acetate = 80:20) to afford **3h** as a white solid in 85% yield (82 mg, 0.26 mmol).

^{1}H NMR (400 MHz, $CDCl_3$) δ (ppm) 7.85 – 7.83 (m, 1H), 7.77– 7.75 (m, 1H), 7.56 (d, *J* = 7.8 Hz, 1H), 7.40 – 7.32 (m, 4H), 7.24 – 7.22 (m, 1H), 5.36 (bs, 1H), 2.41 (s, 3H), 1.15 (s, 9H).

^{13}C NMR (101 MHz, $CDCl_3$) δ (ppm) 168.4, 141.4, 140.2, 140.1, 139.8, 135.1, 131.4, 131.1, 129.3, 128.7, 124.7, 124.5, 123.8, 123.7, 122.1, 51.5, 28.3, 21.2.

2-(Benzo[*b*]thiophen-2-yl)-4-bromo-*N*-(*tert*-butyl)benzamide (3i)

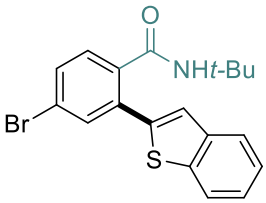

Following the general procedure using 4-bromo-*N*-(*tert*-butyl)benzamide **1h** (76.8 mg, 0.3 mmol, 1 equiv.) and benzo[*b*]thiophene **2a** (48.3 mg, 0.36 mmol, 1.2 equiv.), the product was purified by flash chromatography on silica gel (Petroleum ether/Ethyl acetate = 80:20) to afford **3i** as a white solid in 82% yield (96 mg, 0.25 mmol).

^{1}H NMR (400 MHz, $CDCl_3$) δ (ppm) 7.85 – 7.83 (m, 1H), 7.77 – 7.5 (m, 1H), 7.67 (d, *J* = 1.9 Hz, 1H), 7.54 – 7.46 (m, 2H), 7.40 – 7.33 (m, 3H), 5.45 (bs, 1H), 1.15 (s, 9H).

^{13}C NMR (101 MHz, $CDCl_3$) δ (ppm) 167.4, 140.2, 140.0, 139.5, 136.6, 133.5, 133.1, 131.5, 130.2, 124.9, 124.9, 124.5, 123.9, 123.6, 122.1, 51.8, 28.3.

2-(Benzo[*b*]thiophen-2-yl)-4-chloro-*N*-(*tert*-butyl)benzamide (3j)

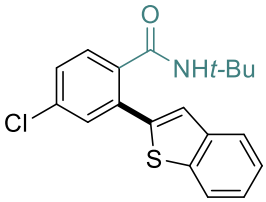

Following the general procedure using 4-chloro-*N*-(*tert*-butyl)benzamide **1i** (63.5 mg, 0.3 mmol, 1 equiv.) and benzo[*b*]thiophene **2a** (48 mg, 0.36 mmol, 1.2 equiv.), the product was purified by flash chromatography on silica gel (Petroleum ether/Ethyl acetate = 80:20) to afford **3j** as a white solid in 80% yield (82.5 mg, 0.24 mmol).

^{1}H NMR (400 MHz, $CDCl_3$) δ (ppm) 7.88 – 7.85 (m, 1H), 7.80 – 7.77 (m, 1H), 7.58 – 7.56 (m, 1H), 7.53 (d, *J* = 2.1 Hz, 1H), 7.43 – 7.36 (m, 4H), 5.49 (s, 1H), 1.18 (s, 9H).

^{13}C NMR (101 MHz, $CDCl_3$) δ (ppm) 167.4, 140.1, 140.0, 139.6, 136.1, 135.4, 133.3, 130.2, 130.0, 128.6, 124.9, 124.9, 124.5, 123.9, 122.1, 51.8, 28.3.

2-(Benzo[*b*]thiophen-2-yl)-*N*-(*tert*-butyl)-5-methylbenzamide (3k)

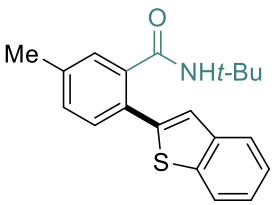

Following the general procedure using *N*-(*tert*-butyl)-3-methylbenzamide **1k** (57.4 mg, 0.3 mmol, 1 equiv.) and benzo[*b*]thiophene **2a** (48 mg, 0.36 mmol, 1.2 equiv.), the product was purified by flash chromatography on silica gel (Petroleum ether/Ethyl acetate = 80:20) to afford **3k** as a white solid in 75% yield (72.8 mg, 0.23 mmol).

^{1}H NMR (400 MHz, $CDCl_3$) δ (ppm) 7.83 – 7.81 (m, 1H), 7.76 – 7.73 (m, 1H), 7.45 – 7.23 (m, 6H), 5.41 (bs, 1H), 2.40 (s, 3H), 1.17 (s, 9H).

^{13}C NMR (101 MHz, $CDCl_3$) δ (ppm) 168.6, 141.3, 140.3, 140.0, 138.8, 137.6, 130.4, 130.3, 129.2, 128.6, 124.63 124.4, 123.6, 123.6, 122.0, 51.6, 28.3, 21.1.

2-(Benzo[*b*]thiophen-2-yl)-*N*-(*tert*-butyl)-6-methylbenzamide (3l)

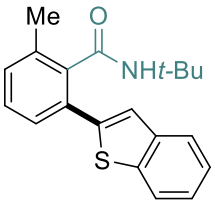

Following the general procedure using *N*-(*tert*-butyl)-2-methylbenzamide **1l** (57.4 mg, 0.3 mmol, 1 equiv.) and benzo[*b*]thiophene **2a** (48.3 mg, 0.36 mmol, 1.2 equiv.), the product was purified by flash chromatography on silica gel (Petroleum ether/Ethyl acetate = 80:20) to afford **3l** as a white solid in 62% yield (60 mg, 0.19 mmol).

^{1}H NMR (400 MHz, $CDCl_3$) δ (ppm) 7.87 – 7.85 (m, 1H), 7.80 – 7.77 (m, 1H), 7.54 (s, 1H), 7.44 – 7.33 (m, 5H), 5.44 (bs, 1H), 2.48 (s, 3H), 1.24 (s, 9H).

^{13}C NMR (101 MHz, $CDCl_3$) δ (ppm) 168.9, 141.3, 140.6, 140.0, 137.8, 135.9, 131.4, 130.3, 128.8, 127.7, 124.7, 124.4, 123.9, 123.8, 122.1, 51.8, 28.5, 19.4.

2-(Benzo[*b*]thiophen-2-yl)-*N*-(*tert*-butyl)-6-fluorobenzamide (3m)

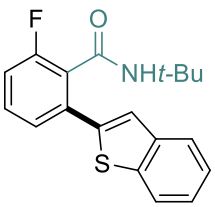

Following the general procedure using *N*-(*tert*-butyl)-2-fluorobenzamide **1m** (58.6 mg, 0.3 mmol, 1 equiv.) and benzo[*b*]thiophene **2a** (48.3 mg, 0.36 mmol, 1.2 equiv.), the product was purified by flash chromatography on silica gel (Petroleum ether/Ethyl acetate = 80:20) to afford **3m** as an orange solid in 65% yield (64 mg, 0.2 mmol).

^{1}H NMR (400 MHz, $CDCl_3$) δ (ppm) 7.84 – 7.82 (m, 1H), 7.77 – 7.74 (m, 1H), 7.57 (s, 1H), 7.39 – 7.34 (m, 4H), 7.12 – 7.07 (m, 1H), 5.53 (bs, 1H), 1.29 (s, 9H).

^{19}F{^{1}H} NMR (376 MHz, $CDCl_3$) δ (ppm) -111.2.

^{13}C NMR (101 MHz, $CDCl_3$) δ (ppm) 163.9, 159.5 (d, *J* = 248.2 Hz), 140.3, 140.0, 139.5 (d, *J* = 2.8 Hz), 133.8 (d, *J* = 4.3 Hz), 130.3 (d, *J* = 8.9 Hz), 126.0, 125.8, 125.7 (d, *J* = 3.2 Hz), 124.7 (d, *J* = 5.4 Hz), 124.1, 124.0, 122.0, 115.5 (d, *J* = 22.1 Hz), 52.2, 28.4.

2-(Benzo[*b*]thiophen-2-yl)-*N*-(*tert*-butyl)-4,6-difluorobenzamide (3n)

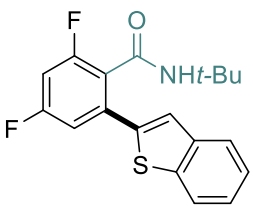

Following the general procedure using *N*-(*tert*-butyl)-2,4-difluorobenzamide **1n** (64.0 mg, 0.3 mmol, 1 equiv.) and benzo[*b*]thiophene **2a** (48.3 mg, 0.36 mmol, 1.2 equiv.), the product was

purified by flash chromatography on silica gel (Petroleum ether/Ethyl acetate = 80:20) to afford **3n** as a red solid in 66% yield (68 mg, 0.2 mmol).

^{1}H NMR (400 MHz, $CDCl_3$) δ (ppm) 7.84 – 7.82 (m, 1H), 7.77 – 7.75 (m, 1H), 7.58 (s, 1H), 7.40 – 7.34 (m, 2H), 7.12 – 7.08 (m, 1H), 6.85 (td, *J* = 8.8, 2.4 Hz, 1H), 5.55 (bs, 1H), 1.28 (s, 9H).

^{19}F{^{1}H} NMR (376 MHz, $CDCl_3$) δ (ppm) -107.8 (d, *J* = 8.2 Hz), -111.7 (d, *J* = 9.0 Hz).

^{13}C NMR (101 MHz, $CDCl_3$) δ (ppm) 162.5 (dd, *J* = 233.3, 13.1 Hz), 163.1, 160.0 (dd, *J* = 232.5, 13.1 Hz), 140.1, 140.0, 138.4 (t, *J* = 2.9 Hz), 135.2 (dd, *J* = 10.1, 6.0 Hz), 125.1, 124.8, 124.7, 124.2, 122.4 (dd, *J* = 20.3, 4.0 Hz), 112.8 (dd, *J* = 22.8, 3.5 Hz), 103.8 (t, *J* = 25.8 Hz), 52.3, 28.4.

***N*-(*tert*-butyl)-2-(5-methylthiophen-2-yl)benzamide (3o)**

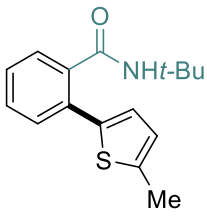

Following the general procedure *N*-(*tert*-butyl)benzamide **1a** (53.1 mg, 0.3 mmol, 1 equiv.) and 2-methylthiophene **2b** (35 µL, 0.36 mmol, 1.2 equiv.), the product was purified by flash chromatography on silica gel (Petroleum ether/Ethyl acetate = 50:50) to afford **3o** as a yellow solid in 78% yield (64 mg, 0.23 mmol).

^{1}H NMR (400 MHz, $CDCl_3$) δ 7.61 – 7.58 (m, 1H), 7.37 – 7.30 (m, 3H), 6.92 (d, *J* = 3.4 Hz, 1H), 6.73 – 6.71 (m, 1H), 5.38 (bs, 1H), 2.51 (s, 3H), 1.25 (s, 9H).

^{13}C NMR (101 MHz, $CDCl_3$) δ (ppm) 168.6, 141.0, 138.8, 137.3, 132.0, 130.5, 129.6, 128.7, 127.9, 127.2, 125.9, 51.6, 28.5, 15.4.

***N*-(*tert*-butyl)-2-(5-cyanothiophen-2-yl)benzamide (3p)**

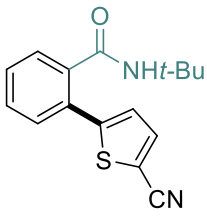

Following the general procedure *N*-(*tert*-butyl)benzamide **1a** (53.1 mg, 0.3 mmol, 1 equiv.) and 2-thiophenecarbonitrile **2c** (34 µL, 0.36 mmol, 1.2 equiv.), the product was purified by flash chromatography on silica gel (Petroleum ether/Ethyl acetate = 50:50) to afford **3p** as a white solid in 62% yield (53 mg, 0.19 mmol).

^{1}H NMR (400 MHz, $CDCl_3$) δ 7.58 (d, *J* = 3.9 Hz, 1H), 7.54 – 7.52 (m, 1H), 7.47 – 7.43 (m, 3H), 7.21 (d, *J* = 3.9 Hz, 1H), 5.36 (bs, 1H), 1.30 (s, 9H).

^{13}C NMR (101 MHz, $CDCl_3$) δ (ppm) 168.0, 148.9, 137.9, 137.7, 130.4, 129.9, 129.4, 129.4, 128.2, 127.3, 114.0, 109.8, 52.0, 28.5.

Ethyl 5-(2-(*tert*-butylcarbamoyl)-5-methylphenyl)thiophene-2-carboxylate (3q)

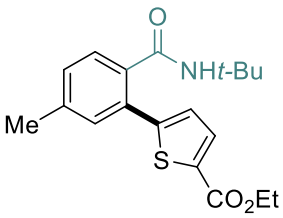

Following the general procedure using *N*-(*tert*-butyl)-4-methylbenzamide **1g** (57.4 mg, 0.3 mmol, 1 equiv.) and ethyl 2-thiophenecarboxylate **2d** (48 µL, 0.36 mmol, 1.2 equiv.), the product was purified by flash chromatography on silica gel (Petroleum ether/Ethyl acetate = 50:50) to afford **3q** as a white solid in 78% yield (81 mg, 0.23 mmol).

^{1}H NMR (400 MHz, $CDCl_3$) (ppm) 7.71 (d, *J* = 3.8 Hz, 1H), 7.44 (d, *J* = 7.8 Hz, 1H), 7.23 (s, 1H), 7.21 – 7.18 (m, 1H), 7.13 (d, *J* = 3.8 Hz, 1H), 5.34 (bs, 1H), 4.34 (q, *J* = 7.1 Hz, 2H), 2.37 (s, 3H), 1.36 (t, *J* = 7.1 Hz, 3H), 1.25 (s, 9H).

^{13}C NMR (101 MHz, $CDCl_3$) δ (ppm) 168.4, 162.2, 148.5, 139.9, 135.1, 133.9, 133.6, 130.9, 130.7, 129.6, 128.6, 127.7, 61.3, 51.8, 28.5, 21.3, 14.4.

***N*-(*tert*-butyl)-2-(5-(cyclopropanecarbonyl)thiophen-2-yl)-4-methylbenzamide (3r)**

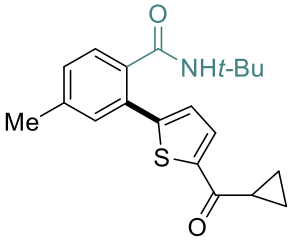

Following the general procedure using *N*-(*tert*-butyl)-4-methylbenzamide **1g** (57.4 mg, 0.3 mmol, 1 equiv.) and cyclopropyl(thiophen-2-yl)methanone **2e** (47 µL, 0.36 mmol, 1.2 equiv.), the product was purified by flash chromatography on silica gel (Petroleum ether/Ethyl acetate = 50:50) to afford **3r** as a white solid in 80% yield (81 mg, 0.24 mmol).

^{1}H NMR (400 MHz, $CDCl_3$) (ppm) 7.74 (d, *J* = 3.9 Hz, 1H), 7.43 (d, *J* = 7.8 Hz, 1H), 7.24 (s, 1H), 7.20 – 7.18 (m, 2H), 5.40 (bs, 1H), 2.55 – 2.49 (m, 1H), 2.37 (s, 3H), 1.26 (s, 9H), 1.24 – 1.21 (m, 2H), 1.04 – 1.00 (m, 2H).

^{13}C NMR (101 MHz, $CDCl_3$) δ (ppm) 192.8, 168.5, 149.6, 144.8, 140.0, 135.0, 131.8, 130.9, 130.8, 129.7, 128.5, 128.1, 51.8, 28.5, 21.3, 18.0, 11.5.

Methyl 5-(2-(*N*-*tert*-butyl)benzamide-3-chlorothiophene-2-carboxylate (3s)

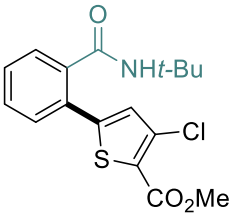

Following the general procedure *N*-(*tert*-butyl)benzamide **1a** (53.1 mg, 0.3 mmol, 1 equiv.) and methyl 3-chlorothiophene-2-carboxylate **2f** (48 µL, 0.36 mmol, 1.2 equiv.), the product was purified by flash chromatography on silica gel (Petroleum ether/Ethyl acetate = 50:50) to afford **3s** as a white solid in 85% yield (90 mg, 0.26 mmol).

^{1}H NMR (400 MHz, $CDCl_3$) (ppm) 7.49 – 7.45 (m, 1H), 7.41 – 7.38 (m, 3H), 7.11 (s, 1H), 5.50 (bs, 1H), 3.87 (s, 3H), 1.30 (s, 9H).

^{13}C NMR (101 MHz, $CDCl_3$) δ (ppm) 168.2, 161.0, 146.0, 137.8, 131.5, 129.9, 129.8, 129.7, 129.6, 129.4, 128.3, 125.4, 52.3, 52.1, 28.5.

Methyl 5-(2-(*N*-*tert*-butyl)benzamide-3-methylthiophene-2-carboxylate (3t)

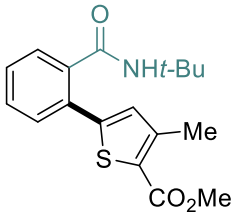

Following the general procedure *N*-(*tert*-butyl)benzamide **1a** (53.1 mg, 0.3 mmol, 1 equiv.) and methyl 3-methylthiophene-2-carboxylate **2e** (48 µL, 0.36 mmol, 1.2 equiv.), the product was purified by flash chromatography on silica gel (Petroleum ether/Ethyl acetate = 50:50) to afford **3t** as a yellow solid in 89% yield (86 mg, 0.27 mmol).

^{1}H NMR (400 MHz, $CDCl_3$) δ (ppm) 7.51 – 7.48 (m, 1H), 7.40 – 7.34 (m, 3H), 6.99 (s, 1H), 5.41 (bs, 1H), 3.83 (s, 3H), 2.51 (s, 3H), 1.25 (s, 9H).

^{13}C NMR (101 MHz, $CDCl_3$) δ (ppm) 168.5, 163.2, 146.7, 145.5, 137.6, 131.8, 130.7, 130.0, 129.7, 128.8, 128.4, 126.6, 51.9, 51.8, 28.4, 16.0.

2-(5-Acetyl-4-chlorothiophen-2-yl)-*N*-(*tert*-butyl)benzamide (3u)

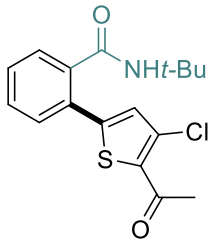

Following the general procedure *N*-(*tert*-butyl)benzamide **1a** (53.1 mg, 0.3 mmol, 1 equiv.) and 2-acetyl-3-chlorothiophene **2d** (44 µL, 0.36 mmol, 1.2 equiv.), the product was purified by flash chromatography on silica gel (Petroleum ether/Ethyl acetate = 50:50) to afford **3u** as a white solid in 85% yield (86 mg, 0.26 mmol).

^{1}H NMR (400 MHz, $CDCl_3$) δ (ppm) 7.49 – 7.39 (m, 4H), 7.15 (s, 1H), 5.53 (bs, 1H), 2.66 (s, 3H), 1.33 (s, 9H).

^{13}C NMR (101 MHz, $CDCl_3$) δ (ppm) 190.0, 168.2, 147.3, 137.6, 137.4, 129.9, 129.9, 129.7, 129.7, 129.4, 128.5, 128.1, 52.1, 29.7, 28.5.

Methyl 5-(2-(*tert*-butylcarbamoyl)-5-methylphenyl)furan-2-carboxylate (3v)

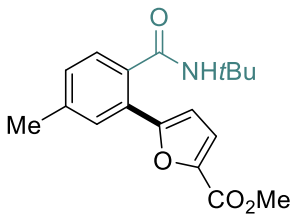

Following the general procedure using *N*-(*tert*-butyl)-4-methylbenzamide **1g** (57.4 mg, 0.3 mmol, 1 equiv.) and methyl furan-2-carboxylate **2i** (38 µL, 0.36 mmol, 1.2 equiv.), the product was purified by flash chromatography on silica gel (Petroleum ether/Ethyl acetate = 50:50) to afford **3v** has a white solid in 65% (61 mg, (0.20 mmol).

^{1}H NMR (400 MHz, $CDCl_3$) δ (ppm) 7.57 (s, 1H), 7.34 (d, *J* = 7.7 Hz, 1H), 7.23 (d, *J* = 3.6 Hz, 1H), 7.20 – 7.17 (m, 1H), 6.78 (d, *J* = 3.6 Hz, 1H), 5.50 (bs, 1H), 3.90 (s, 3H), 2.40 (s, 3H), 1.39 (s, 9H).

^{13}C NMR (101 MHz, $CDCl_3$) δ (ppm) 169.0, 159.2, 155.6, 143.9, 139.7, 133.9, 129.6, 128.6, 127.9, 126.6, 119.80, 110.7, 51.9, 51.8, 28.6, 21.2.

4.5.4. Post-Transformations and Compounds Characterization

2-(Benzo[*b*]thiophen-2-yl)-4-methylbenzamide (4a)

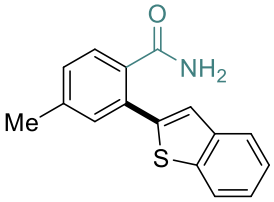

To an oven-dried Schlenk tube was added 2-(benzo[*b*]thiophen-2-yl)-*N*-(*tert*-butyl)-4-methylbenzamide (**3h**) (150 mg, 0.46 mmol) and TFA/H_2O (5 mL, 4:1) under argon atmosphere. The resulting mixture was stirred at 110 °C over 24 h. Then the reaction was cooled to room temperature and neutralized with Na_2CO_3. The aqueous layer was extracted with EtOAc (10 mL x 3). The organic layers were combined, dried over $MgSO_4$ and concentrated. The product was purified by flash chromatography on silica gel (Petroleum ether/Ethyl acetate = 60:40) to afford **4a** as a white solid in 60% yield (74 mg, 0.28 mmol).

^{1}H NMR (400 MHz, $CDCl_3$) δ (ppm) 7.86 – 7.82 (m, 1H), 7.80 – 7.76 (m, 1H), 7.64 (d, *J* = 7.9 Hz, 1H), 7.41 – 7.32 (m, 4H), 7.28 – 7.24 (m, 1H), 5.73 (bs, 1H), 5.62 (bs, 1H), 2.42 (s, 3H).

^{13}C NMR (101 MHz, $CDCl_3$) δ (ppm) 171.2, 141.5, 140.9, 140.4, 140.3, 132.6, 132.0, 131.7, 129.5, 129.2, 124.8, 124.8, 124.0, 123.9, 122.3, 21.4.

Ethyl 5-(2-carbamoyl-5-methylphenyl)thiophene-2-carboxylate (4b)

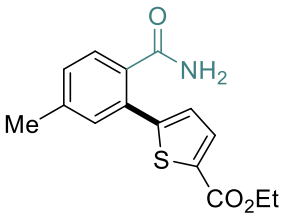

To an oven-dried Schlenk tube was added ethyl 5-(2-(*tert*-butylcarbamoyl)-5-methylphenyl)thiophene-2-carboxylate (**3q**) (150 mg, 0.46 mmol) and TFA/H_2O (5 mL, 4:1) under argon atmosphere. The resulting mixture was stirred at 110 °C over 24 h. Then the reaction as cooled to room temperature and neutralized with Na_2CO_3. The aqueous layer was extracted with EtOAc (10 mL x 3). The organic layers were combined, dried over $MgSO_4$ and concentrated. The product was purified by flash column chromatography on silica gel (Petroleum ether/Ethyl acetate = 50:50) to afford **4b** as a white solid in 32% yield (43 mg, 0.15 mmol).

^{1}H NMR (400 MHz, $CDCl_3$) δ (ppm) 7.69 (d, *J* = 3.9 Hz, 1H), 7.50 (d, *J* = 7.8 Hz, 1H), 7.27 – 7.24 (m, 1H), 7.23 – 7.18 (m, 1H), 7.13 (d, *J* = 3.8 Hz, 1H), 6.22 (bs, 1H), 5.75 (bs, 1H), 4.32 (q, *J* = 7.1 Hz, 1H), 2.38 (s, 3H), 1.35 (t, *J* = 7.1 Hz, 3H).

^{13}C NMR (101 MHz, $CDCl_3$) δ (ppm) 171.4, 162.2, 148.3, 140.8, 134.2, 133.8, 132.7, 131.3, 131.1, 129.6, 128.7, 127.6, 61.3, 21.3, 14.4.

4.6. References

1. (a) Segawa, Y.; Maekawa, T.; Itami, K. *Angew. Chem. Int. Ed.* **2015**, *54*, 66–81; (b) Wu, J.-S.; Cheng, S.-W.; Cheng, Y.-J.; Hsu, C.-S. *Chem. Soc. Rev.* **2015**, *44*, 1113–1154; (c) Surry, D. S.; Buchwald, S. L. *Angew. Chem. Int. Ed.* **2008**, *47*, 6338–6361; (d) Blake, J. F.; Kallan, N. C.; Xiao, D.; Xu, R.; Bencsik, J. R., Skelton, N. J.; Spencer, K. L.; Mitchell, I. S.; Woessner, R. D.; Gloor, S. L.; Risom, T.; Gross S. D.; Martinson, M.; Morales, T. H.; G. Vigers, P. A.; Brandhuber, B. J. *Bioorg. Med. Chem. Lett.* **2010***, 20,* 5607–5612; (e) Mohanakrishnan, A. K.; Lakshmikantham, M. V.; McDougal, C.; Cava, M. P.; Baldwin, J. W.; Metzger, R. M. *J. Org. Chem.* **1998**, *63*, 3105–3112; (f) Lu, R.-J.; Tucker, J. A.; Pickens, J.; Ma, Y.-A.; Zinevitch, T.; Kirichenko, O.; Konoplev, V.; Kuznetsova, S.; Sviridov, S.; Brahmachary, E.; Khasanov, A.; Mikel, C.; Yang, Y.; Liu, C.; Wang, J.; Freel, S.; Fisher, S.; Sullivan, A.; Zhou, J.; Stanfield-Oakley, S.; Baker, B.; Sailstad, J.; Greenberg, M.; Bolognesi, D.; Bray, B.; Koszalka, B.; Jeffs, P.; Jeffries, C.; Chucholowski, A.; Sexton, C. *J. Med. Chem.* **2009**, *52*, 4481–4487.
2. For selected reviews on oxidative C–H/C–H coupling reactions see: (a) Yeung, C. S.; Dong, V. M. *Chem. Rev.* **2011**, *111*, 1215–1292; (b) Yang, Y.; Lan, J.; You, J. *Chem. Rev.* **2017**, *117*, 8787–8863; Li, S.-S.; Qin, L.; Dong, L. *Org. Biomol. Chem.* **2016**, *14*, 4554–4570.
3. Reddy, M. D.; Blanton, A. N.; Watkins, E. B. *J. Org. Chem.* **2017**, *82*, 5080–5095.
4. Wencel-Delord, J.; Nimphius, C.; Wang, H.; Glorius, F. *Angew. Chem. Int. Ed.* **2012**, *51*, 13001–13005.
5. Zhang, X.-S.; Zhang, Y.-F.; Li, Z.-W.; Luo, F.-X.; Shi, Z.-J. *Angew. Chem. Int. Ed.* **2015**, *54*, 5478–5482.
6. Tan, G.; Ran, C.; You, J. *Org. Chem. Front.* **2018**, *5*, 2930–2933.
7. Huang, L.; Weix, D. J. *Org. Lett.* **2016**, *18*, 5432–5435.
8. Zhao, S.; Yuan, J.; Li, Y.-C.; Shi, B.-F. *Chem. Commun.* **2015**, *51*, 12823–12826.
9. Nishino, M.; Hirano, K.; Satoh, T.; Miura, M. *Angew. Chem. Int. Ed.* **2013**, *52*, 4457–4461.
10. Wang, X.; Xie, P.; Qiu, R.; Zhu, L.; Liu, T.; Li, Y.; Iwasaki, T.; Au, C.-T.; Xu, X.; Xia, Y.; Yin, S.-F.; Kambe, N. *Chem. Commun.* **2017**, *53*, 8316–8319.
11. Wencel-Delord, J.; Nimphius, C.; Patureau, F. W.; Glorius, F. *Angew. Chem. Int. Ed.* **2012**, *51*, 2247–2251.
12. Wencel-Delord, J.; Nimphius, C.; Wang, H.; Glorius, F. *Angew. Chem. Int. Ed.* **2012**, *51*, 13001–13005.
13. Dong, J.; Long, Z.; Song, F.; Wu, N.; Guo, Q.; Lan, J.; You, J. *Angew. Chem. Int. Ed.* **2013**, *52*, 580–584.

14. Huang, Y.; Wu, D.; Huang, J.; Guo, Q.; Li, J.; You, J. *Angew. Chem. Int. Ed.* **2014**, *53*, 12158–12162.
15. Qin, D.; Wang, J.; Qin, X.; Wang, C.; Gao, G.; You, J. *Chem. Commun.* **2015**, *51*, 6190–6193.
16. He, S.; Tan, G.; Luo, A.; You, J. *Chem. Commun.* **2018**, *54*, 7794–7797.
17. Tan, G.; You, Q.; You, J. *ACS Catal.* **2018**, *8,* 8709–8714.
18. Colletto, C.; Panigrahi, A.; Fernández-Casado, J.; Larrosa, I. *J. Am. Chem. Soc.* **2018**, *140*, 9638–9643.
19. Piou, T.; Romanov-Michailidis, F.; Romanova-Michaelides, M.; Jackson, K. E.; Semakul, N.; Taggart, T. D.; Newell, B. S.; Rithner, C. D.; Paton, R. S.; Rovis, T. *J. Am. Chem. Soc.* **2017**, *139*, 1296-1310.
20. Shibata, Y.; Tanaka, K. *Angew. Chem. Int. Ed.* **2011**, *50*, 10917-10921.
21. Wodrich, M. D.; Ye, B.; Gonthier, J. F.; Corminboeuf, C.; Cramer, N. *Chem. – Eur. J.* **2014**, *20*, 15409–15418.
22. (a) Shi, Y.; Yang, G.; Shen, B.; Yang, Y.; Yan, L.; Yang, F.; Liu, J.; Liao, X.; Yu, P.; Bin, Z.; You, J. *J. Am. Chem. Soc.* **2021**, *143*, 21066–21076; (b) Tan, G.; Ran, C.; You, J. *Org. Chem. Front.*, **2018**, *5*, 2930–2933.
23. Tanaka, J.; Shibata, Y.; Joseph, A.; Nogami, J.; Terasawa, J.; Yoshimura, R.; Tanaka, K. *Chem. – Eur. J.* **2020**, *26*, 5774–5779.
24. Hoshino, Y.; Shibata, Y.; Tanaka, K. *Adv. Synth. Catal.* **2014**, *356*, 1577–1585.
25. Kashima, K.; Teraoka, K.; Uekusa, H.; Shibata, Y.; Tanaka, K. *Org. Lett.* **2016**, *18*, 2170–2173.
26. Hyster, T. K.; Rovis, T. *Chem. Sci.* **2011**, *2*, 1606–1610.
27. Hyster, T. K.; Rovis, T. *J. Am. Chem. Soc.* **2010**, *132*, 10565–10569.
28. (a) Salvati, E.; Botta, L.; Amato, J.; Di Leva, F. S.; Zizza, P.; Gioiello, A.; Pagano, B.; Graziani, G.; Tarsounas, M.; Randazzo, A.; Novellino, E.; Biroccio, A.; Cosconati, S. *J. Med. Chem.* **2017**, *60*, 3626–3635; (b) Chen, J.; Peng, H.; He, J.; Huan, X.; Miao, Z.; Yang, C. *Bioorg. Med. Chem. Lett.* **2014**, *24*, 2669–2673; (c) Li, D.; Xiao, Z.; Wang, S.; Geng, X.; Yang, S.; Fang, J.; Yang, H.; Ding, L. *Adv. Energy Mater.* **2018**, *8*, 1800397.
29. Deng, H.; Li, H.; Wang, L. *Org. Lett.* **2016**, *18*, 3110–3113.
30. (a) Whitaker, D.; Burés, J.; Larrosa, I. *J. Am. Chem. Soc.* **2016**, *138*, 8384–8387; (b) Lotz, M. D.; Camasso, N. M.; Canty, A. J.; Sanford, M. S. *Organometallics* **2017**, *36*, 165–171.
31. Morris, D. M.; McGeagh, M.; De Peña, D.; Merola, J. S. *Polyhedron* **2014**, *84*, 120–135.
32. For the Synthesis of Cp^{TFT}*, Cp^{DMP}*, Cp^{TMP}*, $[Cp^{TFT}*RhCl_2]_2$, $[Cp^{TMP}*RhCl_2]_2$ and $[Cp^{DMP}*RhCl_2]_2$ see chapter 3 : 3.6.3. Synthesis of Novel Cyclopentadienyl Proligands (Cp^RH), Rhodium Complexes $[Cp^RRhCl_2]_2$ and their Characterizations.

General Conclusion and Perspectives

During this thesis, we developed novel rhodium-catalyzed C−H bond functionalization strategies to access various nitrogen-containing heterocycles from low-functionalized materials in a few steps. These processes are facilitated by forming multiple bonds in a cascade reaction triggered by initial C−H bond activation/functionalization. Unconventional directing groups, such as trivalent phosphorus and nitro, were thoughtfully studied to induce *ortho*-directed C−H bond functionalization selectively. Associated with a deep mechanistic investigation of rhodium catalysis, these strategies provide eco-friendly routes for the formation of valuable nitrogen-containing scaffolds such as 3,4-dihydroquinolin-2-ones, 3,3-disubstituted oxindoles, and bi-heteroaryl compounds.

Our studies began by investigating the previous strategies employing rhodium as catalyst for C−H bond annulation to access nitrogen-containing heterocycles. This literature survey points out the efficiency of rhodium catalysts for regioselective C−H bond transformations involving the formation of multiple bonds. The importance of the catalytic system and the choice of the directing group are underlined and proved to be essential to enhance the reactivity and selectivity. Some of these important contributions to rhodium-catalyzed C−H bond functionalization is discussed in chapter 1.

First, we developed, in chapter 2, an efficient Rh(I)-catalyzed strategy to functionalize anilines in the presence of α–β unsaturated esters (Figure 5.1). As previously reported by our group and Shi's group, the P(III)-atom proved to be an efficient directing group to promote *ortho*-directed C−H bond functionalization. Besides its ability to control the regioselectivity, P(III) moiety can be easily removed after the completion of the C–H bond transformation. We discovered that P(III)-atom associated with Rh(I) catalyst smoothly provided a cascade reaction of C−H bond alkylation and intramolecular amidation. This strategy allowed the simultaneous formation of C−C and C−N bonds leading to dihydroquinolinone scaffolds in a single-step process. Starting from various decorated anilines, eighteen dihydroquinolinone derivatives were successfully isolated in good yields with an excellent functional group tolerance at the *para*-, *meta*- and *ortho*-positions. This methodology was extended to styrene derivatives as coupling partners to deliver *ortho*-alkylated anilines. We also demonstrated the synthetic use of our novel methodology by preparing an *N*-methylated analog of Aripiprazole, a biologically active compound known for treating schizophrenia. In addition, a mechanistic investigation was conducted to bring a comprehensive pathway of this novel Rh(I)-catalyzed cascade reaction. Control experiments revealed that the P(III)-atom acts as a traceless directing group to undergo the selective C−H bond alkylation − amidation in one pot. Notably, water is essential to induce intramolecular amidation by facilitating the hydrolysis of the N−P

bond with the release of hydroxydiisopropylphosphane as a side-product. A full kinetic profile was completed following the consumption of *N*-arylphosphanamine, the evolution of a latent alkylated-*N*-arylphosphanamine intermediate, and the formation of the desired dihydroquinolinone product. These mechanistic insights should pave the way for the development of new P(III)-directed Rh(I)-catalyzed C–H bond transformations to broaden access to complex motifs from raw-functionalized molecules.

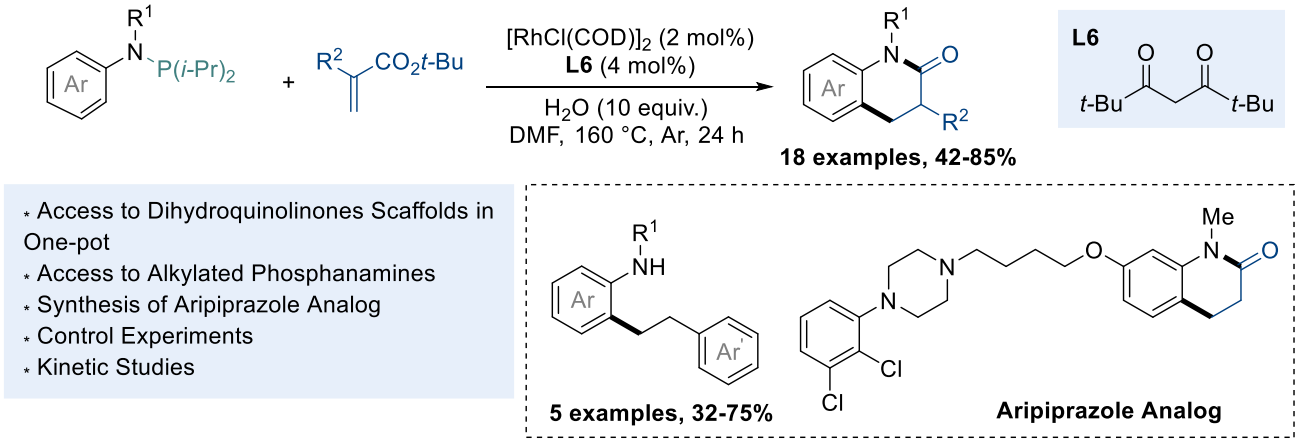

Figure 5.1. Rhodium(I)-Catalyzed Cascade C–H Bond Alkylation – Amidation of Anilines with Trivalent Phosphorus as Traceless Directing Group.

In chapter 3, we explored the reactivity of nitroarenes in C–H bond functionalization using Rh(III) catalysis (Figure 5.2). By merging C–H bond activation and oxygen-atom transfer, we overcame the poor reactivity of nitroarenes in *ortho*-directed C–H bond transformation through the generation of a highly reactive nitroso intermediate under redox-neutral conditions. This elegant cascade reaction delivered 3,3-disubstituted oxindoles from nitroarenes and alkynes in one pot. After optimization and design of new cyclopentadienyl pro-ligands, we observed that this novel reaction is facilitated by the use of $[Cp^{TMP*}RhCl_2]_2$ [Cp^{TMP*} = 1-(3,4,5-trimethoxyphenyl)-2,3,4,5-tetramethylcyclopentadienyl], a Cp ligand combining an electron-rich character with an elliptical shape. The scope of nitroarene, alkyne, and anhydride partners was investigated, allowing the formation of various 3,3-disubstituted oxindoles in one pot in good yields. Besides good functional group tolerance, this strategy allows the formation of oxindoles with a (stereogenic) quaternary carbon stereocenter. Several post-transformations were carried out to illustrate the synthetic value of our novel reaction. The synthesis of valuable indolin-2-one derivatives was achievable in only two steps after the reduction of the amide groups. Several electron-withdrawing groups, such as cyano, formyl, and alkynyl, were introduced by post-functionalization starting from iodo-substituted oxindoles. A deep mechanistic investigation was conducted with the isolation of three

rhodacycle intermediates. These results revealed that the reaction proceeds through a cascade reaction of C–H bond activation – *O*-atom transfer – [1,2]-aryl shift – deoxygenation – acylation. This strategy is one of the rare examples employing a nitro group as a directing group and encourages the exploration of nitroso intermediates to discover novel cascade transformations.

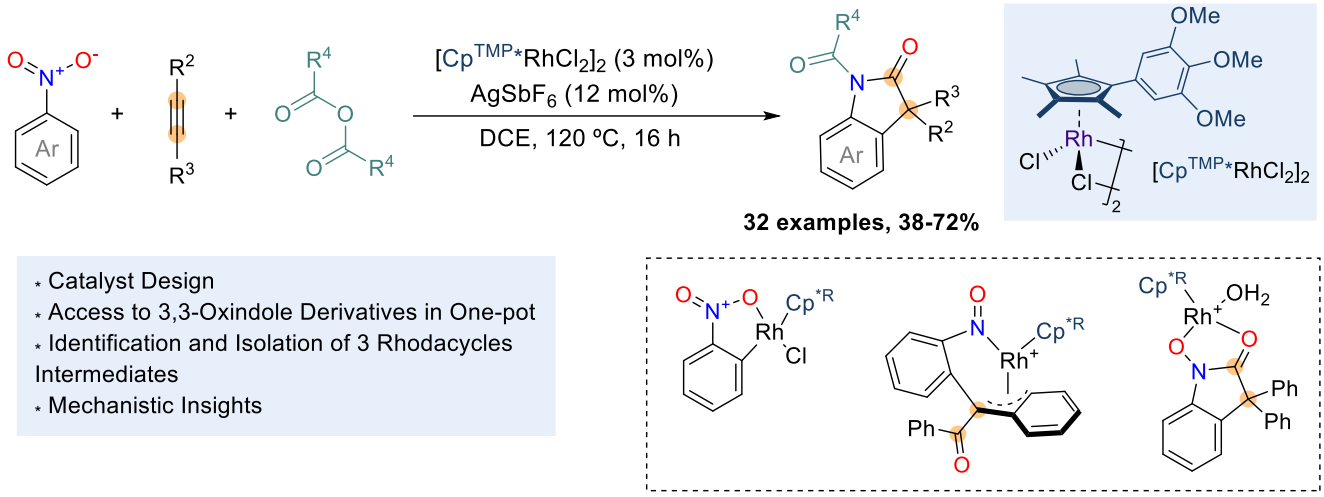

Figure 5.2. Rhodium(III)-Catalyzed Cascade C–H bond Activation – *O*-Atom Transfer – [1,2]-Aryl Shift – Deoxygenation – Acylation to Access *N*-Heterocycles.

Finally, in chapter 4, we reported a novel set of conditions for the regioselective Rh(III)-catalyzed C–H bond heteroarylation of benzamides under mild conditions (Figure 5.3). The reaction occurred through a double C–H bond functionalization strategy under mild conditions to access bi(hetero)aryl compounds. Secondary benzamide was selected as a directing group to undergo this transformation with heteroarenes as coupling partners. This reaction is facilitated by using the η^5-cyclopentadienyl rhodium complex $[RhCp^{*TMP}Cl_2]_2$ that we previously developed in the chapter 3, with the presence of Ag_2O and $Zn(OTf)_2$. Rh(III) and Ag(I) catalyzed double C–H bond activation of benzamide at the *ortho*-position and the C2-position of heteroarenes. A broad scope of the reaction was investigated and tolerated various functional groups, including halogens (Br, F, Cl) at the *ortho*-, *meta*- and *para*-positions. The scope of heteroarenes was extended to mono and di-substituted thiophenes and furans, allowing the formation of the desired compounds in excellent yields. Finally, this eco-friendly strategy allows the rapid formation of bi(hetero)aryl compounds by 2-fold C–H bond activation that exhibits potential in synthesizing various natural products, biologically active compounds, and organic functional materials.

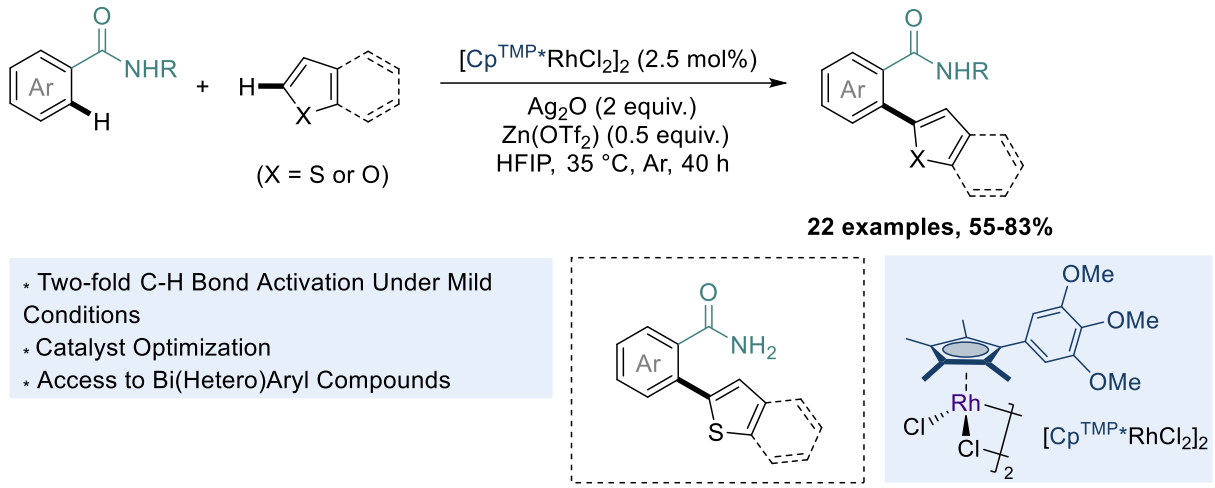

Figure 5.3. Rhodium(III)/Silver(I)-Catalyzed *ortho*-Heteroarylation of Benzamides at Room-Temperature *via* C–H/C–H Bonds Couplings.

These pieces of research, developed during this Ph.D., set the stage for exploring new Rh-catalyzed C–H bond functionalization. For instance, the Rh(I)-catalyzed P(III)-directed cascade reaction from anilines derivatives developed in the first part could be extended to further coupling partners. The introduction of olefin partners with extended carbon chains could give access to more complex nitrogen-containing heterocycles (Figure 5.3-a). Another appealing extension of this research would involve the phosphorus group as a transient directing group to undergo selective C–H bond functionalization (Figure 5.4-b). This challenging approach relying on installing and removing the directing group, often in a catalytic amount, could be considered as another sustainable strategy.

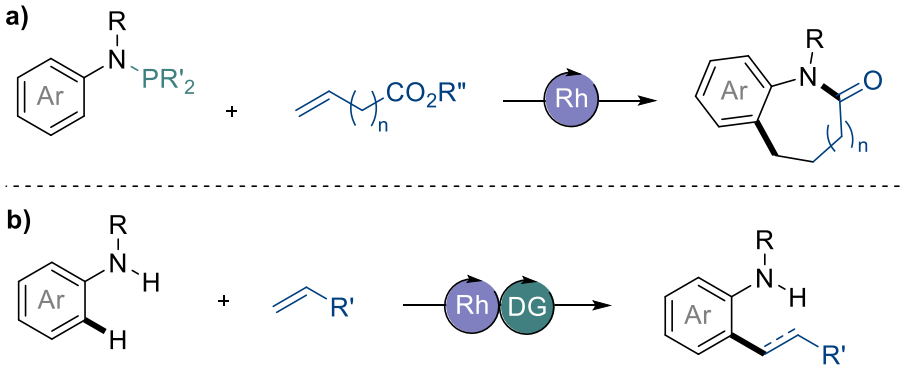

Figure 5.4. Future Diversification of Anilines with Olefins *via* C–H bond functionalization with Traceless or Transient Directing Groups.

The cascade reaction discovered in chapter 3 delivered 3,3-disubstituted oxindoles from nitroarenes and alkynes in a single-step process. Starting from non-symmetrical alkynes, 3,3-disubstituted oxindoles with a quaternary carbon stereocenter were obtained in a racemic

mixture. An asymmetric variant could be explored by controlling the insertion of alkyne and the aryl-shift step to provide enantiopure oxindoles (Figure 5.5-a). The discovery of this new cascade reaction from nitroarenes paves the way to dig deeper into nitroso intermediates reactivity. In association with other electrophile or nucleophile partners, new unpredictable cascade transformations could provide access to nitrogen-containing heterocycles (Figure 5.5-b).

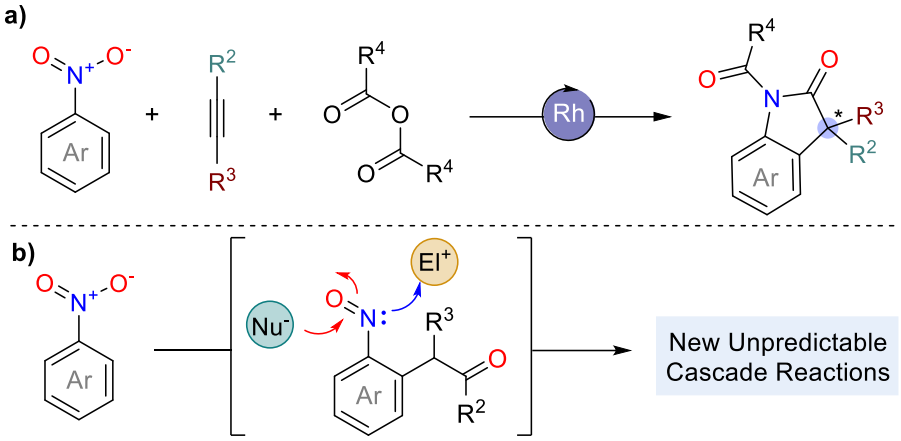

Figure 5.5. Future Diversification of Nitroarenes *via* Asymmetric Functionalization of C–H Bonds and Exploration of the Reactivity of Nitroso Intermediates.

By extension to the research work reported in chapter 4, the development of a novel C–H bond annulation strategy from benzamides could be investigated to build fused isoquinolin-1-*2H*-one scaffolds in a one-pot by using multi-catalysts approaches (Figure 5.6).

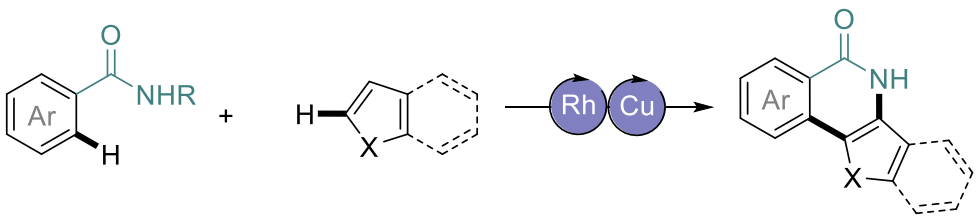

Figure 5.6. Future Diversification of Benzamides *via* C–H Bond Annulation.

Finally, the results presented in this thesis highlighted the importance of the catalytic system to enhance the efficiency and the reactivity to build complex heterocycles in a few steps. Promising performances were provided from the elliptical-shaped catalyst $[Cp^{TMP*}RhCl_2]_2$ that we designed and should stimulate further C–H bond transformations in the future. At last,

elaborating on milder conditions at room temperature would be beneficial to ensure the attractiveness of these novel methodologies, notably in the late-stage functionalization of highly functionalized molecules.

Résumé Français

Ce projet de thèse s'articule autour de la synthèse d'hétérocycles azotés par le développement de nouvelles réactions catalysées par des complexes de rhodium. En effet, les hétérocycles azotés sont des motifs organiques importants de par leur large représentation dans les composés naturels, dans les médicaments ou dans les matériaux organiques. L'accès à ces hétérocycles azotés demeure souvent laborieuse impliquant régulièrement une synthèse multi-étape. Afin de faciliter la synthèse de ces composés aromatiques, l'axe de recherches est porté sur la fonctionnalisation directe de liaisons C−H avec une formation simultanée d'autres liaisons telles que la formation de liaisons C−C ou C−X (X = N ou O). Contrairement aux réactions classiques de couplages croisés nécessitant des étapes de pré-fonctionnalisation, cette méthode permet d'accéder de manière rapide à des complexes (poly)(hétéro)aromatiques favorisant ainsi une économie d'atomes, une économie d'étapes et une réduction des déchets.

Parmi les métaux de transition employés en fonctionnalisation de liaisons C−H, les catalyseurs de rhodium tirent leur épingle du jeu notamment par leur polyvalence. Leur efficacité a été prouvée pour de nombreuses réactions en chimie organométallique telles que les réactions d'activation de liaisons C−H, les réactions d'hydrogénation ou les réactions de carbonylation. Le rhodium présente notamment des propriétés intéressantes en termes de régiosélectivité et de compatibilité avec de nombreux groupes fonctionnels. Les catalyseurs à base de rhodium sont généralement hautement actifs pouvant être utilisés à faible charge. Ces atouts (*i.e.* le taux, la sélectivité et la durée de vie du catalyseur) sont souvent des variables plus importantes que le coût du métal lui-même.

Du fait de l'omniprésence de liaisons C−H dans les composés organiques, le contrôle de la régiosélectivité demeure un enjeu important. Afin de guider sélectivement la fonctionnalisation de liaisons C−H en position *ortho,* plusieurs approches nécessitant l'emploi de groupement directeur ont été envisagées. La première repose sur l'emploi de groupement directeur amovible. Dans ce cas, le groupement directeur est initialement introduit puis sa suppression se produit directement en *one-pot*. La deuxième alternative consiste à employer un groupement directeur se convertissant directement en groupe fonctionnel. Associé à différents partenaires de couplage, ce type de stratégie peut ainsi induire des réactions intramoléculaires avec la formation simultanée de liaisons multiples. Dans ce contexte, l'activation de liaisons C−H est considérée comme un outil intéressant pour déclencher des réactions en cascade facilitant ainsi l'accès à divers hétérocycles azotés en peu d'étapes. Ces réactions en cascade se définissent par la formation d'au moins deux liaisons en une étape

sans ajout de réactif ou de catalyseur. Au-delà de l'économie d'atomes et d'étapes, les réactions en cascade initiée par la fonctionnalisation/ l'activation de liaisons C−H permettent d'enrichir la complexité des composés désirés.

Au cours de ces travaux de recherche, nos efforts sont portés sur l'utilisation de substrats de départ accessibles dans le commerce et sur la formation simultanée de multiples liaisons initiées par la fonctionnalisation de liaisons C−H *ortho*-dirigée. Les objectifs de cette thèse sont multiples et se développent autour de l'étude de complexes de rhodium, l'optimisation des conditions de réactions de fonctionnalisation de liaisons C−H, et l'étude des périmètres de la réaction afin d'élargir l'accès à divers composés azotés. Enfin, ces travaux sont complétés par diverses études mécanistiques afin de rationaliser ces nouvelles réactions.

Dans un premier temps, nous nous sommes intéressés à la fonctionnalisation d'anilines catalysée par le rhodium en présence d'esters α-β-insaturés afin d'accéder à des motifs de type dihydroquinolinones. Ces composés sont des précurseurs dans une multitude de molécules biologiquement actives notamment le Cartéolol, bétabloquant utilisé pour le traitement du glaucome, le Cilostazol employé comme vasodilateur pour traiter des symptômes de claudication intermittente ou le Vesnarinone, médicament cardiotonique prescrit en cas de déficience cardiaque (Figure 1).

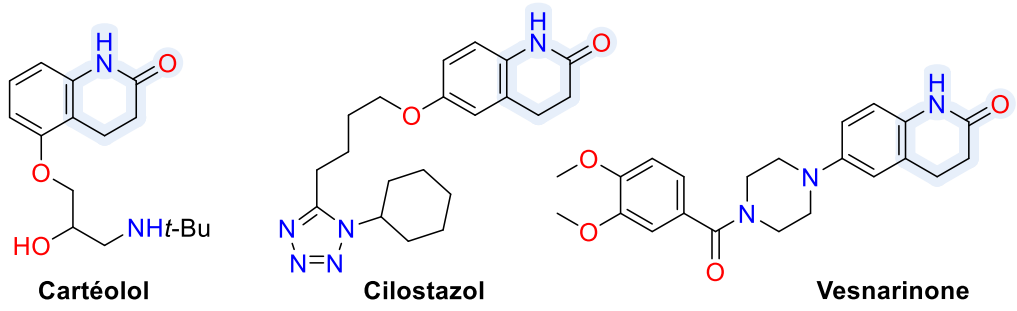

Figure 1. Sélection de médicaments comportant un motif dihydroisoquinolinone.

De par leur importance, le développement de nouvelles stratégies afin d'accéder à des dihydroquinolinones en peu d'étapes est souhaitable. Notre étude s'est donc portée sur l'annulation de liaisons C−H à partir d'anilines afin de former simultanément des liaisons C−C et C−N. La littérature montre que la réactivité des anilines s'effectue habituellement en position *para.* Afin de pouvoir moduler la régiosélectivité, notre avons étudié l'introduction d'un groupement directeur pour favoriser la fonctionnalisation de liaisons C−H en position *ortho* de l'aniline. Notre choix s'est dirigé vers l'emploi de phosphore trivalent. Son efficacité

en tant que groupement directeur a déjà été démontrée pour diverses réactions de fonctionnalisation de liaisons C−H *ortho*-dirigée notamment pour l'alkylation de diarylphosphines. De plus, après hydrolyse de la liaison N−P, une réaction d'amidation intramoléculaire pourrait spontanément se produire afin d'obtenir le motif désiré en une étape. Nous avons ainsi démontré, après optimisation des conditions de réaction, l'accès à divers motifs de type dihydroquinolinones à partir de *N*-arylphosphanamines et d'acrylates. En effet, en présence de $[RhCl(COD)]_2$, de 2,2,6,6-tetramethyl-3,5-heptanedione et d'eau dans le DMF, la réaction en cascade d'alkylation de la liaison C−H – amidation nous permet de générer les hétérocycles azotés désirés en *one-pot*. Dix-huit motifs de type dihydroquinolinones diversement décorés ont pu être obtenus et isolés avec de bons rendements avec une tolérance pour des groupements fonctionnels en positions *para*-, *meta*- et *ortho*- (Schéma 1-a). Cette stratégie a pu être étendue à d'autres substrats comme les styrènes permettant l'accès à diverses anilines alkylées (Schéma 1-b).

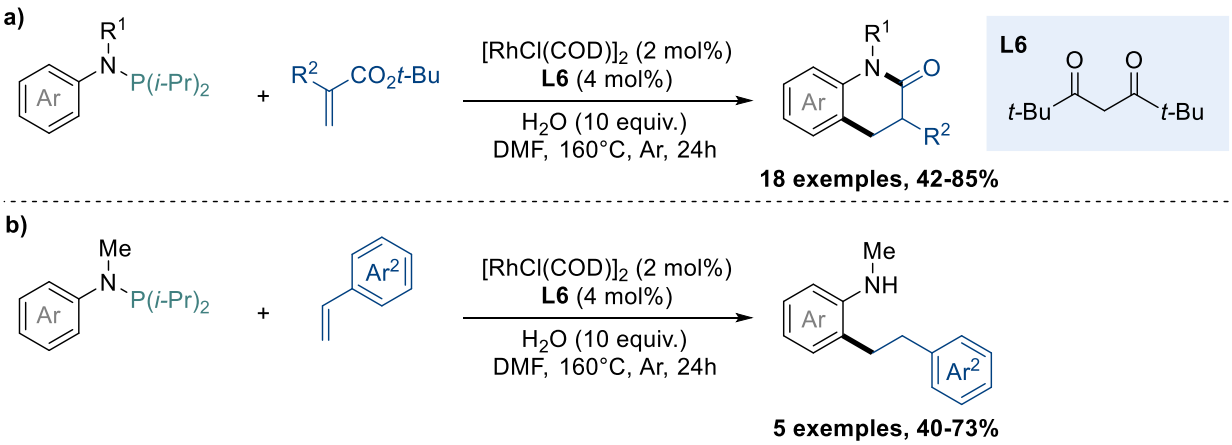

Schéma 1. Fonctionnalisation P(III)-dirigée et catalysée au Rh(I) de *N*-arylphosphanamines : accès à divers motifs dihydroquinolinones et anilines alkylées.

Cette nouvelle réaction en cascade permet notamment de fournir efficacement un précurseur essentiel pour la synthèse d'un anologue *N*-méthylé de l'Aripiprazole, composé biologiquement actif prescrit dans les traitements contre la schizophrénie. (Schéma 2).

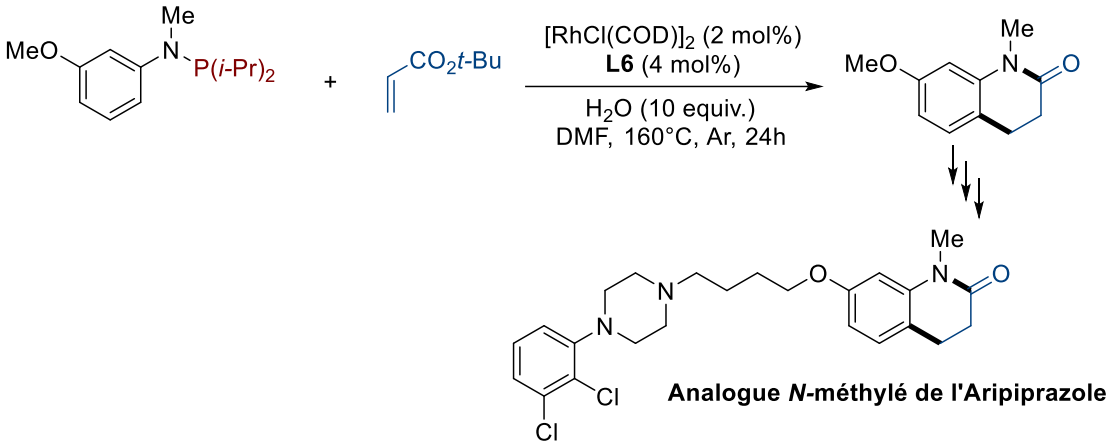

Schéma 2. Synthèse d'un analogue *N*-méthylé de l'Aripiprazole.

Ces résultats ont été complétés par plusieurs études mécanistiques et cinétiques afin de comprendre davantage le système catalytique ainsi que les rôles du phosphore trivalent et de l'eau dans cette réaction en cascade catalysée au Rh(I). Il s'est avéré que le groupement P(*i*-Pr)$_2$ trivalent agit comme un groupement directeur amovible. De plus, nous avons pu démontrer que l'eau était un paramètre essentiel pour induire la réaction d'amidation intramoléculaire en facilitant l'hydrolyse de la liaison N−P. Un profil cinétique complet a pu être dressé en suivant la consommation de *N*-arylphosphanamine de départ, l'évolution d'un intermédiaire alkylé de *N*-arylphosphanamine dit latent ainsi que l'apparition de produit final. Ces résultats nous ont permis de mettre en lumière l'efficacité du phosphore trivalent en tant que groupement directeur pour la réaction d'alkylation de liaison C−H − amidation de *N*-arylphosphanamine en *one-pot.* Cette nouvelle méthodologie catalysée au Rh(I) associé au 2,2,6,6-tetramethyl-3,5-heptanedione nous a permis d'accéder à une vaste bibliothèque de motifs dihydroquinolinones décorés. Cette stratégie P(III)-dirigée catalysée au Rh(I) présentée pourrait être étendue à d'autres partenaires de couplage permettant ainsi l'accès à divers composés poly(hétéro)aromatiques.

Dans un second temps, nous nous sommes intéressés à la réactivité des nitroarènes. Obtenus après réaction de nitration d'arènes, ces composés constituent les premières briques de construction pour la synthèse de nombreux hétérocycles azotés. Son emploi en tant que groupement directeur demeure cependant très limité. En 2008, Fagnou *et al.* a décrit le premier exemple d'arylation pallado-catalysée en position *ortho* de nitroarène en présence de bromure d'aryle, depuis, un seul autre exemple a été reporté par Echavarren *et al.* en 2021 en employant le rhodium pour l'alkynylation en position *ortho* de nitroarènes (Schéma 3).

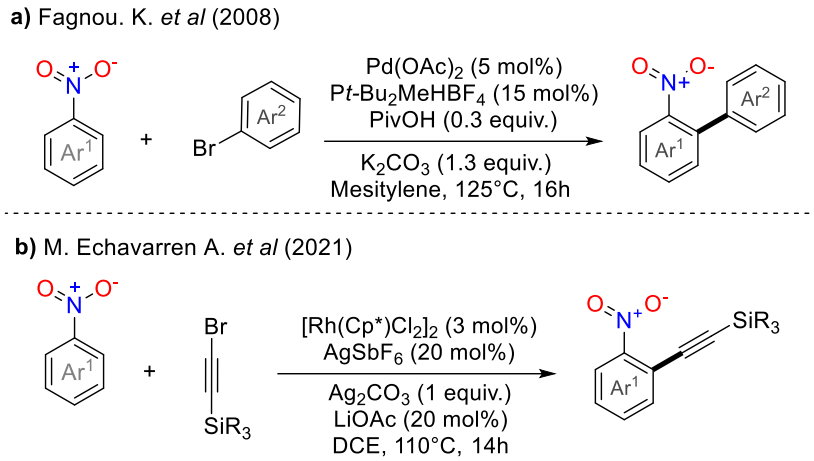

Schéma 3. Précédentes stratégies de fonctionnalisation de liaisons C−H de nitroarènes.

Le caractère électroattracteur du groupement nitro fait de lui un candidat peu attrayant pour diriger sélectivement une fonctionnalisation de liaison C−H en position *ortho*. Il est traditionnellement réduit en aniline pour faciliter l'installation de groupements directeurs plus coordinant pour la fonctionnalisation de liaisons C−H. Nous avons alors envisagé de combiner l'activation de liaison C−H avec un transfert d'atome d'oxygène nous permettant d'employer le groupement nitro comme oxydant naturel et de générer un intermédiaire nitroso potentiellement très réactif enclin à des réactions de réarrangements. L'étude a débuté en employant le nitrobenzène, le diphénylacétylène et l'anhydride acétique en tant que substrats de départ en présence de $[Rh(Cp^*)Cl_2]_2$ dans le dichloroéthane. Nous avons pu générer de manière inattendue des oxindoles disubstitués en position 3,3 en conditions d'oxydo-réduction neutres. Cette nouvelle réaction en cascade nous a permis d'obtenir en une seule étape un motif oxindole à partir de substrats simples et disponibles dans le commerce et représente également le premier exemple de réaction de transfert d'atome d'oxygène à partir d'un groupement nitro. Afin d'optimiser les conditions de réaction, notre étude s'est portée sur le design de pro-ligands de type cyclopentadiène. Divers complexes de rhodium de forme hélicoïdale ont été mis au point et testés pour notre réaction. Le catalyseur riche en électrons et de forme hélicoïdale $[Cp^{TMP}*RhCl_2]_2$ [CpTMP* = 1-(3,4,5-triméthoxyphényl)-2,3,4,5-tetraméthylcyclopentadiène] que nous avons conçu s'est avéré être le plus efficace. Après avoir évalué l'étendue des nitroarènes, des alcynes et des anhydrides, plus de trente dérivés d'oxindoles disubstitués ont pu être isolés avec des bons rendements. De nombreux groupes fonctionnels et halogènes ont pu être tolérés. Il convient de noter que l'utilisation d'alcynes 1,2-diaryl non symétriques a permis de générer six

oxindoles comportant un carbone quaternaire avec un centre stéréogénique ouvrant la voie à une alternative asymétrique (Schéma 4).

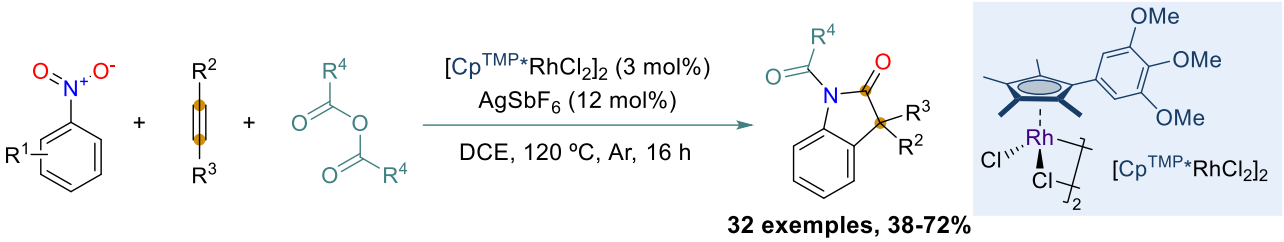

Schéma 4. Réaction multi-composants en cascade de nitroarènes et alcynes : accès à divers oxindoles 3,3-disubstitués.

Cependant, le groupement nitro appauvrissant le système électronique n'est pas compatible avec la présence de substituants électroattracteurs pour cette stratégie. Nous avons ainsi complété l'étendue de cette réaction en réalisant plusieurs transformations post-fonctionnelles à partir de l'oxindole iodo-substitué afin d'introduire différents groupements électroattracteurs comme les groupes cyano-, formyl- ou alkynyl-. Ensuite, plusieurs conditions de réduction de la fonction amide ont été mises en place nous permettant d'accéder à des indolines disubstituées en seulement deux étapes. Enfin, nous avons complété nos recherches par plusieurs études mécanistiques afin d'identifier les étapes clés de cette nouvelle réaction en cascade. Dans un premier temps, l'effet isotopique cinétique a été déterminé en présence de notre catalyseur ainsi que du catalyseur $[Rh(Cp^*)Cl_2]_2$ commercial. L'étude a révélé que l'étape de C–H activation semble être l'étape limitante de cette réaction en cascade. Nos efforts se sont ensuite portés sur l'isolation de différents intermédiaires réactionnels afin d'identifier les étapes clés du cycle catalytique. Nous avons pu identifier et isoler 3 intermédiaires rhodacycles après une analyse complète par RMN, spectroscopie de masse haute résolution et obtention des structures crystallographiques (Schéma 5).

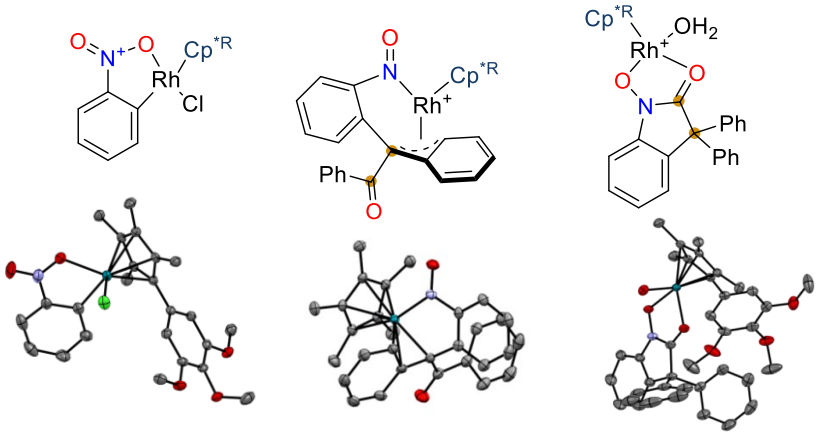

Schéma 5. Intermédiaires de rhodium cyclométallés isolés.

L'efficacité de notre catalyseur de Rh(III) a notamment pu être prouvée grâce à la génération d'un intermédiaire cyclométallé très réactif. Nous avons ainsi démontré que cette nouvelle réaction catalysée au Rh(III) générant des dérivés d'oxindoles en *one-pot* a lieu suite à une réaction en cascade d'activation de liaison C–H – transfert d'atome d'oxygène – migration d'aryl en 1,2 – déoxygénation – acylation. Cette nouvelle stratégie permet d'ouvrir la voie à l'exploration des nitrosoarènes en présence d'autres partenaires de couplage pour le développement de nouvelles réactions en cascade.

Enfin, la dernière partie de ces travaux de recherches concerne l'application des catalyseurs de rhodium précédemment développés pour la fonctionnalisation directe de liaisons C−H entre 2 composés bi(hétéro)aromatiques. En effet, les systèmes pi-conjugués étendus dans les motifs bi(hétero)aromatiques font de ces motifs des précurseurs intéressants pour la synthèse organique. Par extension, l'accès à des structures plus complexes d'hétérocycles azotés est envisageable. Traditionnellement, les bromures ou les iodures d'aryles sont privilégiés en tant que partenaire électrophile de couplage générant inévitablement des déchets halogénés ou des sous-produits issus de réactions d'homo-couplage. Afin de contrer ces problèmes, nos travaux de recherches se sont portés sur la double activation de liaisons C−H, puisque dans les faits, seulement « H_2 » serait généré. Cette stratégie permet de générer rapidement et de manière efficace un composé bi(hétéro)aromatique. Les résultats de recherches préliminaires nous ont permis de mettre en lumière l'importance du groupement directeur afin de diriger sélectivement la fonctionnalisation de liaison C−H en position *ortho*- ainsi que l'importance du système catalytique. Dans ces travaux, nous avons développé une méthode efficace d'hétéroarylation d'amides secondaires catalysée au $[Rh(Cp^{TMP}*)Cl_2]_2$ et à Ag(I) en présence de triflate de zinc en conditions douces à température ambiante. Après optimisation des conditions de réaction, cette stratégie a pu être appliquée à divers hétéroatomes tels que les benzo[*b*]thiophènes, les thiophènes mono-, di-substitués ou les furanes. Au total, plus de vingt produits issus de la double fonctionnalisation de liaisons C−H ont pu être isolés avec de très bons rendements (Schéma 6). La présence de substituants sur les benzamides en positions *ortho-, méta-* et *para-* est également bien tolérée et n'affecte pas la régiosélectivité de la réaction.

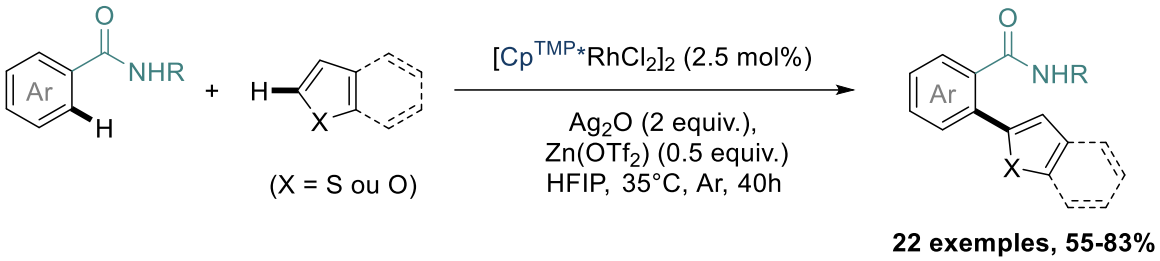

Schéma 6. Synthèse de composés bi(hétéro)aromatiques par fonctionnalisation de liaisons C−H catalysée au Rh(III)/Ag(I) et transformations post-fonctionnelles.

Notre stratégie permet donc de générer ces hétérocycles azotés en peu d'étapes, qui peuvent être employés en tant que précurseurs pour des molécules biologiquement actives ou des matériaux organiques. Enfin, des expériences complémentaires sont en cours afin d'accroître l'étendu des substrats de départ, des études mécanistiques sont également envisagées afin de mieux comprendre le cycle catalytique de cette nouvelle réaction.

Au cours de ces travaux de thèse, nous avons ainsi pu développer trois nouvelles stratégies de fonctionnalisation de liaisons C−H catalysées au rhodium pour l'accès à des hétérocycles azotés en employant des groupements directeurs originaux. Dans un premier temps, nous avons mis en place une nouvelle méthodologie pour accéder à des composés de type dihydroisoquinolinones à partir de *N*-arylphosphanamines et d'acrylates comme substrats de départ. Cette réaction en cascade d'alkylation de liaisons C−H et d'amidation dirigée au P(III) et catalysée au Rh(I) permet d'accéder de manière efficace en une seule étape à une multitude de composés dihydroisoquinolinones et permet l'accès à diverses anilines alkylées avec de bons rendements (Schéma 7-a). Ensuite, nous avons décrit des conditions de réaction permettant l'accès à divers oxindoles 3,3 disubstitués avec création d'un carbone quaternaire asymétrique. Nous avons pu accéder de manière sélective à ces hétérocycles azotés en *one-pot* à partir de nitroarènes, d'alcynes et d'anhydrides (Schéma 7-b). Cette réaction multi-composants en cascade d'activation de liaison C−H – transfert d'atome d'oxygène – migration en 1,2 d'aryl – déoxygénation – acylation est notamment facilitée par l'utilisation d'un catalyseur de rhodium que nous avons développé qui combine un caractère riche en électrons avec une forme hélicoïdale. Enfin, nous avons mis au point les premières conditions douces de double fonctionnalisation de liaisons C−H entre amides secondaires et hétérocycles (benzo[*b*]thiophènes, thiophènes et furanes) catalysée au Rh(III)/Ag(I). Le processus est facilité par le ligand Cp^{TMP*} précédemment développé avec l'assistance d'oxyde d'argent et de triflate de zinc et permet l'accès à une vaste bibliothèque de composés bi(hétéro)aromatiques (Schéma 7-c).

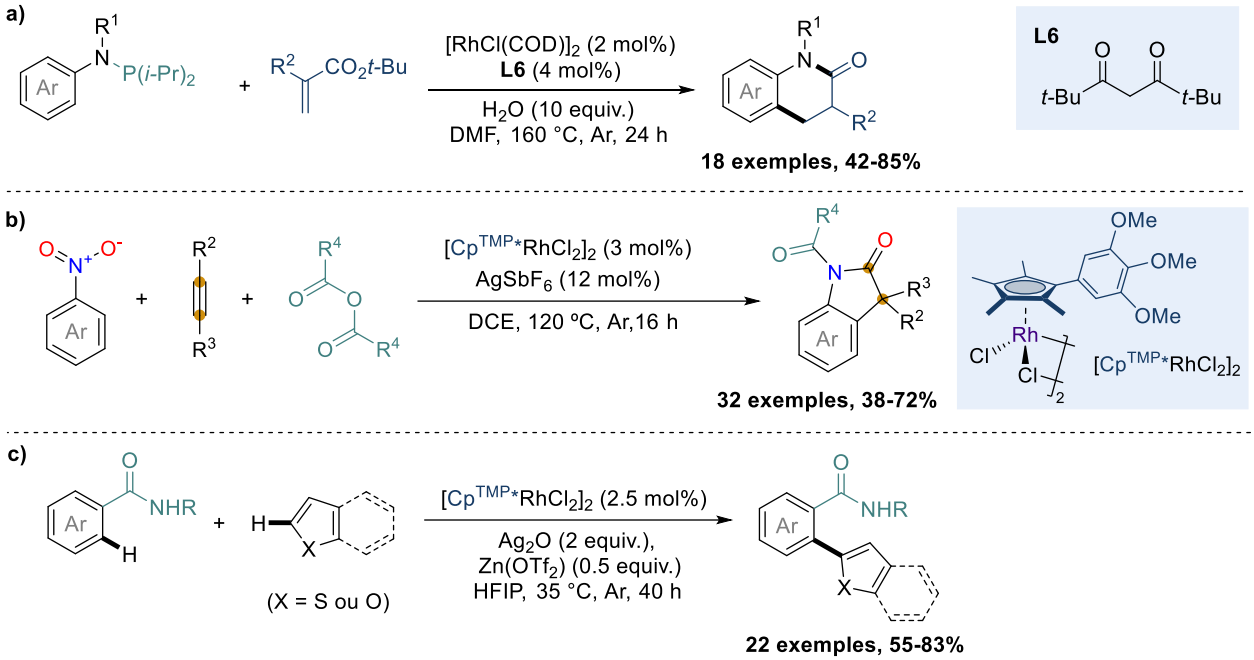

Schéma 7. Nouvelles stratégies de synthèse d'hétérocycles azotés par fonctionnalisations de liaisons C−H en cascade catalysées par des complexes de rhodium.

Les résultats de ces travaux de thèse nous ont permis de mettre en avant plusieurs critères essentiels pour la fonctionnalisation de liaisons C−H. Les différents groupements fonctionnels utilisés nous ont permis d'effectuer sélectivement la fonctionnalisation de liaisons C−H en position *ortho.* Notamment, l'emploi de groupement directeur amovible a permis de faciliter la formation simultanée de multiples liaisons C−C, C−N et C−O. De plus, le choix du système catalytique s'est avéré crucial pour contrôler la régiosélectivité et la réactivité des intermédiaires réactionnels.

Grâce à ces nouvelles réactions de fonctionnalisation de liaisons C−H, divers hétérocycles azotés qui nécessitaient auparavant une synthèse multi-étape peuvent dorénavant être obtenus en très peu d'étapes. De plus, la bonne tolérance pour un large choix de groupes fonctionnels étend les possibilités de transformations post-fonctionnelles et par conséquent, la modification des propriétés de ces composés. A l'avenir, les propriétés prometteuses du catalyseur de rhodium $[Cp^{TMP*}RhCl_2]_2$ que nous avons élaboré pourrait stimuler l'exploration de nouvelles transformations de liaisons C−H catalysées au rhodium. Enfin, le développement de conditions de réaction plus douces pourrait être bénéfique afin d'assurer l'attractivité de ces nouvelles méthodologies de synthèse.

DOCTORAT MATIERE BRETAGNE MOLECULES LOIRE ET MATERIAUX

UNIVERSITÉ DE RENNES 1

Titre : Synthèse d'Hétérocycles Azotés par Fonctionnalisations de Liaisons C–H en Cascade Catalysées par des Complexes de Rhodium

Mots clés : Catalyse, Fonctionnalisation de Liaisons C–H, Hétérocycles Azotés, Réaction en Cascade, Rhodium.

Résumé : Depuis 20 ans, la fonctionnalisation directe de liaisons C–H catalysée par des métaux de transition s'est imposée comme une stratégie de choix pour la construction rapide de liaisons C–C et C–X. Les résultats obtenus lors de ces travaux de recherche visent à développer de nouvelles voies de synthèse permettant l'accès à divers hétérocycles azotés à partir de molécules peu fonctionnalisées disponibles dans le commerce.

Dans un premier temps, nous avons développé des conditions permettant l'accès à des motifs dihydroquinolinones *via* une réaction en cascade d'alkylation et d'amidation d'anilines catalysée au Rh(I). La présence d'un groupement directeur amovible de type phosphore trivalent permet notamment de diriger sélectivement la fonctionnalisation de liaisons C–H en position *ortho* et d'induire l'amidation intramoléculaire après hydrolyse de la liaison N–P.

Dans un second objectif, nous avons élaboré une stratégie de fonctionnalisation de liaisons C–H *ortho*-dirigée de nitroarènes en présence de diarylalcynes et d'anhydrides. Cette réaction en cascade a permis d'obtenir des structures oxindoles 3,3-disubstitués en une seule étape. Cette transformation est notamment facilitée par l'emploi d'un catalyseur de rhodium (Cp^{TMP*})Rh(III) [Cp^{TMP*} = 1-(3,4,5-trimethoxy phenyl)-2,3,4,5-tetramethylcyclopentadienyl] que nous avons mis au point.

L'utilisation de ce catalyseur de Rh(III) a notamment pu être étendu à l'hétéroarylation d'amides par couplages de liaisons C–H/ C–H. Le Rh(III) associé à l'Ag(I) a permis d'obtenir différents complexes bi(hétéro)aromatiques à température ambiante.

Des études mécanistiques approfondies ont été réalisées sur chaque réaction afin de rationaliser les différents processus catalytiques.

Titre : Rhodium Catalyzed Cascade C–H Bond Functionalization for the Synthesis of Nitrogen-Containing Heterocycles

Keywords : Cascade Reaction, Catalysis, C–H Bond Functionalization, Nitrogen-Containing Heterocycles, Rhodium

Abstract : Over the past two decades, the C–H bond functionalization raised as a powerful tool for the rapid construction of C–C bonds et C–X bonds. This research work aimed to demonstrate new methodologies to access nitrogen-containing heterocycles from readily available with diarylakynes and anhydrides. This cascade reaction delivered 3,3-disubstituted oxindoles in a single-step process. Notably, the reactivity is enhanced by using a rhodium complex (Cp^{TMP*})Rh(III) [Cp^{TMP*} = 1-(3,4,5-trimethoxyphenyl)-2,3,4,5-tetramethyl-